



**Universidade do Minho**  
Escola de Engenharia

Tiago Filipe da Silva Miranda

**Geomechanical Parameters Evaluation in  
Underground Structures. Artificial Intelligence,  
Bayesian Probabilities and Inverse Methods.**

Novembro de 2007



**Universidade do Minho**

Escola de Engenharia

Tiago Filipe da Silva Miranda

**Geomechanical Parameters Evaluation in  
Underground Structures. Artificial Intelligence,  
Bayesian Probabilities and Inverse Methods.**

Tese de Doutoramento em Engenharia Civil - Geotecnia

Trabalho efectuado sob a orientação do:

**Professor Doutor António Gomes Correia**

Co-orientação do:

**Professor Doutor Luís Ribeiro e Sousa**

Novembro de 2007

---

# ACKNOWLEDGMENTS

---

The present work was developed at the Civil Engineering Department of the University of Minho in Portugal under the supervision of Professor António Gomes Correia and Luís Ribeiro e Sousa. The development and writing of a PhD thesis is essentially an one-man task but in the end, this three year work would be a lot more difficult to accomplish without the support and help of a considerable amount of people and institutions which directly or indirectly contributed to the achievement of the final work. This way, it is only fair to present to all of them (hoping not to forget anyone) my sincere acknowledgments.

- First of all to Professor Luís Ribeiro e Sousa for the dedication and for always pushing me forward. His expertise and experience turned the last five years working together a continuous professional and personal learning experience.
- Professor António Gomes Correia whose broad view of geotechnics and critical spirit provided an important contribution to the work.
- The financial support granted by FCT (Foundation for Science and Technology) in the scope of the research project POCI/ECM/57495/2004 *Geotechnical Risk in Tunnels for High-Speed Trains*.
- The EDP (Electricity of Portugal) company for making available all the data concerning the Venda Nova II scheme in particular to Professor Celso Lima and Dr. Nadir Plasencia.
- To Professor Manuel Filipe Santos and Paulo Cortez for their explanations and support concerning the Data Mining field and for providing the analysis tools.
- Professor Lino Costa for supplying the evolution strategy algorithm code to be used in the back analysis calculations.
- Professor Daniel Dias and Eng. Stéphanie Eclaircy-Caudron from INSA-Lyon, partners in some of the back analysis work, for their dynamic spirit and friendship which produced very good results.

- To the students Ricardo Sousa, Isabel Nogueira, André Oliveira, José Carvalho, Manuel Pereira and Rosário Costa for the help in some of the developed research tasks.
- To the colleagues of the Geotechnics group, Professor Francisco Martins and Eng. Nuno Araújo, for their team spirit and friendship.
- The interesting discussions and encouragement of some friends (some of them also researchers): Eduardo Pereira, Vítor Cunha, Luís Neves, Sena Cruz, Dinis Leitão, Carlos Cunha, Joel Oliveira, Alexandre Antunes, Jorge Branco, Pina Henriques, Alberto Ribeiro, Gouveia Pereira and Sandra Ferreira.
- The support and encouragement of many of my long time friends was essential. Fortunately they are too many to mention but they all have an essential importance in my life.
- My mother Filomena, my brother Rui and my sister-in-law Ana for being the most caring and supporting family someone could wish for.
- Marta for the unconditional love, for supporting the long days of work and for everything else which is too much to mention.
- For my father Mário for always being my biggest friend and to whom I dedicate this work.

To all my deepest and sincere thank you this work also belongs to you.



---

# ABSTRACT

---

This work aims to improve the numerical methodologies of geomechanical parameters evaluation in rock masses. In particular, the assessment of strength and deformability parameters in underground structures is addressed. In this task, innovative methodologies were developed and validated using real data from the Venda Nova II hydroelectric scheme.

In an underground work, the geomechanical parameters are continuously evaluated in different stages. Three main levels were defined in which this evaluation has to be carried out. Level 1 is correspondent to the preliminary design stage where the geomechanical parameters values estimation has to be made, in many cases, based on scarce and uncertain information. Level 2 is concerned with the parameters updating when new information about the rock mass is available which can happen in both design and service stages. Level 3 identifies the parameter values used in the constitutive models using observation results from the construction and/or service stages to perform inverse calculations. In each level, a certain amount of data concerning the rock mass is available therefore different approaches were carried out.

In relation to level 1, a large database of geotechnical information was gathered and explored using Data Mining techniques. The goal was to develop simple and reliable models for the geomechanical characterisation in order to be used mainly in the preliminary project stages.

In what concerns level 2, a consistent and mathematically valid framework was developed, based on Bayesian probabilities, which is particularly suited to deal with the quantification of uncertainty. The application to real data from *in situ* tests performed by LNEC in the scope of the Venda Nova II project allowed validating the developed methodologies.

In the scope of level 3, different classical and new optimisation algorithms were investigated in the scope of underground works back analysis. Besides, an innovative algorithm - an evolution strategy - was used together with a 3D model of the powerhouse caverns of the Venda Nova II complex for the back analysis of the deformability modulus and *in situ* stress state. The results were compared with the solution provided by an optimisation software based on traditional algorithms.



---

## RESUMO

---

Este trabalho pretende contribuir para melhorar as metodologias numéricas de avaliação de parâmetros geomecânicos em maciços rochosos. Em particular, é abordada a problemática do cálculo de parâmetros de resistência e deformabilidade em obras subterrâneas. Para levar a cabo esta tarefa foram desenvolvidas metodologias inovadoras que foram posteriormente validadas utilizando dados reais do complexo hidroeléctrico da Venda Nova II.

Numa obra subterrânea os parâmetros geomecânicos são continuamente avaliados em diferentes fases. Assim, foram definidos três níveis principais, nos quais esta avaliação deve ser executada. O nível 1 é correspondente à fase preliminar do projecto onde a estimativa dos parâmetros geomecânicos é executada, em muitos casos, baseada em informação escassa afectada por um elevado nível de incerteza. O nível 2 está relacionado com a actualização do valor dos parâmetros quando estão disponíveis novos dados relativos ao maciço rochoso o que pode acontecer durante a fase de projecto de execução e/ou serviço. O nível 3 identifica os valores dos parâmetros utilizados nos modelos constitutivos utilizando resultados de observação provenientes das fases de construção e/ou serviço. Em cada nível existe uma determinada quantidade de dados relativos ao maciço rochoso tendo-se, por isso, levado a cabo diferentes abordagens.

Relativamente ao nível 1 foi reunida uma grande base de dados de informação geotécnica que foi explorada e analisada utilizando técnicas de *Data Mining*. O objectivo foi desenvolver modelos simples e fiáveis para o cálculo dos parâmetros geomecânicos de forma a possibilitar a sua utilização principalmente na fase preliminar do projecto.

No que concerne ao nível 2 procedeu-se ao desenvolvimento de uma metodologia consistente e matematicamente válida, baseada em probabilidades *Bayesianas*, que é particularmente apropriada para lidar com a quantificação da incerteza relativamente ao valor dos parâmetros. A metodologia desenvolvida foi validada pela sua aplicação a dados resultantes de medições de campo efectuadas pelo LNEC no âmbito do projecto da Venda Nova II.

No âmbito do nível 3 foram testados diferentes técnicas de retroanálise em obras subterrâneas. Foi também utilizado um algoritmo inovador (estratégia evolutiva) em conjunto com um modelo 3D das cavernas principais do complexo da Venda Nova II, para a identificação do módulo de deformabilidade do maciço rochoso e do estado de tensão. Os resultados foram comparados com a solução obtida utilizando um programa de optimização baseado em algoritmos tradicionais.



---

# RESUMÉ

---

Ce travail représente une contribution à l'amélioration des méthodologies numériques d'évaluation de paramètres géomecaniques dans les massifs rocheux. La problématique du calcul de paramètres de résistance et de déformabilité dans les ouvrages souterrains est abordée. Des méthodologies innovantes, validées en utilisant des données réelles du complexe hydro-électrique Venda Nova II, ont été développées.

Dans un ouvrage souterrain, les paramètres géomécaniques sont évalués lors des différentes phases. Ainsi, trois niveaux ont été définis dans lesquels cette évaluation doit être exécutée. Le niveau 1 correspond à la phase préliminaire du projet où l'estimation des paramètres géomécaniques est, dans de nombreux cas, basée sur des informations insuffisantes affectées d'un niveau élevé d'incertitude. Le niveau 2 est rapporté à la mise à jour de la valeur des paramètres lié au fait que de nouvelles données relatives au massif rocheux sont disponibles qui peut être dans la phase du projet et dans la phase de service. Le niveau 3 identifie les valeurs des paramètres à utiliser dans les modèles constitutifs utilisant les résultats de l'observation dans la phase de construction et la phase de service. Pour chaque niveau, il existe des données relatives au massif rocheux, différentes approches ont donc été mises en oeuvre.

Relativement a le niveau 1, une base de données d'informations géotechniques a été collectée et analysée en utilisant une technique de *Data Mining*. L'objectif étant de développer des modèles simples et fiables pour le calcul des paramètres géomécaniques utilisables principalement dans la phase préliminaire du projet.

Dans le contexte du niveau 2, on a été développée une méthodologie basée sur des probabilités *Bayésiennes*, qui sont particulièrement appropriées au traitement de la quantification de l'incertitude relative à la valeur des paramètres. La méthodologie développée a été validée par application à des données réelles relatives à des essais *in situ* réalisés par le LNEC dans le contexte du projet Venda Nova II.

Pour le niveau 3, ont été expérimentés différents algorithmes d'optimisation. En outre, une stratégie évolutive a été utilisé conjointement avec un modèle numérique 3D des cavernes principales du complexe de Venda Nova II, pour l'identification du module de déformabilité du massif rocheux et de l'état de contraintes. Les résultats ont été comparés avec la solution obtenue en utilisant un programme d'optimisation basé sur des algorithmes traditionnels.



---

# SYMBOLS

---

## ABBREVIATIONS

---

3D	Three dimensions
AI	Artificial Intelligence
ANN	Artificial Neural Network
$c'$	Effective cohesion
CG	Conjugate gradient optimisation algorithm
CI	Confidence Interval
CRISP-DM	Cross-Industry Standard Process for Data Mining
D	Disturbance factor for the Hoek-Brown strength criterion
DDM	Data-Driven Models
DM	Data Mining
E	Deformability modulus of the rock mass
$E_i$	Elasticity modulus of the intact rock
ES	Evolution Strategy
GA	Genetic Algorithm
GSI	Geological Strength Index
H	Depth
H-B	Hoek-Brown failure criterion
HRMR	Hierarchical Rock Mass Rating
$K_0$	Ratio between the horizontal and vertical effective stresses
KDD	Knowledge Discovery in Databases
LFJ	Large Flat Jack test
LNEC	Portuguese National Laboratory of Civil Engineering
MAD	Mean Absolute Deviation
MCMC	Markov Chain Monte Carlo
MSE	Mean Squared Error
PLT	Plate Load Test
Q	Q-system index
$Q_{TBM}$	Variant of the Q-index for the TBM tunnelling behaviour prediction

## ABBREVIATIONS

---

QN	Quasi-Newton optimisation algorithm
$R^2$	Determination coefficient
RQD	Rock Quality Designation
RMSE	Root Sum Squared Error
RMR	Rock Mass Rating
RST	Random Set Theory
SEMMA	Sample, Explore, Modify, Model, and Assess
SD	Steepest Descent optimisation algorithm
SFJ	Small Flat Jack test
SSE	Sum Squared Error
STT	Strain Tensor Tube test
TBM	Tunnel Boring Machine

## GREEK LETTERS

---

$\epsilon_1$	First stopping criterium for the evolution strategy algorithm
$\epsilon_2$	Second stopping criterium for the evolution strategy algorithm
$\phi'$	Effective friction angle
$\gamma$	Volumic weight
$\mu$	Mean
$\nu$	Poisson coefficient
$\sigma$	Standard deviation
$\sigma^2$	Variance
$\sigma_c$	Unconfined compressive strength of the intact rock
$\sigma_h$	Horizontal effective stress



---

# CONTENTS

---

<b>CHAPTER 1 – Introduction</b>	<b>1</b>
1.1 Background . . . . .	1
1.2 Approach and scope of the work . . . . .	2
1.3 Outline of the thesis . . . . .	5
<b>CHAPTER 2 – Methodologies for Geomechanical Parameters Evaluation in Rock Masses</b>	<b>7</b>
2.1 Introduction . . . . .	7
2.2 Laboratory and <i>in situ</i> tests in rock mechanics . . . . .	12
2.3 Empirical rock mass classification systems . . . . .	20
2.3.1 General . . . . .	20
2.3.2 RMR system . . . . .	22
2.3.3 Q system . . . . .	25
2.3.4 GSI system . . . . .	30
2.3.5 Correlations between parameters and indexes . . . . .	38
2.4 Highly heterogeneous rock masses . . . . .	40
2.5 Conclusions . . . . .	49
<b>CHAPTER 3 – Knowledge Discovery in Databases and Data Mining</b>	<b>51</b>
3.1 Introduction . . . . .	51
3.2 Knowledge Discovery in Databases . . . . .	56
3.3 Data Mining . . . . .	58
3.3.1 Tasks . . . . .	58
3.3.2 Methodologies . . . . .	60
3.3.3 Models and techniques . . . . .	62
Decision trees and rule induction . . . . .	63
Artificial Neural Networks . . . . .	64
Model evaluation . . . . .	69
3.4 Final remarks . . . . .	72

<b>CHAPTER 4 – New Models for Geomechanical Characterisation Obtained Using</b>	
<b>DM Techniques</b>	<b>75</b>
4.1 Introduction . . . . .	75
4.2 Data understanding and preparation . . . . .	78
4.3 Modelling and evaluation . . . . .	85
4.3.1 RMR index . . . . .	88
4.3.2 Q index . . . . .	92
4.3.3 Friction angle ( $\phi'$ ) . . . . .	96
4.3.4 Cohesion ( $c'$ ) . . . . .	102
4.3.5 Deformability modulus (E) . . . . .	107
4.3.6 The Hierarchical Rock Mass Rating (HRMR) . . . . .	110
4.4 Conclusions . . . . .	115
<b>CHAPTER 5 – Updating of Geomechanical Parameters Through Bayesian Prob-</b>	
<b>abilities</b>	<b>119</b>
5.1 Introduction . . . . .	119
5.2 Bayesian Methods . . . . .	122
5.2.1 Introduction . . . . .	122
5.2.2 Bayes theorem . . . . .	124
5.2.3 Choice of a prior . . . . .	126
5.2.4 Bayesian inference . . . . .	128
Normal data with unknown mean ( $\mu$ ) and known variance ( $\sigma^2$ ) - the	
Jeffreys prior . . . . .	128
Normal data with unknown mean ( $\mu$ ) and known variance ( $\sigma^2$ ) - the	
conjugate prior . . . . .	129
Normal data with unknown mean ( $\mu$ ) and unknown variance ( $\sigma^2$ ) - the	
Jeffreys prior . . . . .	130
Normal data with unknown mean ( $\mu$ ) and unknown variance ( $\sigma^2$ ) - the	
conjugate prior . . . . .	131
5.2.5 Posterior simulation . . . . .	132
5.3 Application of the Bayesian framework to update E in a rock mass . . . . .	134
5.3.1 Introduction . . . . .	134
5.3.2 Statistical analysis of the data . . . . .	136
5.3.3 Updating of E considering unknown mean ( $\mu$ ) and known variance ( $\sigma^2$ ) .	138
5.3.4 Updating of E considering normal data and unknown mean ( $\mu$ ) and vari-	
ance ( $\sigma^2$ ) . . . . .	143

5.4	Alternative updating methodology using the Weibull distribution . . . . .	148
5.4.1	Introduction . . . . .	148
5.4.2	The Weibull distribution . . . . .	149
5.4.3	The proposed methodology . . . . .	151
5.4.4	Results . . . . .	152
5.5	Conclusions . . . . .	155
<b>CHAPTER 6 – Application of Inverse Methodologies in Underground Structures</b>		<b>159</b>
6.1	Introduction . . . . .	159
6.2	Main components and methods of inverse analysis . . . . .	162
6.3	Use of classical and new optimisation algorithms in inverse analysis applied to underground structures . . . . .	168
6.4	Application of gradient optimisation algorithms to a verification problem . . . .	173
6.4.1	Introduction . . . . .	173
6.4.2	Numerical model . . . . .	173
6.4.3	Used back analysis techniques . . . . .	176
6.4.4	Obtained results . . . . .	178
6.5	Application of Evolution Strategies (ES) to analytical verification problems . . .	189
6.5.1	Introduction . . . . .	189
6.5.2	Evolution Strategies . . . . .	191
6.5.3	Obtained results . . . . .	193
6.6	Conclusions . . . . .	199
<b>CHAPTER 7 – Venda Nova II Powerhouse Complex - Back Analysis of Geomechanical Parameters</b>		<b>203</b>
7.1	Introduction . . . . .	203
7.2	Analysis of geotechnical information along the hydraulic circuit of Venda Nova II	205
7.3	The underground powerhouse complex . . . . .	210
7.4	Numerical modelling . . . . .	214
7.4.1	Description of the developed models . . . . .	214
7.4.2	Analysis of the results . . . . .	216
7.5	Back analysis of geomechanical parameters . . . . .	223
7.5.1	Used optimisation techniques . . . . .	223
7.5.2	Validation studies . . . . .	225
7.5.3	Results . . . . .	227
7.6	Conclusions . . . . .	235

<b>CHAPTER 8 – Conclusions</b>	<b>239</b>
8.1 Summary and main contributions . . . . .	239
8.2 Future developments . . . . .	244
<b>CHAPTER 9 – References</b>	<b>247</b>
<b>ANNEX I – Histograms of the numerical variables used in the DM process</b>	<b>267</b>
<b>ANNEX II – Correction for <math>\phi'</math> and <math>c'</math> due to H and D</b>	<b>279</b>
<b>ANNEX III – Computed stresses and displacements for the 3D model of Venda Nova II</b>	<b>285</b>

---

# LIST OF FIGURES

---

<b>CHAPTER 1 – Introduction</b>	<b>1</b>
1.1 Scheme of a generic methodology for rock mass characterisation. . . . .	3
1.2 Outline and organisation of the thesis. . . . .	5
<b>CHAPTER 2 – Methodologies for Geomechanical Parameters Evaluation in Rock Masses</b>	<b>7</b>
2.1 Approximate involved volumes for different tests. . . . .	13
2.2 Scheme of two methods for the <i>in situ</i> deformability evaluation: a) Plate Load or Jacking test (with two types of possible measurements layout) and b) Goodman Jack test (adapted from Palmstrom and Singh (2001)). . . . .	15
2.3 Scheme of the methodology for rock formations deformability characterisation. .	17
2.4 Scheme of a PLT layout (Sousa <i>et al.</i> , 1990). . . . .	18
2.5 Equipment for sliding test in discontinuities of LNEC . . . . .	19
2.6 3D laser scanner for measuring the topography of joint surface (Fardin <i>et al.</i> , 2001). . . . .	20
2.7 Scheme for the calculation of the RMR index. . . . .	23
2.8 Scheme for the calculation of the Q and $Q_{TBM}$ indexes . . . . .	26
2.9 Relation between $Q_c$ , the velocity of P seismic waves and E (Barton, 2004). . . .	28
2.10 Variation of m with the Q value (Barton, 2004). . . . .	29
2.11 Chart for the GSI estimation. . . . .	31
2.12 Examples of typical flysch: a) thick bedded blocky sandstone and b) sandstone with thin siltstone layers (Marinos and Hoek, 2001). . . . .	41
2.13 GSI chart for heterogeneous rock masses such as flysch (Marinos and Hoek, 2001).	42
2.14 Histogram of the GSI obtained by a probabilistic methodology (Miranda, 2003) .	44
2.15 Survey of heterogeneous granite formations by boreholes (Medley, 1999). . . . .	45
2.16 Mixed face conditions. . . . .	46
2.17 Model used for homogenisation method: ‘a’ is the radius of the inclusion; ‘b’ is radius of the matrix; and ‘c’ is volume fraction (Chammas <i>et al.</i> , 2003). . . . .	49
<b>CHAPTER 3 – Knowledge Discovery in Databases and Data Mining</b>	<b>51</b>
3.1 Modelling in civil engineering. . . . .	53

3.2	Number of journal publications in the DM and in this area related with engineering and geotechnics (source ISI Web of Knowledge) (Cortez, 2007). . . . .	55
3.3	Phases of the KDD process (Fayyad <i>et al.</i> , 1996). . . . .	56
3.4	Classification example with rock mass classification data. . . . .	59
3.5	Stages of the CRISP-DM process (Chapman <i>et al.</i> , 2000) . . . . .	61
3.6	Stages of the SEMMA methodology (Bulkley <i>et al.</i> , 1999) . . . . .	62
3.7	Example of a decision tree. . . . .	64
3.8	Human neuron. . . . .	65
3.9	Scheme of an artificial neuron configuration. . . . .	66
3.10	Sigmoid activation function. . . . .	66
3.11	Scheme of a multi-layer network. . . . .	67

<b>CHAPTER 4 – New Models for Geomechanical Characterisation Obtained Using DM Techniques</b>		<b>75</b>
4.1	Histogram of the RMR variable. . . . .	79
4.2	Alternative definitions for the deformability of a rock mass. . . . .	83
4.3	Histogram of class frequencies in the database. . . . .	85
4.4	Workflow used for the DM tasks. . . . .	86
4.5	Relative importance of the attributes for the prediction of the RMR variable. . .	88
4.6	Computed versus Predicted RMR values for the regression model with parameters $P_3$ , $P_4$ and $P_6$ . . . . .	90
4.7	Real versus Predicted RMR values for regression model with parameters $P_3$ , $P_4$ and $P_6$ and considering the transformation of RMR. . . . .	91
4.8	Computed versus Predicted Q values for regression models using all attributes (a) without logarithmic transformation and (b) with logarithmic transformation. . .	93
4.9	Relative importance of the attributes for the prediction of the log Q variable. . .	94
4.10	Computed versus Predicted logQ values for regression model with parameters $J_r/J_a$ , SRF and $J_n$ . . . . .	95
4.11	Real versus Predicted log Q values for regression models with (a) parameters $J_r/J_a$ and $J_n$ and (b) parameters $J_r/J_a$ , $J_n$ , $P_3$ , $P_4$ and $P_6$ . . . . .	96
4.12	Relative importance of the attributes for the $\phi'$ prediction. . . . .	97
4.13	Computed versus Predicted $\phi'$ values for regression model with data set 3. . . . .	98
4.14	Real versus Predicted $\phi'$ values for regression model for data set 2. . . . .	99
4.15	Computed versus Predicted $\phi'$ values for regression model with data set 3. . . . .	99
4.16	Relative importance of the RMR weights in the prediction of $\phi'$ . . . . .	100

4.17	Computed versus Predicted $\tan\phi'$ values for regression models with (a) parameters $P_1$ to $P_6$ and (b) parameters $P_1$ , $P_4$ and $P_6$ . . . . .	101
4.18	Computed versus Predicted $\tan\phi'$ values for the correlation with E. . . . .	102
4.19	Computed versus Predicted $c'$ values for regression models which use all attributes (a) without logarithmic transformation and (b) with logarithmic transformation of the target variable. . . . .	103
4.20	Relative importance of the attributes for the $\ln c'$ prediction. . . . .	104
4.21	Computed versus Predicted $c'$ values for regression models for (a) data set 2 and (b) data set 3. . . . .	105
4.22	Relative importance of the RMR classification weights for the $c'$ prediction. . . . .	106
4.23	Computed versus Predicted $c'$ values for regression model with data set 4. . . . .	106
4.24	Computed versus Predicted $\ln E$ values for regression model with the RMR and Q parameters. . . . .	108
4.25	Relative importance of the attributes for the $\ln E$ prediction. . . . .	108
4.26	Computed versus Predicted values for (a) correlation with RMR and (b) correlation with $P_3$ , $P_4$ and $P_6$ . . . . .	109
4.27	The HRMR system. . . . .	112
4.28	Relative importance of the parameters in the HRMR system. . . . .	114
 <b>CHAPTER 5 – Updating of Geomechanical Parameters Through Bayesian Probabilities</b>		<b>119</b>
5.1	The decision cycle (Haas and Einstein, 2002). . . . .	120
5.2	Scheme of the updating process for the deformability modulus during the construction of an underground structure. . . . .	122
5.3	Scheme of the overall updating process (adapted from Faber (2005)). . . . .	125
5.4	Cross-section of the Venda Nova II powerhouse complex caverns. . . . .	135
5.5	Scheme of the performed calculations for the Bayesian updating. . . . .	136
5.6	Histograms of E calculated from the empirical systems application data: (a) raw data (b) logarithmic transformation. . . . .	137
5.7	Histograms of E from the LFJ tests: (a) raw data (b) logarithmic transformation. . . . .	138
5.8	Posterior probability density functions for the mean value of E for both types of distributions using Jeffreys prior. . . . .	139
5.9	Posterior probability density functions for the simulated values of E for the both types of distributions using Jeffreys prior (inferred values for the population). . . . .	140
5.10	Prior and posterior probability density functions for the mean value of E. . . . .	141

5.11	Prior and posterior probability density distributions for E considering the normal distribution (inferred values for the population). . . . .	142
5.12	Posterior probability density distributions for E considering the Jeffreys and conjugate priors. . . . .	143
5.13	Posterior probability density distributions for E for the normal and lognormal case using Jeffreys prior (inferred values for the population). . . . .	144
5.14	Prior and posterior probability density functions for the mean value of E. . . . .	147
5.15	Prior and posterior probability density functions for E (inferred values for the population). . . . .	147
5.16	Posterior probability density functions for E (inferred values for the population). . . . .	148
5.17	Scheme of the alternative Bayesian updating scheme. . . . .	153
5.18	Weibull distributions for the simulated populations. . . . .	154
<b>CHAPTER 6 – Application of Inverse Methodologies in Underground Structures</b>		<b>159</b>
6.1	Scheme of the forward and back analysis (adapted from Sakurai (1997)) . . . . .	160
6.2	Typical topology of a smooth-shaped error function (adapted from Lecampion <i>et al.</i> (2002)) . . . . .	165
6.3	Optimisation of three parameters ( $G_{ref}$ , $\phi'$ and $K_0$ ) in a excavation problem using a GA (Levasseur <i>et al.</i> , 2007). a) Initial population; b) Sixth population; c) Eleventh population; d) Nineteenth population. . . . .	167
6.4	Excavation sequence and field instrumentation of the Estanygento-Sallente powerhouse cavern (Ledesma <i>et al.</i> , 1996). . . . .	169
6.5	Tunnel and field instrumentation layout (Swoboda <i>et al.</i> , 1999). . . . .	170
6.6	Approach to back analysis developed by Sakurai <i>et al.</i> (2003). . . . .	171
6.7	Scheme of the back analysis procedure using gradient optimisation algorithms. . . . .	174
6.8	Adopted models . . . . .	175
6.9	Convergence of the identification process considering two steps for the finite difference calculation for the case of 50%(-) deviation. . . . .	180
6.10	Error function values during the identification process for two different deviations. . . . .	182
6.11	Topology of the error function on the identification of E and $K_0$ of using three measurements. (a) 3D view (b) Plan view. . . . .	183
6.12	Comparison between the algorithms in terms of efficiency. . . . .	185
6.13	Evolution of the error function values during the identification process for the three algorithms. . . . .	186
6.14	Topology of the error function on the identification of $c'$ and $\phi'$ for the case of using two measurements. (a) 3D view (b) Plan view. . . . .	188



6.15	Evolution of the $c'$ and $\phi'$ values during the identification process using the SD algorithm together with different number of available measurements. . . . .	188
6.16	Scheme of the back analysis procedure using the ES algorithm. . . . .	190
6.17	Evolution stages of the $(\mu/\rho + \lambda)$ -ES algorithm (Costa and Oliveira, 2001). . . .	193
6.18	Topology of the error function on the identification of $E$ and $\sigma_H$ for the analytical case in elasticity and using two measurements. (a) 3D view (b) Plan view. . . . .	195
6.19	Topology of the error function on the identification of $c'$ and $\phi'$ for the analytical case in elasto-plasticity (no-yielding) and using two measurements. (a) 3D view (b) Plan view. . . . .	196
6.20	Topology of the error function on the identification of $c'$ and $\phi'$ for the analytical case in elasto-plasticity (with yielding) and using three measurements. (a) 3D view (b) Plan view. . . . .	197
 <b>CHAPTER 7 – Venda Nova II Powerhouse Complex - Back Analysis of Geomechanical Parameters</b>		<b>203</b>
7.1	General perspective of the power reinforcement scheme (adapted from Plasencia (2003)) . . . . .	204
7.2	Scheme of the underground works composing the Venda Nova II complex (adapted from (Lima <i>et al.</i> , 2002)) . . . . .	205
7.3	Geological-geotechnical zones along the hydraulic circuit (adapted from Plasencia (2003)) . . . . .	206
7.4	Histograms of the E values obtained by the dilatometer tests (a) normal distribution (b) lognormal distribution. . . . .	207
7.5	Location and comparison between the results of the SFJ and STT tests. . . . .	208
7.6	Pictures of the powerhouse complex caverns during excavation. . . . .	211
7.7	Powerhouse complex geometry. . . . .	211
7.8	Cross-sections of the monitoring plan. . . . .	213
7.9	Displacements evolution measured by extensometers EF5 and EF11. . . . .	213
7.10	3D mesh developed for the Venda Nova II powerhouse complex. . . . .	215
7.11	Displacement contours for the 3D model in the last excavation stage. . . . .	217
7.12	Displacement contours and vectors for the 2D (upper image) and 3D models . . .	218
7.13	Computed displacements near (a) the wall and (b) arch of the main cavern. . . .	218
7.14	Comparison between computed and measured displacements in the last excavation stage. . . . .	219
7.15	Computed versus real displacements for (a) the 2D and (b) 3D models. . . . .	220
7.16	Absolute error histograms for (a) the 2D and (b) 3D models. . . . .	221

7.17	Computed minimum stresses (negative values translate compression). . . . .	221
7.18	Plastic zones at the last excavation stage. . . . .	222
7.19	Stresses in the fiber sprayed concrete. . . . .	222
7.20	3D visualisation of the shear strain contours for the last non-equilibrium state. .	223
7.21	2D visualisation of the shear strain contours and velocity vectors. . . . .	224
7.22	Topology of the error function on the identification of E and $K_0$ for the validation study using only the displacements measured after the first stage. (a) 3D view (b) Plan view. . . . .	227
7.23	Comparison between the observed measurements and the computed values with the initial and optimised set of parameters obtained by SiDolo in the first identification attempt. (a) Absolute values (b) Error values. . . . .	229
7.24	Comparison between the observed measurements and the computed values with the initial and optimised set of parameters obtained by SiDolo in the second identification attempt. (a) Absolute values (b) Error values. . . . .	230
7.25	Comparison between the observed measurements and the computed values with the initial and optimised set of parameters obtained by the evolution strategy considering $\epsilon_1$ and $\epsilon_2$ equal to $10^{-7}$ . (a) Absolute values (b) Error values. . . . .	231
7.26	Comparison between the observed measurements and the values computed using a) the initial set of parameters and b) the optimised set of parameters. . . . .	232
7.27	Topology of the error function for the plastic model of Venda Nova II powerhouse complex. (a) 3D view (b) Plan view. . . . .	232
7.28	Topology of the error function for the elastic model of Venda Nova II powerhouse complex. (a) 3D view (b) Plan view. . . . .	234
<b>CHAPTER 8 – Conclusions</b>		<b>239</b>
<b>CHAPTER 9 – References</b>		<b>247</b>
<b>ANNEX I – Histograms of the numerical variables used in the DM process</b>		<b>267</b>
<b>ANNEX II – Correction for <math>\phi'</math> and <math>c'</math> due to H and D</b>		<b>279</b>
II.1	Variation of $\phi'$ with a) D and b) H. . . . .	280
II.2	Variation of $c'$ with a) D and b) H. . . . .	280
II.3	Correction factor chart for $\phi'$ concerning D . . . . .	281
II.4	Correction factor chart for $\phi'$ concerning H . . . . .	282
II.5	Correction factor chart for $c'$ concerning D . . . . .	283
II.6	Correction factor chart for $c'$ concerning H . . . . .	283

---

**ANNEX III – Computed stresses and displacements for the 3D model of Venda**

<b>Nova II</b>	<b>285</b>
III.1 Adopted mesh for the 3D model of the Venda Nova II powerhouse complex . . .	285
III.2 Total displacements for cross-section 1. . . . .	286
III.3 Minimum stresses for cross-section 1. . . . .	287
III.4 Maximum stresses for cross-section 1. . . . .	288
III.5 Total displacements for cross-section 2. . . . .	289
III.6 Minimum stresses for cross-section 2. . . . .	290
III.7 Maximum stresses for cross-section 2. . . . .	291



---

# LIST OF TABLES

---

CHAPTER 1 – <b>Introduction</b>	1
CHAPTER 2 – <b>Methodologies for Geomechanical Parameters Evaluation in Rock Masses</b>	7
2.1 <i>In situ</i> and laboratory tests for intact rock and rock formation characterisation. . . . .	13
2.2 Dilatometer test <i>versus</i> Plate Load test - advantages and disadvantages. . . . .	15
2.3 Evaluation of large scale tests needs (Sousa <i>et al.</i> , 1990). . . . .	16
2.4 Analytical expressions for the calculation of $E$ based on the RMR value. . . . .	23
2.5 Analytical expressions for the calculation $E$ based on the $Q$ value. . . . .	27
2.6 Analytical expressions for the calculation $E$ based on the GSI value. . . . .	38
CHAPTER 3 – <b>Knowledge Discovery in Databases and Data Mining</b>	51
3.1 Confusion matrix for two classes . . . . .	71
CHAPTER 4 – <b>New Models for Geomechanical Characterisation Obtained Using DM Techniques</b>	75
4.1 Initial attributes of the database . . . . .	78
4.2 Expressions used for the calculation of $E$ . . . . .	82
4.3 Comparison between calculated and measured values of $E$ . . . . .	82
4.4 Comparison between the number of times the expressions were calculated with the number of times the result was within the considered interval. . . . .	84
4.5 List of attributes added to the original database. . . . .	84
4.6 Results for the models considering all the attributes and the most important ones for the RMR prediction. . . . .	89
4.7 Results for the multiple regression model considering parameters $P_3$ , $P_4$ and $P_6$ and using the transformed form of the target variable. . . . .	91
4.8 Comparison of the main results between the regression models which use RMR and $RMR^2$ as target variables . . . . .	92
4.9 Results for the models considering all the attributes and the most important ones for the $Q$ coefficient. . . . .	93
4.10 Results for the models considering the $J_r/J_a$ , $J_n$ and $J_r/J_a$ , $J_n$ , $P_3$ , $P_4$ , $P_6$ attributes. . . . .	95

4.11	Results for the models using the different data sets for $\phi'$ prediction. . . . .	97
4.12	Results for the models developed for $\tan\phi'$ prediction. . . . .	101
4.13	Results for the models using the different data sets for $c'$ prediction. . . . .	104
4.14	Results for the models which use the RMR and Q coefficients. . . . .	107
4.15	Results for the models which use the RMR and only some few parameter. . . . .	109
4.16	Performance measures for the HRMR system. . . . .	113
 <b>CHAPTER 5 – Updating of Geomechanical Parameters Through Bayesian Prob-</b>		
	<b>abilities</b>	<b>119</b>
5.1	Distribution parameters for the initial values of E (GPa). . . . .	136
5.2	Distribution parameters for the values of E obtained by the LFJ tests (GPa). . .	137
5.3	Posterior estimates of the mean value of E considering Jeffreys prior (GPa). . . .	139
5.4	Prior and posterior estimates of the mean value of E considering the conjugate prior (GPa). . . . .	141
5.5	Posterior distributions considering Jeffreys prior . . . . .	143
5.6	Posterior estimates of the mean value of E (GPa) . . . . .	144
5.7	Prior and posterior distributions considering the conjugate prior. . . . .	145
5.8	Prior and posterior estimates of the mean value of E (normal distribution) (GPa). .	146
5.9	Prior and posterior estimates of the mean value of E (lognormal distribution) (GPa). . . . .	146
5.10	Mean and standard deviation of the Weibull parameters and determination co- efficient from the Weibull analysis fitting (GPa). . . . .	154
5.11	Parameters of the Weibull fit for the simulated population values (GPa). . . . .	154
5.12	E values for different reliability levels (GPa). . . . .	155
 <b>CHAPTER 6 – Application of Inverse Methodologies in Underground Structures</b>		<b>159</b>
6.1	Computed values for the elastic calculation. . . . .	175
6.2	Computed values for the plastic calculation . . . . .	175
6.3	Results of the identification process of $E$ with two displacement measurements. .	179
6.4	Results of the identification process of E and $K_0$ with two displacement mea- surements. . . . .	180
6.5	Results of the identification process of E and $K_0$ with one horizontal and one vertical displacement measurement. . . . .	181
6.6	Results of the identification process of E and $K_0$ with three and four displacement measurements . . . . .	182

6.7	Results of the identification process of $E$ and $K_0$ with one stress and one displacement measurements using the SD algorithm . . . . .	184
6.8	Results of the identification process of $E$ and $K_0$ with one stress and one displacement measurements using the QN algorithm . . . . .	184
6.9	Results of the identification process of $E$ and $K_0$ with one stress and one displacement measurements using the CG algorithm . . . . .	185
6.10	Results of the identification process of $c'$ and $\phi'$ . . . . .	187
6.11	Characteristics of the verification problems. . . . .	189
6.12	Adopted combinations of measurements and parameters for the evaluation of the ES algorithm in back analysis. . . . .	191
6.13	Results of the identification of $E$ with two measurements in the elastic case. . . . .	194
6.14	Results of the identification of $E$ , $\sigma_H$ and $\nu$ with three measurements in the elastic case . . . . .	195
6.15	Results of the identification of $E$ , $c'$ and $\phi'$ and with two measurements in the elasto-plastic case with no-yielding. . . . .	197
6.16	Results of the identification of $c'$ and $\phi'$ with three measurements in the elasto-plastic case with yielding . . . . .	198
<b>CHAPTER 7 – Venda Nova II Powerhouse Complex - Back Analysis of Geomechanical Parameters</b>		<b>203</b>
7.1	Statistical analysis of $E$ in GPa obtained by the dilatometer tests. . . . .	207
7.2	Statistical analysis of $V_p$ and $V_s$ obtained by the ultrasound tests. . . . .	208
7.3	Statistical analysis of $\sigma_c$ and $E_i$ obtained by the laboratory compression tests . . . . .	209
7.4	Statistical analysis of shear tests on discontinuities results. . . . .	209
7.5	Geological-geotechnical zoning of the rock mass . . . . .	212
7.6	Characteristics of the four main families of discontinuities (Plasencia, 2003). . . . .	212
7.7	Adopted construction stages for the 3D numerical model. . . . .	216
7.8	Mean displacements and errors for situation a) and b). . . . .	219
7.9	Results of the validation studies. . . . .	226
7.10	Results of the identification processes using SiDolo. . . . .	228
7.11	Results of the identification processes using the ES algorithm. . . . .	230
<b>CHAPTER 8 – Conclusions</b>		<b>239</b>
<b>CHAPTER 9 – References</b>		<b>247</b>
<b>ANNEX I – Histograms of the numerical variables used in the DM process</b>		<b>267</b>

ANNEX II – Correction for $\phi'$ and $c'$ due to H and D	279
---	-----

ANNEX III – Computed stresses and displacements for the 3D model of Venda Nova II	285
--	-----



---

# CHAPTER 1

---

## Introduction

### 1.1 Background

The prediction of rock formations behaviour due to changes in the stress/strain field caused by the excavation of an underground structure is a complex issue. The main reason for such complexity is mainly related with the uncertainties concerning the rock mass characterisation. Beyond a certain discontinuities density, the rock mass can be approximated as a continuous medium with average properties. In this case, the behaviour of the rock mass is controlled not only by the properties of the intact rock but also by the discontinuities characteristics (both geometrical and mechanical), groundwater conditions, between others. Also, micro and macro-scale heterogeneities may have a significant impact on their behaviour.

The evaluation of geomechanical parameters is normally carried out by means of laboratory and *in situ* tests. In the specific case of rock formations they can be complemented by indirect methodologies like the empirical rock mass classification systems (Bieniawski, 1989; Hoek *et al.*, 2002; Barton *et al.*, 1974). The advantages and limitations of each methodology are well known. In the case of laboratory tests the stress/strain distribution and boundary conditions are well defined. However, there are difficulties on obtaining undisturbed samples. Besides, these type of tests raise representativeness issues related to the sample size compared with the formation which is necessary to reproduce. In the case of *in situ* tests, these drawbacks are reduced, but, in the other hand, the stress/strain distribution, is not well known. The empirical methods application is relatively simple and straightforward and their use is widespread. Nevertheless, they present several limitations mostly related to their empirical base.

Recently, developments on both testing equipments and instruments were achieved allowing a more thorough characterisation of the geotechnical materials behaviour. For instance, deformability characteristics can now be assessed in laboratory for very small strain levels interesting the serviceability of the geotechnical structures (Gomes Correia *et al.*, 2004). The

empirical systems were also object of several updates and improvements during the years. However, the potentialities of the available numerical tools have exceeded the capability of accurately characterise the geotechnical materials.

Ground properties behaviour can, nowadays, be numerically translated by a wide range of constitutive models ranging from the simple elastic isotropic to complex coupled and multiscale ones. Pre and post failure behaviour, dilation, damage, creep and strain-hardening/softening are only some of the aspects covered by currently available constitutive models. However, there are high uncertainties related to the evaluation of strength and deformability properties even for the simplest ones (Einstein, 2006). This fact hinders the definition of a standard methodology to obtain characteristic values for these properties. Concerning this subject, Eurocode 7 (Eurocode, 2004) is very general and only provides guidelines. It establishes that the choice of characteristic values for the properties of soils and rocks should be supported by the results of laboratory and *in situ* tests. It also mentions that the determination of characteristic values should also be based in experience (engineering judgment) and to the project inherent risk. Concluding, this code establish that the characteristic value of a property should be understood as a cautious estimate of the mean value that the property can assume. In this context, the definition of design parameters, even though these guidelines, is still a subjective and user-dependent exercise involving a great deal of uncertainties.

## 1.2 Approach and scope of the work

The goal of this work is to improve the way strength and deformability parameters are obtained in the several phases of an underground work project and considering different levels of available geotechnical data.

Figure 1.1 presents a generic methodology for the rock mass characterisation normally used in large geotechnical projects. It starts with a preliminary research based on geological data and some tests in order to define an initial geotechnical model which is used to support the decision about location, orientation and other generic issues. Afterwards, a more thorough characterisation is carried out and the previous results can be updated with this new data to form a geotechnical model of the interested formations. These updated parameters are used in numerical modelling and geotechnical design. During construction, stresses and displacements can be monitored. This observational data can be used to re-evaluate the established geotechnical model by back analysis. In this overall methodology, geomechanical parameters have to be assessed in three levels considering completely different conditions of available geotechnical data, i.e. knowledge about the rock mass. In the next items, a succinct outline of the problem in each level and the research approach are presented.

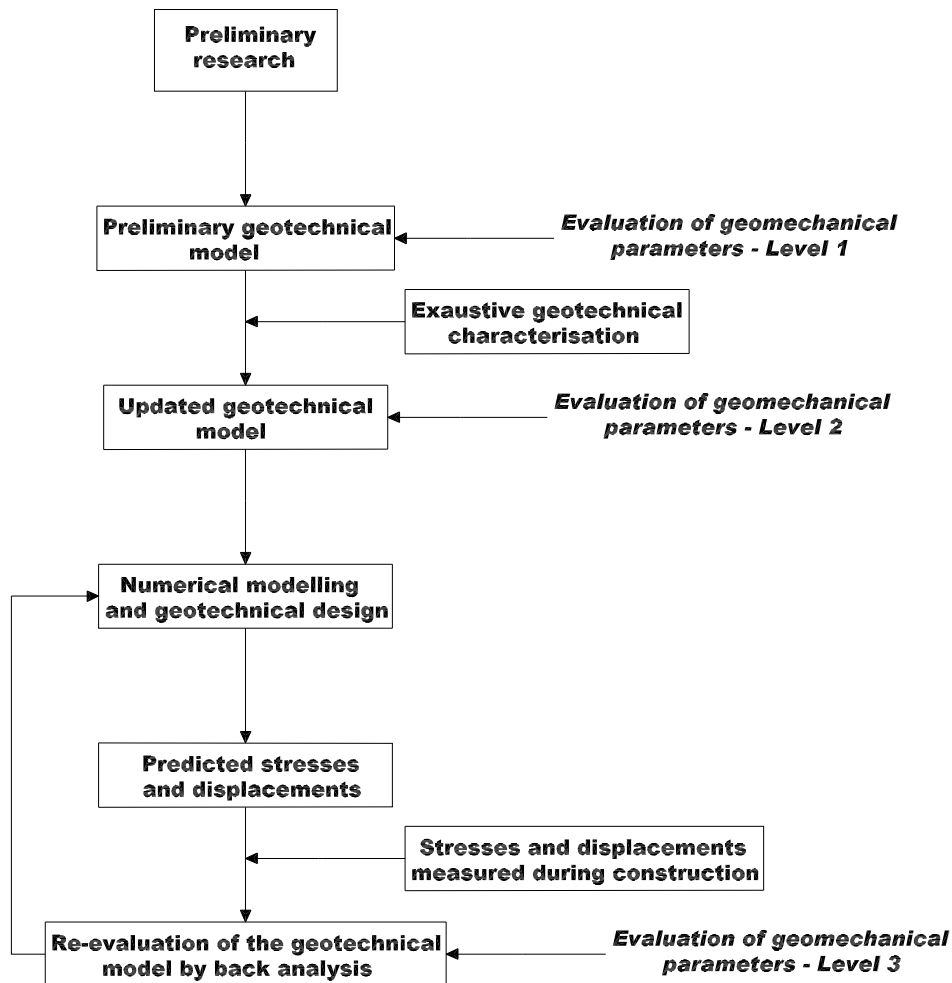


*Figure 1.1:* Scheme of a generic methodology for rock mass characterisation.

- *Level 1:* The number and type of tests performed in geotechnical site investigation is related with the importance of the work, the inherent risk and budget issues. In small projects, normally, only a few or even no tests are carried out and the parameters are set based on local experience and conservative engineering judgment. However, in large geotechnical projects, a great amount of data is produced and used to establish near-homogeneous geotechnical zones. This information could be important not only for the analysed project but to smaller ones where only scarce geotechnical information is available. Currently, this data is analysed using simple statistical tools which can not take full advantage of the knowledge that can be embedded in such databases. Nowadays, there are automatic tools, from the fields of artificial intelligence and pattern recognition for instance, which allow to have a deeper understanding of large and complex databases exploring and discovering potential embedded knowledge (Hand *et al.*, 2001). In the ini-

tial project stages information is scarce to allow defining an accurate geotechnical model. In this context, it is intended to gather a large database of geotechnical data and use these innovative tools to analyse and induce new and useful knowledge. The main goal is to develop new, simple and reliable models to predict geomechanical parameters values mainly in the initial stages of design.

- *Level 2*: The collection of geomechanical information is a complex and dynamic process. In large geotechnical projects, several geotechnical survey campaigns can be carried out in different project stages. This way, as new information is available, it is necessary to update the geotechnical model. However, this is not a straightforward process since tests have different characteristics and reliability levels. Once more, this is a process based on judgment and experience. It lacks a systematic and mathematically valid process, which considers also the important contribution of experience, to deal with this problem and use new information to update the model parameters in a process to reduce uncertainties. It is believed that this problem can be treated within the scope of Bayesian (subjective) probabilities (Bernardo and Smith, 2004). In this context, it is intended to develop a generic Bayesian framework that allows geomechanical parameters to be updated in a proper mathematical sense and apply it to a real case.
- *Level 3*: The observation of the geotechnical structures real behaviour during construction, namely by monitoring stresses and displacements, allow to update the geomechanical parameters to values closer, in mean terms, to the real ones (Gioda, 1980; Ledesma *et al.*, 1996). In this process, called back analysis, the parameters of the geotechnical model are adjusted in order to match, under a certain tolerance, the monitored and predicted measures. Many times, this process is carried out by means of ‘hand adjustment’ or using a method that searches within all (or almost) the parameters space. These methods can be very time-consuming (specially when complex computational models are used) and the best set of parameters may not be reached. Mathematical tools from the classical optimisation field are available to perform this task. Recently, new algorithms based on artificial intelligence, in particular evolutionary computation (like genetic algorithms and evolution strategies), have appeared as a good alternative surpassing some limitations of the previously mentioned techniques (Holland, 1975; Rechenberg, 1994; Schefel, 1995; Costa, 2007). In this sense, it is important to better characterise the application domain of these techniques (advantages, drawbacks and application limits) for the case of geomechanical parameters identification. It is intended to carry out this task using verification problems of a tunnel excavation. Afterwards, the innovative algorithm based on evolution strategies will be applied to a real case study.

Concluding, the idea for this thesis was not to concentrate the research effort on a small topic but to enhance the geomechanical parameter evaluation in different stages using innovative numerical methodologies. This motivated a broader treatment of the subject and the development of several research topics that deserved to be addressed. It can be understood that the complete solution to all of these issues is not achieved but relevant and original contributions were accomplished and many basis for future research were established.

All the data used in this thesis was gathered from the Venda Nova II hydroelectric scheme courtesy of EDP (Electricity of Portugal) company. This large underground project is composed by important underground works built in a predominantly granitic rock mass. This data provided the basis for the developed methodologies and their posterior application and validation.

### 1.3 Outline of the thesis

The present thesis is composed by eight chapters organised as schematised in Figure 1.2.

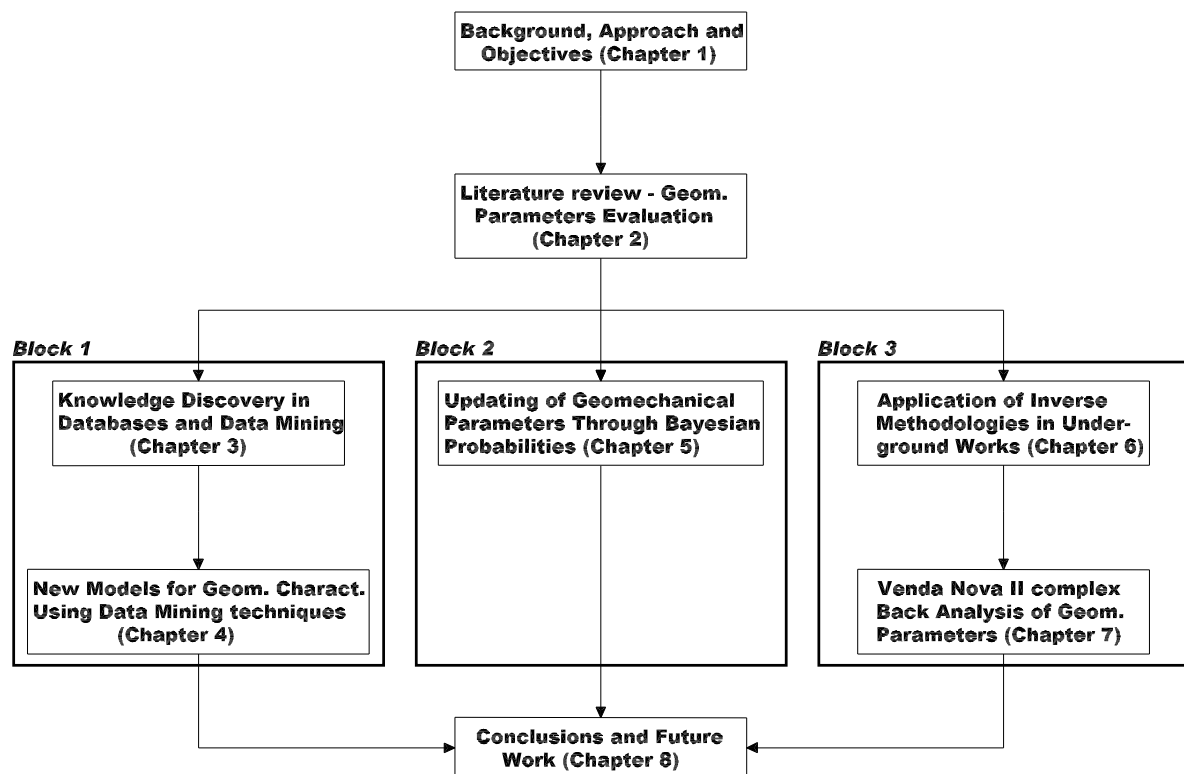


Figure 1.2: Outline and organisation of the thesis.

Following this introduction, part of Chapter 1, a comprehensive literature review on the subject of strength and deformability parameters determination in rock masses is presented in Chapter 2. The current state-of-the-art regarding this subject is presented with special emphasis to the advanced methodologies and highly heterogeneous rock masses characterisation.

The work developed after this Chapter falls into three different blocks of chapters and form the backbone of the thesis. Each block addresses one of the issues raised in the previous section. This approach allows treating the different problems independently in order to reach an acceptable solution for each one of them with an integrated view. Every block starts with an outline of the problem being addressed and a concise state-of-the-art. Because of the innovative aspects of some of the used techniques their main issues are described.

Block 1 is composed by Chapters 3 and 4. The first is related with recent techniques concerning the exploration of knowledge embedded in large and complex databases commonly known as Knowledge Discovery in Databases and Data Mining. The main tasks, methods, models and techniques are presented and explained. In the last, a case study is developed and presented. A large database of geotechnical information was gathered and organised. This database was then explored using the mentioned techniques in order to develop new alternative methods to obtain geomechanical parameters in the early stages of design.

Block 2 is composed only by Chapter 5 where the fundamentals of Bayesian probabilities are presented. Issues like Bayes' theorem, the choice of proper prior distributions and Bayesian inference are explained. Bayesian frameworks are developed for the updating of the geomechanical parameters considering different levels of uncertainties. An application of these frameworks is carried out considering the updating of the deformability modulus in an underground work.

Chapters 6 and 7 form the last block. Chapter 6 concerns the main components and methods of back analysis in geotechnical problems. Classical and new optimisation algorithms are presented and applied in verification problems considering different circumstances in order to check their performance. In Chapter 7 the Venda Nova II underground project is described. Numerical models for the powerhouse complex are developed in 2D and 3D. Its structural behaviour is analysed and compared with the observed data. Finally, a new optimisation algorithm based on evolution strategies is used to back analyse geomechanical parameters considering the observed behaviour of the structure, in terms of displacements, in the different construction stages. Its performance is compared with an optimisation software based on classical algorithms.

Finally, conclusions from the conducted research are drawn in Chapter 8 and some recommendations for future work are outlined. It is believed that the original contributions and innovative aspects of this thesis are a step forward in the subject of geomechanical parameters evaluation intending to be a contribution to a closed form solution for the problem.

# Methodologies for Geomechanical Parameters Evaluation in Rock Masses

## 2.1 Introduction

Due to the natural variability of the rock formations, the geotechnical properties evaluation is one of the issues with largest uncertainty degree. This fact is a consequence of the complex geological processes involved and to the inherent difficulties of geomechanical characterisation.

In the last years, the evaluation of geomechanical parameters, in both rock and soil formations, has gone through some changes and developments which are due to several factors.

- New instruments and equipments for *in situ* and laboratory tests which allow a higher accuracy in the evaluation of both materials and formations behaviour.
- The improvement of the empirical rock mass classification systems and geomechanical parameters quantification.
- The development of more powerful numerical tools which allow performing backanalysis in complex models.
- Improvement of the monitoring techniques providing higher accuracy in the observed measurements.
- New probabilistic methodologies for rock mass characterisation.
- Development of innovative tools based on Artificial Intelligence (AI) techniques for decision support.

In the case of rock formations, the calculation of the geomechanical parameters is mainly carried out through *in situ* and laboratory tests and also by the application of empirical methodologies such as the RMR (Bieniawski, 1989), GSI (Hoek *et al.*, 2002) and Q (Barton *et al.*, 1974) systems.

Rock formations may present discontinuous, heterogeneous and anisotropic characteristics. This way, *in situ* tests for the evaluation of geomechanical parameters are, in large scale, influenced by the tested volumes. The rock masses may only be considered homogeneous at a large scale, therefore, it might not be economically sustainable to perform tests in a significant volume. However, insufficient test volumes may cause scale effects, namely at the strength level, and higher dispersion in the deformability results (Cunha and Muralha, 1990).

The *in situ* tests for the deformability characterisation, like the Large Flat Jack (LFJ) test, are normally carried out by applying a load in a certain way and measuring the correspondent deformations in the rock mass. The tests for the strength characterisation are yet not fully satisfactory and are normally materialised through shear or sliding tests in low strength surfaces (Rocha, 1971). However, these tests are time consuming and expensive and the strength parameters determination is normally carried out indirectly by means of the Hoek and Brown (1980) strength criteria (H-B) associated with the GSI. Even though the limitations of this approach, it has been extensively used in projects developed in rock masses and have been through several changes and updates. For instance, Hoek *et al.* (2002) presented an important update of the criterion expressions and introduced a disturbance factor (D) to account with degradation due to blasting and stress relaxation. Douglas (2002) presented new expressions in order to contemplate rock types and formations for which the initial criterion did not present a satisfactory performance.

Laboratory tests interest a relatively small rock volume and, consequently, it is necessary to perform a considerable number of tests in both the rock material and discontinuities surfaces, in order to contemplate the variability in the obtained geomechanical parameters. Laboratory tests like the determination of the uniaxial compressive strength, the point-load and sliding of discontinuities tests are also very important for the empirical classification systems application. In the cases where the rock masses present time-dependent properties, namely due to creep and expansibility phenomena, more specific laboratory and *in situ* tests are necessary (Rocha, 1971; Wyllie, 1992).

As it was referred, the preliminary calculation of the geomechanical parameters can be carried out also using the empirical classification systems. These systems consider, between others, properties like: the strength of the rock, density, condition and orientation of the discontinuities, groundwater conditions and the stress state. To the evaluated properties a numerical measure is given and, subsequently, a final geomechanical index is obtained by the



application of a numerical expression associated with the system. The result allows classifying the rock mass in a certain class which is associated to important information for design like construction sequences, support needs and geomechanical parameters.

The most widely used systems are the RMR, Q and GSI. The last one can not be formally considered a classification system since it was developed mainly to the calculation of the H-B failure criterion strength parameters. However, because of its simple application characteristics, normally it is used as a classification system as well. For the deformability evaluation there are several analytical solutions relating the deformability modulus (E) with geomechanical coefficients. These expressions should always be used considering their application limits. As it was already referred, the determination of strength parameters is normally carried out using the H-B and the Mohr-Coulomb criteria based on the results of the GSI application.

The development of the  $Q_{TBM}$  system (Barton, 2000), starting from the Q system, allows the prediction of several parameters related to the excavation in TBM tunnels, and also constitutes an important development for the characterisation of geomechanical parameters. It is also worth mentioning also the development of a new empirical system specially for the characterisation of volcanic rocks (Menezes *et al.*, 2007).

In highly heterogeneous rock formations the geomechanical characterisation becomes more complex. The deterministic definition of the parameters and zoning are very difficult or even impossible tasks. In this context, alternative characterisation methodologies have been proposed that combine, in different ways, probabilistic tools, *in situ* and laboratory tests, numerical methods, application of the empirical systems and monitoring data.

The monitoring of the structures allows, among other things, the validation and calibration of the geotechnical models. This is a main issue for understanding the mechanisms that rule the formations and the geotechnical structures behaviour. Through the comparison between predicted and observed measurements, the assumed hypotheses and the geomechanical model reliability can be assessed. In this particular aspect, back analysis techniques are important for they allow, through formally appropriate mathematical techniques, to obtain the model parameters based in the real behaviour of the structure. This information can then be used to update the geotechnical model reducing the uncertainties.

In the design and construction of underground structures, experience plays an important role. The fundamental reason lies in the difficulty of gathering enough geological-geotechnical information to correctly evaluate the geomechanical behaviour of the rock mass. Therefore, there are indubitable advantages in congregating the experience and knowledge of one or several specialists in a specific field of knowledge. New tools of computer sciences, namely those based on AI, can play an important role in the generation of calculation means that make possible the inclusion of that experience and knowledge (Russell and Norvig, 1995).

Specialised knowledge can be easily implemented once it possesses a very well established area of application and a context of concepts and rules to be applied for the resolution of a specific problem. One of the branches of AI are the expert systems that began to be developed in the 80's. Starting from a properly structured and validated knowledge base, they develop processes of reasoning simulation to present recommendations seeking the resolution to a given problem. These systems are normally used for decision support in a limited domain of knowledge.

In the 90's the trend shifted to the development of intelligent systems that learn from the data or use hybrid approaches. There are several techniques in the AI field. Artificial neural networks (ANN), genetic algorithms (GA) and evolutive strategies (ES), support vector machines are only some examples. Methodologies of Knowledge Discovery in Databases (KDD) or Data Mining (DM), in the scope of intelligent systems development, use different AI techniques together with tools from statistics, machine learning, pattern recognition, between others. Some of these techniques and methodologies are used in this thesis and will be described more thoroughly in the next chapters.

The necessary input parameters for the development of numerical models are generally imprecise. The high uncertainty degree associated with the determination of these parameters may lead to erroneous results if their values are treated as deterministic. Rock properties values used for design purposes are affected by several sources of uncertainties (Popescu *et al.*, 2005).

- Inherent random heterogeneity or spatial variability.
- Measurement errors.
- Statistical errors, for instance, due to small sample sizes.
- Uncertainty in transforming the test results in proper geomechanical properties.

There is no agreement about what method should be used to account with these uncertainties, in particular for geotechnical problems where usually information is scarce and may contain high uncertainty levels. Currently, there are many techniques to deal with uncertainty in the scope of reliability analysis. Some of these techniques are: probability and random set theories, fuzzy sets and stochastic analysis. Some of them can be used together forming hybrid methodologies to solve a specific problem.

Advanced probabilistic approaches to safety and reliability are common nowadays and started to be already used into practical applications and code making (Rackwitz, 2000). Probability theory has been extensively and successfully used in reliability analysis and is the most used technique to deal with uncertainties. In opposition to the traditional frequentist probability view, it is also possible to use subjective probability methodologies. Using Bayes theorem

and considering suitable assumptions on uncertainties statistics, it is possible to combine different sources of information like the opinion from experts and results from *in situ* tests.

Random Set Theory (RST), even though providing a poorer model than in the probabilistic approach, provides an appropriate framework to deal with uncertainty specially in the cases, as it happens often in rock mechanics, when information about the geomechanical properties is not point-valued but varies within a certain range. In these cases RST allows to calculate (Tonon *et al.*, 2000): upper and lower bound of the probability of occurrence of a certain outcome; and for a fixed value of probability, the interval of values of a given rock mass parameter.

Information regarding a rock mass is affected by "dissonance" and "non-specificity" or "imprecision" which are sub-classes of "ambiguity". RST allows treating the problem of "ambiguity" as opposed to "vagueness" which is properly formalised by the concept of fuzzy set. The theory of fuzzy sets, also known as possibility calculations, is an alternative to model uncertainties and provide conservative bounds for probability. Fuzzy sets allow to compute the membership function of a certain system from the membership functions of the uncertain variables (Peschl and Schweiger, 2003).

A realistic consideration is that the strength and deformability parameters distribution within a rock or soil formation is random. These random heterogeneities can be modelled probabilistically using stochastic field theory. Geomechanical properties are considered as homogeneous non-Gaussian (since they can not assume negative values) random fields and the Monte Carlo method is used for the stochastic analysis.

The random fields approach starts with the generation of several random fields based on: i) the probabilistic distributions assumed for the parameters; ii) the correlation length concerning the distance for which there are significant differences in the material properties; iii) the cross-correlation between the parameters. Each generated random field is a possible realisation of the geomechanical properties spatial variation and is deterministically computed using the finite element method. The results of every realisation allows a probabilistic analysis of the formation behaviour.

Fenton and Griffiths (2003) applied this principle to model a spatially varying shear strength soil using elasto-plastic finite element analysis to evaluate the effect of spatial variability and cross-correlation between cohesion ( $c'$ ) and friction angle ( $\phi'$ ) in bearing capacity. Cohesion was assumed a lognormal random variable while  $\phi'$  was assumed to have a bounded normal distribution. The authors concluded that the cross-correlation between the parameters have only minor influence on the stochastic behaviour and that for small variability of the parameters, results tend to the deterministic solution. However, as variability increases, the mean bearing capacity becomes significantly lower as the failure surface tends to follow the weakest path. This means that inherent spatial variability affects the mechanical behaviour of the formations

in particular in the failure mechanism form. This conclusion highlights the importance of the randomness consideration for proper design and prediction of the real formations behaviour.

In this chapter, the main methodologies for estimating strength and deformability parameters in rock formations are presented. Aspects related with hydromechanics are not addressed and are outside the scope of this thesis. The main *in situ* and laboratory tests are briefly described and contextualised in a broader approach of rock mass characterisation. Even though they are widely known and used, the RMR, Q and GSI empirical systems are presented highlighting the most innovative aspects. Emphasis is given to the GSI system for it is the only one specially developed for an integrated approach of strength and deformability parameters calculation. A section is devoted to the special challenges raised in the characterisation of highly heterogeneous rock masses. Some methodologies to deal with different types of heterogeneities are also described.

## 2.2 Laboratory and *in situ* tests in rock mechanics

The mechanical characterisation of the rock formations can be carried out through *in situ* tests in representative volumes, including the rock material and the main discontinuities, which constitute a reliable source of geomechanical information. However, they are normally expensive, time consuming and also subjected to errors or uncertainties due to *in situ* measurements, blasting damage, test procedure and others that should be taken into account when analysing the results. A good site characterisation together with an indirect method like the use of empirical classification systems should be used in the assessment of the geomechanical parameters design values.

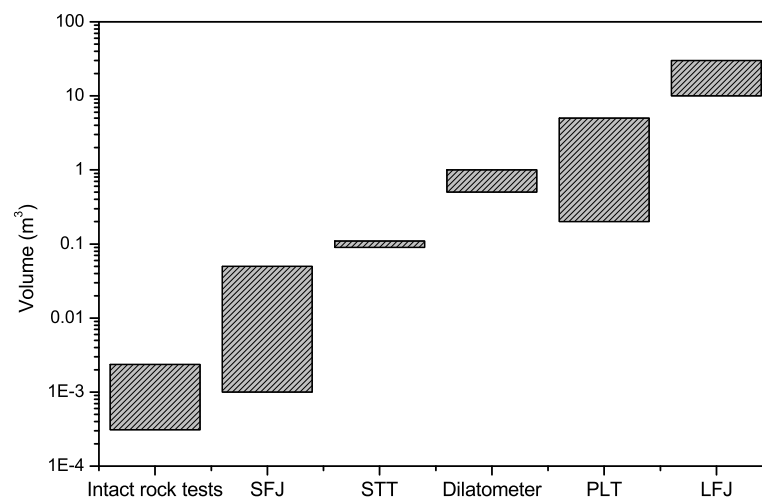
The characterisation can also be indirectly carried out through laboratory tests on discontinuity surfaces and in the intact rock material. The main problems are related with sampling and representativeness of the tests due to the small volume of the samples. This is why it is recommended that their results should always be calibrated by *in situ* tests. In Table 2.1, a summary of the main laboratory and *in situ* tests for the mechanical characterisation of intact rock and rock formations is presented.

In what concerns the evaluation of the deformability parameters, the *in situ* tests can involve small volumes as in the case of the dilatometer, or large volumes, as in case of the LFJ. In Figure 2.1, approximate values of the involved volumes, reporting mainly to the experience of LNEC, are presented for some of the most common tests (Cunha and Muralha, 1990).

The *in situ* tests are performed inside a borehole or inside a gallery or adit excavated for this purpose. In the case of boreholes they normally involve small volumes of rock mass and can be grouped in two main types, depending on the way the pressure is applied to the walls

**Table 2.1:** *In situ* and laboratory tests for intact rock and rock formation characterisation.

<i>In situ</i> tests	
Static tests in boreholes	Load tests
Dilatometer Pressiometer Borehole jacks	Plate Load Test (PLT) Goffi Method
Compression tests	Pressure tests on adits
Uniaxial Triaxial	Chamber pressure method Radial (or Goodman) jack
Tests in opened slots	Dynamic tests
Circular jacks Large Flat Jacks (LFJ) Small Flat Jacks (SFJ) Strain Tensor Tube (STT)	Propagation of seismic waves
Laboratory tests	
Static tests	Dynamic tests
Uniaxial, diametral and point load compression Shear and triaxial Flexural, torsion and uniaxial tension Sliding of discontinuities	Resonance method Ultrasonic pulse method

**Figure 2.1:** Approximate involved volumes for different tests.

of the borehole (Pinto, 1981; Sousa *et al.*, 1990):

- Application of the pressure through a flexible membrane completely adapted to the walls of the hole with a rotational symmetrical pressure. In the case of the dilatometer, radial deformations are measured while for the pressiometer a global volumetric deformation is considered. The last is more often used for soft rocks and present precision limitations

since it measures volumes instead of displacements.

- Application of the pressure through rigid plates in two circumference arches (borehole jacks). They correspond to more complex load situations and, consequently, their interpretation raises larger difficulties.

The tests carried out inside a gallery can involve larger volumes therefore being more representative (Figure 2.2). However, they are more expensive and time consuming. The main *in situ* tests that can be performed inside a gallery are the following:

- Plate Load or Plate Jacking tests - the load is applied by means of a jack and the rock displacements are measured at the surface of the rock or in boreholes behind each loaded area using extensometer anchors.
- Radial (or Goodman) Load tests - a uniform radial pressure is applied in a part of a gallery or inside an NX size borehole and radial deformations are measured by means of two transducers. They have larger precision than the plate tests and are able to evaluate hydromechanical properties and the anisotropy of the rock formation.
- Large Flat Jacks (LFJ) and Small Flat Jacks (SFJ) - the load is applied in the walls of one or more opened slots. The SFJ test has the additional advantage of allowing to evaluate, besides the deformability parameters, stress state components.
- Seismic tests between holes or galleries - allow determining the dynamic modulus measuring the S and P waves velocities. The values of these modulus are different from the static ones due to the differences in time and deformation levels applied to the formation during the test. Depending on the distance between holes or galleries, they involve considerable volumes and can be correlated with the results of static tests.
- Biaxial or triaxial *in situ* tests - rarely used for they involve high costs and have low accuracy.

When the tests are carried out inside a gallery, the results can be very much affected by damage due to blasting. The damage is mainly caused by development of cracks, displacements in joints and changes in the stresses. This effect is particularly important near the surface of the adit where the displacement measures can take place. In this situation, the results of the test are normally conservative estimations of the rock mass modulus. Palmstrom and Singh (2001) stated that when blasting is used to excavate the adit, the measurements should be performed inside a borehole at a minimum depth of 0.5-0.8 m, i.e outside the damaged zone.

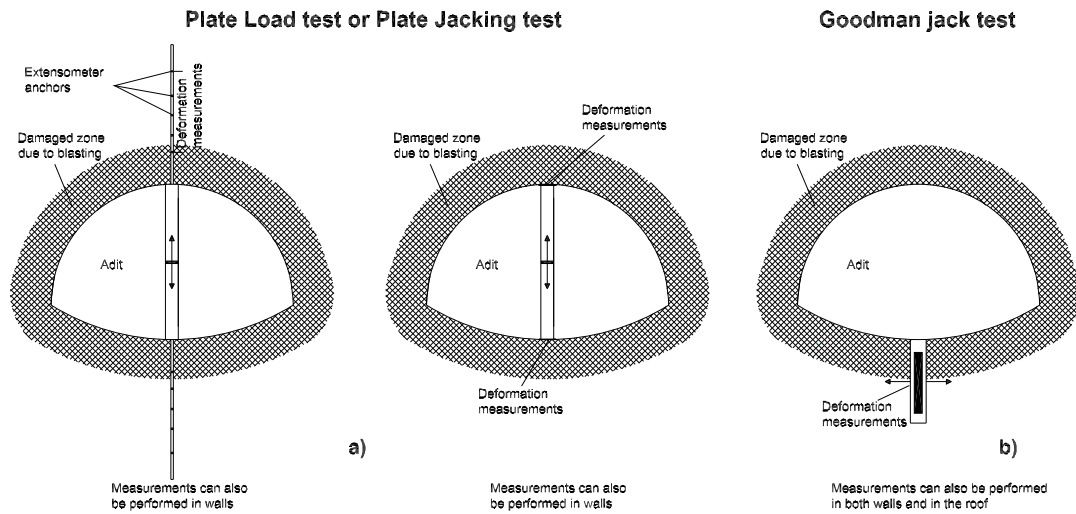


**Figure 2.2:** Scheme of two methods for the *in situ* deformability evaluation: a) Plate Load or Jacking test (with two types of possible measurements layout) and b) Goodman Jack test (adapted from Palmstrom and Singh (2001)).

During the tests the deformation modulus increase with the applied pressure. This is due to closure of cracks and joints of the rock mass during the first loading cycle. This is why this cycle should never be considered when interpreting the results since it can lead to erroneous conclusions.

There are no universal rules to define which tests should be carried out for a given situation since every test presents advantages and drawbacks. A good characterisation plan should rely on engineering experience and the project particular issues. For illustrative purposes, Table 2.2 compares some characteristics of a small scale test (dilatometer) and a large scale test (PLT).

**Table 2.2:** Dilatometer test *versus* Plate Load test - advantages and disadvantages.

<b>Dilatometer test</b>		<b>Plate Load test</b>	
<i>Advantages</i>	<i>Disadvantages</i>	<i>Advantages</i>	<i>Disadvantages</i>
Modulus obtained at considerable distances from the surface	Small volume of rock mass involved	The load can be applied in its real direction	It is slow, expensive and very difficult to materialise the test load
Different geological conditions are examined and fast execution	Only normal measurements to the borehole axis are carried out	Significant volume of rock mass is involved	The load is only applied in one direction

In the cases where the rock masses present high anisotropy levels the tests should be carried

out in order to define the parameters that characterise that anisotropy. This is normally done by computing indexes which relate rock properties (for instance the uniaxial compressive strength, point load strength and longitudinal wave velocity) perpendicular and parallel to planes of anisotropy (Saroglou and Tsiambaos, 2007).

In some types of rock masses the time-dependent behaviour is an important parameter for the prediction of the long-term stability in rock engineering. Creep, relaxation and loading tests at different stress or strain rates can be carried out for rheological experiments (Li and Xia, 2000). These tests are very difficult to be carried out *in situ* therefore, to obtain creep and relaxation laws, normally laboratory tests on intact rock samples are conducted using simple mechanical or servo-controlled testing machines.

To quantify the deformability of the rock masses, the number of *in situ* tests should be rationalised. Typically, a methodology that combines a small number of large scale tests with a larger number of small scale tests is adopted. The methodology can be resumed in three main tasks:

- Zoning of the rock mass considering the available geological information, the type of rock formations and their weathering degree, the main discontinuities and the use of empirical classification systems.
- For each zone, execution of small scale tests, in boreholes and eventually in galleries. They should be in enough number to assure a good characterisation of the rock mass. Their location can be chosen randomly in order to obtain a mean value of the deformability modulus or in zones in which lower values of this parameter are expected.
- For each zone, execution of a small number of large scale tests due to the involved costs. The results should be calibrated with the values obtained with the small scale tests. Depending on the deformability modulus value, it is considered that three different situations exist in what concerns the needs of large scale tests as it is indicated in Table 2.3.
- Individual analysis of the most important faults. Carry out representative tests on the fault filling material.

**Table 2.3:** Evaluation of large scale tests needs (Sousa *et al.*, 1990).

Situation	E (GPa)	Large scale tests
I	$E \geq 10$	Advisable
II	$5 \leq E < 10$	Necessary
III	$0.1 \leq E < 5$	Necessary with high precision



Figure 2.3 presents a scheme of the described methodology for the rock mass characterisation through *in situ* tests.

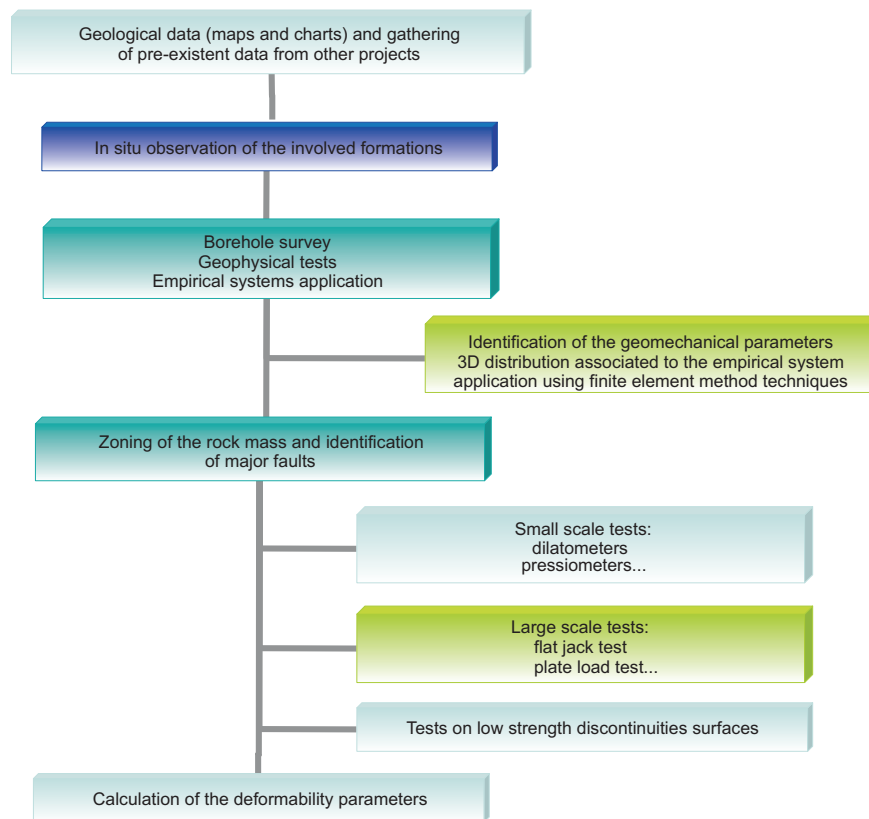


**Figure 2.3:** Scheme of the methodology for rock formations deformability characterisation.

In the deformability characterisation tests, the scale effect is mainly translated by the highest variability in the results of the small scale tests. In order to account with this effect, the number of tests should be enough to compensate this variability.

If the tests are carried out at randomly chosen sites, the obtained values should present the same mean and a standard deviation proportional to the square root of a significant dimension of the tested volume. Figure 2.4 presents the layout of two PLT with 30 and 60 cm diameter in a highly heterogeneous conglomerate rock mass. As it can be seen, the test with larger diameter plate includes a larger volume of rock elements with higher rigidity. This fact implies that the obtained modulus is higher in this case compared with the smaller diameter plate situation. Deformability modulus values of 621 and 896 MPa for the 30 and 60 cm diameter plates, respectively, were obtained (Sousa *et al.*, 1990).

For the determination of the rock masses strength parameters, large scale *in situ* and laboratory tests for the intact rock material and discontinuities can be executed. The main *in situ*

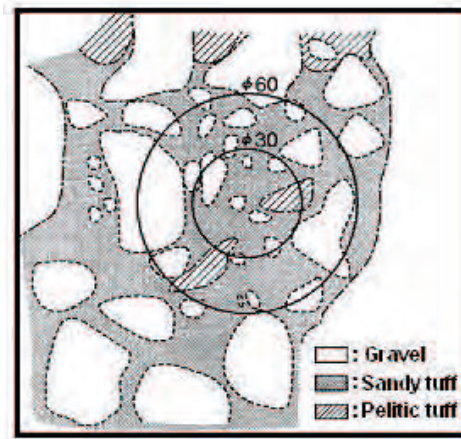


**Figure 2.4:** Scheme of a PLT layout (Sousa *et al.*, 1990).

tests are, normally, sliding or shearing in discontinuities, in the faults filling material and other low strength surfaces and in the rock mass/structure interfaces. The main goal of this kind of tests consist on the determination of the strength parameters for the Mohr-Coulomb or Barton (Barton *et al.*, 1974) criteria. Other tests of smaller use are the triaxial and torsion tests.

One of the main difficulties in performing large scale *in situ* tests for the strength parameters evaluation is to apply a load to a large volume of rock mass until it reaches ultimate failure. Normally, these tests are carried out until a certain stress is applied to the rock mass allowing to obtain E but without reaching failure. In this context, it is important to point out the contribution of Singh and Rao (2005) that, based on a extensive experimental study, presented expressions to predict the strength of the rock mass ( $\sigma_{cj}$ ).

$$\frac{\sigma_{cj}}{\sigma_c} = \left( \frac{E_j}{E_i} \right)^{1/\text{gradient}} \quad (2.1)$$

where  $E_j$  and  $E_i$  are the tangent moduli (tangent) of the rock mass and intact rock, respectively, and  $\sigma_c$  is the uniaxial compressive strength of the intact rock. The gradient is a parameter which is dependent of the type of failure expected for the rock mass. The probable mode of failure may be assigned depending on the orientation and interlocking of joints. It assumes the values of 0.56 for splitting and shearing, 0.66 for sliding and 0.72 for rotation. To obtain a rough estimate of the rock mass strength a mean value of 0.63 can be used. This way, it is possible to predict the rock mass strength based on  $E_i$  and  $\sigma_c$  that can be easily obtained by laboratory tests and  $E_j$  obtained by *in situ* tests like the PLT.

The main laboratory tests for the intact rock strength evaluation are: uniaxial compression, triaxial, diametral, linear (Brazilian test), point load, uniaxial tension, shear and flexural. There are also special diametral compression tests for the determination of anisotropic materials elastic

properties. The uniaxial compressive test is often used for the intact rock strength and deformability characterisation. It allows not only the calculation of the uniaxial compressive strength but also the deformability modulus since it is possible to obtain all the load-displacement curve. However, the triaxial test is the most accurate and reliable for this purpose since it simulates the *in situ* stress conditions and the adequate stress path. Nevertheless, this test involves more sophisticated equipment, is more time-consuming and expensive. Another very common test is the point load in rock samples whose result is, usually, correlated with the uniaxial compressive strength (Goodman, 1989; Miranda, 2003). The mechanical characterisation of discontinuities is carried out through sliding, triaxial, shear and torsion tests (Bandis, 1990). In Figure 2.5 the equipment for discontinuities sliding test of LNEC is presented.



**Figure 2.5:** Equipment for sliding test in discontinuities of LNEC

In this context, the accurate characterisation of surface roughness of joints at a relevant scale is very important since it is closely related to the overall behaviour of a rock mass. To quantify the rock joint surface roughness a great number of parameters have been proposed. However, this is normally carried out using the joint roughness coefficient (JRC) proposed by Barton (Barton *et al.*, 1974). The JRC roughness ranges from 0 (smooth) to 20 (rough) and can be determined by tilt, push or pull tests on rock samples.

It is also possible to characterise geometrically the discontinuities surfaces by means of laboratory tests using a mechanical system (Silvestre, 1996). The geometry of the discontinuity

is evaluated in several discrete points and the overall surface can be approximated numerically using a finite element mesh. More recently, Lanaro *et al.* (1998) used tree-dimensional laser scanning for digitising the topography of rock joint surfaces. Fardin *et al.* (2001) used this same method to characterise the joint roughness using fractal models investigating also the scale effects of roughness parameters (Figure 2.6).



*Figure 2.6:* 3D laser scanner for measuring the topography of joint surface (Fardin *et al.*, 2001).

## 2.3 Empirical rock mass classification systems

### 2.3.1 General

With the progressive increase of the underground space use, classification systems of empirical nature were developed to aid design support of underground structures. In the process of their application, qualitative and quantitative data is collected and organised in order to obtain indexes which provide descriptive information about the rock mass, support needs and geomechanical parameters estimation. This process includes core and borehole logging, scanline surveying, geological structure mapping and rock testing (Cai and Kaiser, 2007). Also, new technologies, such as digital and laser image processing of fractures and joint roughness can be used. Miranda (2003) stated that an empirical system should have the following characteristics:

- easily measurable parameters from outcrops, boreholes and tunnels;
- insensitive to variations of the rock mass, robust and repeatable;
- calibrated against test cases representative of the application field;

- practical and complete including all relevant parameters;
- result in an economic and safe design.

Most of the classification systems were developed based on experience from case histories. They can be very useful in the preliminary stages of design and during tunnel construction to quickly obtain a description of the actual ground conditions. Rocha (1976), who developed the MR empirical system for the calculation of loads in the support systems of tunnels, argued that the difficulties in the mechanical characterisation of rock masses due to their heterogeneity justified the use of less refined methods for support design. Rock mass classifications are the most important part of the empirical design methods. In the early stages of a project, the rock mass classification systems can be applied as an useful tool to establish a preliminary design. At least two systems should always be applied in order to reduce uncertainty (Bieniawski, 1989). It is not recommended their use in final design, especially for complex geotechnical structures or rock mass conditions like swelling or squeezing rock. From the application of the classification systems three types of outputs can be obtained:

- characterisation of the rock mass expressed as an overall rock mass index considering the effects of different geological parameters;
- empirical design with guidelines for support needs, method of excavation, stand-up time, support pressure, etc;
- estimates of rock mass properties like deformability modulus and strength parameters for a given failure criterion.

The classification of rock masses continues to be a discussion subject. Several new proposals have being made in the literature and also several papers have been published on their use and misuse (Bieniawski, 1989; Palmstrom, 1995; Riedmüller and Schubert, 1999; Hoek *et al.*, 2002; Stille and Palmstrom, 2003; Barton, 2004). The systems present several drawbacks and intrinsic limitations that should be known by practitioners for their correct use. For instance, the application of the RMR and Q systems for support design is suited for rock masses with relatively simple behaviour. However, they are less reliable for squeezing, swelling, and rock-burst conditions resulting of very high stresses and when failure can be defined by an important geological structure. Moreover, the ability to consider strain softening and strength anisotropy is limited. This way, the empirical systems should only be used within the limits of experience from which their rules have been derived and always calibrated with a good field survey and tests to the intact rock and rock mass.

In this context, it is interesting to refer the innovative work developed by Mas Ivars *et al.* (2007) in order to overcome the problems of rock mass classification systems. The authors presented a new approach to better understand and predict the rock mass behaviour called the Synthetic Rock Mass approach. It is based on the bonded-particle model for rock developed by Potyondy and Cundall (2004) and involves the construction of a discontinuum 3D sample of the rock mass composed by spherical particles embedded in a fracture network. The results can be used as input in large scale continuum models.

In recent years, classification systems have often been used together with analytical and numerical tools. They are used to obtain parameters to the numerical models consequently their importance has increased over time.

The empirical systems with wider application for the preliminary calculation of geomechanical parameters are the RMR, Q and GSI systems. They provide a quantitative estimation of the rock mass quality associated with empirical design rules and quantification of geomechanical parameters. The advantages of these systems are the large database that support them and the simplicity of application. They are widely known and their use is widespread. Therefore, in this text, only the most innovative issues of these systems are presented.

### 2.3.2 RMR system

The RMR system is based on the consideration of six geological-geotechnical parameters to which relative weights are attributed. The RMR index value, which can vary between 0 and 100, is then obtained through the algebraic sum of the referred weights (Figure 2.7). The one due to discontinuities orientation was introduced by Bieniawski (1989) as an adjustment of the sum of the remaining five. The application of this correction is not straightforward since a given orientation can be favourable or unfavourable, depending on the underground water condition. The calculated RMR value allow to classify the rock mass in one of five classes describing the rock mass condition ranging from "very poor rock" to "very good rock". To these classes several important informations are assigned like support needs, stand-up time and range of geomechanical parameters.

The deformability evaluation is carried out using the final RMR index and correlations developed by several authors. In Table 2.4 some of these expressions are presented. Their limitations, and the ones of the different expressions relating classification indexes and E presented in this Chapter, were established by the authors and by Miranda (2003) after a comparative study of the results given by the expressions in the context of the development of a knowledge based system.

The RMR system also provides a range of values for the Mohr-Coulomb parameters for

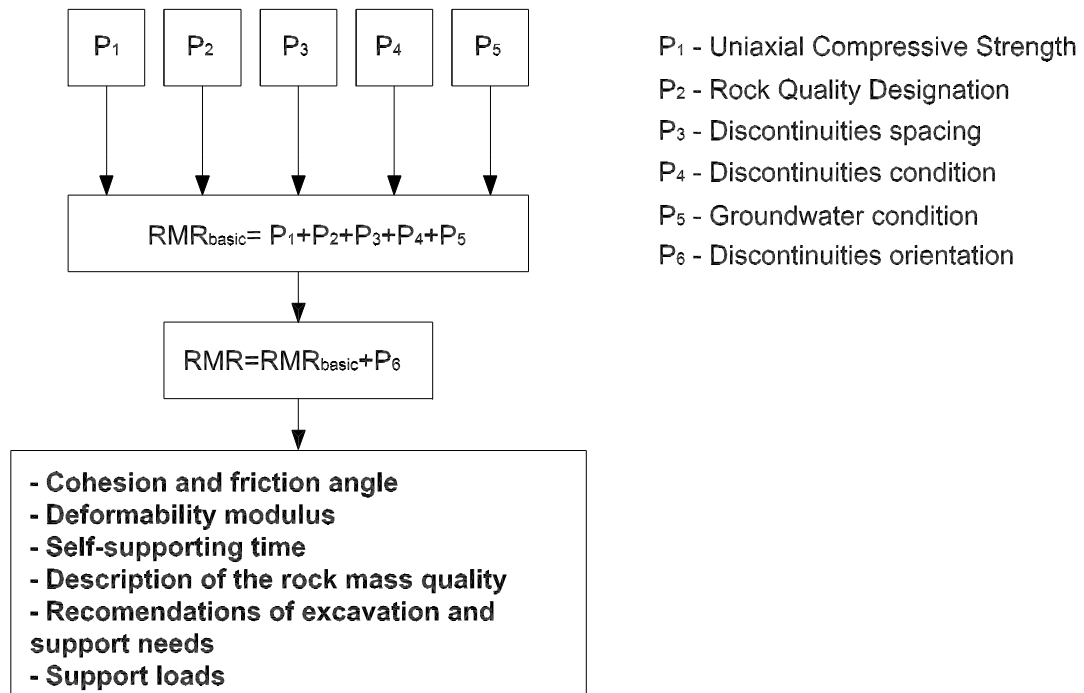


**Figure 2.7:** Scheme for the calculation of the RMR index.

**Table 2.4:** Analytical expressions for the calculation of  $E$  based on the RMR value.

Expression	Limitations	Reference
$E(GPa) = 10^{(RMR-10)/40}$	$RMR \leq 80$	Serafim and Pereira (1983)
$E(GPa) = 2 \cdot RMR - 100$	$RMR > 50$ and $\sigma_c > 100MPa$	Bieniawski (1978)
$E(GPa) = \frac{\sqrt{\sigma_c}}{10} \cdot 10^{(RMR-10)/40}$	$\sigma_c \leq 100MPa$	Hoek and Brown (1997)
$E = \frac{E_i}{100} \cdot 0.0028 \cdot RMR^2 + 0.9 \cdot e^{(RMR/22.28)}$	-	Nicholson and Bieniawski (1997)
$\frac{E}{E_i} = 0.5 \cdot (1 - \cos(\pi \cdot RMR/100))$	-	Mitri <i>et al.</i> (1994)
$E(GPa) = 0.3 \cdot H^\alpha \cdot 10^{(RMR-20)/38}$	$\sigma_c > 100MPa$ and $H > 50m$	Verman (1993)
$E(GPa) = 0.1 \cdot (RMR/10)^3$	-	Read <i>et al.</i> (1999)

$\alpha$  varies between 0.16 and 0.30 (higher for poorer rock masses); H is depth.

each class. However, the values which are pointed seem to be deeply conservative and research should be carried out in order to update these intervals.

The system can be represented in matrix form. This is done considering that each parameter  $P_i$  ( $i = 1$  to 6) is composed by two parts, the maximum weight of the parameter and its percentage evaluation (Castelli, 1992). The maximum values of the RMR system weights are represented by the following vector  $w_i = [15, 20, 20, 30, 15]$ . It is assumed that the evaluation

can be done, quantitatively, in an interval ranging from 0 to 1. The  $RMR_{basic}$  matrix can, then, be represented as follows:

$$RMR_{basic} = [w_1; w_2; w_3; w_4; w_5] \cdot [E_1; E_2; E_3; E_4; E_5]^T = [W] \cdot [E]^T \quad (2.2)$$

where  $E_i$  is the quantitative evaluation of the rock mass for the  $P_i$  parameter with  $0 \leq E_i \leq 1$ . Then,

$$P_i = w_j \cdot E_j \quad (j = 1, 2, \dots, 5) \quad (2.3)$$

The sixth parameter, that is used as an adjustment parameter to consider the influence of discontinuities orientation, can be considered in the following way:

$$P_6 = -(P_{1,or} + P_{2,or} + P_{3,or} + P_{4,or} + P_{5,or}) \quad (2.4)$$

in which,

$$P_{j,or} = w'_j \cdot E_{j,or} \quad (j = 1, 2, \dots, 5) \quad (2.5)$$

the  $P_{j,or}$  represent the adjustment parameters for each  $P_i$ . The values of the  $w'_j$  vector are constant and dependent on the type of work being analysed. In the case of tunnel, for instance, this value is equal to -12. This way, the vector can be represented by a constant C. The  $E_{j,or}$  are the quantitative influence of the discontinuities orientation in parameter  $i$  with  $0 \leq E_{j,or} \leq 1$ . In this case, the  $E_{j,or}$  sum can not be greater than 1 so that the value of  $P_6$  is kept below its maximum. The main difficulty of this methodology is the evaluation of the discontinuities orientation influence in each of the remaining parameters. This way, the adjustment parameter  $P_6$  can be represented by the following matrixes:

$$P_6 = -C \cdot [E_{1,or}; E_{2,or}; E_{3,or}; E_{4,or}; E_{5,or}]^T = -C \cdot [E_{j,or}]^T \quad (2.6)$$

as result,

$$RMR = RMR_{basic} + P_6 = [W'] \cdot [E]^T - [W] \cdot [E_{j,or}]^T \quad (2.7)$$

Random set theory (RST) can be applied to rock mass classification systems to deal with the two types of uncertainties related to their application: imprecision and dissonance. When a rock mass classification system is applied, a range of values for each parameter  $i$  is normally obtained within a lower ( $\delta_i^L$ ) and an upper bound ( $\delta_i^R$ ) (Tonon *et al.*, 2000). To deal with imprecision a range for the final index value is obtained using interval analysis. For the RMR system it is translated by the following expression:



$$\Delta RMR = [RMR^L, RMR^R] = \left[ \sum_{i=1}^6 \delta_i^L, \sum_{i=1}^6 \delta_i^R \right] \quad (2.8)$$

Dissonance refers to the fact that different observations generally provide different results, in this case different values of  $\Delta RMR$ . After  $M$  observations,  $N$  intervals  $\Delta RMR_i$  ( $i = 1, \dots, N$ ) will be available, each one with frequency  $m(\Delta RMR_i) = c_i/M$  where  $c_i$  is the number of occurrences of  $\Delta RMR_i$ . This way, to eliminate dissonance, the expectation value is the interval:

$$\mu_{RMR} = \left[ \sum_{i=1}^N (m_i RMR_i^L), \sum_{i=1}^N (m_i RMR_i^R) \right] \quad (2.9)$$

This random set approach can account for the two uncertainty types present in the application of the classification systems. This model is more adapted than probability theory to the real information that it is possible to obtain in the field by geomechanical survey and experts opinion.

### 2.3.3 Q system

The Q system was proposed by Barton *et al.* (1974) and since then it has been updated and some innovative concepts in what concerns aspects like supports design have been introduced (Barton, 2004). It proposes a quality index for the rock mass classification and determination of support needs. Using this index the rock mass is classified in one of nine different classes ranging from "exceptionally poor" to "exceptionally good". This system is schematized in Figure 2.8 (Miranda *et al.*, 2006).

It is important to mention that, in fractured rock masses, the parameters related with the discontinuities characteristics ( $J_r$  and  $J_a$ ) should refer to the discontinuity family which is more probable to initiate a failure process.

The Q value can, also, be matricially represented using a logarithmic transformation in the following sense:

$$Q = \frac{RQD}{J_n} \cdot \frac{J_r}{J_a} \cdot \frac{J_w}{SRF} \Leftrightarrow \log Q = \log RQD + \log \frac{1}{J_n} + \log J_r + \log \frac{1}{J_a} + \log J_w + \log \frac{1}{SRF} \quad (2.10)$$

This way,  $\log Q$  can be represented by equation 2.11:

$$\log Q = P'_1 + P'_2 + P'_3 + P'_4 + P'_5 + P'_6 \quad (2.11)$$

Using the same procedure as for the RMR system, the following matricial formulation is obtained:

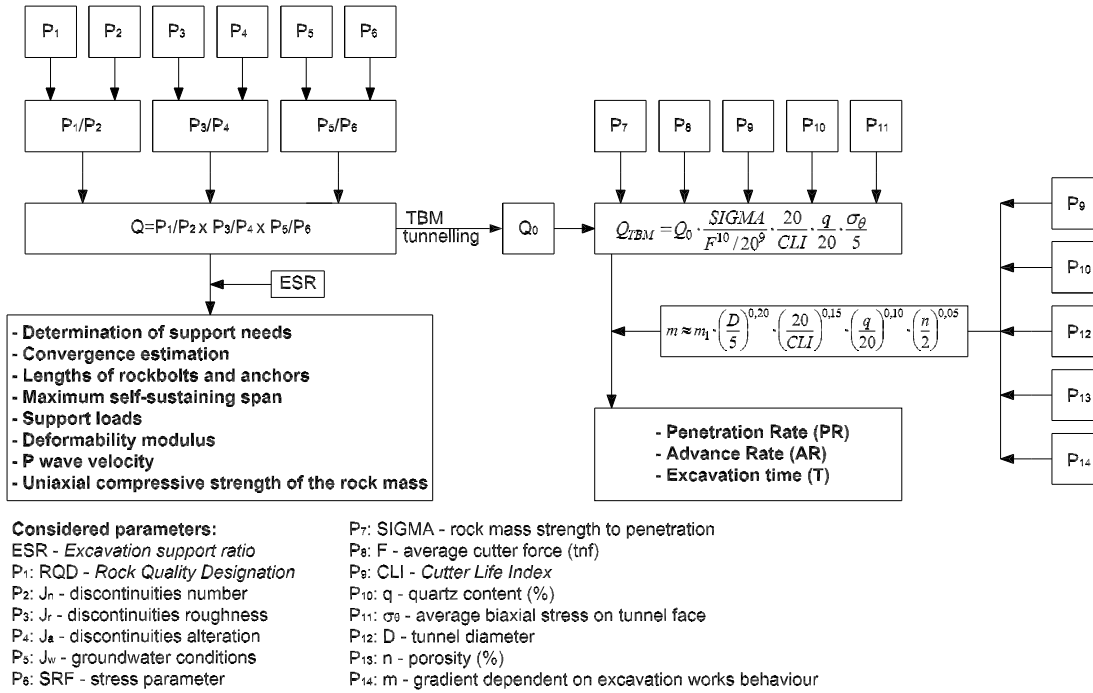


Figure 2.8: Scheme for the calculation of the Q and  $Q_{TBM}$  indexes

$$\log Q = [w_1; w_2; w_3; w_4; w_5; w_6] \cdot [E_1; E_2; E_3; E_4; E_5; E_6]^T = [W] \cdot [E]^T \quad (2.12)$$

$P'_i$  is calculated using a equation similar to 2.3. The maximum values of the Q system weights are represented by the vector  $w_i = [2, 0.30, 0.60, 0.13, 0, 0.30]$ .

Some expressions have been presented in order to predict the rock mass strength using this system. Singh (1997), based on the back analysis of several tunnels, have suggested the following expressions for rock mass strength:

$$\sigma_{cj} = 7 \cdot \gamma \cdot Q^{1/3} \quad (2.13)$$

where  $\gamma$  is the unit weight of the rock. Barton and Quadros (2002) modified equation 2.13 and included in it the uniaxial compressive strength of the intact rock ( $\sigma_c$ ) and suggested the following expression:

$$\sigma_{cj} = 5 \cdot \gamma \cdot \left( \frac{Q \cdot \sigma_c}{100} \right)^{1/3} \quad (2.14)$$

The Q value can also be correlated with E using several analytical expressions. In Table 2.5 some of these expressions are presented.

**Table 2.5:** Analytical expressions for the calculation E based on the Q value.

Expression	Limitations	Reference
$E(GPa) = 25 \cdot \log Q$	$Q > 1$	Barton <i>et al.</i> (1980)
$E(GPa) = 10 \cdot Q_c^{1/3}$ ; $Q_c = Q \cdot \sigma_c / 100$	$Q \leq 1$	Barton and Quadros (2002)
$E(GPa) = H^{0.2} \cdot Q^{0.36}$	$H > 50m$	Singh (1997)
$E(GPa) = 1.5 \cdot Q^{0.6} \cdot E_i^{0.14}$	$E_i \leq E$ and $Q \leq 500$	Singh (1997)
$E(GPa) = 7(\pm 3) \cdot \sqrt{Q'}; Q' = \frac{RQD}{J_n} \cdot \frac{J_r}{J_a}$	not limited	Diederichs and Kaiser (1999)

As for the RMR system, the random set theory can also be applied to the Q system. In this case, to deal with imprecision, and in accordance with interval analysis, the RST approach is translated by the following equation:

$$\Delta Q = [Q^L, Q^R] = \left[ \frac{RQD^L}{J_n^R} \cdot \frac{J_r^L}{J_a^R} \cdot \frac{J_w^L}{SRFR}, \frac{RQD^R}{J_n^L} \cdot \frac{J_r^R}{J_a^L} \cdot \frac{J_w^R}{SRFL} \right] \quad (2.15)$$

With respect to dissonance, and under the same previous assumptions referred for the RMR system, the expectation value is the interval:

$$\mu_Q = \left[ \sum_{i=1}^N (m_i Q_i^L), \sum_{i=1}^N (m_i Q_i^R) \right] \quad (2.16)$$

Recently, from the analysis of 145 projects, Barton (2000) established an empirical methodology for the performance prediction of TBM tunnelling which operate in rock masses and in open mode called  $Q_{TBM}$ . It is an expanded form of the Q system to account for important parameters in the tunnelling process. The base of the  $Q_{TBM}$  sub-system consists on the use of a  $Q_0$  index, that is calculated using the same equation as for the Q system with some differences. They consist on the use of a RQD value obtained in the tunnel axis direction ( $RQD_0$ ) and on the use of a  $J_r/J_a$  ratio (that represents the discontinuities shear strength) related to the most important family of discontinuities in the tunnelling process. The value of  $Q_{TBM}$  is calculated starting from  $Q_0$  and including other parameters which are related with the TBM performance (Figure 2.8).

A key aspect of this system is the comparison between the shear strength produced by the TBM (F) and an empirical measure of rock mass penetration strength, designated SIGMA, that is highly orientation dependent. The calculation of this value incorporates ( $\gamma$ ) and other normalised parameter  $Q_c$  or  $Q_t$ . This way SIGMA can take one of two different values:

$$SIGMA_{CM} = 5 \cdot \gamma \cdot Q_c^{1/3} \quad (2.17)$$

$$SIGMA_{TM} = 5 \cdot \gamma \cdot Q_t^{1/3} \quad (2.18)$$

The normalised values of  $Q_c$  and  $Q_t$  can be calculated, respectively, by:

$$Q_c = Q_0 \cdot \frac{\sigma_c}{100} \quad (2.19)$$

$$Q_t = Q_0 \cdot \frac{I_{50}}{4} \quad (2.20)$$

in which  $I_{50}$  is the point load index.  $SIGMA_{CM}$  should be used when the failure mode of the rock mass to TBM penetration is mainly compression controlled and  $SIGMA_{TM}$  when is mainly by tension (Barton, 2000). In a simpler way, when the discontinuities inclination is favourable to the excavation (low inclinations), the correct approach consists on using  $SIGMA_{TM}$ ; when it is unfavourable (high inclinations),  $SIGMA_{CM}$  should be used. This approach makes  $Q_{TBM}$  orientation dependent. The value of  $Q_c$  can be correlated with the P seismic waves velocity and with E by the plot of Figure 2.9.

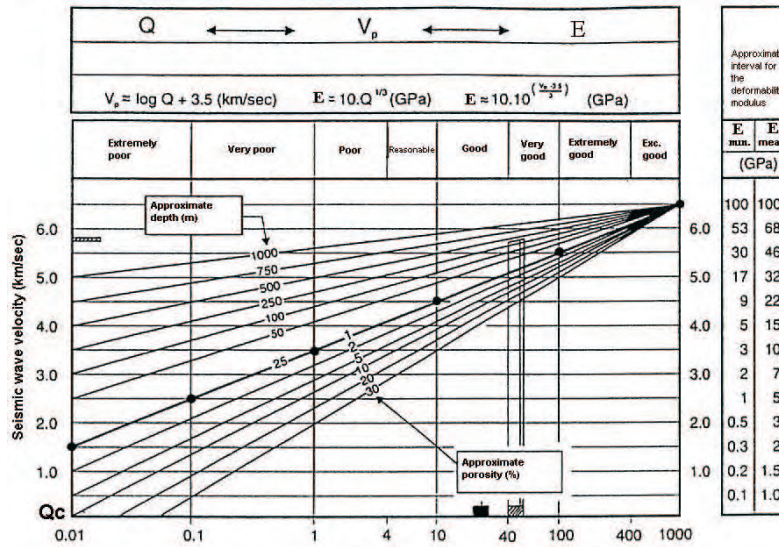


Figure 2.9: Relation between  $Q_c$ , the velocity of P seismic waves and E (Barton, 2004).

The fundamental parameters calculated by this methodology for TBM performance evaluation are the penetration rate (PR) and the advance rate (AR). For PR, Barton found a power increase of penetration with decreasing of  $Q_{TBM}$  translated by 2.21 in m/hour:

$$PR \approx 5 \cdot (Q_{TBM})^{-0.2} \quad (2.21)$$

This relation is only valid for  $Q_{TBM} > 1$  because in very poor rock masses the penetration rate is reduced by the operator to avoid problems with the TBM machine. The AR is related with the PR through equation 2.22:

$$AR = PR.U \quad (2.22)$$

where U is the level of utilisation which is time dependent (T) and can also be expressed in function of  $T^m$ . This way equation 2.22 can take a different form:

$$AR \approx 5. (Q_{TBM})^{-0.2} . T^m \quad (2.23)$$

m is a negative gradient which translates the decelerating average AR as the unit of time increases and T is the time unit (day, week, month...) for which a medium value of AR, expressed in hours, is necessary. The mean value of AR decreases with the increase of the considered time unit. The reason is the successive decline in the U value, corresponding to the TBM use. This decrease is quantified through the m coefficient. The initial value of the decline coefficient m ( $m_1$ ) can be estimated through a relation with the Q value (Figure 2.10). The initial value is modified to consider: the abrasivity of the rock through the CLI coefficient; the quartz percentage (q); the porosity (n); and the tunnel diameter (d), through equation 2.24.

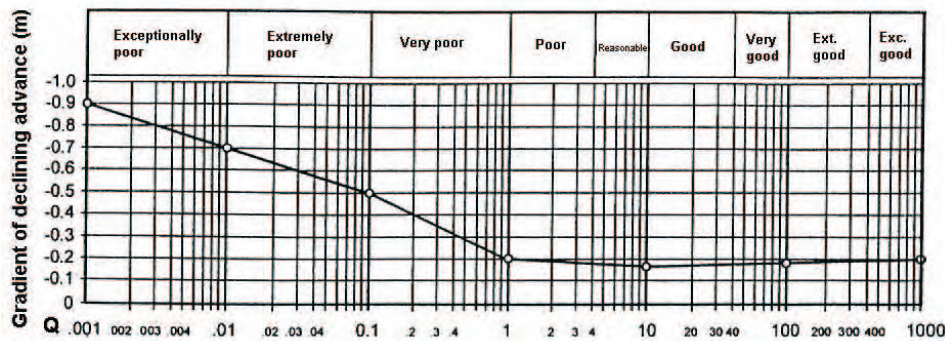


Figure 2.10: Variation of m with the Q value (Barton, 2004).

$$m \approx m_1 \cdot \left(\frac{d}{5}\right)^{0.20} \cdot \left(\frac{20}{CLI}\right)^{0.15} \cdot \left(\frac{q}{20}\right)^{0.10} \cdot \left(\frac{n}{2}\right)^{0.05} \quad (2.24)$$

The time of excavation of a tunnel segment with a certain length (L) and approximately

homogeneous characteristics, can be calculated by equation 2.25:

$$T = \left( \frac{L}{PR} \right)^{\frac{1}{1+m}} \quad (2.25)$$

Some correlations to predict PR and AR based on the RMR index were also developed by different authors. Sapigni *et al.* (2002) based on the data of 14 km of TBM tunnels found a second-degree polynomial relation between PR and RMR. However, due to the very high scatter of the data, the correlation has a limited use. Innaurato *et al.* (1991) found a correlation between PR, the Rock Structure Rating (RSR) (Wickham *et al.*, 1974) and  $\sigma_c$ :

$$PR = 40.41 \cdot \sigma_c^{0.44} + 0.047 \cdot RSR + 3.15 \quad (2.26)$$

where PR is in mm/round and  $\sigma_c$  in MPa. The RSR is related with RMR by (Bieniawski, 1989):

$$RSR = 0.77 \cdot RMR + 12.4 \quad (2.27)$$

Sapigni *et al.* (2002) applied this methodology to their database and a poor fit was found. The probable cause of the low relationship between RMR and tunnelling parameters is the lack of specific TBM and TBM-rock mass interaction factors in the original RMR formulation. Several improvements are needed to the conventional RMR system in order to be capable of predicting TBM performance parameters.

#### 2.3.4 GSI system

The GSI - Geological Strength Index - is a rock mass characterisation system specially developed to obtain strength parameters. It is the only system which provides an integrated procedure to estimate the parameters for the H-B and Mohr-Coulomb failure criteria. Using this index it is also possible to estimate the value of E. This way, it is possible to obtain these parameters based on geological observations of the rock mass in borehole cores, outcrops, surface excavations and tunnel faces.

The system uses the qualitative description of two fundamental parameters of the rock mass namely its structure or blockiness and the discontinuities conditions. The present form of the GSI system is presented in Figure 2.11 (Hoek and Brown, 1997; Marinos and Hoek, 2001; Hoek *et al.*, 2002). The authors also extended its application to heterogeneous rock masses which will be described later in this chapter.







GEOLOGICAL STRENGTH INDEX FOR JOINTED ROCKS (Hoek and Marinos, 2000)		SURFACE CONDITIONS				
<p>From the lithology, structure and surface conditions of the discontinuities, estimate the average value of GSI. Do not try to be too precise. Quoting a range from 33 to 37 is more realistic than stating that GSI = 35. Note that the table does not apply to structurally controlled failures. Where weak planar structural planes are present in an unfavourable orientation with respect to the excavation face, these will dominate the rock mass behaviour. The shear strength of surfaces in rocks that are prone to deterioration as a result of changes in moisture content will be reduced if water is present. When working with rocks in the fair to very poor categories, a shift to the right may be made for wet conditions. Water pressure is dealt with by effective stress analysis.</p>		DECREASING SURFACE QUALITY →				
		VERY GOOD Very rough, fresh unweathered surfaces	GOOD Rough, slightly weathered, iron stained surfaces	FAIR Smooth, moderately weathered and altered surfaces	POOR Slackensided, highly weathered surfaces with compact coatings or fillings or angular fragments	VERY POOR Slackensided, highly weathered surfaces with soft clay coatings or fillings
STRUCTURE		DECREASING INTERLOCKING OF ROCK PIECES ↓				
	INTACT OR MASSIVE - intact rock specimens or massive in situ rock with few widely spaced discontinuities	90			N/A	N/A
	BLOCKY - well interlocked undisturbed rock mass consisting of cubical blocks formed by three intersecting discontinuity sets	80	70			
	VERY BLOCKY - interlocked, partially disturbed mass with multi-faceted angular blocks formed by 4 or more joint sets		60	50		
	BLOCKY/DISTURBED/SEAMY - folded with angular blocks formed by many intersecting discontinuity sets. Persistence of bedding planes or schistosity			40	30	
	DISINTEGRATED - poorly interlocked, heavily broken rock mass with mixture of angular and rounded rock pieces				20	
	LAMINATED/SHEARED - Lack of blockiness due to close spacing of weak schistosity or shear planes	N/A	N/A			10

Figure 2.11: Chart for the GSI estimation.

In the first stages of development, it was proposed to calculate the GSI using correlations with modified forms of the RMR and Q systems. The authors considered that the groundwater and discontinuities orientation parameters in RMR and the groundwater and stress parameters in Q should be dealt explicitly in numerical analysis and, therefore, it was inappropriate to incorporate them in the estimation of rock mass strength parameters. This way, the proposed correlations to calculate GSI used RMR' (RMR without  $P_5$  and  $P_6$ ) and Q' (Q without  $J_w$  and SRF) and are translated by the following equations:

$$GSI = RMR' - 5 \quad (RMR \geq 23) \quad (2.28)$$

$$GSI = \ln Q' + 44 \quad (RMR < 23) \quad (2.29)$$

In a recent publication, Marinos *et al.* (2005) argued that the use of these correlations is not recommended for weak and very weak rock masses ( $GSI < 35$ ) and for those with high heterogeneity levels. However, the relation with RMR' is acceptable for reasonable quality rock masses.

The GSI system is based on the assumption that the rock mass behaves isotropically and uses a continuous medium approach. Hence, it should not be used in rock masses which present a dominant geological structure that clearly defines the behaviour of the rock mass. Also, the GSI is inappropriate for massive hard rock with discontinuities spaced at distances of similar magnitude to the dimension of the work under consideration.

A point value deterministic definition of the GSI (or any other empirical system indexes) for a rock mass is not realistic. In the use of the GSI, a range of values should be assigned (considering a normal distribution within the range, for instance) instead of a precise number.

Due to the qualitative nature of the inputs, the application of the GSI involves some subjectivity and experience is needed to obtain satisfactory results. Some attempts have been made in order to reduce the inherent uncertainties by complementing the qualitative descriptions of the rock mass and discontinuities with easy to obtain quantitative inputs.

Sonmez and Ulusay (1999) presented a methodology to provide a quantitative numerical basis for evaluating GSI introducing two new parameters to the GSI chart namely, the surface condition rating (SCR) and structure rating (SR). SR and SCR are calculated based on the volumetric joint count ( $J_v$ ) and from input parameters of the RMR system like roughness, weathering and infilling.

Cai *et al.* (2004) followed a similar methodology and proposed an approach based on the concepts of block volume ( $V_b$ ) and joint condition factor ( $J_c$ ). The first complements the geological structure description while the latter complements the discontinuities conditions.  $V_b$  is determined from geometric characteristics of the discontinuities like spacing, orientation and persistence. On the other hand, the calculation of  $J_c$  is dependent on the intrinsic characteristics of discontinuities. It is obtained by rating joint roughness depending on their large-scale waviness and small-scale smoothness and by rating alteration depending on weathering and infilling conditions.

In this quantitative approach, the GSI can be determined by an adapted GSI chart or using the following equation:

$$GSI(V_b; J_c) = \frac{26.5 + 8.79 \cdot \ln J_c + 0.9 \cdot \ln V_b}{1 + 0.0151 \cdot \ln J_c - 0.0253 \cdot \ln V_b} \quad (2.30)$$

Cai and Kaiser (2007) extended this approach in order to cover the residual strength of jointed rock masses. The main concept is to obtain the peak GSI value from field mapping and adjust it to the residual  $GSI_r$  based on the residual block volume ( $V_b^r$ ) and the residual joint surface condition ( $J_c^r$ ). Once  $GSI_r$  is obtained, the residual H-B parameters can be calculated using the abovementioned equations replacing GSI by  $GSI_r$ . In this case the intact rock parameters should be kept unchanged. Even though the rock is broken into smaller pieces,



fracturing and shearing do not weaken the intact rocks.

The reduction from peak to residual GSI, as it happens with the strength parameters, is a gradual process linked to the post-peak strain softening of the rock mass. Cai and Kaiser (2007) based on the analysis of some case studies, developed an equation to estimate  $GSI_r$  from GSI:

$$GSI_r = GSI \cdot \exp(-0.0134 \cdot GSI) \quad (2.31)$$

These approaches add quantitative measures to the system inputs increasing its objectivity and turning it less dependent on experience. However, Marinou *et al.* (2005) argued that, in spite of the interest of these approaches, they should be used with caution since the quantification process is limited to rock masses where the quantitative inputs can be easily measured.

As it was referred, given the complexity of the rock masses, composed by a rock matrix and discontinuities surfaces, the strength quantification can be carried out using the method developed in the scope of the GSI system. Based on experimental data and through theoretical knowledge of fracture mechanics in rocks, Hoek and Brown (1980) established, for intact rocks, the H-B strength criterium. Its actual version for rock formations, resulting from the generalisation of the intact rock criterium, is given by the following expression:

$$\sigma'_1 = \sigma'_3 + \sigma_c \cdot \left( m_b \cdot \frac{\sigma'_3}{\sigma_c} + s \right)^a \quad (2.32)$$

where  $\sigma'_1$  and  $\sigma'_3$  are, respectively, the maximum and minimum effective principal stresses;  $m_b$  is the reduced value of the  $m_i$  parameter which is a constant of the intact rock; and  $s$  and  $a$  are parameters that depend on the rock formation characteristics.

Serrano *et al.* (2007) developed an extension of this failure criterion to three-dimensions in order to consider the importance of the intermediate principal stress ( $\sigma'_2$ ) in the failure strength of rocks. This extension requires the introduction of two new parameters -  $\alpha$  and  $\eta$  - and it is translated by the following expression:

$$\frac{\sigma'_1 - \sigma'_3}{\sigma_c} = \left( m_b \cdot \frac{\sigma'_3}{\sigma_c} + \alpha \cdot \frac{(\eta \cdot \sigma'_1 - \sigma'_2) \cdot (\sigma'_2 - \sigma'_3)}{\sigma_c^2} + s \right)^a \quad (2.33)$$

The new introduced parameters are dependent on the rock type. Triaxial tests pointed to values between 0.90 and 1.50 for  $\alpha$  and 1.1 and 1.4 for  $\eta$ . However, as stated by the authors, more tests are needed for a better understanding of the new parameters involved. For  $\alpha=0$ , this extension reproduces the Hoek-Brown failure criterion for two dimensions.

When possible, the constants for the intact rock should be determined through the statistical analysis of a set of triaxial tests carried out according to the ISRM (1981) recommendations.

The values of the  $m_i$  parameter can be estimated for different rock types through the data supplied by Hoek (1994). Douglas (2002) based on the results of an extensive tests database, stated that the published values for  $m_i$  by Hoek are not accurate since this value is not related with the rock type. According to this author, the relation given by the uniaxial compression and tension strengths is a more reasonable approach for the calculation of this parameter. This relation was used with success in practical cases for granite formations in the Metro do Porto project (Normetro, 2001). In this case a correlation between the uniaxial compression and tension strengths was developed using 40 samples. It presents a determination coefficient ( $R^2$ ) equal to 0.93 and is translated by the following equation:

$$\sigma_t = 0.062 \cdot \sigma_c \quad (2.34)$$

where  $\sigma_t$  is the tension strength obtained by diametral compression tests. This correlation indicates that, for a large range of  $\sigma_c$  values, the tension strength is approximately 6% of that value.

In spite of the wide application of the H-B criterion it presents some limitations that should be taken into account. Considering the way how currently is formulated, this criterion does not correctly evaluate the strength of the rock mass in the transition from intact to weathered rock. Moreover, it is not valid for soft rocks (when applied to intact rock) since it was developed for hard rocks and is not adequate to model the intact rock behaviour when subjected to low confinement stress (Douglas, 2002). These limitations are often unknown or ignored in practice and the criterion is applied indiscriminately to all rock types in every condition.

Considering these limitations, Douglas (2002) presented a modified H-B criterion based in an extensive database of tests which, in the case of intact rocks, is expressed by the following equations:

$$\sigma'_1 = \sigma'_3 + \sigma_c \cdot \left( \frac{m_i \cdot \sigma'_3}{\sigma_c} + 1 \right)^a \quad \text{for } \sigma'_3 > -\sigma_c/m_i \quad (2.35)$$

$$\sigma'_1 = \sigma'_3 \quad \text{for } \sigma'_3 \leq -\sigma_c/m_i \quad (2.36)$$

Using this modified criterion it is possible to predict the uniaxial compressive and tension strengths with higher accuracy. The variance of this adjustment is approximately half of the one given by the original formulation. Using the generalized criterion a relationship was developed between  $a$  and  $m_i$ :

$$a_i \approx 0.4 + \frac{1.2}{1 + \exp\left(\frac{m_i}{7}\right)} \quad (2.37)$$

Once the GSI of the rock mass is defined, the parameters of the H-B criterium can be calculated through the following equations (Hoek *et al.*, 2002):

$$m_b = m_i \cdot \exp\left(\frac{GSI - 100}{28 - 14 \cdot D}\right) \quad (2.38)$$

$$s = \exp\left(\frac{GSI - 100}{9 - 3 \cdot D}\right) \quad (2.39)$$

$$a = \frac{1}{2} + \frac{1}{6} \cdot (\exp(-GSI/15) - \exp(-20/3)) \quad (2.40)$$

where D is a parameter that depends on the disturbance to which the formation was submitted due to the use of explosives during excavation and to the stress release (Hoek *et al.*, 2002). This value varies between 0 for undisturbed and 1 for very disturbed rock masses. The authors provided some orientations for the choice of values for this parameter but there is still relatively little experience on its use. The value of  $m_b$  can also be calculated using expression 2.41 (Hoek and Brown, 1997), valid for  $GSI > 25$ :

$$m_b = m_i \cdot s^{1/3} \quad (2.41)$$

The H-B failure criterion have been successfully applied for estimating rock mass strength where block size and discontinuity controlled shear failure dominates ground behaviour. However, this failure criterion present some difficulties to estimate the strength parameters at the extreme ends of rock competence scale (Carter *et al.*, 2007). For poorer rock formations ( $\sigma_c \ll 15MPa$ ) accuracy is lost because the rock mass behaviour is matrix controlled. In the case of massive rock masses failure demands the creation of new fractures.

For the low range of GSI values, Carvalho *et al.* (2007) developed alternative functions to evaluate the H-B parameters in the transition from rock to soil:

$$m_b^* = \frac{(m_b + (m_i - m_b) \cdot f_T(\sigma_c))}{(4 \cdot a^* - 1)} \quad (2.42)$$

$$s^* = s + (1 - s) \cdot f_T(\sigma_c) \quad (2.43)$$

$$a^* = a + (1 - a) \cdot f_T(\sigma_c) \quad (2.44)$$

where,

$$f_T(\sigma_c) = \left\{ 1, \sigma_c \leq 500kPa; \exp\left(-\frac{(GSI - 0.5)^2}{25}\right), \sigma_c > 500kPa \right\} \quad (2.45)$$

For the highest geomechanical quality rock masses, a transition in behaviour occurs between an inter-block shear dominated rock mass controlled by discontinuities and rock masses which behaviour is dominated by rock material strength. In this transition, the following procedure can be used to model the spalling initiation or "damage threshold" (Martin *et al.*, 1999):

- determine the unconfined compressive strength ( $\sigma_c^*$ ) which corresponds to the start of "systematic cracking" in an uniaxial testing. This can be carried out by means of acoustic emission or radial strain data and set  $a_{sp}$  to 0.25;
- obtain a reliable estimation of tensile strength (T) for instance using the Brazilian test;
- compute the H-B parameters from the following equations:

$$s_{sp} = \left(\frac{\sigma_c^*}{\sigma_c}\right)^{1/a} \quad (2.46)$$

$$m_{sp} = s_{sp} \cdot \left(\frac{\sigma_c}{T}\right) \quad (2.47)$$

$$a_{sp} = 0.25 \quad (2.48)$$

In the transition between discontinuities controlled and massive rock masses the strength parameters can be computed by the following function:

$$X_{trans} = X_{GSI} + (X_{GSI} - X_{sp}) \cdot f_{sp} \quad (2.49)$$

where,

$$f_{sp} = \frac{1}{1 + \exp\left[100 \cdot \left(2 + \frac{D}{5}\right) - \left(\frac{GSI}{60}\right)^{1/3} - \left(\frac{\sigma_c}{34 \cdot T}\right)^{1/5}\right]} \quad (2.50)$$

$X'$ s represent the values of  $a$ ,  $s$  and  $m$ . According to their subscripts, GSI means the conventional calculation while  $sp$  corresponds to their value for spalling assessment.

In rock masses with brittle failure lower  $m_b$  and higher  $s$  values than those provided by the equations 2.38 and 2.39 were necessary to match predictions with observations (Cai *et al.*, 2004). Martin *et al.* (1999), based on analysis of underground excavations built in massive to moderately fractured brittle rocks, proposed the following H-B parameters for this type of rock mass:  $m_b = 0$  and  $s = 0.11$ . However, more research is required in order to validate and fine-tune these values and to define the border between brittle and shear failure.

Douglas (2002) also presented new equations to calculate the H-B parameters considering very bad quality rock formations:

$$m_b = \max \left\{ m_i \cdot \frac{GSI}{100}; 2.5 \right\} \quad (2.51)$$

$$m_b = \min \left\{ \exp \left( \frac{GSI - 85}{15} \right); 1 \right\} \quad (2.52)$$

$$a_b = a_i + (0.9 - a_i) \cdot \exp \left( \frac{75 - 30 \cdot m_b}{m_i} \right) \quad (2.53)$$

Given that in many cases the geotechnical software uses the Mohr-Coulomb strength parameters, it is convenient to evaluate the equivalent  $c'$  and  $\phi'$  angle to the H-B strength parameters. This procedure consists in adjusting a line to the curve generated by the H-B criterion balancing the areas above and below this line for a expected range of stresses considering the work being analysed. The range of stresses should be within  $\sigma_{t, mass} < \sigma_3 < \sigma'_{3max}$ . The value of  $\sigma'_{3max}$  should be determined for each specific case. In the case of underground structures the following expression should be used:

$$\frac{\sigma'_{3max}}{\sigma'_{cm}} = 0.47 \cdot \left( \frac{\sigma'_{cm}}{\gamma \cdot H} \right)^{-0.94} \quad (2.54)$$

where  $\sigma'_{cm}$  is the rock mass strength and  $H$  the tunnel depth. The rock mass strength can be determined by equation 2.55.

$$\sigma'_{cm} = \sigma_c \cdot \frac{(m_b + 4 \cdot s - a \cdot (m_b - 8 \cdot s)) \cdot (m_b/4 + s)^{a-1}}{2 \cdot (1 + a) \cdot (2 + a)} \quad (2.55)$$

This way, the equivalent values of the friction angle and cohesion are given by the following expressions, respectively:

$$\phi' = \arcsin \left[ \frac{6.a.m_b.(s + m_b.\sigma'_{3n})^{a-1}}{2.(1+a).(2+a) + 6.a.m_b.(s + m_b.\sigma'_{3n})^{a-1}} \right] \quad (2.56)$$

$$c' = \frac{\sigma_c. [(1+2.a).s + (1-a).m_b.\sigma'_{3n}].(s + m_b.\sigma'_{3n})^{a-1}}{(1+a).(2+a).\sqrt{1 + \left(6.a.m_b.(s + m_b.\sigma'_{3n})^{a-1}\right) / ((1+a).(2+a))}} \quad (2.57)$$

where,

$$\sigma'_{3n} = \frac{\sigma'_{3max}}{\sigma_c} \quad (2.58)$$

The GSI value can also be used for an indirect calculation of E of the rock mass. Several expressions have been presented. In Table 2.6 some of the developed analytical correlations are presented.

**Table 2.6:** Analytical expressions for the calculation E based on the GSI value.

Expression	Limitations	Reference
$E = \left(1 - \frac{D}{2}\right) \cdot \sqrt{\frac{\sigma_c}{100} \cdot 10^{(GSI-10)/40}}$	$\sigma_c \leq 100MPa$	Hoek <i>et al.</i> (2002)
$E = \left(1 - \frac{D}{2}\right) \cdot 10^{(GSI-10)/40}$	$\sigma_c > 100MPa$	Hoek <i>et al.</i> (2002)
$E(GPa) = 100000 \cdot \left(\frac{1 - D/2}{1 + \exp((75 + 25 \cdot D - GSI)/11)}\right)$	not limited	Hoek and Diederichs (2006)
$E(GPa) = E_i \cdot \left(\frac{1 - D/2}{1 + \exp((60 + 15 \cdot D - GSI)/11)}\right)$	not limited	Hoek and Diederichs (2006)
$E(GPa) = E_i \cdot (s^a)^{0.4}$	not limited	Sonmez <i>et al.</i> (2004)
$E(GPa) = E_i \cdot s^{1/4}$	not limited	Carvalho (2004)

### 2.3.5 Correlations between parameters and indexes

In literature, several correlations between the RMR and Q indexes can be found (Rutledge and Preston, 1978; Bieniawski, 1989; Barton, 2000; Yanjun *et al.*, 2007). In spite of the natural differences between these correlations, a common point is the logarithmic relation between the two indexes. In this work, and using a large database of the RMR and Q systems application in a granite rock mass, also a correlation was developed which is translated by the following equation:

$$RMR = 8.4 \cdot \ln Q + 49.8 \quad (2.59)$$

This equation resembles the one presented by Bieniawski (1989):

$$RMR = 9 \cdot \ln Q + 44 \quad (2.60)$$

Goel *et al.* (1995) defined RCR (Rock Condition Rating) as the RMR without considering the weights correspondent to the intact rock strength and discontinuities orientation; and N (Rock Mass Number) as the Q without the stress factor (SRF). These indexes can also be used to indirectly correlate the values of RMR and Q. The authors proposed the following correlation between RCR and N:

$$RCR = 8 \cdot \ln N + 30 \quad (r = 0.92) \quad (2.61)$$

It is proposed an alternative correlation which was developed considered the cited database:

$$RCR = 7.9 \cdot \ln N + 44.9 \quad (r = 0.90)^1 \quad (2.62)$$

Tzamos and Sofianos (2007) argued that, since there are parameters which are not common for the different classification systems, a large scatter should be expected when trying to correlate them. Therefore, it would be more appropriate to correlate the common parts of the systems which concern to the rock mass only. This way, they defined the Rock Mass Fabric Index (F) which is a scalar function of the rock structure and joints condition. Concerning the RMR, this parameter ( $F_{RMR}$ ) is then composed by the sum of the weights related to the RQD, discontinuities spacing and conditions ( $P_2$ ,  $P_3$  and  $P_4$ ). In relation to the Q system,  $F_Q$  is equal to  $Q'$ . The correlation between the two parameters is translated by equation 2.63.

$$F_{RMR} = 15 \cdot \ln F_Q + 32 \quad (r = 0.96) \quad (2.63)$$

In the scope of this work, also a correlation was developed between these two parameters valid for granite rock formations:

$$F_{RMR} = 7.4 \cdot \ln F_Q + 31.6 \quad (r = 0.90) \quad (2.64)$$

---

<sup>1</sup>It is considered that the correlation coefficient (r) is not the best way to assess the quality of a correlation. However, it is presented for comparison purposes.

## 2.4 Highly heterogeneous rock masses

Rock masses present different levels of heterogeneity. However, in some cases, these heterogeneities turn the rock mass extremely difficult to characterise due to their geological, tectonic and geomechanical complexity. For instance, it is inappropriate and simplistic to use traditional rock mass classification systems such as the RMR or the Q systems. They were developed for relatively simple rock masses and fail to adequately determine optimum support requirements, appropriate excavation methods and geomechanical parameters estimation. This factor raises several issues with direct impact on the geomechanical properties determination and hinders the establishment of a proper geotechnical model. This section briefly deals with tools and methodologies that have been developed to deal with this type of rock masses in order to obtain a less uncertain characterisation.

As it has been referred in this Chapter, the traditionally employed tools to obtain parameters and analyse the data consist of direct (laboratory and *in situ* tests) and indirect methods (empirical classification systems). In any case, it is recognised that these methods are insufficient and do not give adequate answer to the problem of a reliable characterisation of rock masses with high heterogeneity levels. In this context, different authors are attempting to progress developing research in different fields of study (Morales *et al.*, 2004):

- Enhancing test methods in order to obtain representative strength and deformability parameters.
- Studies to adapt and modify geomechanical characterisation systems aimed at better characterising rock masses in relation to different materials and engineering projects.
- The development of correlations between characteristic geomechanical parameters.
- Use of probabilistic tools to deal with uncertainty related with the geomechanical properties.
- Development of AI based tools for decision-making support.
- Application of homogenisation techniques.
- Use of state-of-the-art observation and monitoring techniques.

High heterogeneity can be found in many types of rock masses and under several forms. The GSI has been adapted in order to be applicable on some of the most variable rock masses, including extremely poor quality sheared rock masses of weak schistose materials (such as siltstones, clay shales or phyllites) sometimes inter-bedded with strong rock (Figure 2.12). In



this context, Marinós and Hoek (2001) adapted the GSI system for heterogeneous rock masses such as flysch, based on the application of the H-B criterion (Figure 2.13). Flysch consists on alternations of clastic sediments that are associated with orogenesis. Geotechnically, a flysch rock mass has the following characteristics: high heterogeneity with the presence of clay materials; tectonic fatigue and sheared discontinuities, often resulting in a soil-like material; and low permeability due to the presence of clay minerals.

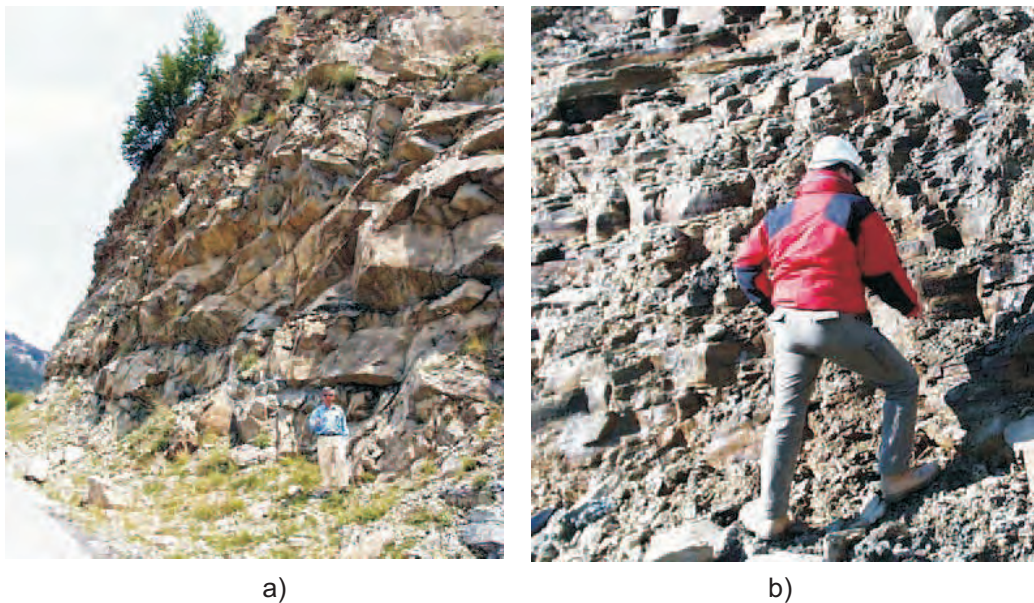


**Figure 2.12:** Examples of typical flysch: a) thick bedded blocky sandstone and b) sandstone with thin siltstone layers (Marinós and Hoek, 2001).

Determination of the GSI for these rock masses, composed of frequently tectonically disturbed alternations of strong and weak rocks, present some special challenges. The authors described eight classes of heterogeneous rock units and for each a range of GSI values is suggested. In addition to the GSI values, they considered the selection of the intact rock properties  $\sigma_c$  and  $m_i$  for heterogeneous rock masses, adopting a "weighted average" of the intact strength properties of the strong and weak layers.

Different adaptations of the GSI system have been carried out for other types of heterogeneous rock masses. Hoek *et al.* (1998) presented some alterations for very weak and sheared rock masses. For lithologically varied but tectonically undisturbed rock masses, such as molasses, a new GSI chart was presented by Hoek *et al.* (2005).

When dealing with heterogeneities due to weathering, like in granite rock masses, the initial chart can be used taken into account some specific issues. The GSI values for weathered rock

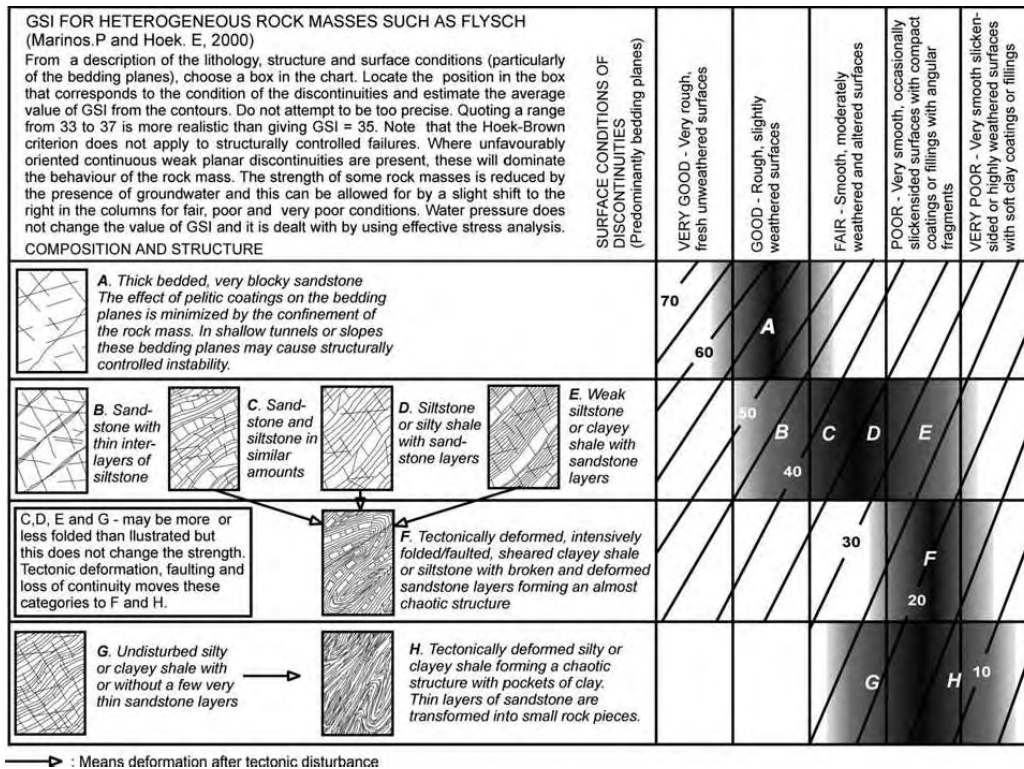


Figure 2.13: GSI chart for heterogeneous rock masses such as flysch (Marinos and Hoek, 2001).

masses can be obtained shifting to the right in the GSI chart in relation to the unweathered rock material. If the weathering has reached the intact rock, which is also very common in weathered granites, the  $\sigma_c$  and the  $m_i$  constant must also be reduced. If the weathering has penetrated the rock to the extent that the discontinuities and the structure has been lost, then the rock mass must be assessed as a soil and the GSI no longer applies. In the particular case of granite weathering profiles characterisation it is important to mention the work developed by Viana da Fonseca and Coelho (2007). They used drilling parameters of boreholes (advance rate, thrust penetration, rod torque, rotation rate, water pressure and vibration) to calculate the Somerton index in order to differentiate weathering degrees.

Some authors, based on the GSI system together with intensive *in situ* and laboratory testing, developed local classification systems for specific rock masses (Morales *et al.*, 2004).

In what concerns the underground works, some measures can be adopted to make possible the fine-tuning of the geotechnical model, for instance: boreholes in the excavation face; use of geophysical methods; displacements evaluation using the monitoring data; and combinations between these methods (Moritz *et al.*, 2004). However, the boreholes in the excavation face and the geophysical methods cause delays due to the temporary stops they compel and can become expensive. Moreover, boreholes only supply discrete information and the geophysical

data interpretation is difficult and need to be improved.

In the construction of a tunnel the total excavation time, and consequently its cost, is highly dependent on the geomechanical formation characteristics. The natural variability of these formations does not allow these geomechanical parameters to be estimated in a deterministic way. This way, probabilistic methods can be used, as the Monte Carlo, to obtain the parameters distribution for areas considered with nearly constant geomechanical characteristics. It becomes evident that probabilistic distributions that adapt to the elementary properties distributions of the formation are of primordial importance.

In this context, some probabilistic methods have been developed for tunnels design like the ones developed by Goricki *et al.* (2003) and Costa *et al.* (2003) for the specific case of heterogeneous volcanic formations. Miranda (2003) developed a similar approach as the latter, generalising the approach for granite rock formations. The methodology was based in the calculation of a statistical distribution of the RMR index. Considering the mean value and the standard deviation of each weight of this classification, and assuming a normal distribution, the Monte Carlo method was used to generate a thousand random values for each weight. The obtained values were added to obtain a probabilistic distribution of RMR. Afterwards, a range of GSI values was obtained through correlations, for the H-B strength parameters and E calculation. For each geomechanical area the mean and characteristic values (corresponding to the 5, 50 and 95% percentiles) were considered which allow to cover practically all the variability of the geotechnical materials. Figure 2.14 presents a histogram of the GSI generated by this methodology.

For the short term behaviour prediction of the rock mass in the front and around the tunnel, the evaluation of the 3D displacements from the observed data is very effective (Moritz *et al.*, 2004). This prediction is possible based on the displacement vector direction evaluation which relates the vertical and longitudinal displacements. The displacement vector is considered positive when it points in the excavation direction and negative otherwise.

When a tunnel is being bored in a homogeneous formation the normal direction of the displacement vector is slightly positive (up to  $10^\circ$ ). When a weaker formation approaches the displacements direction suffers a significant deviation in the positive sense, in other words, the longitudinal displacement grows significantly while settlement remains almost constant. After entering in the weak area the displacement vector returns to normal. On the other hand, if a more rigid formation is approaching the front of the tunnel the displacement vector inclination changes to negative values and smaller displacements are expected when entering that formation. When the excavation approaches a more rigid zone the displacement vector changes from the normal position i.e slightly positive to negative values.

The "normal" vector orientation is between  $8^\circ$  and  $10^\circ$  against the excavation. Increasing

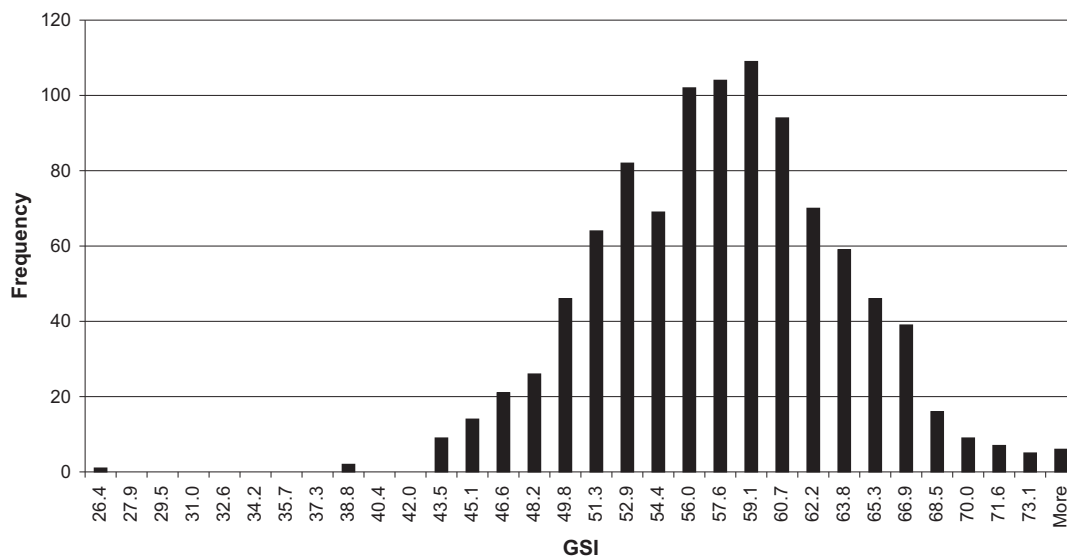


**Figure 2.14:** Histogram of the GSI obtained by a probabilistic methodology (Miranda, 2003)

trends indicate weaker material ahead of the face, while decreasing trends indicate stiffer material. If the cross-section displacements are asymmetrical this means that a weaker formation will first appear on the largest displacements side. Sudden changes in the displacements will impose high stresses in the support. This estimate allows designers to act proactively in the adjustment of the excavation and support methods to avoid unexpected events.

In some types of formations frequently occur geotechnical situations without space, lithological and mechanical continuity. They are commonly known as tectonic melanges or block-in-matrix rocks (bimrocks) and are defined as chaotic, heterogeneous geological mixtures of blocks, with different types, lithologies and sizes, surrounded by weaker, sheared, finer-grained rocks and a soil matrix (Button *et al.*, 2004; Wakabayashi and Medley, 2004). Sometimes, as it happens in granite formations, the soil matrix also presents different weathering degrees in a metric scale transforming the characterisation system a more difficult process. They are deeply heterogeneous and very difficult to characterise, since they present a soil matrix with a set of randomly distributed blocks. In a borehole, the intersection of a rigid boulder can induce that the bedrock was reached (Figure 2.15). Samples of soil for laboratory testing are also affected by rock inclusions.

The main geotechnical problem results from the significant spacial variations in rock mass stiffness and strength, which reduce the confidence of predictions. The heterogeneity of a melange rock mass demands comprehensive characterisation of the geological, geometrical, mechanical and hydraulic properties, even more than in other rock mass types. However, even when comprehensive investigations are performed, the complexity of the internal block/matrix

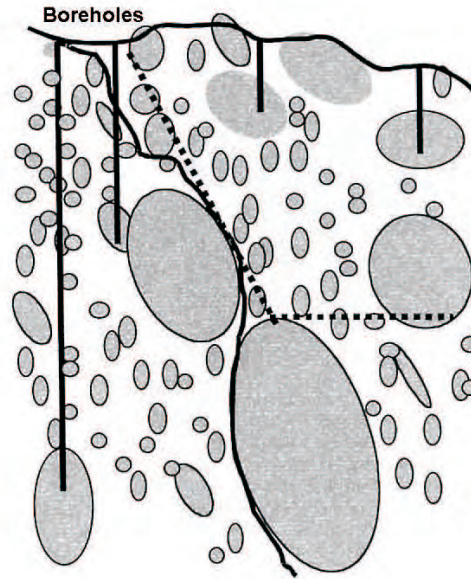


**Figure 2.15:** Survey of heterogeneous granite formations by boreholes (Medley, 1999).

structure may prevent the geotechnical investigations from yielding sufficiently precise rock mass models (Button *et al.*, 2004).

The enormous heterogeneity of a melange poses severe engineering problems. In tunnelling, one of the main construction problems is working with mixed face conditions, in which the working face contains materials with different excavation characteristics. In this case, the rock mass behaviour is much more unpredictable and incidents are more possible to occur if adequate measures are not considered like continuous characterisation of the tunnel face, real-time monitoring, etc. In the case of the Metro do Porto project (Figure 2.16), developed in a highly heterogeneous granite rock mass and in urban environment, there were severe problems in the initial stages of tunnelling related to these heterogeneities, resulting in several delays and an accident. The solution was to use the TBM in closed mode, i.e. using a support pressure applied in the TBM front, which allowed the excavation to be carried out with minor problems.

Many times, the presence of rigid inclusions within a soil matrix, even though raising higher uncertainties in the geomechanical behaviour of the rock mass, enhances the overall strength and deformability characteristics of the rock mass. However, in practice, geotechnical design is only based on the soil matrix properties. This simplification can lead to a very conservative or inappropriate design. As the block volume increases, so does the strength since the shear planes in the formation have to be tortuous around the blocks. The mechanical properties are affected by the mechanical properties of the main matrix, volumetric block proportion, distribution of the block size and block orientation relatively to the shear planes (Wakabayashi and Medley,



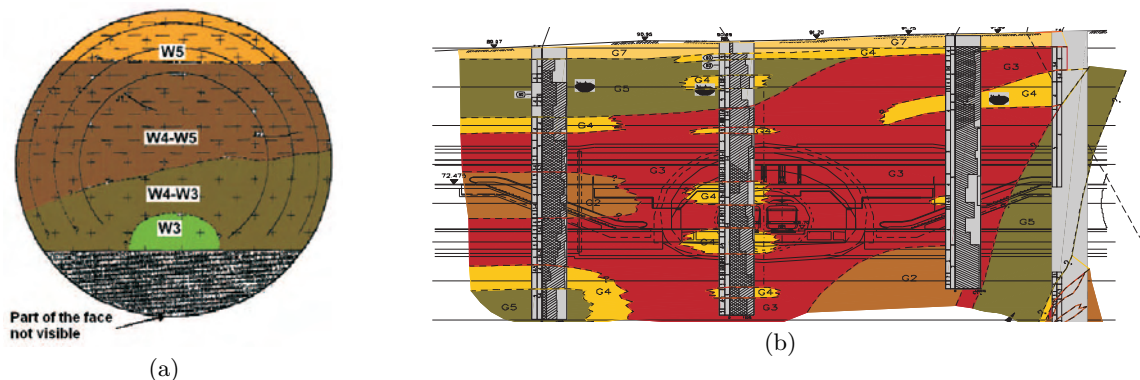


**Figure 2.16:** Mixed face conditions found during the construction of the Metro do Porto project built in a highly heterogenous granite rock mass: (a) View of the tunnel face with different weathering degrees; (b) Cross-section of Bolhão underground station (Babendererde *et al.*, 2004).

2004).

In the case of the existence of boulders or more rigid blocks in the middle of a soft rock or soil matrix, these should just be considered if their influence is significant. They will be relevant for the global geomechanical behaviour of the formation if (Medley, 1999):

- the blocks present considerable mechanical contrast with the matrix, for instance, ratio between  $\phi'$  of the block and the matrix higher than 2;
- the size of the blocks is between 5 and 75% of the elementary characteristic dimension or *characteristic engineering length* that describes the problem in analysis (tunnel diameter, thickness of landslide, laboratory rock sample diameter);
- the volumetric proportion of the blocks, or in other words, the ratio between the total volume of blocks and the formation volume being analysed is between 25 and 75%.

The rock mass strength of block-in-matrix rocks, is mainly governed by the strength contrasts between the blocks and the matrix, the sizes, proportion and orientation of the blocks (Mandrone, 2006). The rock mass behaviour, particularly during tunnelling, is primarily influenced by the local rock mass strength and, very importantly, by the location and size of significant blocks. When the existence of these blocks is, in fact, significant for the global behaviour of the formation, they influence in the following way (Medley, 1999):

- when the volumetric proportion of the blocks is less than 25%, their influence in the global behaviour of the formation can be ignored and only the properties of the matrix are considered;
- between 25 and 75%,  $\phi'$  and E increase and  $c'$  decreases due to the presence of the blocks;

- above 75%, the blocks tend to be in contact, and no longer supported by the matrix which implicates that no increase of strength is verified;
- the global strength of the formation is, normally, independent of the blocks internal strength;
- shear failure tend to begin in the perimeter of the blocks.

Barbero *et al.* (2007) stated that, in these formations, the block size distribution is scale independent, i.e., the laboratory and site size scale behaviour is the same. The authors numerically simulated compression tests on bimrocks to identify strength and deformability laws to model the material as a homogenised equivalent continuum. The blocks were generated according to a random process producing samples of block populations with certain statistical properties. The results showed that both  $\sigma_c$  and E increase with the block volume proportion (BVP). The value of E is proportional to the BVP, and can be computed as a simple weighted mean between the matrix and the blocks properties. Moreover, yielding starts and spreads in the matrix. Finally, modelling this kind of materials using a continuum model provides a reasonable approach. However, since the mechanical behaviour of bimrocks is a three-dimensional problem, more calculations are needed to validate these conclusions.

To define heterogeneous formations it is necessary to carry out a more intensive characterisation to: determine the external contacts of the formation (if possible); to determine the borders of the larger blocks; and to predict the blocks proportion and different lithological units. Usually, there is no order in the blocks distribution, nevertheless, sub-areas may exist that can be mapped. These sub-areas can evidence differences in the blocks lithology and number and type of matrix.

These features of a melange, which are particularly important for the prediction of the rock mass behaviour during tunnelling, can only be revealed by geotechnical investigations that are combined with detailed structural-geological analysis and, during excavation, by state-of-the-art techniques to interpret the results of real-time monitoring.

To interpret and complement the information gathered in the boreholes it can be necessary to execute trenches. The ratio between the lengths of intersection of all boreholes with the blocks and the boreholes total length can give a rough estimate of the blocks proportion. The unidimensional (1D) evaluation of blocks proportion underestimates this value for greater blocks happening the inverse for the smaller ones. This way, 3D mapping tools have been developed. Haneberg (2004) showed that there is no solution for the inverse problem of rebuilding the 3D distribution of blocks starting from 1D measurements in boreholes and 2D from outcrops. The same author stated that, if there is information about the shape, orientation and size

distribution of the blocks, indirect methods allow to obtain a 3D statistical distribution starting from 1D and 2D information. These methods use the Monte Carlo method to generate 3D populations of blocks from which the blocks size distribution is determined and compared with the observed information.

In the characterisation of heterogeneous formations, dynamic methodologies are gaining increasing importance. These methods are capable of identifying the dynamic shear modulus at various depths which can then be related to the static deformation modulus by means of the elasticity theory which provide a valuable geomechanical mapping or zoning. In particular, surface analysis of Rayleigh waves allow to obtain this data only requiring access to the surface and without any boreholes.

The interaction between Rayleigh waves and the heterogeneities allow a good understanding of the overall deformability characteristics of the formation. By analysing Rayleigh waves velocities it is possible to study the macroscopic effect of inclusions and provides an insight to the macroscopic behaviour of the equivalent homogeneous medium.

Chammas *et al.* (2003) demonstrated numerically that Rayleigh waves are well-suited for determining the effective shear modulus of a heterogeneous medium. In the simulations, the heterogeneous medium was composed by a soil matrix and random stiff inclusions modelled using time-domain finite element simulations. The results showed the dependence of shear wave velocities on the nature and concentration of inclusions and that Rayleigh waves can differentiate inclusion sizes, which can serve as valuable information.

Homogenisation techniques can also be used in order to calculate the characteristics of a homogeneous medium with the same geomechanical behaviour as the heterogeneous one. This problem is within the scope of the composite material theory and deals with the prediction of effective or average macroscopic properties of the medium and their connection with the properties of the individual materials. Most of these techniques, commonly used to predict the elasto-plastic behaviour of heterogeneous materials, are only valid over quite specific spatial distributions of the constituent phases (Herve and Zaoui, 1990). They can be applied to periodic media with uniform stress/strain field and periodic cell models and disordered media or self-consistent schemes. The latter, initially developed by Kröner (1978), can be adapted to heterogeneous soils. Their main principle is the translation of the interaction between inclusions, as well as with the homogenous matrix. One example of this self-consistent schemes is the one presented by Christensen and Lo (1979). They developed the exact analytical solution based on elasticity for calculating the effective stiffness of a material with cylindrical inclusions. The model considers three phases namely: an outer region of equivalent homogeneous material or "effective medium", the cylindrical inclusions and a cylindrical ring of matrix material (Figure 2.17).



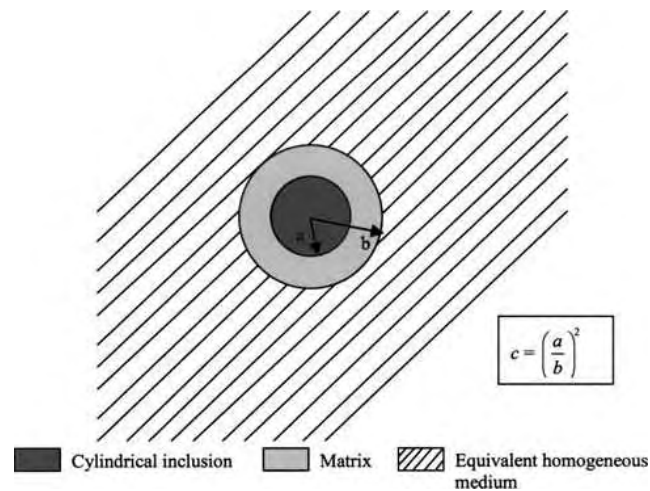


**Figure 2.17:** Model used for homogenisation method: ‘a’ is the radius of the inclusion; ‘b’ is radius of the matrix; and ‘c’ is volume fraction (Chammas *et al.*, 2003).

Many other homogenisation techniques were developed and can be applied to obtain mean properties of rock masses that allow a more accurate modelling of such formations (Maghous *et al.*, 1998; Yufin *et al.*, 2007). However, as it was already referred, the application of these techniques are limited to rock masses with certain well established characteristics, in particular, regularity of the joints network. In this case, the homogenisation approach provides a potentially efficient computational tool. In highly heterogeneous rock masses these techniques are obviously less applicable.

In spite of these new developments and even carrying out extensive survey campaigns and tests, still persists considerable uncertainties in design phase regarding high heterogeneities. These uncertainties request continuous investigations on the formation and permanent updating of the geological-geotechnical model during construction. This is of fundamental importance to make possible to adapt the project for the real characteristic of the interested formation.

## 2.5 Conclusions

In geotechnical design it is very difficult to obtain reliable results without a thorough characterisation of the involved materials. Due to the formations variability, the geotechnical properties evaluation is the issue with higher uncertainty degree. Eurocode 7 (Eurocode, 2004) recommends that the characteristic value of a property should be a cautious estimate of its mean value and that its evaluation should be based also in experience and inherent risk to the work.

In this Chapter, a critical analysis of the different methods to evaluate strength and deformability parameters in rock and heterogeneous formations was carried out. The main *in situ* and laboratory tests for geomechanical characterisation and the main indirect methods like the

empirical systems were described. In particular, the most innovative aspects of the RMR, Q,  $Q_{TBM}$  and GSI empirical systems were pointed out. It is worth mentioning the innovative approaches of the RMR and Q systems in what concerns their matrix form and RST approach. A methodology was defined for the deformability characterisation combining small and large scale tests. Also, an outline of expressions to compute E was carried out.

An original contribution was given in the development of correlations between rock mass indexes (RMR-Q, RCR-N and  $F_{RMR-F_Q}$ ) valid for granite rock masses, based on a database of more than a thousand records.

In heterogeneous rock formations (like granites, flysch and bimrocks), the geomechanical characterisation is a substantially more complicated task. The current methodologies and the deterministic definition of the parameters do not conveniently translate their real behaviour. Research in this area is being developed following different paths and important advances have been achieved in the last years. However, this is still an open research field since more work is needed to develop tools to more accurately characterise and predict the behaviour of highly heterogeneous formations. In this context, some methods specially developed for the characterisation of highly heterogeneous rock formations were described. Between others, adaptations of the GSI system, probabilistic tools and geophysical methods can be mentioned.

It is important to point out the fundamental role of the underground structures monitoring for the validation, calibration and updating of the geotechnical models and of the assumed hypothesis. In this domain, back analysis techniques are very important for they allow to obtain the parameters that best translate the observed behaviour based on appropriate mathematical tools.

# Knowledge Discovery in Databases and Data Mining

## 3.1 Introduction

The concept of artificial intelligence (AI), formally initiated in 1956, is related with the attempt of qualifying the computer with an intelligent behaviour which is understood as the set of activities that only a human being is capable of fulfil. In the AI domain, in the 70s there was a great emphasis in expert systems which tried to mimic the expert and served as tools in the decision making process. The trend shifted in the 90s to the intelligent systems which could learn directly from the data or use hybrid approaches.

In the current information age, due to the advances in information and communication technologies, there is an extraordinary expansion of data generation that needs to be stored. In some areas, this fast-growing amount of data is collected and stored in large and numerous databases that have exceeded our human ability for comprehension without using computational tools. As a result, data collected in large databases, which often presents high complexity, is not properly explored. This data can hold valuable information, such as trends and patterns, that can be used to improve decision making and optimise processes (Goebel and Gruenwald, 1999).

In the past, two major approaches have been used for this goal: classical statistics, used to uncover relationships in data, and the use of knowledge from experts. Nevertheless, the number of human experts is limited and they may overlook important details, while classical statistic analysis may break down when vast amounts of complex data are available. The alternative is to use automated discovery tools to analyse the raw data and extract high-level information for the decision-maker (Hand *et al.*, 2001).

Due to the awareness of the great potential of this subject there has been an increasing interest in the Knowledge Discovery from Databases (KDD) and Data Mining (DM) fields that led to the fast development of electronic data management methods. These terms are often confused. KDD denotes the overall process of transforming raw data into high-level knowledge and DM is just one step of the KDD process, aiming at the extraction of useful patterns from observed data. The knowledge derived through DM is often referred to as models or patterns and it is very important that this knowledge is both novel and understandable.

DM is a relatively new area of computer science that lies at the intersection of statistics, machine learning, data management and databases, pattern recognition, AI and other areas. DM is thus emerging as a class of analytical techniques that go beyond statistics and concerns with automatically find, simplify and summarise patterns and relationships within large data sets that have business or scientific value. In other words, it allows finding trends and relationships between variables characterising systems and processes with the objective of predicting their future state. A practical and applied definition of DM is the analysis and non-trivial extraction of data from databases for the purpose of discovering new and valuable information, in the form of patterns and rules, from relationships between data elements (Fayyad *et al.*, 1996).

There are several DM techniques, each one with its own purposes and capabilities. Examples of these techniques include Decision Trees and Rule Induction, Neural and Bayesian Networks, Learning Classifier Systems and Instance-Based algorithms (Lee and Siau, 2001; Berthold and Hand, 2003). DM is receiving widespread attention in the academic and public literature and case studies suggest companies are increasingly investigating the potential of DM technology to deliver competitive advantage. These techniques are widely used in the business field such as direct target marketing campaigns, fraud detection, and development of models to aid in financial predictions.

In the civil engineering field, several applications using these techniques have been developed. The following examples can be mentioned (Solomatine and Dulal, 2003; Quintela, 2005):

- applications to data obtained by structures monitoring to predict their future behaviour;
- use of rainfall data and past river flows to predict the flows and floods;
- application to large construction databases to generate knowledge in order to improve future planning of construction projects;
- bridge deterioration and behaviour;
- prediction of maximum loads in steel beams.

Modelling in civil engineering can be carried out following three different approaches (Figure 3.1). It is often based on good understanding of the underlying processes and use "knowledge-driven" behavioural models (Bhattacharya and Solomatine, 2005). These simulation models use techniques like the finite-difference or the finite-element methods. In "knowledge-driven" models the observed data is used during the model calibration. Used in a lower extent, the "expert-driven" models are based on the subjective evaluation of a panel of specialists which normally provide guidelines to the way the project should be carried out.

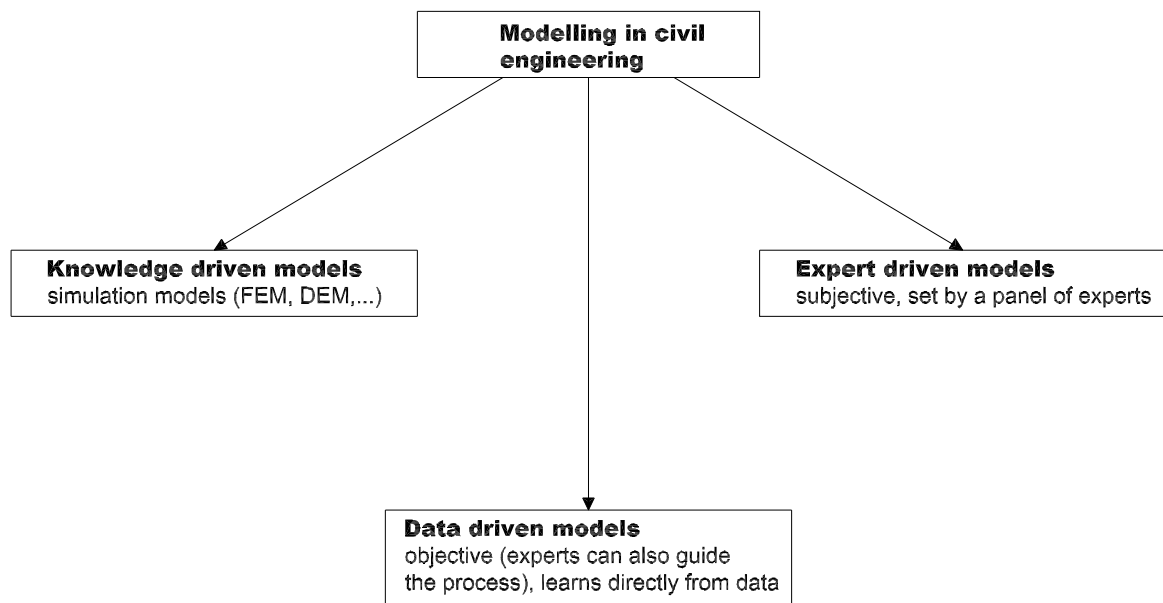


*Figure 3.1:* Modelling in civil engineering.

In contrast, the so-called "data-driven" models (DDM) are based on the establishment of a mathematical model to be adjusted to the data. A DDM of a system is defined as a model connecting the system state variables (input, internal and output variables) with only a limited knowledge of the details about the behaviour of the system. Probably the simplest DDM is a linear regression model. Hybrid models combine both types of models and are the current trend.

Generally speaking, the physically-based "knowledge-driven" models are more accurate and general. The problem is that sometimes it is not possible to build reliable models. In such cases, if the observation data is available, DDM may help. DDM complements the simulation modelling and in some cases could replace it. These models can be developed using DM techniques.

DDM are already often used in geotechnical engineering in their simpler forms like the

correlations between parameters. However, they can constitute a more powerful tool in the decision support process in geotechnical projects. This can be achieved if the models are developed using more powerful tools and more complete information.

In large underground geotechnical projects, for instance, a quite considerable amount of data about the involved formations is produced coming from different sources, namely:

- laboratory and *in situ* tests;
- application of the empirical classification systems in the case of rock masses;
- monitoring and observation of the structures behaviour;
- data from the Tunnel Boring Machines (TBM);
- data from accidents and unexpected events.

Normally, for schedule reasons, it is difficult for practitioners to properly analyse this data in order to obtain deeper knowledge concerning the involved formations. The analyses are normally carried out using statistic tools which do not give adequate response when dealing with large and complex databases.

Much of this data interest and have significant value to the broad geotechnical engineering and construction community, as well as for research. Nevertheless, in particular in Europe, all this data is not properly stored and explored in order to take full advantage of the potentially embedded knowledge. There is a necessity to define standard ways of creating organised repositories of data (Data Warehouses) in order to simplify its exchange and analysis. With this kind of structures and using DM techniques it would be easier to induce more complex DDM that could enhance the comprehension of the structure behaviour and interested formations and help in the decision making process.

The obtained models could be used in future projects, integrated in empirical or in hybrid systems in which they are used together with numerical and analytical methodologies. In the geotechnics field, there are some successful applications of DM techniques to different kinds of problems.

Bhattacharya and Solomatine (2005) applied Decision Trees, Artificial Neural Networks (ANN) and Support Vector Machines for classifying sub-surface soil characteristics using measured data from the Cone Penetration Test. Lehman (2004) identified cause-effect relationships between specific drilling and construction practices with resulting production levels using ANN to mine huge volumes of historical field data. Some applications have been developed for soil slope stability prediction based on field data (Zhou *et al.*, 2002; Souza, 2004; Sakellariou and Ferentinou, 2005). Guo *et al.* (2003) developed a model to identify probable failure on rock

masses bases on ANNs. Also using ANNs Basheer and Najjar (1995) developed a model for soil compaction control. Klose *et al.* (2002) applied DM techniques on geological and seismic data for the prediction of small-scale hazardous geotechnical structures. Hanna *et al.* (2004) developed a model for efficiency prediction of pile groups installed in cohesionless soil and subjected to axial loading based on ANNs. Motta (2004) implemented a classification algorithm for geotechnical risk evaluation and accidents prediction in roads. Rangel *et al.* (2005) presented an alternative strategy to evaluate the stability of tunnels during the design and construction stages. They developed a hybrid system, composed by ANN and neuro-fuzzy networks and analytical solutions. Suwansawat and Einstein (2006) applied with success ANN for predicting maximum surface settlement due to tunnelling in soft ground. The authors used data from the Bangkok Subway Project excavated using earth pressure balance (EPB) shield machines.

In spite of the presented cases, in geotechnical engineering the use of these methodologies is not yet generalised and the geotechnical community is not aware of their potential applications. Figure 3.2 presents an overview of the number of journal publications in the areas of DM and in this area related with engineering and geotechnics since 1996. It clearly shows that, although the increasing interest in this area even in the broad field of engineering, in geotechnics the research in this area is still incipient and the field almost unknown.

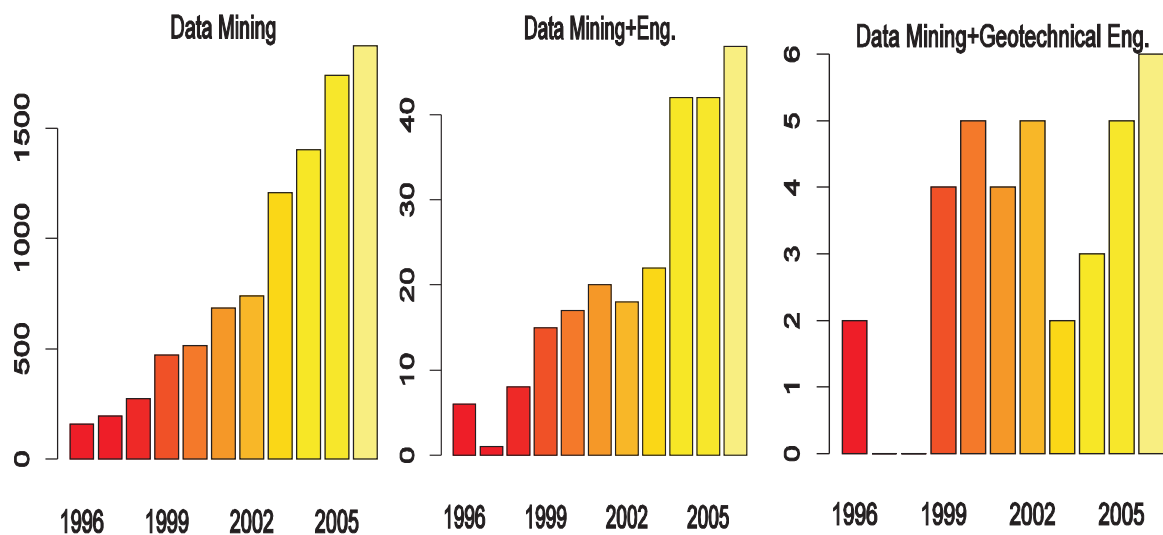


**Figure 3.2:** Number of journal publications in the DM and in this area related with engineering and geotechnics (source ISI Web of Knowledge) (Cortez, 2007).

Due to this almost lack of knowledge concerning these techniques in the geotechnics field, in this Chapter, the main tasks, methods and techniques of DM and KDD are described. This

conceptual principles are the basis of the work developed using a large database of geotechnical data together with these tools in order to develop new and reliable models for geomechanical characterisation which will be presented in Chapter 4.

## 3.2 Knowledge Discovery in Databases

Data can be stored in many different types of databases. Data Warehouse is a database architecture that has recently emerged. It can be described as a repository of clean, aggregated and organised data from multiple data sources, in order to enhance and support the decision making process. This structure can be analysed by OLAP (On-Line Analytical Processing) tools, which are analysis techniques oriented to test a given hypothesis posed by the user or simply to make random consults. However, this approach which is user dependent, can hinder the establishment of patterns in an "intelligent" way. Although OLAP tools support complex consults and multidimensional databases, for a thorough analysis more advanced tools are required. This overall process of discovering useful knowledge from databases is called Knowledge Discovery in Databases (KDD). In this process, Data Mining (DM) is a step related to the application of specific algorithms for extracting models from data (Fayyad *et al.*, 1996). The KDD process consists in five main steps (Figure 3.3).

- Data selection: the application domain is studied and relevant data is collected from the database.
- Pre-processing or data preparation: noise or irrelevant data is removed (data cleaning) and multiple data sources may be combined (data integration). In this step appropriate prior knowledge can be also incorporated.
- Transformation: data is transformed in appropriate forms for the Data Mining process.
- Data Mining: intelligent methods are applied in order to extract models or patterns.
- Interpretation: results from the previous step are studied and evaluated.

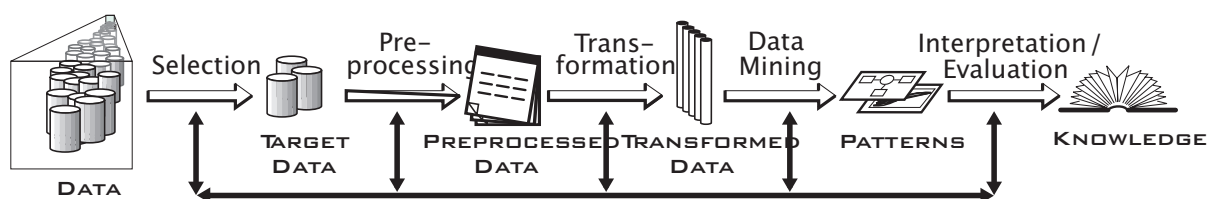


*Figure 3.3:* Phases of the KDD process (Fayyad *et al.*, 1996).



In the data selection phase the main objective is to learn and comprehend the application domain and selecting the data to be analysed. In the first stage, the fundamental concepts have to be acquired and the main goals of the process clearly established. This means that, normally, a multidisciplinary team of specialists is needed. Some cleaning tasks are performed in this step like removing attributes which are considered to have little influence in the output. Afterwards, data is selected to limit the search field in order to carry out the process focusing in the defined goals.

Pre-processing includes the procedures to correct inconsistencies in data to improve its quality. Among others, the main tasks include removing noise or outliers and mapping missing values and selection of attributes. Noise can cause problems in the construction of the models. In certain circumstances, it is useful the use filters to remove the noise from data. Outliers can be detected using statistical techniques and based on experts knowledge. There are several techniques to deal with missing values. The most simple imputation method, valid when missing values affect a small set of data, is simply eliminate the records with missing data. Other imputation methods consist on filling the missing values by the most common, mean or median value of the attribute. The different attributes do not influence the results in the same way. It is necessary to choose the main attributes and eliminate the ones that can hinder the learning process. This can be done using experts analysis or *a priori* knowledge, correlations, sensibility analysis among others.

Data transformation is related with the manipulation of data in order to be in the correct form for the application of the DM algorithms. For instance, in numerical variables with highly skewed distributions, a logarithmic transformation can help the learning process.

The DM step includes choosing the most suited algorithms for the type of analysis and the searching of patterns and models is carried out in a certain figurative type (classification, regression, rule induction, etc). This step will be analysed in detail later in this Chapter.

The last stage is the interpretation of the discovered patterns possibly using visualisation tools. Normally, it is necessary to clean the obtained results because superfluous or irrelevant patterns can be achieved together with important ones. It can be necessary to return to any of the previous step in an iterative process of correcting options and errors in order to improve the final results.

After interpretation, the important patterns transform into knowledge that can be used directly in a decision support process or incorporated in other intelligent systems like the expert or knowledge based systems.

Even though all steps in the KDD process are important, focus will be drawn on the Data Mining section which has received most attention in literature and is many times referred as the KDD process itself.

## 3.3 Data Mining

Data Mining (DM) consists in the searching and inference of patterns or models in the data which can represent useful knowledge. Depending on what kind of patterns to be found, DM tasks are normally classified into two categories: descriptive and predictive. Descriptive tasks characterise the general properties of the data while predictive perform inference on data in order to make predictions (Han and Kamber, 2000). Descriptive models intend to summarise data in convenient ways to improve its understanding while predictive models aim to forecast the unknown value of a variable given known values of other variables (Hand *et al.*, 2001). In the following items the main DM tasks, methodologies, models and techniques will be described.

### 3.3.1 Tasks

**Classification** is the process of finding a model (or function) which describes different classes in data in order to allow associating a new object to a class according to its characteristics. Normally, the derived model is induced by the classification algorithm based on the analysis of a training set of data. In other words, classification categorises a certain object into one of several predefined classes. Each object belongs to a certain class among a pre-defined set of classes. The objective of the classification algorithm is to find some relation between attributes and one class in order that the classification process can use that relation to predict the class of a new and unknown object.

The classification process can be divided in two parts. In the first part, the model is built describing the characteristics of the classes based on the attributes of a randomly chosen set of examples from the population (training set). Since the class label of each training example is known, this process is called supervised learning. In the unsupervised learning, also called clustering, the class labels are unknown. This technique is used to enhance the understanding of the database finding embedded patterns which can then be used to categorise new examples. In the second part, the accuracy of the model is estimated by its application on a testing set which does not incorporate data from the training set. The accuracy is measured as a percentage of correctly classified examples. If the model accuracy is considered adequate than it can be used to classify future cases in which the class is unknown.

Figure 3.4 presents a hypothetical classification example of a rock mass classification system. It is intended to develop a simpler system only based on the uniaxial compressive strength ( $\sigma_c$ ) and the Rock Quality Designation (RQD) as classification parameters based on the results of application of another more complex system. The algorithm is applied over a set of examples of the classification system (training data) to find the classification rules. Their accuracy is tested over a different set of examples not used for training (testing data). If the model shows

acceptable results it can be used to classify new cases.

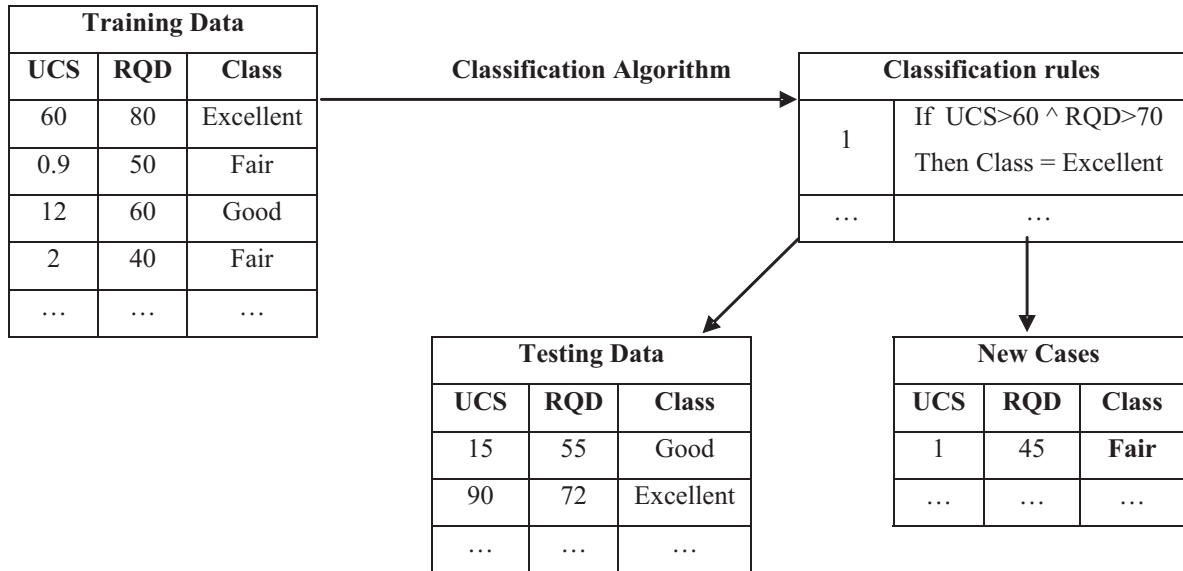


*Figure 3.4:* Classification example with rock mass classification data.

**Regression** is a predictive model, very similar to classification, used for continuous values (in classification the variables are categorical). In fact, the main difference is the nature of the response variable which is, in this case, numerical instead of nominal.

The regression process is also very similar. The main difference is the estimation of the inferred model accuracy. Instead of calculating a percentage of correct classifications, several error measures between real values of the training set and the predicted ones can be calculated. The mean squared error (MSE) and the mean absolute deviation (MAD) are only two examples of these measures. They can be used not only to evaluate the prediction accuracy of a model but also for choosing between alternative ones.

Regression allows obtaining other important information. Using this technique, it can be possible to know the relative importance of each parameter in the prediction of the target variable. This information can be very useful for the comprehension of the physical phenomena supporting the inferred model. Moreover, regression presents flexibility concerning the input parameters allowing that empirical and/or specialised knowledge is considered in the models. For instance, it is possible to consider an input variable that, based on experience, should be in the model, even though it leads to a small predictive improvement. Inversely, it is possible to exclude variables which one considers should not appear in the model or lead to a substantially reduced model complexity in exchange of some predictive accuracy loss. Finally, it is possible

to explore interaction between input variables in the sense that the influence of one input in the target variable depends on the values taken by others.

**Association or dependencies** deal with finding interesting relationships between items of a given data set. These models describe significant dependencies between variables through the identification of groups of highly associated data. These dependencies can exist at two levels:

- structural: the model presents locally dependent variables in a graphical way;
- quantitative: the model specifies the strengths of the dependencies using a numerical scale.

**Summarisation** supplies a succinct description for the data. It can be used for *characterisation* which provides a concise summarisation of the data; and *comparison* which summaries and differentiates one set of data from other sets. These two techniques used together form the *concept description*, a very important component of DM. A very simple example of summarisation could be a histogram or a statistical measure of a certain attribute of data.

**Clustering** is the process of grouping *similar* objects into classes. In classification an object is associated in one of several predefined classes while in clustering the classes must be determined by the data. It is a kind of learning by observation other than learning by examples as in classification. Cluster analysis is also referred to as unsupervised learning. The clusters are defined by finding groups in data which present certain similarities. These similarities are evaluated by metrics or probability tools.

**Data visualisation** supports the understanding of complex data relationships. It deals with displaying, the intermediate or final results, in multiple forms like rules, tables, pie or bar charts, decision trees and other visual representations. These technologies comprise sophisticated techniques for viewing high-dimensional data and 3D renderings. Visualising the results in different forms together with *interestingness* measures help to:

- enhance comprehension of the domain;
- selection of the patterns which represent useful knowledge;
- provide guidelines for further discovery.

### 3.3.2 Methodologies

The increasing interest on DM led to the necessity of defining standard procedures to carry out this task. In this context, the two most used methodologies in DM are the CRISP-DM (Cross-Industry Standard Process for Data Mining) and the SEMMA (Sample, Explore, Modify, Model, and Assess) which are going to be briefly described.

The CRISP-DM methodology was developed by a group of companies to respond to this necessity. It is described as an iterative and interactive hierarchic model which develops in six phases (Figure 3.5).

- Problem understanding: recognize the objectives and conceive the DM problem and a preliminary plan to achieve the goals.
- Data understanding: involve data collection and activities to get an insight in data like inference of data quality, detecting subsets or trends and form hypotheses.
- Data preparation: construction of the final dataset to be modelled from the initial raw data. This phase includes tasks like data cleaning, data transformation and attribute selection.
- Modelling: modelling techniques are selected and applied to find patterns within the data.
- Evaluation: assess the induced models and review the previous steps in order to assure the models accomplish the objectives.
- Deployment: organise the obtained knowledge and make it available in order to be used.

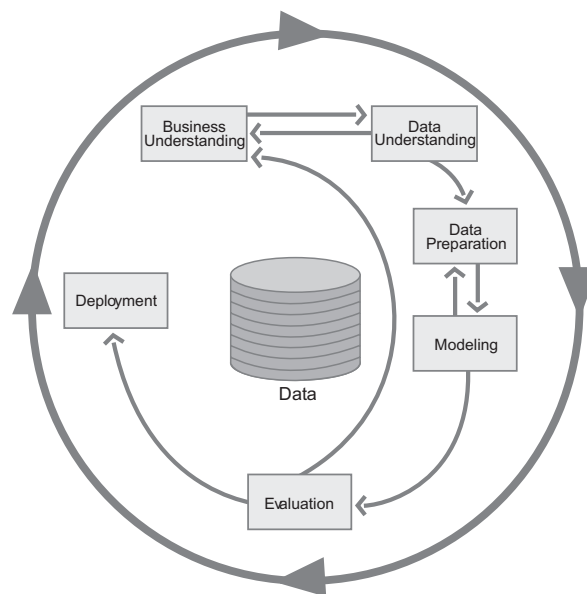


**Figure 3.5:** Stages of the CRISP-DM process (Chapman *et al.*, 2000)

The SEMMA methodology was developed by the SAS institute which is a company that delivers services in the areas of DM and decision support. It is composed by five main stages (Figure 3.6):

- **Sample:** selection of a representative sample from the studied universe.
- **Explore:** using statistical and visualisation techniques to get an insight on the data in order to discover tendencies and/or anomalies.
- **Modify:** proceed with the transformations identified in the previous step if any. An example of these transformations is the inclusion of new attributes.
- **Model:** definition and application of the appropriate DM techniques in order to achieve the objectives of the study.
- **Assess:** evaluation of the obtained models in order to infer about their performance.

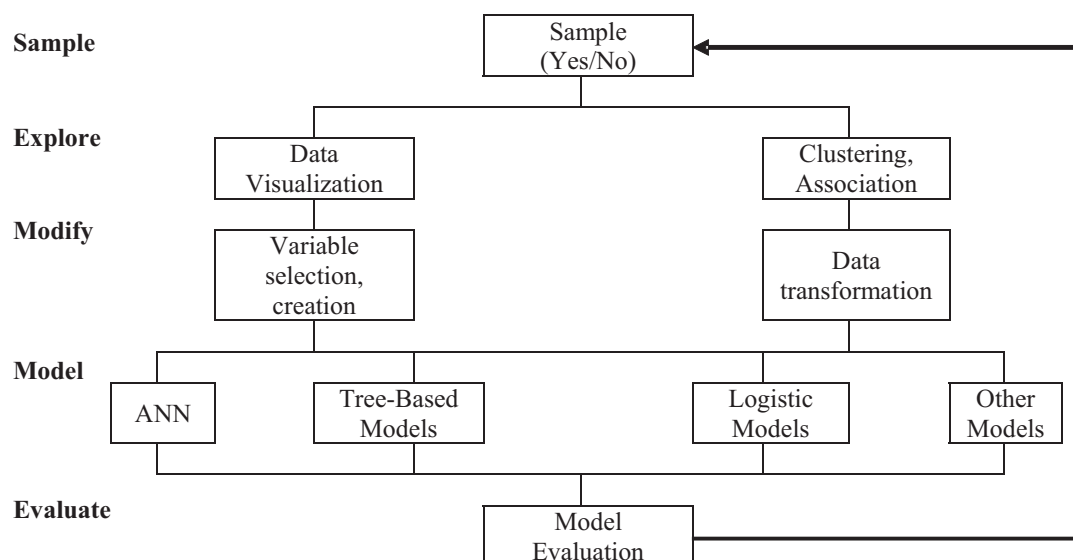


*Figure 3.6:* Stages of the SEMMA methodology (Bulkley *et al.*, 1999)

### 3.3.3 Models and techniques

The main issue of the DM task is building a model to represent data. In this step of the KDD process, learning occurs by adopting a search algorithm for training. This process occurs over a training set until a given criteria is met. After training, the model is built and its quality is normally evaluated over a test set not used for training.

There are several different models but there is no universal one to efficiently solve all the problems (Harrison, 1998). Each one presents specific characteristics (advantages and drawbacks) which make them better suited in a certain case. This section will present the modelling

techniques used in this work with exception to the linear and multiple regression which are widely known.

### Decision trees and rule induction

A decision tree is a direct and acyclic flow chart that represents a set of rules distinguishing classes or values in a hierarchical form. These rules are extracted from the data, using rule induction techniques, and appear in an "If-Then" structure, similar to the rule presented in Figure 3.4, expressing a simple and conditional logic. Source data is splitted into subsets, based on the attribute test value and the process is repeated in a recursive manner. Graphically they present a tree structure and are formed by three main components.

- The top node or root that represents all the data.
- Branches which connect nodes. Each internal node represents a test to an attribute while the branches denote the outcome of the test.
- Leafs which are terminal nodes represent classes or values.

Considering again the previously described example of the hypothetical classification system, in Figure 3.7 it is presented a possible classification tree for this case where the different components are identified. Each path between the root to a leaf correspond to a decision rule. In this case an example of a decision rule could be:

$$\text{If } \sigma_c < 70 \text{ and } RQD < 50 \text{ then class} = \text{Bad} \quad (3.1)$$

After a tree is learned it can be used to classify or calculate the value of a new object. There are two types of decision trees, namely classification and regression trees (Berry and Linoff, 2000). These two types of trees use the same structure. The only difference is the type of the target variable. Classification trees are used to predict the class to which data belongs while regression trees are used to estimate the value of a continuous variable based on induced mathematical expressions.

The CART algorithm, the acronym for Classification And Regression Trees, developed by Breiman *et al.* (1984), is one of the most popular algorithms used for inducing decision trees. It splits the data using a predictor that can be used several times at different levels. At each stage data is partitioned so that the cases of the two created subsets are more homogeneous than the previous one. It grows only binary trees (i.e., trees where only two branches can attach to a single root or node) so, even though its high flexibility, it can sometimes be unreliable and computationally slow.

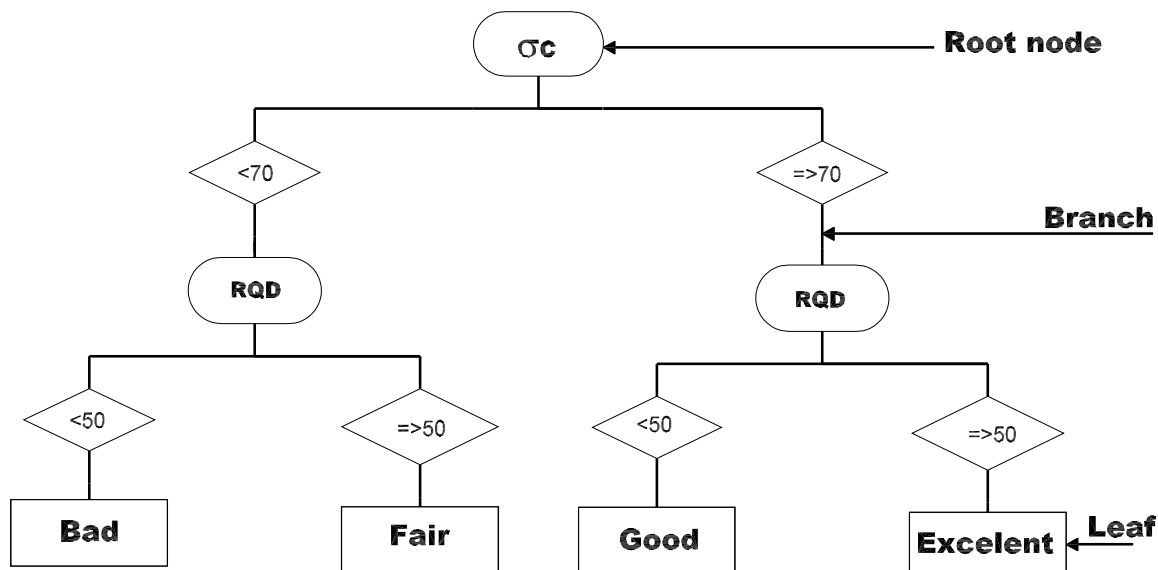


Figure 3.7: Example of a decision tree.

Other very common algorithm is CHAID (CHI-square and Automatic Interaction Detection). Developed by Kass (1980) it is one of the oldest algorithms. CHAID is able to grow non-binary trees. For each potential predictor CHAID merges all values judged to be statistically homogeneous with respect to the target variable and then the best predictor is chosen. For classification problems it relies on the Chi-square test to determine the best next split at each step while for regression problems it computes the F-test. The process is repeated until the tree is fully grown.

Both CART and CHAID algorithms are capable to construct trees which can be applied to analyse regression or classification problems with good results. Nevertheless, the fully automated process may result in an overstructured inefficient tree. Moreover, many of the branches may reflect noise or outliers in the training data. Tree pruning attempts to identify and remove such branches and simplify the tree, with the goal of improving accuracy on new data.

The greatest benefits of decision trees approach are that they are easy to understand and interpret. They use a "white box" model, i.e. the induced rules are clear and easy to explain as they use a simple conditional logic. Additionally, they can deal with categorical and continuous variables. The main drawback is that they get harder to manage as the complexity of data increases leading to a higher number of branches in the tree.

### Artificial Neural Networks

Artificial Neural Networks (ANN), developed in the scope of AI, were conceived to imitate the biological networks of neurons found in the brain. They are formed by groups of connected



artificial neurons in a simplified but very similar structure to the brain neurons. Like the biological structures, ANN can be trained and learn from a set of examples to find solutions to complex problems, recognise patterns and predict future events. The acquired knowledge can then be generalised to solve new problems. This means that they are self-adaptive systems.

Biological neurons are composed by a nucleus and are connected with millions of other neurons (Figure 3.8). They receive electrochemical inputs from their neighbours through connections called synapses. The synapses are formed by axons and dendrites. Neurons form complex, non linear and highly parallel structures.

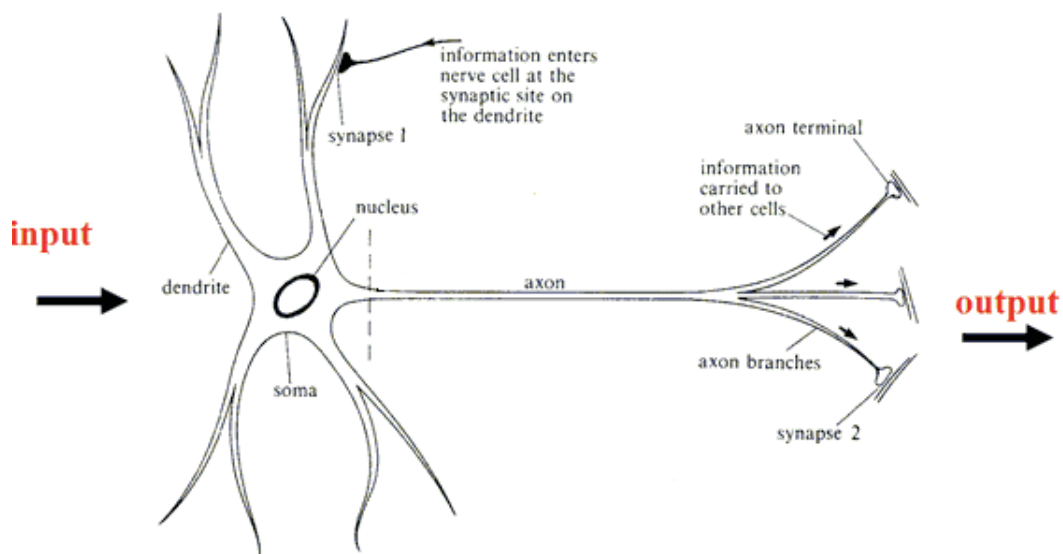


*Figure 3.8:* Human neuron.

The principles of ANN were established by McCulloch and Pitts (1943) and have been developed since. ANN are complex parallel computational structures based on connected processing units (neurons) organised in layers. Neurons communicate using signals through input/output connections and each connection has an associated weight. The neuron multiplies each input with the weight of the associated connection. The total input is the sum of all weighted inputs. Finally, an activation function is applied in order to relate the input (stimulation) to the output (response) (Sakellariou and Ferentinou, 2005). Figure 3.9 presents a scheme of an artificial neuron. It is composed by three main elements (Cortez, 2002):

- a set of connections which represent synapses.

- the neuron which reduce several inputs to one output.
- an activation function which limits the output amplitude of the neuron and introduce a non-linear component.

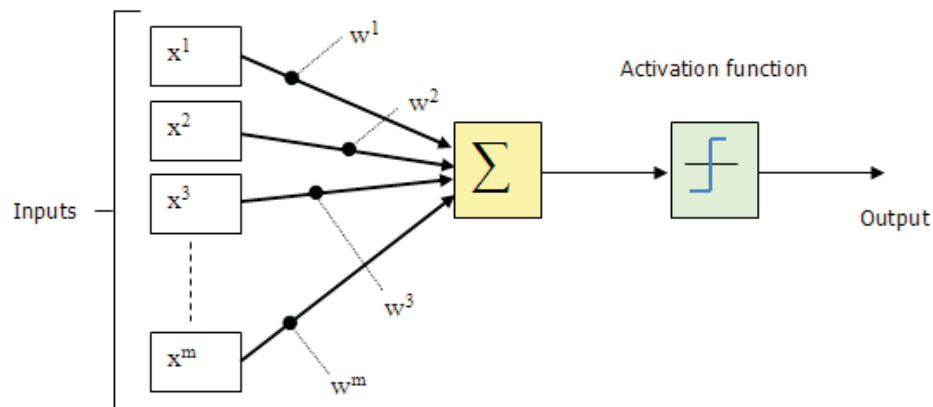


**Figure 3.9:** Scheme of an artificial neuron configuration.

The most used activation function is the sigmoid (Figure 3.10). It is translated by the following equation:

$$f(x) = \frac{1}{1 + e^{(-ax)}} \quad (3.2)$$

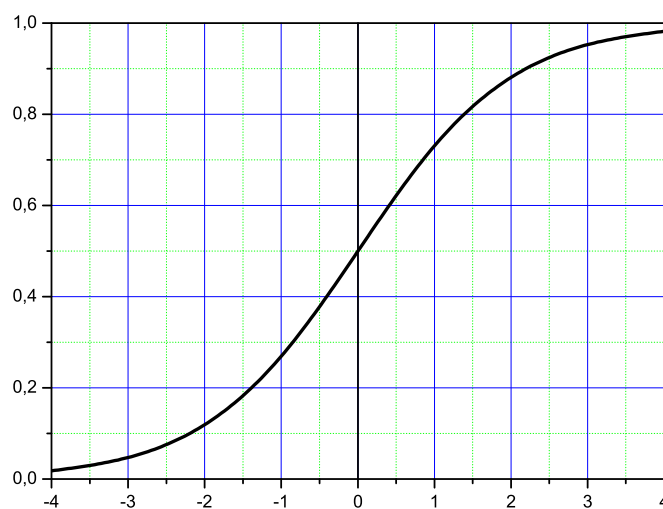


**Figure 3.10:** Sigmoid activation function.

In an ANN, neurons can be connected and organised in many different ways (Santos and Azevedo, 2005).

- Fully connected networks: each neuron is connected to all neurons in the net.
- One layer networks: composed by two layers - input and output. The input layer is not considered because it does not perform any calculations.
- Multi-layer networks: composed by different parallel layers. The first is the input and the last the output layer. Intermediate ones are called hidden layers (Figure 3.11). This is the most common type of network.

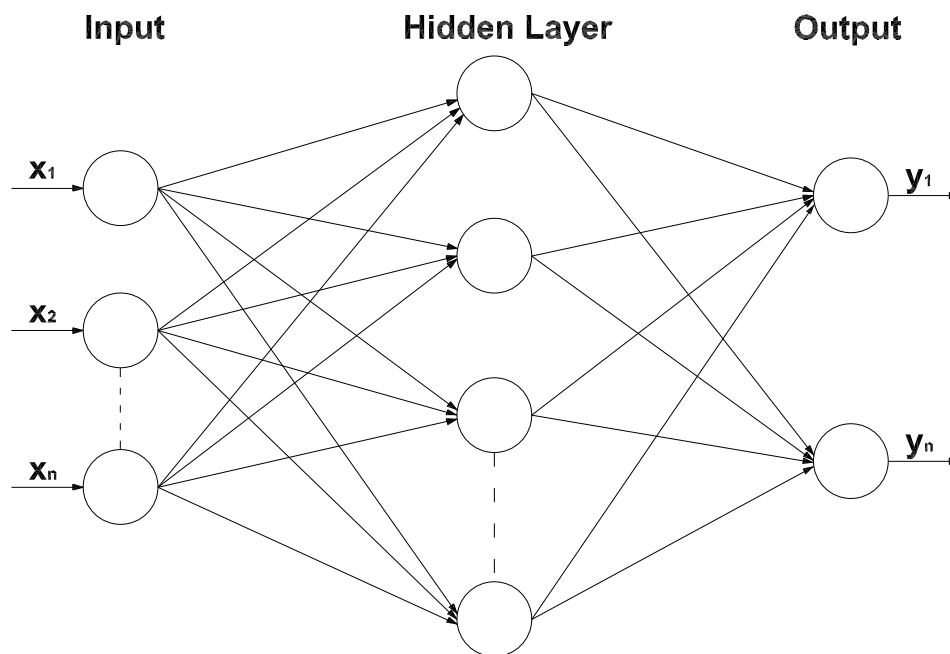


*Figure 3.11:* Scheme of a multi-layer network.

The connection structure of neurons in a network is normally called architecture or topology. There are several architectures, each one with its own potentialities, but the most used is the multilayer feed-forward (also represented by Figure 3.11). In this type of topology, connections are unidirectional (from input to output) and there are no connections between neurons in the same layer forming an acyclic network. On the other hand, in the recurrent topology, the output neurons can be connected with input ones forming cycles, conferring a spatial and/or temporal non linear behaviour to the network.

Optimising a network topology is a trial and error process for there is no rule to define *a priori* the best topology. The initial values of the weights, which are initialised by the user

normally with small random numbers, may affect the results accuracy. This way, when the accuracy of the network is not acceptable, it is common to define a different topology and to initialise the weights with a different set of values.

The learning process of an ANN is carried out using specific algorithms with very well defined rules. In this context, there are three main methods, normally called paradigms, where learning of ANN lies:

- supervised learning;
- unsupervised learning;
- reinforcement learning.

In supervised learning, examples of the inputs together with the correspondent outputs are used in the training process. This allows the network to learn the patterns embedded in the examples. During training, the outputs of the network are compared with the real values resulting in an error measure. This error is used to adjust the weights of the connections in order to minimise it in an iterative process. This type of learning is typically used for modelling dynamic systems, and in classification and prediction problems.

In unsupervised learning the outputs are not presented to the network. Learning is carried out through the identification of certain characteristics within the input data like statistical regularities and clusters. It is mostly used to discovery non-linear patterns within the data.

Reinforcement learning lies close to the supervised learning with the difference that the correct answer is not given to the network. Only a warning about if the network answer is correct is provided. Using this information the network adjusts itself in order to optimise its efficiency.

Concerning supervised learning, which was used in this work, there are several different models that have been implemented on ANN. Perceptron networks were the first to be developed. They are one layered feed forward networks with several inputs and outputs. Perceptrons are very simple to use however they are only applicable to problems with low complexity.

Back-propagation networks appeared latter as a solution to many of the restrictions in perceptron type networks and are the most widely used paradigm in supervised learning. They are a non linear extension of perceptrons and consist in networks where neurons are distributed in two or more layers. The back-propagation algorithm performs learning in multilayer feed-forward networks. It is based on the selection of an error function whose value is determined by the difference between the outputs of the network and the real values. This function is minimised through the correction of the weights in an iterative process normally using the steepest descent method (Hush and Horne, 1999). The objective is to move in the "weight

space” down the slope of the error function with respect to each weight. The slope is the partial derivative of the error with respect to the weight. The learning is ended when the stopping criterion is met. This may be when a sufficiently low error is reached or when there is a low rate of error change in consecutive iterations. The rule for the adaptation of weights is called the generalised delta rule.

The training consists in two distinct phases.

- Forward phase: the input vector is given to the network and the weights are fixed.
- Backward phase: the weights are adjusted in accordance with the error which is propagated backwards against the direction of the connections.

Back-propagation networks are powerful learning tools and have been used with success in several applications. They are able to learn from noisy and highly non linear data and can recognise different sets of data within a broader data set. Moreover, they do not require any pre-existing knowledge and statistical models. However, there are some disadvantages that have to be considered. The computational time during training process can be very high. As they use a minimisation technique like the steepest descent, convergence can be attained to a local minimum which is not an issue if a significant number of cases are used for training. The induced models can perform poorly outside its range of training. Attention may be drawn to the possibility of overtraining the network. Networks with many hidden nodes have the ability to ”memorise” the desired output instead of learning the patterns. The problem of how many hidden neurons to have in a network is still an active research issue. The last and probably the main drawback is that the models induced by the networks are not comprehensible to the user. They are known as ”black box” models since they give the answer but do not transmit the knowledge behind that answer. This way, there is lack of any theoretical basis for validation of the outcomes produced by the networks. Nowadays, research is ongoing for the development of algorithms for the extraction of rules from trained neural networks. This factor contributes toward the usefulness of ANNs in DM.

### **Model evaluation**

After generating the models it is necessary to evaluate their future performance. Normally, this is carried out applying the model to a set of examples not used to induce it. Holdout and cross-validation are two common techniques for assessing the models accuracy, based on randomly-sampled partitions of the data.

In the holdout method data is randomly partitioned into two independent sets, a training set and a test set. Typically, two thirds of the data are allocated to the training set and the

remaining to the test set. Nevertheless, there is no theoretical background to support these values. The training set is used to induce the model whose accuracy is estimated with the test set. The estimate is pessimistic since only a portion of the initial data is used to derive the classifier.

In cross-validation, data is randomly partitioned into  $k$  mutually exclusive subsets randomising for each one the cases within the training and test set. Training and testing is performed  $k$  times and the overall error of the model is taken as the average of the errors obtained in each iteration. The values of  $k$  can vary between 2 and  $n$  (number of cases) however a commonly considered value is 10. It allows using all the available cases in training and testing. The accuracy of this technique involves a considerable computational effort (Cortez, 2002).

There are several evaluation techniques that can be applied to the models depending if it is a regression or a classification problem. In regression problems the goal is to induce the model which minimises an error measurement between real values and the ones predicted by the model. The most used error measurements are the following:

$$\text{Mean Absolute Deviation} = \text{MAD} = \frac{\sum_{i=1}^N |e_i|}{N} \quad (3.3)$$

$$\text{Sum Squared Error} = \text{SSE} = \sum_{i=1}^N e_i^2 \quad (3.4)$$

$$\text{Mean Squared Error} = \text{MSE} = \frac{\text{SSE}}{N} \quad (3.5)$$

$$\text{Root Mean Squared Error} = \text{RMSE} = \sqrt{\text{SSE}} \quad (3.6)$$

where  $N$  is the number of examples. More than one measurement should be used when evaluating the performance of a model since they measure different types of errors. For instance, MSE penalises the models which commit extreme errors since it uses the square of the distance between the real and predicted values. Even if the model presents very low errors in most of the cases the MSE will be high if only in a few cases the error is very high. In the other hand, the MAD will be relatively low if in most of the times the model presents a good behaviour even though with some extreme values. This way, these error measurements give different and complementary perspectives about the behaviour of the induced models.

Another way to evaluate the capabilities of the models is to compute the determination coefficient ( $R^2$ ) which is very common in many statistical applications. This parameter is a measure of variability explained by the model but should not be used alone for it can lead to

wrong conclusions. It varies between 0 and 1 and a value near 1 may mean that the model explains most of the data.

The observation of the residuals plot against the independent variable or simply a histogram of errors can help the model performance evaluation and the outlier detection. Non-normality in an error histogram suggests that the model may not be a good summary description of the data. In a residual plot against the independent variable there should be no discernible trend or pattern for a satisfactory behaviour of the model. In fact, an increasing pattern for the error may mean that the linear relation is not the most suitable for the data. In this case, for instance, a logarithm transformation of the variables can be tried. If one residual is much higher than the others it suggests that there is one unusual observation or outlier distorting the fit. This value should be verified and can be eliminated if there is a concrete or empirical reason to do it.

For classification problems one of the most used techniques is the confusion matrix (Kohavi and Provost, 1998). It is used to evaluate the results of a classification indicating the predicted values versus the correct ones. In the lines are disposed the real classes while in the columns the predictions performed by the model. In the main diagonal it is indicated the number of correct guesses while the remaining indicate errors. In Table 3.1 it is presented the confusion matrix for an example with two classes. In this example the classes are designated as positive and negative.

**Table 3.1:** Confusion matrix for two classes

<b>Class</b>	<b>Predicted <math>C_1</math></b>	<b>Predicted <math>C_2</math></b>
<b>Real <math>C_1</math></b>	True Positive TP	False Negative FN
<b>Real <math>C_2</math></b>	False Positive FP	True Negative TN

With this matrix it is possible to calculate important measures for the model evaluation:

$$\textit{Specificity} = \textit{spec} = \frac{TN}{TN + FP} \times 100\% \quad (3.7)$$

$$\textit{Sensitivity} = \textit{sens} = \frac{TP}{TP + FN} \times 100\% \quad (3.8)$$

$$\textit{Accuracy} = \textit{tacc} = \frac{TP + TN}{N} \times 100\% \quad (3.9)$$

$$\textit{Precision} = \textit{prec} = \frac{TP}{TP + FN} \times 100\% \quad (3.10)$$

Another way of evaluating classification models is the ROC (Receiver Operating Characteristic) curve. It is appropriate when there are only two classes as in the previous example. The ROC curve establishes the relation between the specificity and sensitivity of a model. In the ideal situation the model should have maximum values of these indicators equal to one. The AUC (Area Under Curve) is a performance measure obtained by the calculation of the area under the ROC curve. It can assume values from 0 to 1 and can be interpreted as the probability of a "true" example, chosen randomly, to be classified as such.

### 3.4 Final remarks

The vast amounts of data which are produced in the different activity fields can not be adequately explored and analysed using classical tools like statistics. Deeper understanding of data and relationships or patterns embedded in highly complex databases urge the need of using "intelligent tools" to uncover them and transform it into useful knowledge. The overall process of the intelligent knowledge discovery in complex databases is called Knowledge Discovery in Databases (KDD). Data Mining (DM) is only a step of this process related to the application of the algorithms to induce the models.

DM is a recent field of computer science that is related with several fields like statistics, machine learning and AI. These tools are currently used in many fields like economics, insurances and medicine among others. In the particular case of geotechnical engineering, vast quantities of data are produced associated, for instance, to important underground structures. However, and in spite of some successful applications which were briefly cited, its use it is not yet widespread.

In civil engineering, modelling is normally carried out by means of "knowledge-driven" models through techniques like the finite element methods. In some areas, like in geotechnics, experience plays an important role mainly in the decision support under uncertainty. In this case, normally a set of specialists guide the process in what was called "expert-driven" models. Finally, the data from the actual and past projects can also be used to guide the decisions concerning a certain project. This "data-driven" models are already used in practice at a certain extent (in the form of correlations, for instance) but the application of DM techniques could enhance the way the geotechnical data is managed. If standard ways of organising and exchanging data were defined and followed by the overall geotechnical community, at short term very large databases of important data should be available and ready to be analysed using these automated tools. The knowledge that could be inferred from such databases could turn the "data-driven" models as an invaluable tool in geotechnical projects with direct implications in reliability, safety and costs.

The main contribution of this chapter is the positioning of this problem and the description



of the potentialities of the DM tools in the improvement of the "data-driven" models in geotechnics and more specifically in the underground works field. Since it is an area which is not widely known the fundamentals of KDD and DM were presented. The DM step was particularised in its main features namely tasks, methodologies, models and techniques with especial emphasis to the ones which are going to be applied in the following Chapter.



# New Models for Geomechanical Characterisation Obtained Using DM Techniques

## 4.1 Introduction

The evaluation of geomechanical parameters in underground works correspondent to the preliminary stages of design, defined as level 1 of decision in Chapter 1, is normally carried out based on scarce and uncertain data. The overall methodologies to obtain the parameters at this point of the project are similar to the ones used in more advanced stages. As stated in Chapter 2, this task can be carried out directly by means of *in situ* and laboratory tests and indirectly by the application of empirical methodologies. These methodologies allow obtaining an overall description of the rock mass and the calculation, through analytical solutions, of strength and deformability parameters which are determinant in design. The analytical solutions should be used with caution outside the boundaries of the rock formations based on which they were developed.

However, in the preliminary stages of design of an underground structure, some data about the rock mass can be difficult to obtain and it is possible that the complete information for the empirical systems application may not be available. Moreover, only a limited number of *in situ* and laboratory tests are possible to perform.

It is then rational to think that, when a small amount of data from the present project is available, as it happens in the preliminary stages, geomechanical information concerning other works, developed in similar rock masses, can help in the task of defining values for the parameters. It is indubitable that this data exists for instance when large underground

structures are built.

The fundamental question that needs to be addressed is how this data can be used in a rational way in order to provide some background for future projects. It is believed that the automated tools of data analysis like DM are capable to help in this task allowing to develop what was called in the previous Chapter as "data-driven" models. These tools could be used to explore the geotechnical information gathered in large and organised databases to find patterns and models, i.e. to uncover new and useful knowledge embedded in the data. It is not only a question of applying some tools which can by themselves analyse and interpret the data substituting the human experts. A KDD process must always be developed or at least supervised by experts in the field in order to make decision along the process and analyse the outputs. These tools only allow to more deeply analyse the data which would be very difficult using classical tools like statistics or through one or even a panel of human experts that could overlook important details. The knowledge discovered in the process must be explainable at the light of science and experience and must be always validated before being used in other applications.

In this work, it is intended to develop an innovative study using DM analysis tools applied to a database of geotechnical information. The broad goal is to show, in practical terms, the potentialities of DM techniques in the geotechnics field and how a study of this nature can be carried out providing a contribute for bridging the gap between the areas of data analysis and geotechnics. More specifically, it was intended to develop new and reliable alternative regression and classification models that could be used for geomechanical characterisation of rock masses, especially when only scarce information is available. The innovative character of the study implies the existence of some flaws and limitations that will be properly pointed out.

The data used in this study was assembled from the Venda Nova II powerhouse complex which is an important underground work recently built in the North of Portugal. The interested rock mass is a granite formation so the conclusions drawn in this study are only applicable to formations with similar characteristics. The overall DM process was carried out in three main steps.

- Collect geotechnical data from the Venda Nova II powerhouse complex mainly from the empirical classification systems application.
- Build and organise a database with the data.
- Explore the data using DM techniques to induce the models.

Concerning the regression models, the main goal was to develop alternative ways for the prediction of coefficients (RMR and Q) and geomechanical parameters (deformability modulus

-  $E$ ; friction angle -  $\phi'$ ; cohesion -  $c'$ ) (Oliveira *et al.*, 2006). The Mohr-Coulomb strength parameters were chosen because it is possible to obtain the Hoek-Brown (H-B) parameters using relatively simple expressions based on the GSI. In fact, the calculation of the Mohr-Coulomb parameters, from the linearisation of the H-B failure envelope, is more complex and it was thought that developing models that could simplify this process could be more useful.

These models were expected to have higher accuracy than the existing ones or that they use less information but maintaining a high predictive accuracy. This last group is the one that can be more useful in the preliminary design stages in any case where geological/geotechnical information is limited. Also, it is aimed that the models provide an insight of which parameters are the most influent on the structural behaviour of the rock mass and find possible physical explanations. The used DM techniques were multiple regression analysis and ANN.

The RMR system allows classifying the rock masses into five different classes related to their geomechanical properties. For each class it is possible to obtain support needs, type and excavation sequence, a range for the geomechanical parameters, stand-up time, among others. For the classification process, the values of the six weights -  $P_1$  to  $P_6$  - are needed in order to compute the RMR, which means that a great amount of geomechanical information has to be available. As mentioned, this information can be difficult to obtain. All the classification process is deterministic, since the evaluation of the weight values to the final definition of the class. This can be a drawback since normally it is only possible to obtain approximate values of the weights or a possible range for them.

In this context, it was intended to develop an alternative classification scheme that could overcome the mentioned difficulties. This way, DM classification techniques, particularly decision trees, were applied to the same database used for the regression models. Decision trees are branching structures based on split nodes, that test a given feature, and leaves, which assign a class label. Thus, it was possible to develop a new system based on the RMR which was called Hierarchical Rock Mass Rating (HRMR). The HRMR does not need the deterministic calculation of the RMR value to obtain a certain classification to the rock mass. It adapts to the level of knowledge about the weights used by this system and provides a probabilistically-based classification with a certain degree of accuracy. Obviously, as more information is gathered the accuracy of the system increases.

For both regression and classification models the CRISP-DM methodology was applied in the process of knowledge discovery. In the next sections, the main issues concerning the different steps of the process are presented as well as the main results and their interpretation.

## 4.2 Data understanding and preparation

The available data were mainly applications of the empirical systems and results from laboratory (uniaxial compression strength and sliding of discontinuities) and *in situ* tests (SFJ, LFJ and dilatometers) (LNEC, 1983, 2003, 2005). Concerning the empirical classification systems applications, data was dispersed into 110 spreadsheet files. It was necessary to perform data cleaning tasks by removing duplicated records contained in these files. Data was then organised and structured in a database composed of 1230 examples and 22 attributes which are described in Table 4.1.

**Table 4.1:** Initial attributes of the database

Name of the attribute	Description
RQD	<i>Rock Quality Designation</i>
$J_w$	Factor related with the underground water
$J_n$	Factor related with the number of discontinuities sets
$J_r$	Factor related with discontinuities rugosity
$J_a$	Factor related with the weathering degree of discontinuities
SRF	Factor related with the stress state in the rock mass
Q	Rock mass quality index proposed by Barton <i>et al.</i> (1974)
Q'	Altered form of the Q index ( $Q' = RQD/J_n \cdot J_r/J_a$ )
RCU	Uniaxial compressive strength (or $\sigma_c$ )
$P_1$	Weight related with the uniaxial compressive strength of the intact rock
$P_2$	Weight related with the RQD
$P_3$	Weight related with discontinuities spacing
$P_4$	Weight related with discontinuities conditions
$P_5$	Weight related with the underground water conditions
$P_6$	Weight related with discontinuities orientation
$P_{41}$	Discontinuities conditions - persistence
$P_{42}$	Discontinuities conditions - aperture
$P_{43}$	Discontinuities conditions - rugosity
$P_{44}$	Discontinuities conditions - filling
$P_{45}$	Discontinuities conditions - weathering
RMR	Rock Mass Rating proposed by Bieniawski (1978)
class	Classification of the rock mass based on the RMR value

Some of the variables histograms (in Annex I are reported the histograms of all variables) presented skewed distributions and others only assumed a few different values. Figure 4.1 presents the histogram of the RMR variable which is one example of a skewed distribution. This fact can influence the quality of the induced models specially those based on ANN since this kind of algorithms can learn better the behaviour of normally distributed variables. In some

cases, a variable transformation (logarithmic, exponential, etc.) helps to increase its normality. Some preliminary trial calculations pointed out to the improvement of the results when this transformation was carried out. This way, it was decided to proceed to the transformation of some variables in order to maximise their normality.

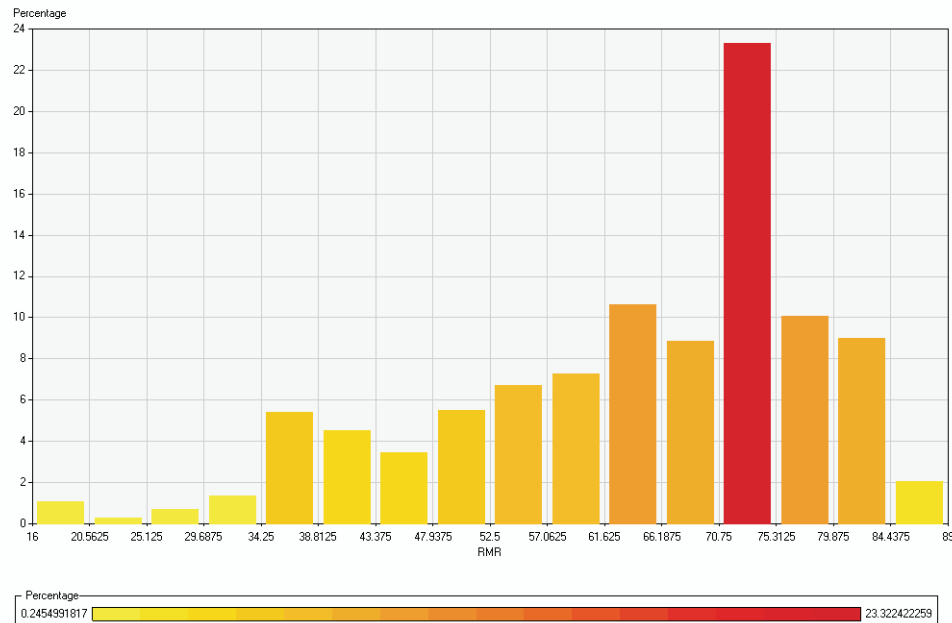


**Figure 4.1:** Histogram of the RMR variable.

From the attributes of the database it was possible to calculate others including the geomechanical parameters. First, the H-B strength parameters were computed and then  $c'$  and  $\phi'$  were derived by fitting an average linear relationship to the generated failure envelope which is formulated in effective stresses (Hoek *et al.*, 2002).

The Mohr-Coulomb parameters derived from the H-B criterion are peak values. For poorer rock mass conditions the peak and residual parameters can be considered similar, since a perfectly plastic post-peak behaviour can be assumed. For average and good rock masses, they exhibit, respectively, a strain softening and a brittle post-peak behaviour, with associated dilatancy which is more pronounced for the last case. For good quality rock masses, a null residual  $c'$  and a  $\phi'$  25% lower than the peak value can be considered (Hoek, 2001). Alternatively, as referred in Chapter 2, it is possible to use the formulation proposed by Carvalho *et al.* (2007) to obtain the H-B parameters for the extreme ends of the rock competency scale. For average rock mass conditions it is reasonable to assume that the residual strength parameters can be obtained using the H-B failure criterion using a reduced GSI value which characterises the

broken rock mass.

For the calculation of the H-B strength parameters, a comparative study between the methods proposed by Hoek *et al.* (2002) and Douglas (2002), described in Chapter 2, was carried out.

The mean  $\phi'$  derived using Douglas formulae ( $57.2^\circ$ ) is approximately 6% higher than the value correspondent to the Hoek *et al.* methodology ( $53.9^\circ$ ) which means that the difference in this particular case is not significant. The main difference is found in the  $c'$  values. In fact, the ones obtained using Douglas method (mean value of 11.6 MPa) are much higher than those by Hoek *et al.* which mean value is only about 33% (3.8 MPa) of the mean  $c'$  obtained with Douglas method. Based on experience and empirical knowledge, the computed values by the methodology developed by Hoek *et al.* are more reasonable. The reasons for such difference are outside the scope of this work but it can be related with the fact that Douglas method was developed mostly to enhance H-B criterion for poor rock mass conditions. The studied database presents a small number of records concerning this type of rock mass, therefore, probably Douglas method needs to be fine tuned for better geomechanical properties rock masses. Thus, in this work, the adopted methodology for the calculation of strength parameters was the one defined by Hoek *et al.*

The prediction models for  $\phi'$  and  $c'$  were developed considering a reference depth (H) of 350 m (the depth of the main caverns of the powerhouse complex) and a disturbance factor (D) of 0. To allow a simple and direct transformation of the values predicted by the models for another conditions (different H and D) a parametric study was carried out. Based on this study, a generic methodology for transforming the geomechanical parameters for a given H and D to another different pair of values was developed and then particularised for the DM models. The generic methodology is based on the application of two correction factors, one for each parameter, and is described in Annex II along with a calculation example.

The deformability modulus (E) is an important input parameter in any rock mass behaviour analysis. However, this parameter is not an intrinsic material characteristic since it depends on other variables, mainly the associated strain level. In fact, there are several different deformability moduli that can be defined. The value to use in design should be associated to the expected level of strains according to the serviceability limit state of the structure.

Generally, there is an agreement that the strains interesting the serviceability of geotechnical structures ranges from 0.001% to 0.5% (Gomes Correia *et al.*, 2004). Consequently, ground behaviour from small to medium strains should be accurately characterised. Both soils and rocks demonstrate an approximate elastic behaviour at very small and small strains and a non-linear pre-failure behaviour at medium strains. This way, it is very important to define and identify the type of modulus that will be adopted for design purposes.



This subject has been an important research issue mostly in the particular case of soil formations and many advances have been reached in the last years. For instance, the development of high precision deformation measurement devices for the triaxial test, which allow assessing very small and small strains, can be mentioned. This important improvement provides a more correct definition of E versus strain levels curve.

However, the question is substantially different in rock formations. The intact rock is not representative of the overall rock mass deformability behaviour like it happens in a larger scale with soil samples. To a more correct definition of E considering all factors which govern the deformation behaviour of the rock mass, large scale *in situ* tests are needed. They can be very time consuming, expensive and their reliability can be sometimes doubtful (Hoek and Diederichs, 2006). Because of these difficulties, back analysis procedures can constitute a source of reliable information about the rock masses characteristics.

This way, most procedures that can be found in literature to estimate this parameter for isotropic rock masses, are based on simple expressions related to the empirical systems or other index values like the RQD (Zhang and Einstein, 2004) and the intact rock modulus (Mitri *et al.*, 1994; Sonmez *et al.*, 2004; Carvalho, 2004).

Miranda (2003), in the framework of the development of a knowledge based system for the calculation of geomechanical parameters, carried out a comparative study of these expressions selecting those which presented best results based on empirical judgment. In the present work, to calculate E of the granite rock mass, the expressions selected in that comparative study were used. Complementarily, the results of other expressions found in the meantime were also studied and it was decided to add to the first selection some other expressions: the one by Read *et al.* (1999) and the two proposed by Hoek and Diederichs (2006). The first was chosen because all exponential equations give poor fits to the experimental data for very good quality rock masses. This is because of the inadequately definition of the asymptotes and this equation uses a third power curve to better define them. The expressions by Hoek and Diederichs (2006) were also added because they are based in a very large database of cases gathered in China and Taiwan and validated by historical measurements from several countries. Some expressions use the elasticity modulus of the intact rock ( $E_i$ ) in order to compute E. That parameter was not available in a great amount of cases and therefore to estimate  $E_i$  a correlation with  $\sigma_c$  developed by Miranda (2003) was applied. The used expression together with their limitations and authors are presented in Table 4.4.

It is important though to define what kind of E these equations lead to. As shown in Figure 4.2, there are several alternative types of E values that can be defined for a specific rock mass. Most authors have based their expressions on field test data reported by Serafim and Pereira (1983) and Bieniawski (1978) and, in some cases, by Stephens and Banks (1989). They mostly

**Table 4.2:** Expressions used for the calculation of E.

Expression	Limitations	Reference
$E(GPa) = 10^{(RMR-10)/40}$	$RMR \leq 80$	Serafim and Pereira (1983)
$E(GPa) = 2 \cdot RMR - 100$	$RMR > 50$ and $\sigma_c > 100MPa$	Bieniawski (1978)
$E = \frac{E_i}{100} \cdot 0.0028 \cdot RMR^2 + 0.9 \cdot e^{(RMR/22.28)}$	not limited	Nicholson and Bieniawski (1997)
$E(GPa) = 0.1 \cdot (RMR/10)^3$	not limited	Read <i>et al.</i> (1999)
$E(GPa) = 25 \cdot \log Q$	$Q > 1$	Barton <i>et al.</i> (1980)
$E(GPa) = 10 \cdot Q_c^{1/3}$ ; $Q_c = Q \cdot \sigma_c/100$	$Q \leq 1$	Barton and Quadros (2002)
$E(GPa) = 1.5 \cdot Q^{0.6} \cdot E_i^{0.14}$	$E_i \leq E$ and $Q \leq 500$	Singh (1997)
$E = \left(1 - \frac{D}{2}\right) \cdot \sqrt{\frac{\sigma_c}{100}} \cdot 10^{(GSI-10)/40}$	$\sigma_c \leq 100MPa$	Hoek <i>et al.</i> (2002) (a)
$E = \left(1 - \frac{D}{2}\right) \cdot 10^{(GSI-10)/40}$	$\sigma_c > 100MPa$	Hoek <i>et al.</i> (2002) (b)
$E(GPa) = 100000 \cdot \left(\frac{1 - D/2}{1 + \exp((75 + 25 \cdot D - GSI)/11)}\right)$	not limited	Hoek and Diederichs (2006) (a)
$E(GPa) = E_i \cdot \left(\frac{1 - D/2}{1 + \exp((60 + 15 \cdot D - GSI)/11)}\right)$	not limited	Hoek and Diederichs (2006) (b)

refer to the secant modulus, typically for deformations correspondent to 50% of the peak load. It is thought that this deformation is higher than the serviceability levels present in most of the geotechnical works built in rock masses. This way, it is expected that this expressions typically provide conservative estimates of E.

To validate the obtained values, the results of a LFJ test (LNEC, 1983, 2003), which allowed obtaining 160 values of E due to several performed loading/unloading cycles, were compared with the calculated values of E obtained near the zone where the test took place. Table 4.3 resumes some statistical results of this assessment.

**Table 4.3:** Comparison between calculated and measured values of E.

<b>E(GPa) - LFJ</b>				<b>E(GPa) - calculated</b>			
N	Mean	95% confidence interval for the mean	Std. deviation	N	Mean	95% confidence interval for the mean	Std. deviation
160	36.9	35.9-37.8	6.1	76	38.5	34.5-42.5	16.6

The mean values of E are very similar. The main difference is the higher variation in the

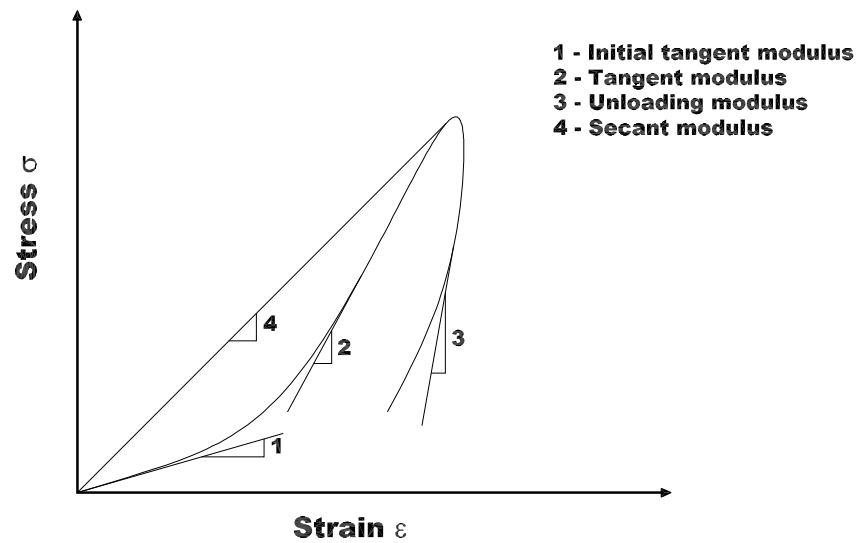


*Figure 4.2:* Alternative definitions for the deformability of a rock mass.

calculated values. This fact can be considered normal since the LFJ tests are much more accurate for measuring  $E$  than the empirically based expressions. Thus, it can be concluded that the calculated values agree well with those obtained by reliable *in situ* tests and can be considered as realistic and precise prediction.

In order to have an insight of the results from the analytical expression application, in Table 4.4 it is presented, for each expression: the number of times it was calculated, the number of times the result was within a considered reasonable interval ( $\pm$  one standard deviation from the mean value given by all expressions) and the ratio between these two previous values.

In general, the expressions gave similar results and most of the times they laid within the considered interval with the exceptions of those proposed by Hoek and Diederichs (2006) (a) and Bieniawski (1978). Normally, the results of these expressions were lower than the ones obtained by the described methodology and should be used with caution when analysing granite formations.

After their calculation, the geomechanical parameters were added to the database along with other attributes in order to check their possible influence on the models. Globally, 10 new attributes were added and are presented in Table 4.5.

As it can be observed, some variables are directly dependent on other variables. This way, it is expected that this dependency will be translated when analysing the most important parameters for each of the target variables. For instance,  $\phi'$  and  $c'$  are computed based on the H-B parameters which by their turn are directly dependent on the GSI. This way, it is expected that when analysing  $\phi'$  and  $c'$ , the GSI value appears as an important parameter. This can happen with other parameters and caution should be made to distinguish when the importance

**Table 4.4:** Comparison between the number of times the expressions were calculated with the number of times the result was within the considered interval.

Author(s)	Number of times it was calculated (1)	Number of times within the considered interval (2)	Ratio (2)/(1) %
Serafim and Pereira (1983)	1114	1094	98.2
Bieniawski (1978)	773	447	57.8
Nicholson and Bieniawski (1997)	1222	1221	99.9
Read <i>et al.</i> (1999)	1222	1180	96.6
Barton <i>et al.</i> (1980) and Barton and Quadros (2002)	1215	1055	86.8
Singh (1997)	1209	1088	90.0
Hoek <i>et al.</i> (2002) (a) and (b)	1223	1223	100
Hoek and Diederichs (2006) (a)	1229	36	2.9
Hoek and Diederichs (2006) (b)	1222	1003	82.1

**Table 4.5:** List of attributes added to the original database.

Name of the attribute	Description
$RQD/J_n$	Ratio which represents the compartmentation of the rock mass
$J_r/J_a$	Ratio which represents the shear strength of discontinuities
$J_w/SRF$	Ratio which represents an empirical factor named "active stress"
$\log Q$	Base 10 logarithm of the Q value
$\log Q'$	Base 10 logarithm of the Q' value
GSI	<i>Geological Strength Index</i> proposed by Hoek <i>et al.</i> (2002)
N	Altered form of the Q index ( $N = RQD/J_n \cdot J_r/J_a \cdot J_w$ )
RCR	Altered form of the RMR index ( $RCR = P_2 + P_3 + P_4 + P_5 + P_6$ )
$\phi'$ (D=0)	Friction angle for a disturbance factor D equal to 0
$c'$ (D=0)	Effective cohesion for a disturbance factor D equal to 0

of a variable has physical meaning or if it is the result of a calculation dependency.

There were some missing values within the database. It would be possible to apply a replacement strategy to fill these missing fields like using the most common or the mean value of the attribute. The replacement strategies should only be used when the elimination of the records with missing values can have a significant influence on the quality of the results. The number of records with missing data represent only 2.2% of all the records therefore the choice was to eliminate them.

The final database was composed of a total of 32 attributes. Only the one related with

the class of the rock mass was not numerical. The number of cases within the database was significant and the missing values low.

Almost 60% of the cases in the database were classified as "class II" considering the RMR classification system (Figure 4.3) which means that the data is based on the results obtained in a granite rock mass with an overall good quality. However, and with the exception of "class V", there could be enough cases for the remaining classes (over 100) to consider that the conclusions drawn out from this study are extensive to these classes also.

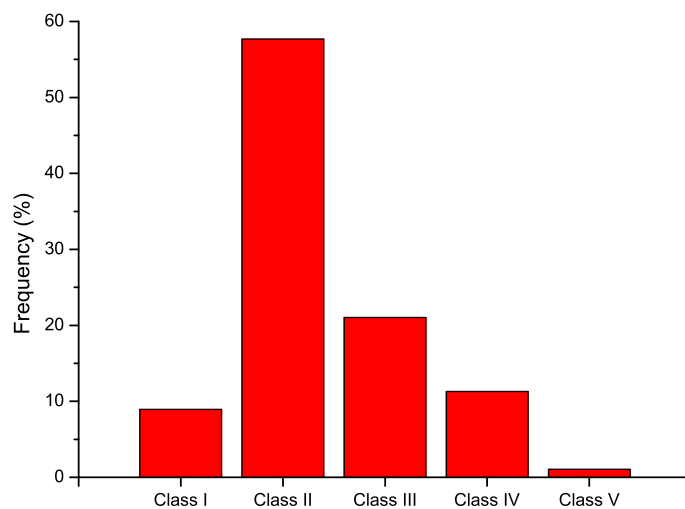


**Figure 4.3:** Histogram of class frequencies in the database.

More specifically, and considering the histograms of each variable of interest, the main limitations that should be considered are: high uniaxial compressive strength ( $\sigma_c > 100MPa$ ), RQD values over 65% and slightly wet to dry rock mass. The models developed in this work should only be applied to rock masses with similar characteristics.

### 4.3 Modelling and evaluation

For the regression models, a methodology was established to define sets of attributes to analyse for each parameter (Oliveira *et al.*, 2006). In general terms, three analysis steps were carried out.

- Induction of models using all the attributes in the database to analyse which were the most important for the considered parameter.

- Induction of models using only a set of the most important attributes.
- Induction of models using a set of easy to obtain attributes or ones which, based on an empirical evaluation, can be related with the parameter.

The SAS Enterprise Miner software, registered trademark of the SAS Institute Inc., was used as modelling tool ([www.sas.com](http://www.sas.com)). It combines statistical analysis with graphical interfaces and delivers a wide range of predictive models. In the SAS Enterprise Miner the DM tasks are carried out programming and connecting nodes in a graphical workspace, adjust settings, and run the constructed workflow. The evaluation of the models was carried out using the results provided by this software and complementary calculations on spreadsheets. In Figure 4.4 the workflow used for in this work is presented.

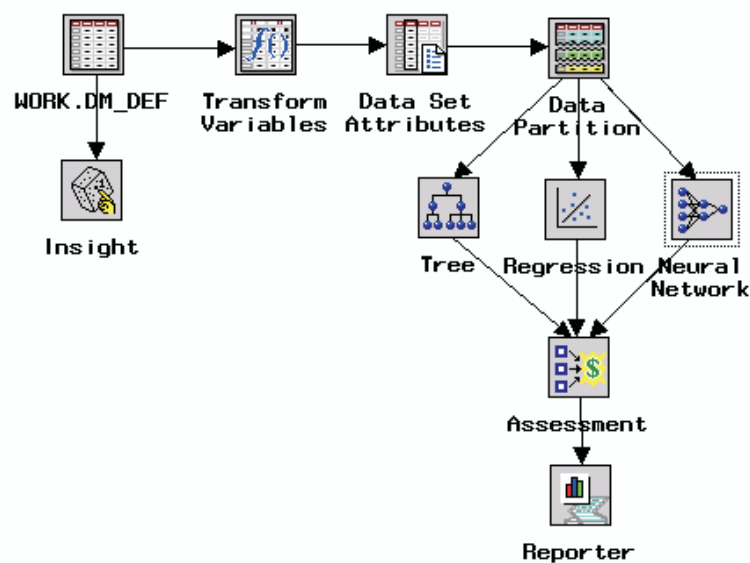


Figure 4.4: Workflow used for the DM tasks.

Each node has a specified role in the process. The node denoted by *Work.DM\_DEF* is responsible for the importation of the data from the database. With the *Insight* it is possible to evaluate and analyse the data. It allows the visualisation of histograms and presents the main statistical parameters. In the *Transform Variables* node the already mentioned transformations for the highly skewed data are performed. *Data Set Attributes* is related with the definition of the role of each attribute in the induced model, i.e., which attributes are going to be included and which is the target variable.

The *Data Partition* node allows splitting data in training and testing sets for the holdout method application. In this case, two thirds of the data was used for training and one third for testing. For each model 10 runs were performed randomising the data within the training and testing sets. These 10 runs allow validating the relations between the attributes and the target variable and to evaluate the final model performance. The evaluation is performed calculating the mean and confidence interval for the error measures obtained for each run. The confidence interval is computed considering a T-Student distribution since the standard deviation of the population is unknown and it is better suited for small samples (in this case 10). These statistical measures define the range of expected errors for future predictions of the final model which is induced using all the data for training.

The algorithms used for the regression models were multiple regression and ANN. The *Regression* and *Neural Network* nodes allow the application of these algorithms. The applied ANN was a multilayer feed-forward network with one hidden layer of six neurons. This topology was decided after some trial calculations which showed that good results could be reached with this configuration.

Focus was drawn to the multiple regression models because it was intended to obtain the explanatory physical knowledge behind the models (for instance, which were the main attributes in the prediction of a certain variable). Moreover, these models are simpler to use and to implement. The ANNs were used more for comparison purposes. The adopted topology and number of neurons in the network were not optimised along the several calculations that were performed and are an open issue for further research. This could enhance the ANN performance in some cases. For the classification model, a decision tree was applied (*Tree* node). The goal was to develop a hierarchical model with different accuracy levels and this type of data representation revealed to be very well suited for this purpose.

The *Assesment* node deals with the evaluation of the models. It allows the visualisation of different plots and graphs, the calculation of error measures and details about the learning process. The regression models based on multiple regression were evaluated using the measures MAD and RMSE together with the determination coefficient ( $R^2$ ). For the ANN, only the RMSE was used due to computational limitations. In fact, the MAD calculation is not performed by the used software. For the multiple regression models, this task was carried out, as well as the  $R^2$  computation, in a post-processing calculation using a spreadsheet. Since it was not possible to obtain the network outputs in a proper way to be manipulated in a spreadsheet, the computation of the MAD and  $R^2$  for the ANN was not viable.

For the evaluation of the parameters importance in the models, plots of significance levels were used. For the classification model the assessment was carried out computing the confusion matrix and from it several different measures for the model evaluation (sensitivity, specificity,

accuracy and precision).

The *Reporter* node provides an overview of the overall DM process since the description of the data until the results. In the following items the main issues and results of the performed studies will be presented.

### 4.3.1 RMR index

As it was described, the study of all target variables started considering firstly all the attributes. This model itself is not relevant for prediction purposes since it uses more information than the original expression with no profit. This was done to determine, for the linear regression models and among all the possible attributes, which were the most important in the prediction of this variable. In Figure 4.5, a plot of the relative importance of the main attributes for the RMR variable is presented.

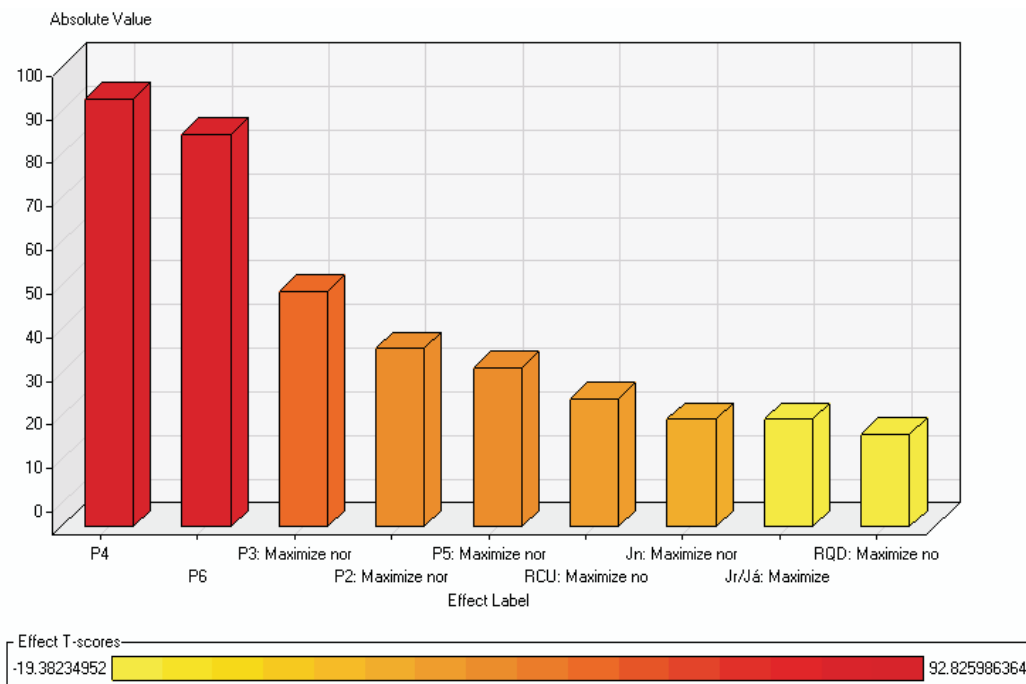


**Figure 4.5:** Relative importance of the attributes for the prediction of the RMR variable.

As it was expected, the main parameters which influence the prediction of RMR are the ones directly related to its calculation even though  $P_1$  appears only in an indirect way in the form of the unconfined compressive strength (defined as RCU in the plot). It is important to notice that, among these parameters, the most important are, by far, the ones related with the discontinuities. In particular, the parameters related with conditions ( $P_4$ ) and orientation



of discontinuities ( $P_6$ ) are very good predictors of RMR. Moreover, in the scale of relative importance, the parameters of the Q system also related with discontinuities appear ( $J_n$  and  $J_r/J_a$ ). These facts point out to the conclusion that, in granite formations, the data related with the discontinuities is a good predictor of the overall quality of the rock.

It is expected that the RMR value translates the overall condition of the rock mass. If a certain parameter does not appear to have a considerable importance in the RMR value prediction, it could mean that indirectly it is not a good predictor of the rock mass conditions. If in one hand it would be expectable that the parameters related with the discontinuities conditions, in particular  $P_3$  and  $P_4$ , should be well related with the RMR and the rock mass conditions, in the other hand the high importance of  $P_6$  which is not directly related with the rock mass state and the low importance of  $\sigma_c$  appear as strange conclusions. This may have to be concerned with limitations of the database or even with the RMR system. If these conclusions are confirmed with a larger database it can be possible to discuss the relative importance given by this system to the mentioned parameters, at least in granite formations.

Even though these limitations, the next step was to induce models considering only the previously determined most important parameters, namely:  $P_3$ ,  $P_4$  and  $P_6$ . The obtained regression model was the following:

$$RMR = 35.77 + 0.065 \times P_3^2 + 1.369 \times P_4 + 0.977 \times P_6 \quad (4.1)$$

In Table 4.6 the results for the regression and ANN models are presented in terms of average errors,  $R^2$  and correspondent t-student 95% confidence intervals. These results are concerned only with the testing set since these are the ones related with the behaviour of the models when facing new cases. The results for the models which use all the attributes are presented only for comparison matters.

**Table 4.6:** Results for the models considering all the attributes and the most important ones for the RMR prediction.

All attributes				$P_3, P_4$ and $P_6$			
Regression			ANN	Regression			ANN
$R^2$	MAD	RMSE	RMSE	$R^2$	MAD	RMSE	RMSE
0.995 ±	0.650 ±	1.094 ±	1.070 ±	0.944 ±	2.565 ±	3.522 ±	2.857 ±
0.001	0.050	0.073	0.070	0.005	0.083	0.169	0.114

As it was expected, the models which use all attributes are very accurate. The error measures are low and  $R^2$  is close to 1. Using only the three main parameters, the error significantly increases. This is because only half of the parameters used in the original expression are

applied. Nevertheless, the error can be considered low for engineering purposes. Analysing the MAD and RMSE values a prediction error around 3 is expected. This means that, for instance, if a rock mass has a "real" RMR value of 65, a value within [62; 68] will be predicted which is acceptable. This expression can be useful in the preliminary stages of design or when only information about discontinuities is available or is reliable.

Considering the RMSE, the ANN slightly outperforms the regression models. Only for the ones with less attributes the difference can be considered significant. In this case the RMSE for the ANN is approximately 20% less than the correspondent value of the regression model. In Figure 4.6 the plot of computed versus predicted RMR values is presented for the simplest case.

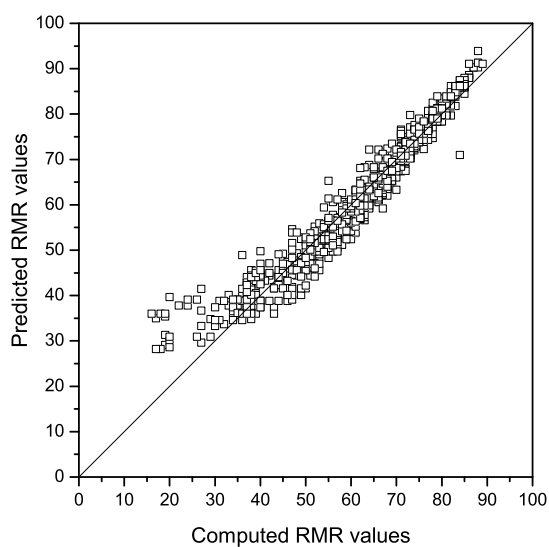


**Figure 4.6:** Computed versus Predicted RMR values for the regression model with parameters  $P_3$ ,  $P_4$  and  $P_6$ .

It can be seen that the values lay near a 45 degree slope line which means that the prediction model shows a good accuracy. However, the deviations between real and predicted values increase with decreasing rock mass quality. For RMR values below 30-35 the prediction error increases and the model tends to overestimate the RMR. Above RMR values of around 85 this overestimation trend is also observed. Since the model is based in the discontinuities characteristics this fact can be explained by the importance loss of discontinuities for poorer and massive rock masses.

The plot of Figure 4.6 shows a tail with an almost quadratic trend. In order to minimise this fact a transformation of the RMR variable was performed. Calculations were repeated using the squared value of RMR and the following regression model was obtained.

$$RMR^2 = 1036.7 + 7.148 \times P_3^2 + 166.3 \times P_4 + 116.7 \times P_6 \quad (4.2)$$

Table 4.7 resumes the results and Figure 4.7 presents a plot of real versus predicted values for this model.

**Table 4.7:** Results for the multiple regression model considering parameters  $P_3$ ,  $P_4$  and  $P_6$  and using the transformed form of the target variable.

Regression		
$R^2$	MAD	RMSE
$0.954 \pm 0.004$	$2.179 \pm 0.081$	$3.172 \pm 0.119$

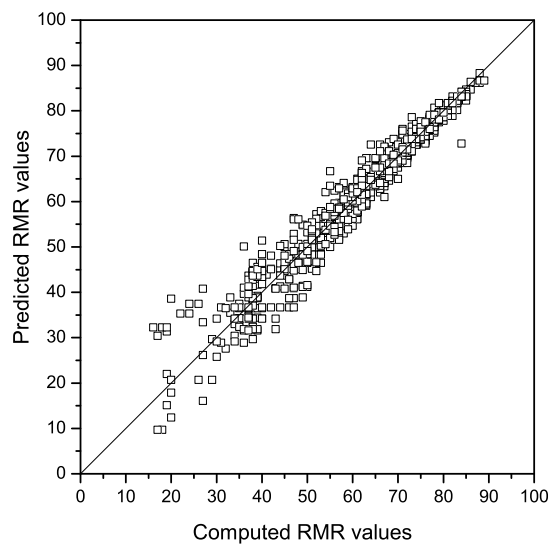


**Figure 4.7:** Real versus Predicted RMR values for regression model with parameters  $P_3$ ,  $P_4$  and  $P_6$  and considering the transformation of RMR.

This transformation led to a slight reduction on the error measurements (approximately 0.4 for each) and confidence intervals and a small increase on  $R^2$ . In Figure 4.7, a loss of accuracy for lower RMR values can still be observed. However, this happens with higher significance for RMR values below 30 and the overestimation trend is no longer observed as in the previous model. The points are almost equally distributed along the 45 degree slope line which means that the mean prediction error is close to 0. Table 4.8 summarises the main issues of the regression models for the two approaches, considering RMR and  $RMR^2$  as the target variables.

In a merely statistic point of view, the model which uses  $RMR^2$  as the target variable

**Table 4.8:** Comparison of the main results between the regression models which use RMR and  $RMR^2$  as target variables

RMR	$RMR^2$
<ul style="list-style-type: none"> <li>• Overestimation trend for <math>RMR &lt; 35</math> and <math>RMR &gt; 85</math>.</li> </ul>	<ul style="list-style-type: none"> <li>• Very good results for <math>RMR &gt; 50</math>.</li> </ul>
<ul style="list-style-type: none"> <li>• Good behaviour in a central range of RMR values.</li> </ul>	<ul style="list-style-type: none"> <li>• Higher dispersion than previous model in a central range of RMR values (<math>35 &lt; RMR &lt; 50</math>).</li> </ul>
<ul style="list-style-type: none"> <li>• Accuracy lost for poorer rock masses.</li> </ul>	<ul style="list-style-type: none"> <li>• For the lower range also accuracy lost with no specific trend.</li> </ul>

presents a better performance since it has lower error measures and higher  $R^2$ . Also, in this case the error does not follow a specific trend presenting a mean value close to 0. However, for design purposes, the conclusion may not be necessarily the same. In fact, the error measures are very close but when using the model with RMR, one knows that in a certain range of values, an overestimation trend is expected. When using the other model the expected error is random.

As it was already referred, the Q system related parameters  $J_n$  and  $J_r/J_a$  are also important to the RMR prediction. These attributes were added to this model and calculations were again performed. However, only negligible increased performance was achieved.

### 4.3.2 Q index

The preliminary runs for the Q variable using all attributes indicated that a variable transformation would be needed. Figure 4.8 (a) shows a plot of computed versus predicted values for the regression model and a highly non linear relation can be observed. The performance of this model was extremely poor resulting, in some cases, in negative values for the value of Q, which as it is well known, is always positive.

On the other hand, ANN had a very good performance with a mean RMSE value ten times lower than the correspondent for the linear regression model. This means that the ANN captured the non-linearity relationship with high accuracy. However, focus was drawn to improve the linear models. In this context, a variable transformation was implemented to linearise the relation. It resembles a logarithmic relation and the preliminary runs confirmed that this was the best suited transformation. This way the target variable turned to be the base 10 logarithm of Q ( $\log Q$ ) which was already an attribute of the database. Figure 4.8 (b) presents the results

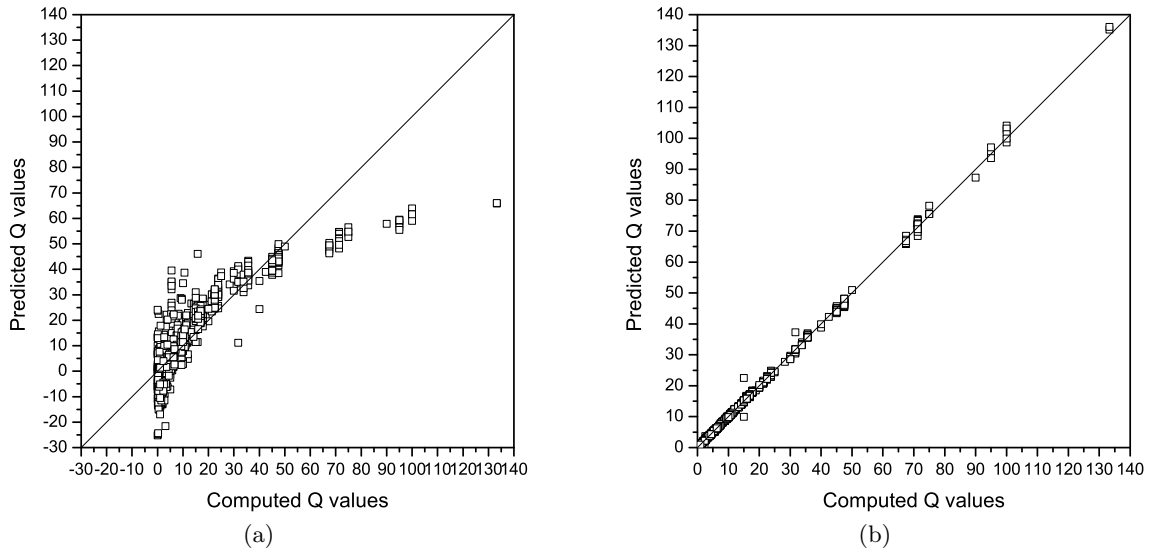


**Figure 4.8:** Computed versus Predicted Q values for regression models using all attributes (a) without logarithmic transformation and (b) with logarithmic transformation.

of the regression model considering this transformation. The results were converted again to a linear scale in order that both plots could be compared. It is possible to observe an outstanding improvement in the model performance with the consideration of the transformed form of the variable.

Table 4.9 shows the results for the models which use all the attributes and the most important ones. As it can be observed in Figure 4.9, the most important attributes are the  $J_r/J_a$  ratio (which is a measure of the shear strength of the discontinuities) and the SRF and  $J_n$  variables. The regression model using this variables is translated by equation 4.3:

$$\log Q = 2.00 + 0.47 \times \ln \left( \frac{J_r}{J_n \times J_a \times SRF^{1.07}} \right) \quad (4.3)$$

**Table 4.9:** Results for the models considering all the attributes and the most important ones for the Q coefficient.

All attributes				$J_r/J_a, J_n$ and SRF			
Regression			ANN	Regression			ANN
$R^2$	MAD	RMSE	RMSE	$R^2$	MAD	RMSE	RMSE
$0.997 \pm$	$0.016 \pm$	$0.031 \pm$	$0.030 \pm$	$0.989 \pm$	$0.049 \pm$	$0.075 \pm$	$0.075 \pm$
0.000	0.001	0.003	0.003	0.001	0.002	0.004	0.005

As it happened for the RMR, the parameters related with discontinuities have a significant effect on the prediction of this quality index together, in this case, with the parameter related

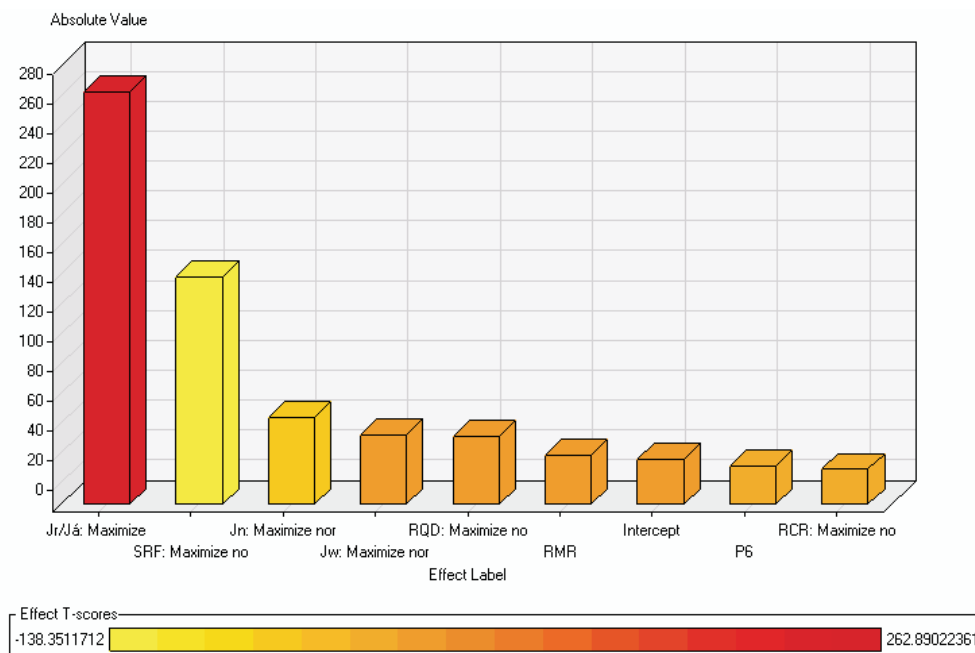


**Figure 4.9:** Relative importance of the attributes for the prediction of the log Q variable.

with the stress state. This point corroborates the previous conclusion that the discontinuities characteristics are good predictors of the overall rock mass quality.

The lower importance of the RQD (which was already observed for the RMR) can be related to the unbalanced distribution of this variable. This is translated by a reduced number of cases correspondent to RQD values lower than, approximately, 65 which hinders the correct evaluation of the importance of this parameter. There are some balancing techniques but they were not applied in this case.

In line with what was stated for the RQD, the low importance of the underground water conditions ( $J_w$ ) may be related with the almost dry in hydrological conditions. In other conditions this influence could be higher since it is well known that the water conditions strongly influence the behaviour of a rock mass.

The attribute "intercept" in Figure 4.9 has no physical meaning. It is related with the importance of the ordinate value correspondent to a null abscissa in the prediction of target variable (logQ).

Analysing the values of  $R^2$  in Table 4.9 it can be seen that the values are very high for both models. The error values are low considering that the target variable ranged approximately from -1.85 to 2.13. Figure 4.11 shows the plot of computed against predicted values and a good relation can be observed.

Since it was concluded that the parameters related with the discontinuities are very much

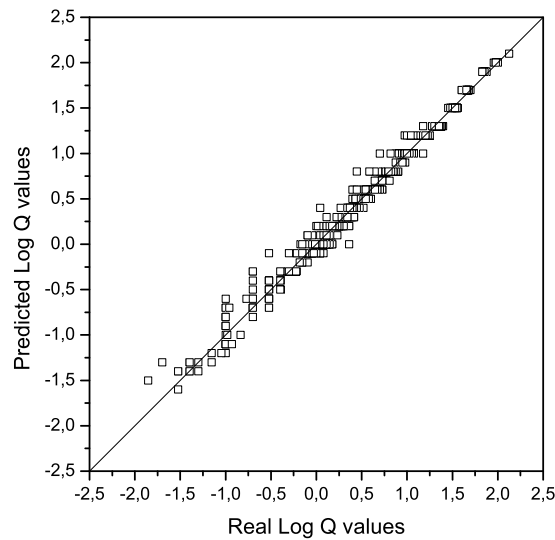


**Figure 4.10:** Computed versus Predicted  $\log Q$  values for regression model with parameters  $J_r/J_a$ , SRF and  $J_n$ .

related with both studied indexes, two more sets of variables were tested: one using only the variables  $J_r/J_a$  and  $J_n$ ; and other using these variables together with the parameters related with the discontinuities of the RMR system ( $P_3$ ,  $P_4$  and  $P_6$ ). The latter is justified since once it is possible to obtain information for the  $J_r/J_a$  and  $J_n$  variables it is not difficult to deduce values for  $P_3$ ,  $P_4$  and  $P_6$ . The regression models are translated by equations 4.4 and 4.5 and the overall results are presented in Table 4.10 and in Figure 4.11.

$$\log Q = 2.17 + 0.57 \times \ln \left( \frac{J_r}{J_n^{1.03} \times J_a} \right) \quad (4.4)$$

$$\log Q = 1.27 + 0.43 \times \ln \left( \frac{J_r}{J_n^{0.95} \times J_a} \right) + 0.0015 \times P_3^2 + 0.015 \times P_4 + 0.0094 \times P_6 \quad (4.5)$$

**Table 4.10:** Results for the models considering the  $J_r/J_a$ ,  $J_n$  and  $J_r/J_a$ ,  $J_n$ ,  $P_3$ ,  $P_4$ ,  $P_6$  attributes.

$J_r/J_a$ and $J_n$				$J_r/J_a$ , $J_n$ , $P_3$ , $P_4$ and $P_6$			
Regression		ANN		Regression		ANN	
$R^2$	MAD	RMSE	RMSE	$R^2$	MAD	RMSE	RMSE
0.908 ±	0.149 ±	0.214 ±	0.204 ±	0.933 ±	0.128 ±	0.184 ±	0.152 ±
0.009	0.007	0.013	0.010	0.005	0.004	0.009	0.007

Even though the  $R^2$  value is still within acceptable values, for the simpler model the errors significantly increase. This is especially true again for poorer rock mass conditions (lower

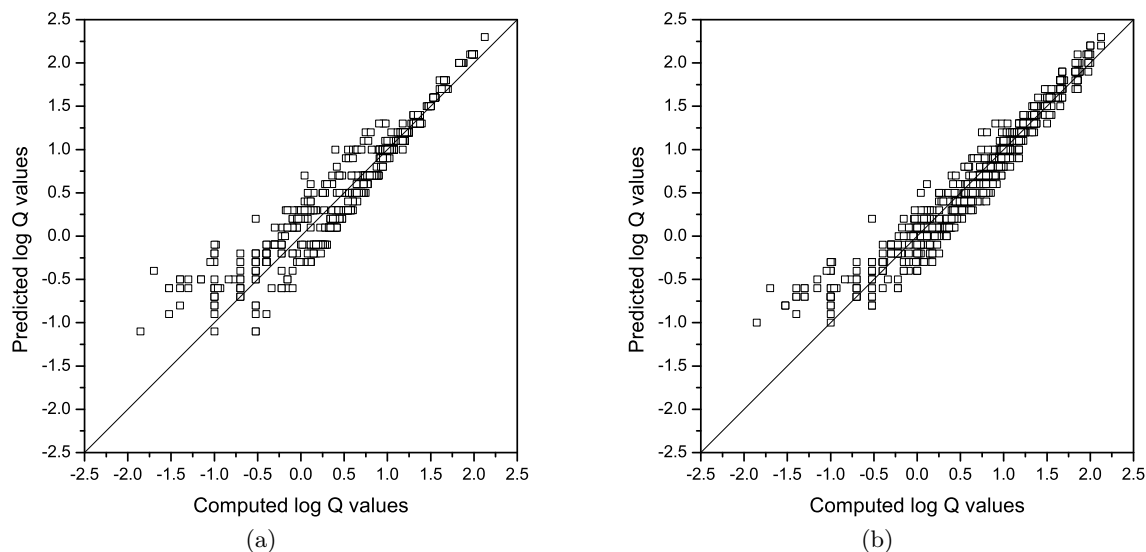


**Figure 4.11:** Real versus Predicted log Q values for regression models with (a) parameters  $J_r/J_a$  and  $J_n$  and (b) parameters  $J_r/J_a$ ,  $J_n$ ,  $P_3$ ,  $P_4$  and  $P_6$ .

logQ values). In fact, Figure 4.11 shows high dispersion for logQ values approximately below  $-0.5$  ( $Q < 0.3$  or  $RMR < 35$ ). This is also due to the loss of discontinuities importance for rock masses with low geomechanical characteristics as discussed before and shows the importance of the stress parameter consideration. The results also show that the behaviour of the models is significantly enhanced with the inclusion of the discontinuities parameters of the RMR system resulting in reduced dispersion and error values. A thorough discretisation about the discontinuities minimises the lack of information about the stress state parameter.

### 4.3.3 Friction angle ( $\phi'$ )

The observation of the most important parameters chart (Figure 4.12) allows concluding that there is a great amount of variables related to the prediction of this geomechanical parameter. Several variables present similar importance levels. However, it is important to notice that the most important ones are: (i)  $\sigma_c$ , which could be expected since this value is also a strength measure, and (ii) the Q index (with logarithmic transformation) and other variables related with the Q system. This fact is unexpected since the Q system is normally used only for classification matters and not for strength parameters calculation. Nevertheless, the Q index is very complete and should be used in models for the prediction of geomechanical parameters.

In this context, several sets of parameters were tested, in conformity with the previously defined criteria, in order to obtain the best prediction models and others that could simplify the way  $\phi'$  is calculated. This way, the data sets which presented the best results were the following:



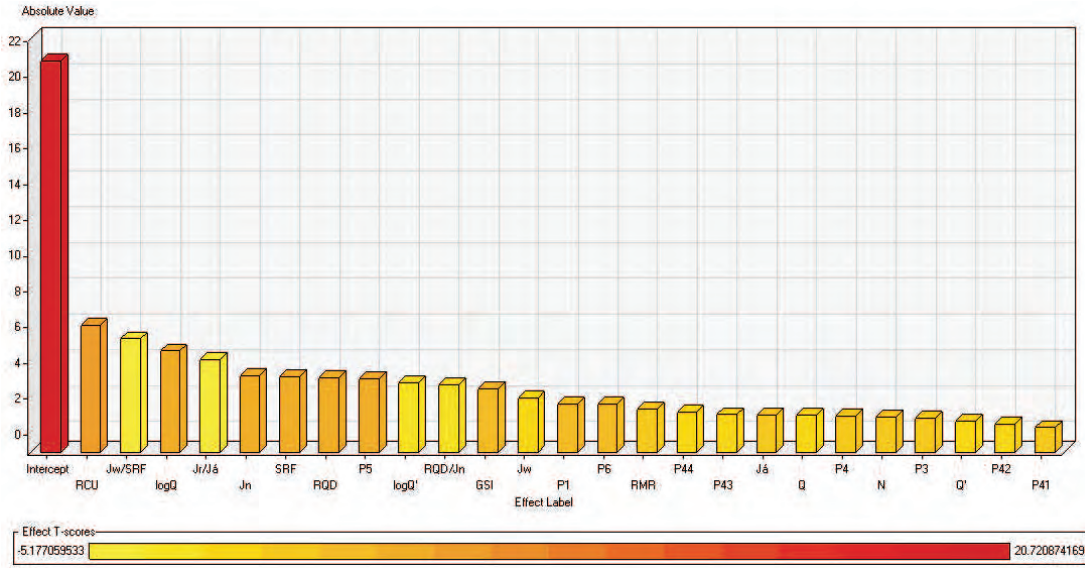


**Figure 4.12:** Relative importance of the attributes for the  $\phi'$  prediction.

- Data set 1: all variables.
- Data set 2: Q; logQ; Q'; logQ'; RMR.
- Data set 3: all RMR parameters ( $P_1, P_2, \dots, P_6$ ).
- Data set 4: RMR parameters  $P_1, P_4$  and  $P_6$ .

The results for the different data sets are presented in Table 4.11. The expressions for the regression models of data sets 2, 3 and 4 are the following:

$$\phi' = 40.566 - 0.398 \times Q + 0.342 \times Q' + 6.726 \times \log Q - 4.853 \times \log Q' + 0.260 \times RMR \quad (4.6)$$

$$\phi' = 27.143 + 1.867 \times P_1 + 0.184 \times P_2 + 0.145 \times P_3 + 0.165 \times P_4 + 0.246 \times P_5 + 0.181 \times P_6 \quad (4.7)$$

$$\phi' = 32.146 + 2.123 \times P_1 + 0.229 \times P_4 + 0.211 \times P_6 \quad (4.8)$$

**Table 4.11:** Results for the models using the different data sets for  $\phi'$  prediction.

Data set	Regression			ANN
	$R^2$	MAD	RMSE	RMSE
1	$0.968 \pm 0.004$	$0.521 \pm 0.020$	$1.002 \pm 0.106$	$0.672 \pm 0.195$
2	$0.869 \pm 0.012$	$1.162 \pm 0.043$	$2.019 \pm 0.154$	$1.970 \pm 0.502$
3	$0.965 \pm 0.001$	$0.600 \pm 0.021$	$1.051 \pm 0.068$	$0.807 \pm 0.092$
4	$0.952 \pm 0.002$	$0.776 \pm 0.019$	$1.226 \pm 0.071$	$2.290 \pm 0.303$

As it was expected, the models which used data set 1 were the most accurate. Nevertheless, the remaining also present very good predictive performances. Data set 3, which uses all the RMR parameters, is only slightly outperformed by data set 1. In fact, the error measures and  $R^2$  are very close. The good behaviour of this model is also observed in the plot of computed versus predicted values (Figure 4.13). For a wide range of values, approximately from  $35^\circ$  to  $63^\circ$ , the prediction capacity is very uniform and reliable since the plotted values lie near the  $45^\circ$  line, even though a small accuracy reduction can be observed for the lower values of  $\phi'$ . This range of values covers a great variety of possible weathering states of the granite rock mass from fresh rock to transition from rock to soil, i.e. excludes only the soil state.

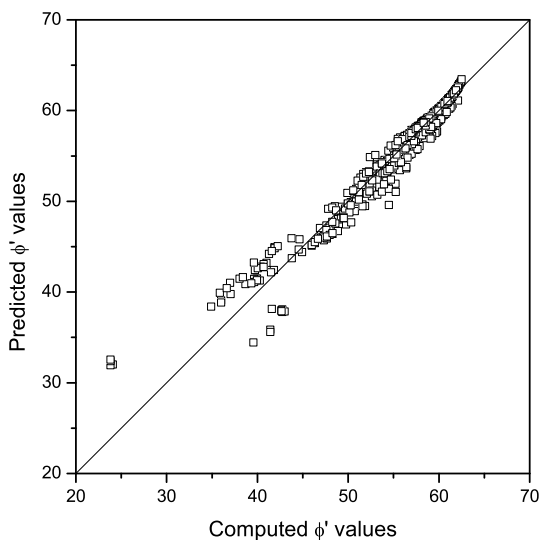


**Figure 4.13:** Computed versus Predicted  $\phi'$  values for regression model with data set 3.

Data set 2 presented the worst performance. In spite of using information from the RMR and Q coefficients it was outperformed by the other simpler models. For the case of the  $\phi'$ , the use of specific information about the rock mass characteristics presented better results than using overall quality indexes like the RMR and Q. The plot in Figure 4.14 shows that this model has worst performance within the range of  $35^\circ$  to  $45^\circ$  approximately, in which absolute errors up to  $10^\circ$  can be found and should be used with caution in this range. Nevertheless, the MAD and RMSE values point to a mean expected overall prediction error between  $1^\circ$  and  $2^\circ$  which is small.

From the RMR parameters, the most important is, by far, the one related with  $\sigma_c$  (Figure 4.15). This means that in granite rock masses  $\phi'$  is closely related with this strength measure which can be considered expectable. The variables related with the discontinuities conditions

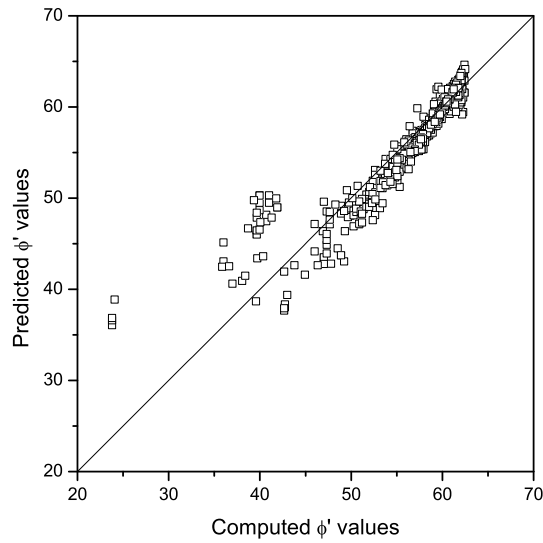


**Figure 4.14:** Real versus Predicted  $\phi'$  values for regression model for data set 2.

and orientation ( $P_4$  and  $P_6$ , respectively) also appear as good predictors.

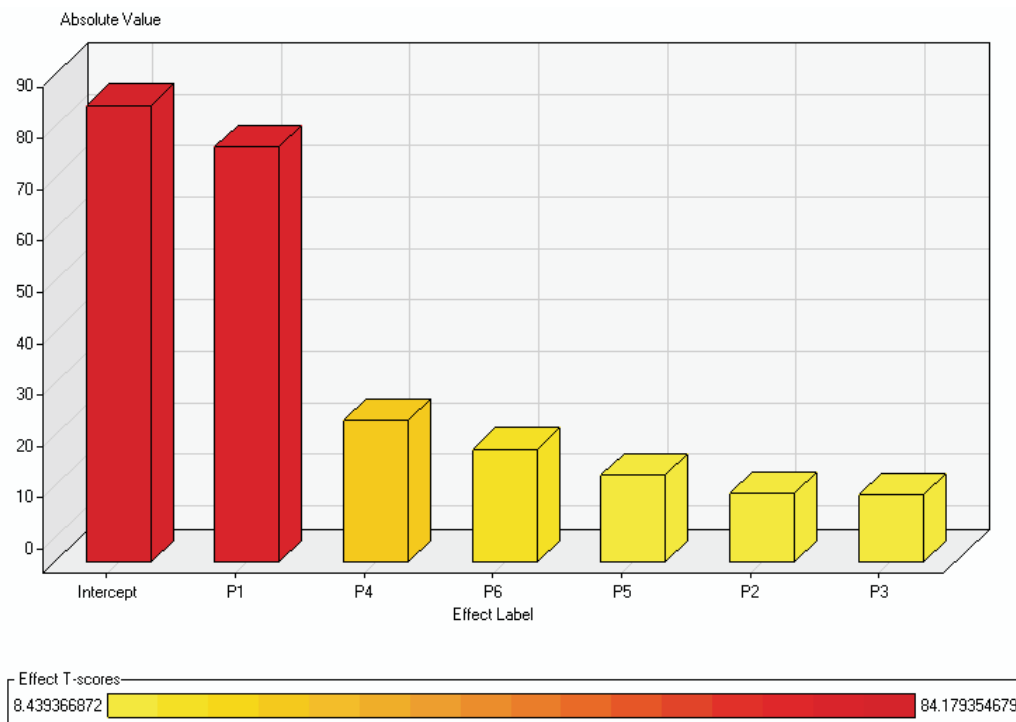


**Figure 4.15:** Computed versus Predicted  $\phi'$  values for regression model with data set 3.

Data set 4 uses these three parameters for the prediction of  $\phi'$  with very good results (Figure 4.16). Comparing with data sets 1 and 3, the error measures are higher but it has the advantage

of being very simple since it uses only three parameters. In fact, and considering the MAD and RMSE values from Table 4.11, the mean expected error for this model, as well as for the cited ones, is only approximately  $1^\circ$  which can be considered negligible for engineering purposes.

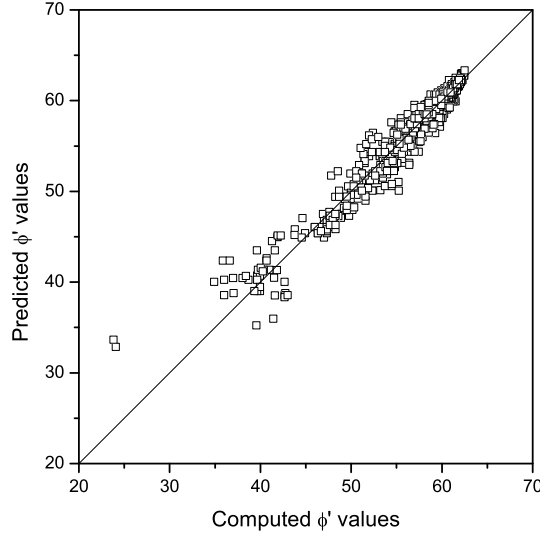


**Figure 4.16:** Relative importance of the RMR weights in the prediction of  $\phi'$ .

The ANN outperformed the regression models for data sets 1 to 3 in terms of the RMSE. This is especially true for data set 1 where the error was reduced in more than 30%. For data set 4 the RMSE of the ANN is 87% higher than the one for the regression model. The ANN performs worst when using less number of parameters. Nevertheless, the RMSE of all the trained ANN point out to acceptable mean errors for every considered model, which mean that they present high accuracy in the  $\phi'$  prediction.

It was decided to carry out some calculations considering  $\tan\phi'$  as the target variable because of its physical meaning. The preliminary runs pointed out to the significant importance of the GSI which is normal since  $\phi'$  is indirectly dependent on this parameter. Moreover, also with significant importance appear the RMR parameters mainly the one related with  $\sigma_c$  ( $P_1$ ) and some parameters related with discontinuities ( $P_4$  and  $P_6$ ) as it happened for  $\phi'$ . This way, regression models were developed considering all the RMR parameters and a simpler solution considering only the parameters  $P_1$ ,  $P_4$  and  $P_6$ . The equations obtained for the multiple regression models were the following:

$$\tan\phi' = 0.245 + 0.070 \times P_1 + 0.010 \times P_2 + 0.012 \times (P_3 + P_4) + 0.013 \times P_5 + 0.011 \times P_6 \quad (4.9)$$

$$\tan\phi' = 0.526 + 0.084 \times P_1 + 0.084 \times P_4 + 0.014 \times P_6 \quad (4.10)$$

Table 4.12 and Figure 4.17 present the overall performance of both models.

**Table 4.12:** Results for the models developed for  $\tan\phi'$  prediction.

Data set	$R^2$	Regression		ANN
		MAD	RMSE	RMSE
$P_1$ to $P_6$	$0.976 \pm 0.003$	$0.025 \pm 0.015$	$0.046 \pm 0.013$	$0.057 \pm 0.006$
$P_1, P_4$ and $P_6$	$0.953 \pm 0.008$	$0.045 \pm 0.014$	$0.062 \pm 0.015$	$0.070 \pm 0.006$

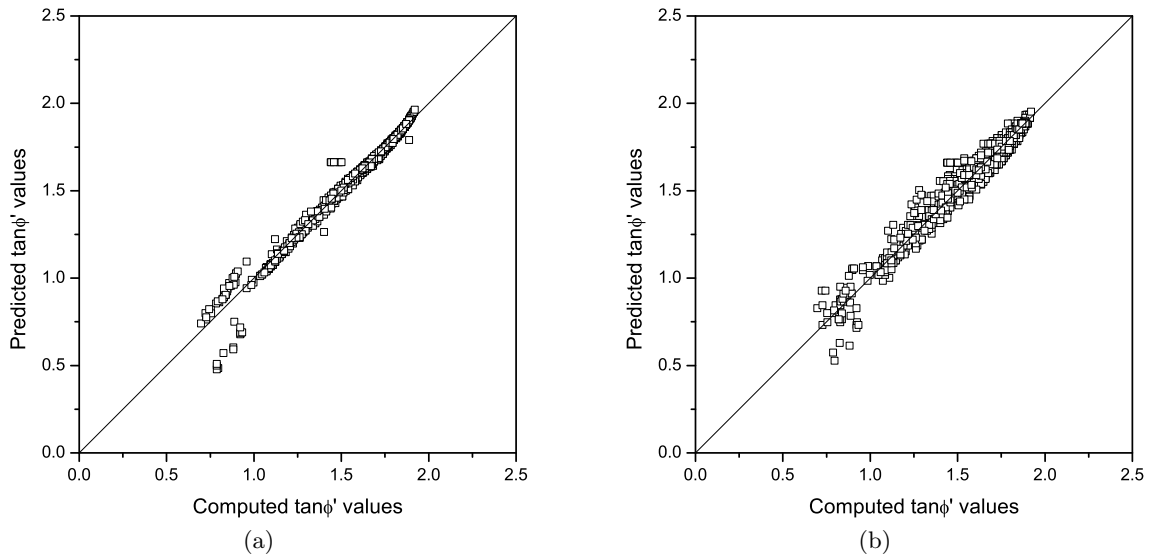


**Figure 4.17:** Computed versus Predicted  $\tan\phi'$  values for regression models with (a) parameters  $P_1$  to  $P_6$  and (b) parameters  $P_1, P_4$  and  $P_6$ .

The results are very similar to those obtained for  $\phi'$  with the same sets of parameters. When using all the RMR parameters, the value of  $\phi'$  can be estimated with acceptable accuracy even though a slight loss of accuracy for the lower values when comparing with the remaining range. The consideration of only the three most important parameters increases, as expected, the mean errors but the models have the advantage of being simpler. In both cases, and considering only the RMSE, the multiple regression models outperformed the ANN in the prediction of the target variable.

It is also interesting to note the correlation found between  $\tan\phi'$  and  $E$  which is translated by the following equation:

$$\tan\phi' = 0.772 + 0.287 \times \ln E \quad (4.11)$$

This correlation presents a  $R^2$  of 0.953. Concerning the error measures the MAD and RMSE take the values 0.0387 and 0.059. These values translate a performance which is comparable to the previously presented models being closer to the simpler one. This conclusion can be corroborated by the plot of computed and predicted values in Figure 4.18. This correlation presents the intrinsic interest of allowing to evaluate a strength parameter from an estimation of a deformability parameter and vice-versa.

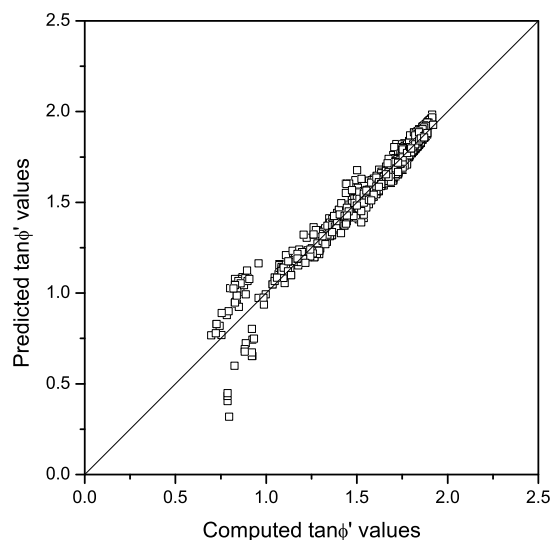


**Figure 4.18:** Computed versus Predicted  $\tan\phi'$  values for the correlation with E.

Also interesting and simple correlations were found, in this case as it should be expected, between  $\tan\phi'$  and the value of GSI from which it is derived. These correlations are translated by the following equations:

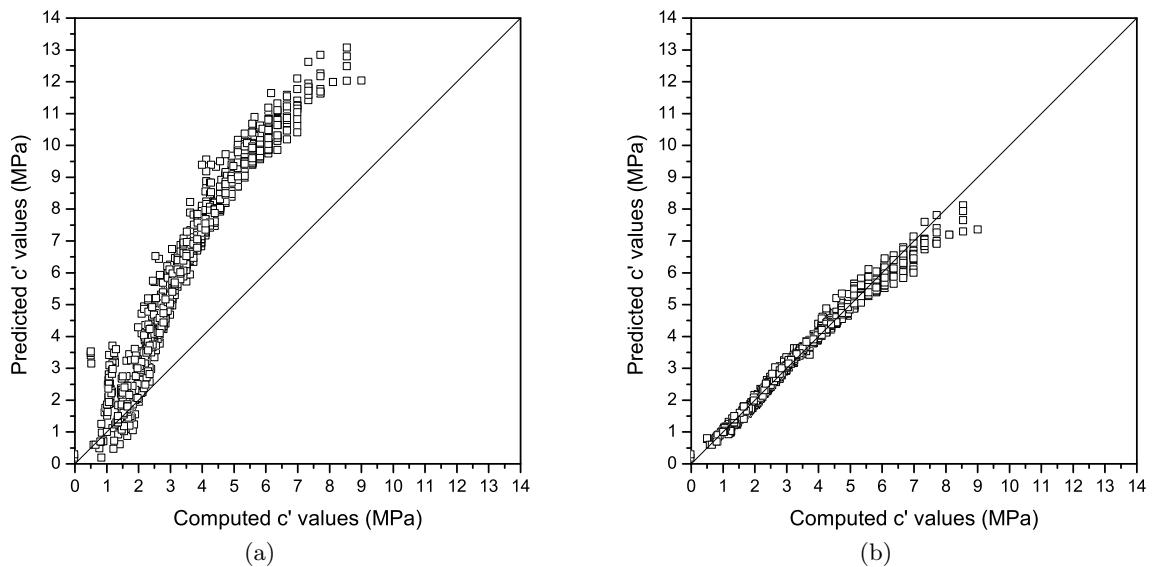
$$\tan\phi' = 0.0181 \times GSI + 0.5331; R^2 = 0.889 \quad (4.12)$$

$$\tan\phi' = 0.93 \times \ln GSI - 2.1574; R^2 = 0.909 \quad (4.13)$$

#### 4.3.4 Cohesion ( $c'$ )

As it happened for the Q index, the preliminary runs for this variable pointed out for the necessity of a variable transformation in order to enhance the prediction capacity of the models. After some tests, it was concluded that the logarithmic transformation ( $\ln c'$ ) was the best suited for this case. Figure 4.19 show the plots of computed versus predicted values for the regression models which use all attributes with and without the logarithmic transformation. It is clear the enhancement of prediction capacity using the transformation of the variable. Nevertheless,

a loss of accuracy for higher cohesion values (approximately above 6 MPa) can still be observed in this case.



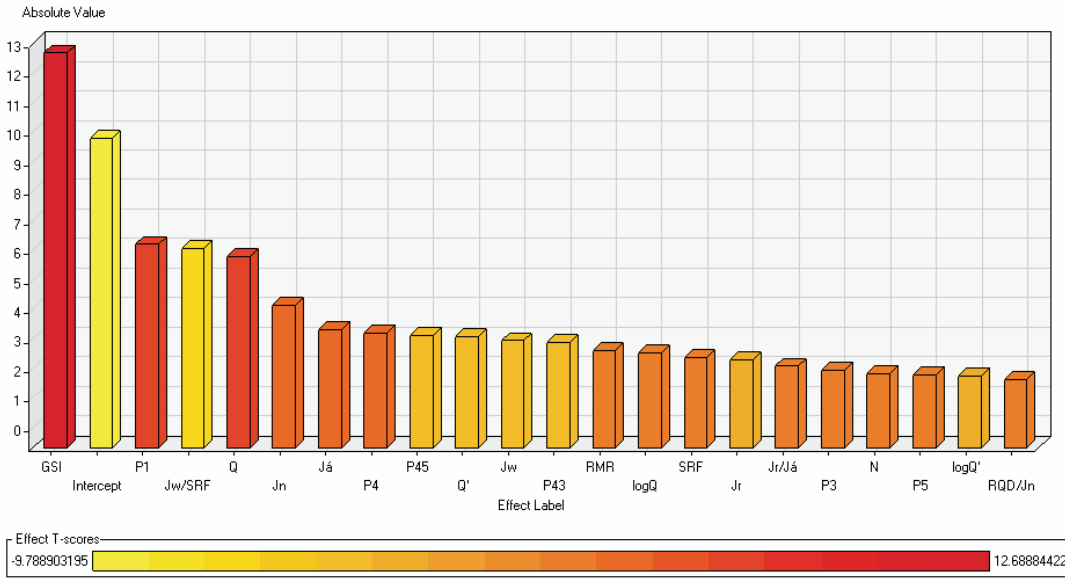
**Figure 4.19:** Computed versus Predicted  $c'$  values for regression models which use all attributes (a) without logarithmic transformation and (b) with logarithmic transformation of the target variable.

Figure 4.20 shows that, as for  $\phi'$ , a great number of variables have similar importance levels. GSI appears as the main parameter for  $c'$  prediction. This fact can be considered normal since GSI is used in the original formulation of the  $c'$  calculation. GSI was not considered for the development of the new models since the main goal was to develop alternative ones which use different parameters. This way, several data sets were tested. The ones which presented best results were similar to those for  $\phi'$ . It means that these variables are the ones most related with the geomechanical parameters. Thus, the most accurate data sets were the following:

- Data set 1: all variables.
- Data set 2:  $Q$ ;  $\log Q$ ;  $Q'$ ;  $\log Q'$ ; RMR.
- Data set 3: all RMR parameters ( $P_1, P_2, \dots, P_6$ ).
- Data set 4: RMR parameters  $P_3, P_4$  and  $P_6$ .

In Table 4.13 the main results are presented. The expressions for the regression models of data sets 2, 3 and 4 are the following:

$$\ln c' = -0.743 + 0.00099 \times Q + 0.0394 \times \log Q' + 0.0298 \times RMR \quad (4.14)$$



**Figure 4.20:** Relative importance of the attributes for the  $lnc'$  prediction.

$$lnc' = -0.906 + 0.067 \times P_1 + 0.022 \times P_2 + 0.027 \times P_3 + 0.033 \times P_4 + 0.021 \times P_5 + 0.022 \times P_6 \quad (4.15)$$

$$lnc' = -0.191 + 0.059 \times P_3 + 0.046 \times P_4 + 0.021 \times P_6 \quad (4.16)$$

**Table 4.13:** Results for the models using the different data sets for  $c'$  prediction

Data set	$R^2$	Regression		ANN
		MAD	RMSE	RMSE
1	$0.986 \pm 0.002$	$0.038 \pm 0.002$	$0.058 \pm 0.005$	$0.055 \pm 0.006$
2	$0.963 \pm 0.002$	$0.054 \pm 0.002$	$0.092 \pm 0.004$	$0.085 \pm 0.006$
3	$0.973 \pm 0.002$	$0.054 \pm 0.001$	$0.078 \pm 0.003$	$0.043 \pm 0.006$
4	$0.913 \pm 0.007$	$0.097 \pm 0.003$	$0.143 \pm 0.008$	$0.128 \pm 0.009$

The results for data sets 2 and 3 are quite similar in terms of the error measures and  $R^2$ . However, Figure 4.21 shows different behaviours in the range of  $c'$  values. For data set 3 the predicted values show a relatively stable trend until values of, approximately, 6 MPa. For higher values, a strong accuracy loss is observed and the model tends to make underestimations. On the other hand, data set 2 shows a higher dispersion than the previous set for values below 6 MPa. For values above this threshold there is also an underestimation tendency which is not so pronounced. Data set 3 has the advantage of being a simpler model because it requires less information.

The  $c'$  values ranged from 0.5 MPa to 9 MPa. The apparently high upper bound value is explained by the consideration, in the calculations, of undisturbed conditions ( $D=0$ ) and 350m



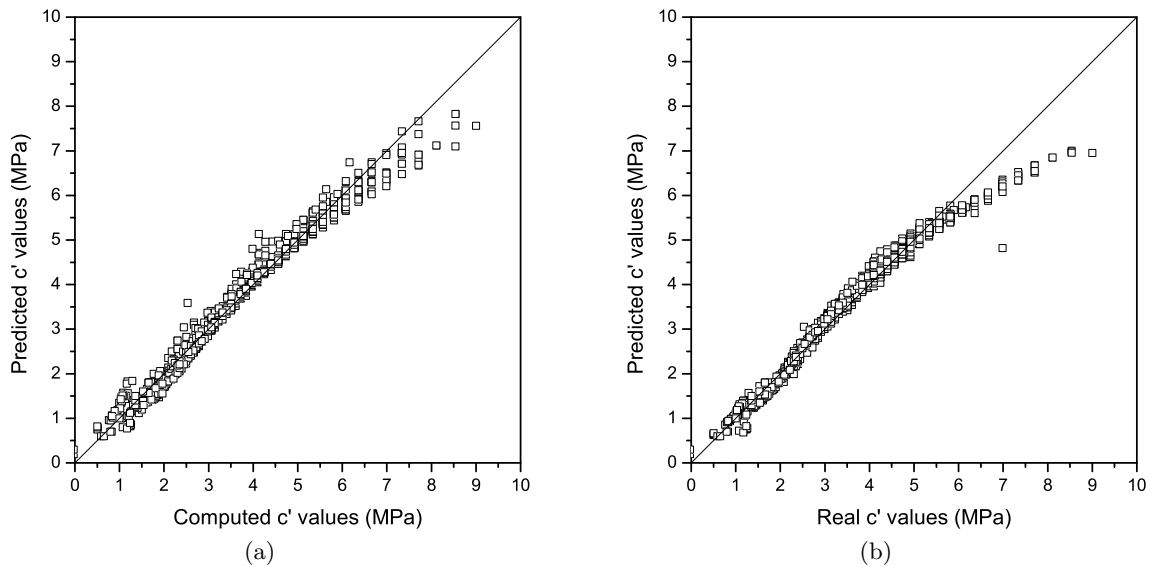


**Figure 4.21:** Computed versus Predicted  $c'$  values for regression models for (a) data set 2 and (b) data set 3.

depth which translates a high confining stress. In fact, when computing the Mohr-Coulomb parameters from the H-B strength criterion, by adjusting a line to the curved failure envelope, the consideration of increasing confining stresses mean higher  $c'$  and lower  $\phi'$  values. Moreover,  $c'$  values around 9 MPa were obtained for almost fresh rock mass with RMR values higher than 85.

The expected error for these regression models is, in linear terms, approximately 0.21 MPa ( $\approx 2.5\%$ ) which can be considered acceptable. When using the models, attention should be paid for the conservative estimation trend for high  $c'$  values. Although the logarithmic transformation, a slight non-linear trend is still observed. This is probably the main reason for the enhanced behaviour of ANN, especially for data set 3 where the RMSE value is reduced for almost half of the regression model value.

From data set 3, it was observed that the most important RMR parameters for  $c'$  prediction, when analysed separately from the remaining variables, were those related to the discontinuities ( $P_3$ ,  $P_4$  and  $P_6$ ) as shown in Figure 4.22. This fact can be considered strange since, as it was shown in Figure 4.20, the parameter  $P_1$  presented a high influence on the prediction of  $c'$ , fact that is also corroborated by engineering practice. Again, the parameter  $P_6$  appears with an overstressed importance which can be, as stated before, due to limitations of the database or of the RMR system itself.

Nevertheless, data set 4 was created considering only the three abovementioned parameters. As it was expected, an accuracy loss is observed (Figure 4.23). Again, a non linear trend is present with an overestimation tendency for the lowest values ( $<1.1$  MPa) and underestimation

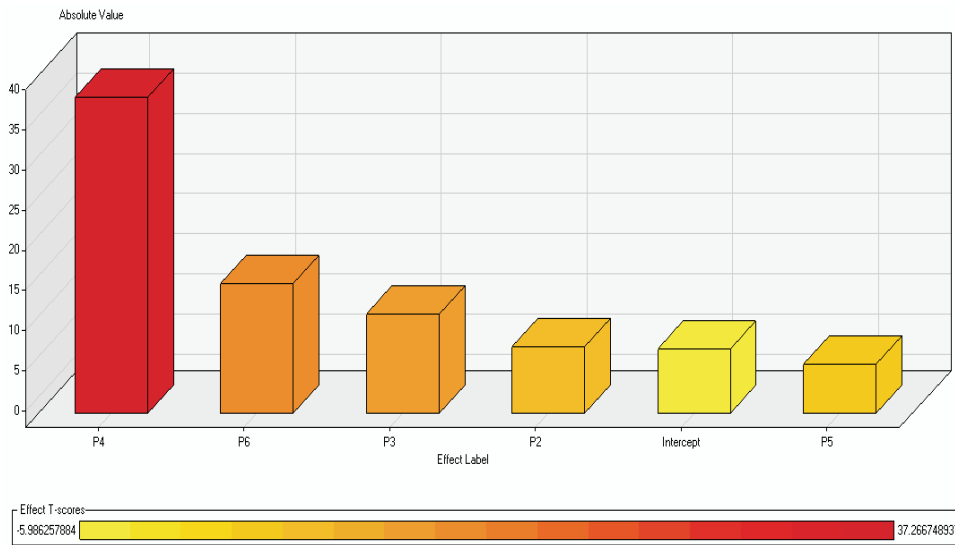


**Figure 4.22:** Relative importance of the RMR classification weights for the  $c'$  prediction.

for the highest ones ( $>6.4$  MPa). In these ranges, especial care should be used when applying the model. Still, the average expected error, in linear terms, is about 0.32 MPa ( $\approx 3.8\%$ ). Considering the range of  $c'$  values it can be considered that this regression model provides a reasonable preliminary estimation. It is outperformed by the ANN which presents a RMSE value about 10% lower.

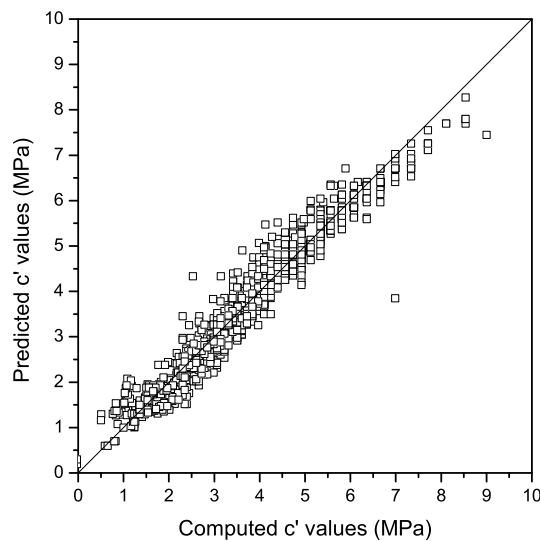


**Figure 4.23:** Computed versus Predicted  $c'$  values for regression model with data set 4.

### 4.3.5 Deformability modulus (E)

For the E parameter, as well for the strength parameters, it was intended to induce prediction models for the values obtained through the previously described methodologies. The models should use different levels of information in order to allow using them in different design stages. In this context, the study started developing the most accurate models and then simplifying them to obtain simpler ones maintaining acceptable accuracy levels.

The preliminary runs for E showed that a logarithmic transformation was necessary ( $\ln E$ ). This transformation led not only to improved results (even though a minor enhancement was observed) but the main reason was to avoid the prediction of negative values for poor rock mass conditions which was observed in some runs for the linear case.

The parameters that produced the most accurate model were the ones directly related with the geomechanical coefficients, namely the RMR and Q values. This is explained by their use in most of the analytical expressions that were in the origin of the E values. Moreover, these indexes assemble a set of important information for the rock mass deformability prediction. The results are presented in Table 4.14 and the regression model is described through expression 4.17.

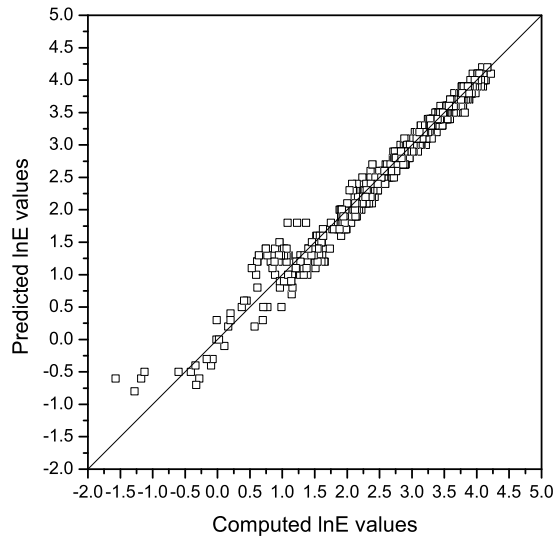
$$\ln E = -2.622 + 0.2594 \times Q^{0.25} + 0.1185 \times RMR - 0.00058 \times RMR^2 \quad (4.17)$$

**Table 4.14:** Results for the models which use the RMR and Q coefficients.

<b>RMR and Q coefficients</b>			
	<b>Regression</b>		<b>ANN</b>
$R^2$	<b>MAD</b>	<b>RMSE</b>	<b>RMSE</b>
0.978 ± 0.001	0.088 ± 0.004	0.137 ± 0.009	0.141 ± 0.016

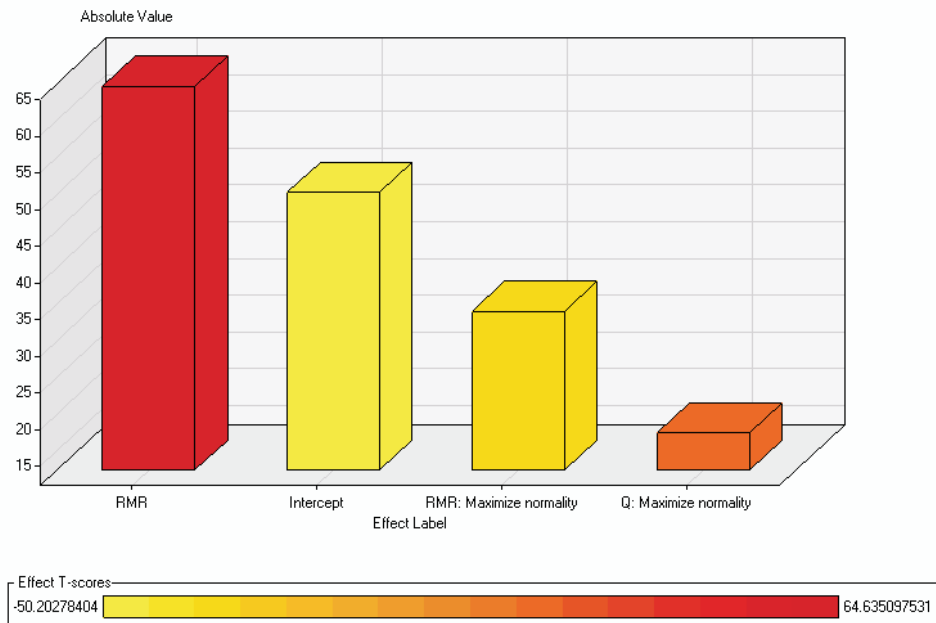
The results show very high accuracy for the linear regression model that even outperforms the ANN model in terms of the RMSE. Since  $\ln E$  ranged from, approximately, -1.57 to 4.22, the error can be considered negligible for engineering practice. The plot of Figure 4.24 shows that this high accuracy is stable for all range of values. These models should be used for the E prediction when a thorough characterisation of the rock mass is available.

Figure 4.25 shows that the most important parameter is the RMR coefficient. In fact, several simpler linear regression models were tested but the most reliable were the ones based on this index. A simple correlation between E and RMR using all available data led to very acceptable results. The expression for this correlation is the following:



**Figure 4.24:** Computed versus Predicted lnE values for regression model with the RMR and Q parameters.

$$E(GPa) = 3 \times 10^{-5} \times RMR^{3.2388} \tag{4.18}$$



**Figure 4.25:** Relative importance of the attributes for the lnE prediction.

When only parameters related to the discontinuities are available ( $P_3$ ,  $P_4$  and  $P_6$ ), the procedure that leads to better results is firstly to calculate the RMR value from equation 4.1

and then, with equation 4.18, calculate the value of E. In Table 4.15 the results for these two methods are presented. In these cases there are no confidence intervals since the results were based in a simple correlation procedure using all data. The error measures, as well as the plots of real versus predicted values (Figure 4.26), are also presented in logarithmic form for the sake of comparison with the previous models.

**Table 4.15:** Results for the models which use the RMR and only some few parameter.

	Correlation with RMR			Correlation $P_3, P_4$ and $P_6$ - RMR - E		
	$R^2$	MAD	RMSE	$R^2$	MAD	RMSE
linear	0.962	2.357	3.156	0.930	3.120	4.138
logarithmic	0.970	0.116	0.164	0.889	0.192	0.319

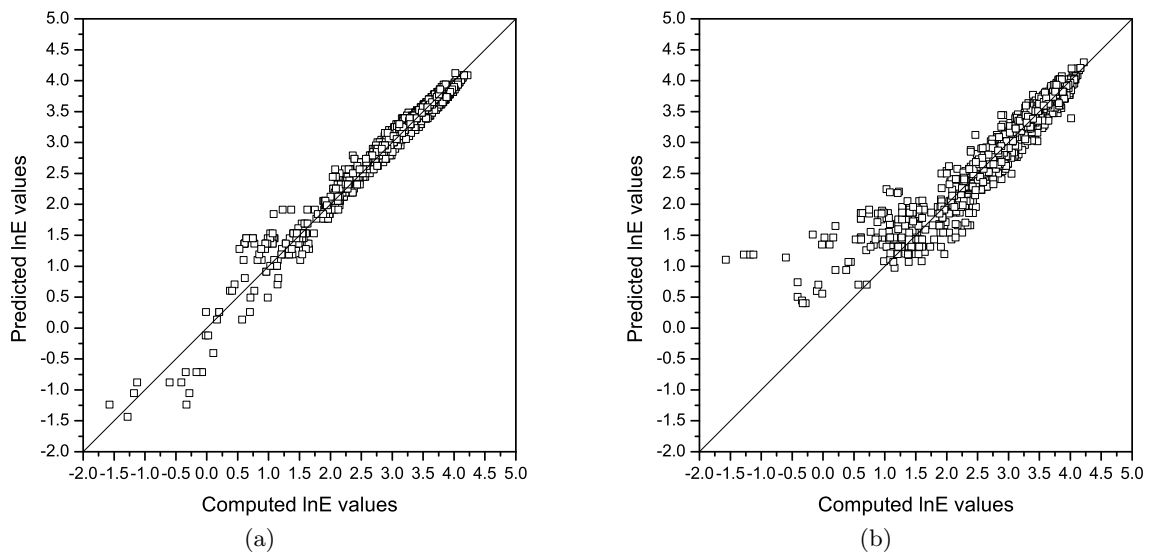


**Figure 4.26:** Computed versus Predicted values for (a) correlation with RMR and (b) correlation with  $P_3, P_4$  and  $P_6$ .

The correlation with the RMR value presents very good results. The loss of accuracy can be considered extremely reduced when compared with the previous more complex model. The plot of real versus predicted values corroborates this conclusion. This correlation has the advantage of avoiding the Q index evaluation. However, it does not have the statistical validation present in the previous more complex model.

For the last method, the decreasing accuracy is much more significant especially for E values correspondent to poorer rock masses ( $\ln E < 1$  or  $RMR < 34$ ). This fact was expected since the expression to calculate RMR from  $P_3, P_4$  and  $P_6$  presented the same drawback. This method

can be used in preliminary studies to obtain a first approach for  $E$  or when only information about the discontinuities is available. It should be used with caution for rock masses with low geomechanical properties.

It is important to mention that the rock mass presented very closed discontinuities in an important area. In this case, it was expected that  $E$  could be related with the deformability modulus of the intact rock ( $E_i$ ). Some values of this parameter were available from the laboratory tests performed by LNEC (1983, 2005). However, their reduced number (in comparison with the number of records in the database) and difficulties to proceed to a correspondence between the data of these tests and the records in the database hindered the inclusion of this information in the process. In the calculation of  $E$ , some expressions used  $E_i$  and this value was estimated by means of a correlation with  $\sigma_c$ . However, it was thought inappropriate to use this approximation in the overall DM process since it could lead to erroneous conclusions. Nevertheless, it is thought that, if this information was available,  $E_i$  should appear as a very important parameter in the prediction of  $E$ .

#### 4.3.6 The Hierarchical Rock Mass Rating (HRMR)

It was intended to develop an alternative classification system, based on the RMR, that could adapt to the level of knowledge about the parameters of the rock mass surpassing the deterministic definition of the classification weights. It was decided to use a decision tree model which structure adapts very well to the objectives of this classification problem.

Applying this algorithm to the database it was possible to develop and validate the new system. This way, the HRMR is a classification system, with a decision tree configuration, which uses intervals for the weights of the RMR system to classify the rock mass. It is called hierarchical because it uses different levels of knowledge about the parameters and the classification accuracy is dependent of this knowledge level.

Since the database was gathered in a granite rock mass, the system is more appropriate to be applied in similar formations. However, the methodology for the development of this system is general and can be applied to other types of rock masses.

To validate the system and establish its performance, and similarly to what was used for the regression models, the hold-out method was applied with 10 runs. In each run the data was randomly partitioned between the training and testing set and the accuracy of the different levels, determined with the testing set, was computed from the confusion matrix. This allowed defining the overall accuracy for each level with the correspondent T-student intervals. Moreover, for each level, a cumulative confusion matrix was built considering the results of all the runs of the hold-out process. It allowed the calculation of particular confusion matrixes for

each class and consequently determine the sensibility, specificity, precision and accuracy. The final tree was obtained using all the cases in the database for training.

The HRMR system is presented in Figure 4.27. The decision tree is composed by four levels of classification. Each level provides the class of the rock mass with different accuracy degrees. The upper levels of the tree need less information but have lower accuracy occurring the opposite for the lower levels.

The results of the classification are presented in the rectangular boxes in a similar way to the RMR system (class I, II,..., V). In the upper part of the box is the class with higher probability to be the correct one and in the lower part the second most probable. Next to the class is a percentage. From the cases in the database which obey to the rules that led to the classification, it is the percentage of cases of that specific class.

In Table 4.16 the overall performance of the HRMR is presented in terms of sensitivity, specificity, accuracy and precision for each class and level. These measures range from 0 to 100%. A low value of one of the four measures indicates problems with the classifier even if the remaining are high. The overall accuracy for each level is also presented. It distinguishes the case when only the most probable class is considered to define accuracy and when the two classes are considered for this purpose. As it was already referred, the results were computed over the test set which was not used for training.

As it was expected, the overall accuracy considering only the most probable class, increases with the number of levels, i.e. as more specific knowledge about the weights is available. The highest increase is from level 1 to level 2 where accuracy increases almost 6%. The accuracy increase from level 2 to level 3 is residual (1.4%) while level 4 means a 3.3% enhancement in relation to the previous level. There is an approximately 10% higher prediction capacity for level 4 in comparison to level 1. In conclusion, the overall accuracy of the system can be considered as very acceptable even for level 1.

If the goal is only to have an approximate idea of the class of the rock mass and the consideration of two classes is enough for some specific purpose, than the different levels have similar high accuracy levels (approximately 97%).

Analysing the results for each class, again a performance increase is observed for every class with the number of levels. The class with best performance is clearly class II. It has high values for the four measures from level one. This is closely related to the high number of cases classified as class II in the database which is almost 60% of the total number (Figure 4.3). In contrast, class V has a very low number of cases (13). This way the algorithm has difficulties to learn its main features and the classification tree performs poorly for this class. In fact, sensitivity values are very low for class V in every level reaching a maximum value of 54.5% for level 4 which is still a low value. This means that the system has difficulties to classify as class V and





**Table 4.16:** Performance measures for the HRMR system.

	Class	Sensitivity (%)	Specificity (%)	Accuracy (%)	Precision (%)	Overall accuracy (%) 1 class	Overall accuracy (%) 2 classes
Leve 1	I	79.1	99.9	94.1	65.6	80.0 ± 1.3	96.8 ± 0.9
	II	87.4	84.6	86.2	88.2		
	III	60.5	94.1	87.1	72.9		
	IV	87.1	94.6	93.7	68.6		
	V	0	100	98.9	0		
Leve 2	I	89.2	97.5	96.7	78.6	85.9 ± 1.1	97.0 ± 0.4
	II	90.7	90.5	90.6	92.6		
	III	72.0	94.8	90.0	78.4		
	IV	90.2	95.9	95.3	75.1		
	V	22.7	100	99.2	100		
Leve 3	I	89.2	97.7	96.9	79.9	87.3 ± 1.4	96.9 ± 0.6
	II	91.3	91.2	91.2	93.1		
	III	78.0	94.6	91.1	79.2		
	IV	87.1	97.3	96.1	81.5		
	V	47.7	99.9	99.3	80.8		
Leve 4	I	87.8	99.3	98.3	93.3	90.6 ± 0.9	96.8 ± 0.6
	II	95.4	92.4	94.1	94.3		
	III	82.1	95.8	93.0	83.7		
	IV	88.1	97.7	96.5	83.6		
	V	54.5	99.9	99.4	82.8		

**Precision** is the percentage of cases which were classified within a certain class and that classification was correct. **Sensitivity** or recall is the percentage of cases that belong to a certain class that were classified as being of that particular class. **Specificity** is the percentage of cases which were not of that class and were classified as such. **Accuracy** is the percentage of correct predictions.

should be used with caution for very poor rock masses. This may not be a decisive issue since very poor rock masses can be more easily classified as such in practice by experts than other classes.

Concerning the remaining classes the system presents the best performance for class IV even though the difference is not relevant. The database has almost twice the cases for class III than for class IV and a much better prediction performance should be expected for this class which is not verified. Classes I, III and IV all have more than 100 cases in the database and this can be a threshold of number of cases to have a satisfactory performance. Classes I and IV present very good performance measures from level one excepting precision which can only be considered satisfactory. For class III the main problem is sensitivity for level 1 which is only about 60%.

In a decision tree, the top nodes represent the most important data for classification. In Figure 4.28 the relative importance of each parameter for classification matters (correspondent to level 4 which is more explanatory) is presented.

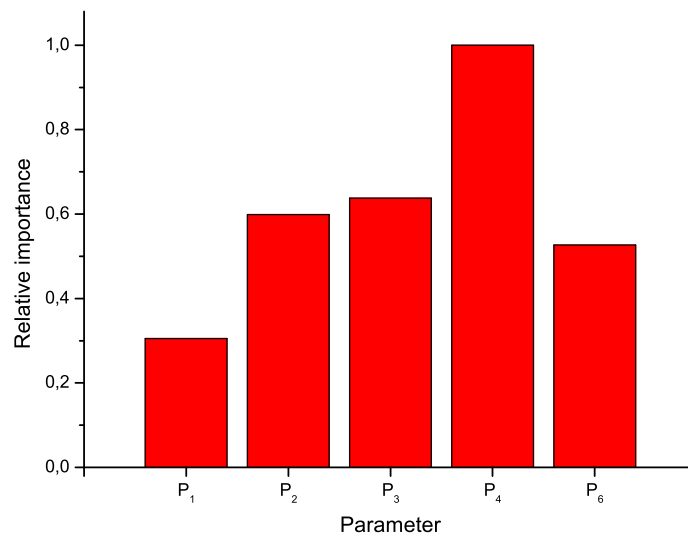


**Figure 4.28:** Relative importance of the parameters in the HRMR system.

It is interesting to notice that the most important attribute is  $P_4$  which appear in the root node. This fact corroborates the previous conclusions (from the regression models) that the discontinuities conditions are particularly relevant to explain the conditions of granite rock masses. The parameters  $P_2$  and  $P_3$ , related with the rock mass fracturing degree, are almost equally important followed by the parameter related with discontinuities orientation ( $P_6$ ). This means that the parameters related with the discontinuities are the main predictors of the overall conditions of the rock mass.

These conclusions are in line with what was observed in the regression models for the prediction of RMR. In fact, the low importance of the parameter related with  $\sigma_c$  ( $P_1$ ), does not necessarily mean that it has a low importance in the overall prediction of the rock mass state. This fact can be related with limitations of the RMR system and the relative importance given to this parameter. Moreover, it is also important to mention that the database comes from a rock mass with high  $\sigma_c$  values which means that in other conditions the conclusions may be different.

Another important point is the absence of the parameter related with the underground water conditions. In fact, as it was observed in the regression models, water has a limited

influence probably because of the almost dry to slightly wet conditions.

In conclusion, the HRMR system can constitute as an interesting classification tool. It adapts to the level of knowledge about the rock mass providing a classification with different accuracy levels. It is based on a large database of cases and was properly validated in statistical terms. Its performance is very acceptable excepting for class V rock masses. However, at this development stage, the system has some limitations that were already pointed out which are related with the original database.

## 4.4 Conclusions

In the context of rock mechanics, the evaluation of strength and deformability parameters presents a fundamental importance in underground structures design. This task is carried out considering the results of *in situ* and laboratory tests and analytical solutions based on application of empirical classification systems.

However, in the preliminary stages of design, the decision about the parameters values have to be performed based on limited data. This way, the use of data from past projects to help in this task appears as a rational solution for this problem. The application of DM techniques to well organised data gathered from large geotechnical works like underground structures can provide the base to the development of important and reliable "data-driven" models that can be very useful in future projects. This process must be always supervised by experts in the field that need to validate the knowledge discovered using these tools.

In this context, an innovative work was carried out considering this idea of using DM tools to uncover new and useful knowledge in a database of geotechnical data. In particular, it was intended to develop new models for geomechanical characterisation that could be used mainly when information about the rock mass is insufficient.

This way, in this Chapter several new models for geomechanical characterisation were presented. They were developed applying DM techniques to a large database of geomechanical information gathered from Venda Nova II powerhouse complex. This is an underground structure built in the North of Portugal in a predominantly granite rock mass.

Regression models for the RMR and Q coefficients, Mohr-Coulomb strength parameters and E were developed using multiple regression and ANN. In all cases it was possible to induce accurate and reliable models that can be helpful in the decision-making process for practitioners and researchers using different sets of parameters. Even though the good performance of the multiple regression models in many cases they were slightly outperformed by the ANN. Most of the induced models have the advantage of using less information than the original ones maintaining high accuracy levels. Moreover, they allowed drawing some conclusions about the

physical aspects and main phenomena behind the behaviour of granite rock masses.

In what concerns the RMR and Q coefficients, the most important parameters for their prediction are the ones related with the discontinuities. This means that in good quality granite formations this data is a very good predictor of the overall quality of the rock masses. The prediction models loose accuracy for poorer rock formations which lay in the border between hard-soil and soft rock due to the loss of discontinuities importance.

However, if a relevant importance of the discontinuities on the rock mass conditions prediction was expected, the lack of importance of other important parameters like the ones related with  $\sigma_c$  and with the underground water conditions (and also the relative high importance of parameter  $P_6$ ) may be related with limitations of the database or even of the empirical systems in particular the RMR.

On the other hand, the Mohr-Coulomb geomechanical parameters are influenced by several different factors. One main issue is the inclusion of the Q index as one of the most important. This is especially interesting since this very complete index is not normally taken into account in the geomechanical parameters calculation.

As it happened for the RMR and Q coefficients, the RMR discontinuities parameters also appear as good predictors of  $\phi'$  and  $c'$ . The  $\sigma_c$  value is also a very good predictor in the particular case of  $\phi'$ . This fact is explained since the  $\sigma_c$  is also a strength measure. The transformed variable  $\tan\phi'$  was also considered as a target variable due to its physical meaning. Similar results were obtained in terms of importance of parameters and in the models accuracy. It was also possible to develop a correlation between this parameter and E.

To validate the previous conclusion, a more thorough analysis was performed. Additional calculations were carried out for the same target variables but considering separately the cases classified as class II (good quality rock mass) and class IV (bad quality rock mass) following the RMR classification system. The results of this analysis showed that, in fact, for class II, the discontinuities characteristics appear as the main parameters for the prediction of the different parameters and indexes. However, when analysing the results for class IV an importance decreasing of these parameters is observed. In this case, there is no particular parameter that is clearly more important. The effects are much more random with no prominence of any parameter. This means that to obtain reliable models for poorer rock masses more parameters are needed. This explains the accuracy lost of almost every developed model for this type of rock mass since it was tried that these models were kept simple and with a low number of parameters. This conclusion corroborates the statement that the developed models should be used with caution when dealing with granite formations with lower geomechanical characteristics.

In literature, a great number of expressions can be found to compute E. A methodology was established in order to calculate, from a selected set of expressions, one final value of E

that could be a reliable estimate. The obtained values were validated by the results of a large number of E values obtained by a LFJ test. Afterwards, regression models were also developed for the calculation of this E value.

For classification purposes a new system based on the RMR was developed called Hierarchical Rock Mass Rating (HRMR). This system tries to overcome some practical problems, namely in what concerns the difficulties to obtain some of the data needed for the RMR system application. As well as for other important classification systems, the RMR needs a precise definition of several parameters which involve the assembly of a considerable amount of geotechnical information. Some of this information can be difficult or expensive to obtain in the different design and construction stages.

The HRMR was developed using the same database as for the regression models and by applying a decision tree algorithm. It was statistically validated using several performance measures. It is called hierarchical because it has four levels which provide a classification for the rock mass. Each level needs a different kind of knowledge about the rock mass, i.e. the deeper the knowledge the higher the classification accuracy.

The most important parameters in the system are the ones related with the discontinuities and fracturing degree. The parameter related with  $\sigma_c$  has a minor contribution and the one related with the underground water conditions is absent. In conclusion, the main characteristics of the HRMR are resumed in the following items.

- Does not need the deterministic definition of the weights of the RMR classification but only a range of values.
- Adaptation to the level of knowledge about the rock mass.
- Mainly uses data concerning discontinuities and fracturing.
- It is based on a large number of cases and a solid statistical validation.
- Presents a good overall performance except in the prediction of poor rock mass conditions (class V).

However, it is important to point out the application field of the system at this development stage which is closely related to the limitations of the database. First of all, obviously, it should only be applied to granite rock masses. The other limitations are more specifically related with the rock mass characteristics, namely:

- high values of  $\sigma_c$  (>100MPa);
- RQD values over 65%;

- Slightly wet to dry rock mass.

Moreover, it presents the already mentioned difficulties of classifying correctly class V rock masses. To improve the system it is necessary to add more cases to the database that cover and go beyond these limitations. Other issue that can enhance the system performance is an effort for optimising the decision tree. This can be carried out by different ways like using non-binary trees (trees with more than two splits for each test), considering interactions between the parameters and using other training algorithms. It would be very interesting also to carry out similar analysis to databases of other types of rock masses.

# Updating of Geomechanical Parameters Through Bayesian Probabilities

## 5.1 Introduction

In the construction of underground works several decisions are carried out under uncertainty. These uncertainties are related with two major problems, namely the geological/geotechnical conditions and questions related with the construction itself (advance rates, costs, etc) (Haas and Einstein, 2002). This Chapter is concerned with the first issue, in particular, the problem of dealing with uncertainty about the geomechanical parameters values in underground works.

Figure 5.1 represents, in general terms, the decision cycle proposed by Raiffa and Schlaifer (1964) and Holstein (1974), adapted for engineering purposes, which is also applied to the underground structures construction. In a first step, parameters are determined and included in engineering models. Then, based on their results, decisions are made with a given uncertainty degree. After new information is gathered the knowledge about the analysed problem can be updated and reused in the models to obtain new results and perform decisions based on less uncertain data.

The formal assignment of uncertainties and the updating procedure in order to improve the predictions are two critical aspects of this approach. The first has been already performed in many areas of geotechnical engineering like landslides (Cruden and Fell, 1997; Hungr *et al.*, 2005) and tunnelling. In this field, the "Decision Aids for Tunnelling" can be referred (Einstein *et al.*, 1999; Einstein, 2004; Min *et al.*, 2005). It is a procedure and a computer code which allows formalising uncertainties related with geological and construction aspects.

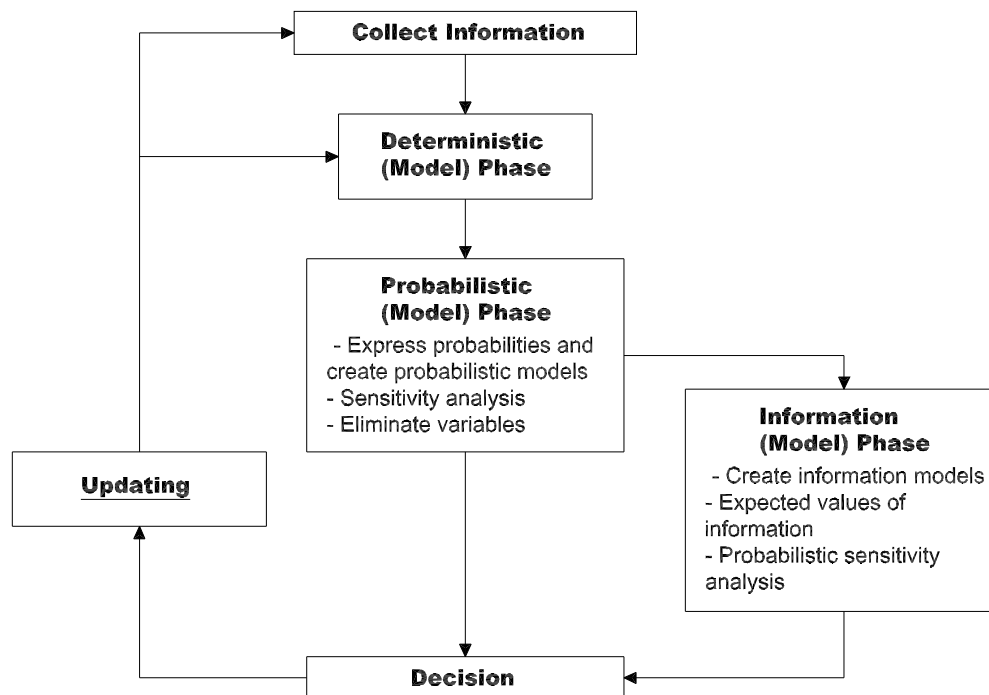


*Figure 5.1:* The decision cycle (Haas and Einstein, 2002).

However, only a few formal and mathematical consistent updating schemes have been developed in geotechnics. This is normally carried out using methodologies based on Bayes theorem. Dershowitz (1992) developed a Bayesian approach to update fracture characteristics with the results of flow tests. Einstein (1988) used the observation of cracks in pavements to refine uncertainties concerning surface creep in slopes. Concerning the tunnelling field, Haas and Einstein (2002) used the Bayesian framework together with a Markov process to update the mean length of the state of a geotechnical parameter (like "intense jointing"). Karam (2005) also used a Bayesian approach in order to update cost in tunnels construction. Concerning the geomechanical parameters updating it is not known any study to implement a formal updating framework.

It was already referred in the previous chapters that the geomechanical parameters determination is an exercise of subjective nature. The inherent uncertainty about their real value hinders the establishment of a deterministic set of values for the parameters. In practice, for each geotechnical zone, a range of values is assigned to the parameters based on the geotechnical survey and, in the case of rock masses, often by application of the empirical classification systems.

In the initial stages, the available information about the rock masses is limited. However, the construction of geotechnical models is a dynamic process and, as the project advances, it can be updated as new data is gathered. Data can have different sources each with its own precision and



accuracy. Data uncertainty involves an objective (frequentist) and subjective component: the latter is usually dependent on the geotechnical engineer's experience. Nowadays, a methodology to consistently treat the problem of geomechanical parameters updating is needed in order to reduce the uncertainties related to this subject.

The characteristics of the Bayesian methods of data analysis make them well suited for geotechnical purposes where uncertainty is present at several levels and data is compiled in different stages and with different properties.

Figure 5.2 presents a general scheme concerning the several stages where an updating process can be applied to reevaluate the geomechanical parameters (in this case particularly for the deformability modulus) in an underground work project. In the initial stages, the value of  $E$  can be evaluated based on preliminary research. As the project advances, more geotechnical information is gathered from *in situ* and laboratory tests which can be used to update the prediction. The geomechanical parameters are used in the numerical models for design purposes calculating among other things stresses and displacements. During construction, new information concerning  $E$  is obtained from several sources, for instance using data related to the mapping of the tunnel front and field measurements in back analysis calculations. This information can be used to update the value of  $E$  in a dynamic process that improves the prediction about the parameter as the quantity of data increases.

In this Chapter, a general Bayesian framework for the geomechanical parameters updating is presented. By applying this framework, it is shown how data from a preliminary geotechnical survey can be updated using *in situ* tests. More specifically, information about  $E$  is available by application of the empirical systems and then it is updated using the results of LFJ tests. Real data from the Venda Nova II powerhouse complex was used for the updating process (LNEC, 1983, 2003). In this approach  $E$  is considered a random variable with a given distribution function - normal or lognormal. Uncertainty about the parameter is represented by its standard deviation which can be reduced as more data is obtained. Different levels of initial information and uncertainty levels were considered and results were compared to evaluate the sensitivity of the results to prior assumptions.

In order to overcome the problem of choosing of a given probability distribution function to the data, an alternative Bayesian methodology was developed and tested. It uses the more flexible Weibull distribution to model the data providing more adaptability and objectivity to the Bayesian updating procedure. Moreover, it allows the introduction of the reliability concept in the overall methodology.

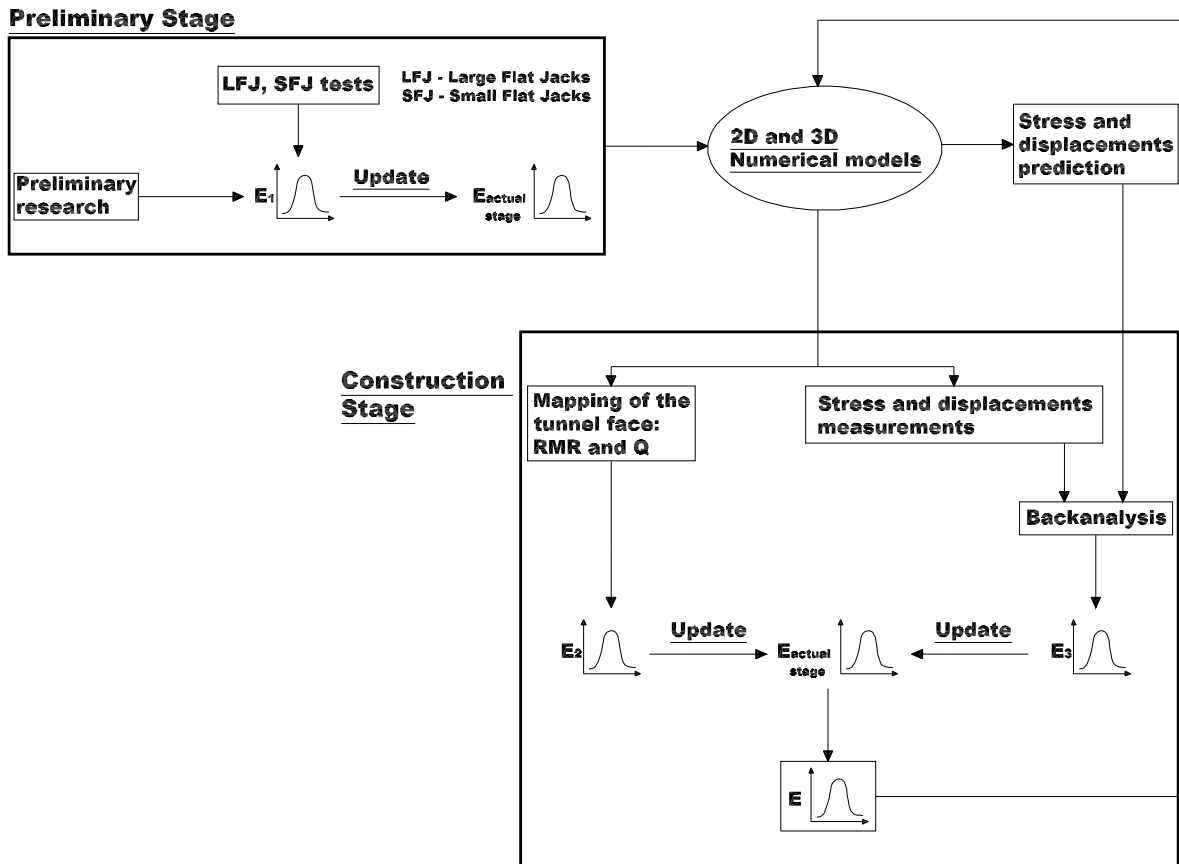


*Figure 5.2:* Scheme of the updating process for the deformability modulus during the construction of an underground structure.

## 5.2 Bayesian Methods

### 5.2.1 Introduction

Risk and reliability analysis are gaining increasing importance in decision support for civil engineering problems. Risk management includes the consideration of the uncertainties included in a given problem and possible consequences. Uncertainties from all essential sources must be evaluated and integrated into a reliability model. Three types of uncertainties may be identified Baker and Calle (2006):

- inherent physical variability or uncertainty which can and cannot be affected by human activities;
- uncertainty due to inadequate knowledge or model uncertainty related with the idealization on which the physical model is based;
- statistical uncertainty due to limited information.

In particular for geotechnical engineering, Einstein and Baecher (1983) distinguished the following main sources of uncertainty:

- spatial and temporal variability;
- measurement errors;
- model and load uncertainty;
- omissions.

Uncertainties can be represented in terms of mathematical concepts based on probabilistic theory (Ditlevsen and Madsen, 1996; Einstein, 2006). In many cases it is enough to model the uncertain quantities using random variables with given distribution functions and parameters estimated on the basis of statistical and/or subjective information (Faber, 2005). The principles and methodologies for data analysis that derive from the subjective point of view are often referred to as Bayesian statistics. Its central principle is the explicit characterisation of all forms of uncertainty in a data analysis problem. The knowledge about an unknown parameter is described by a probability distribution which means that probability is used as the fundamental measure of uncertainty. Bayesian methods are suited for making inferences from data using probability models.

The Bayesian (subjective) perspective of probability is different from the frequentist which has been the prevailing one. The frequentist view takes the perspective that probability is an objective concept while from the Bayesian perspective probability is the individual degree of belief that a given event will occur (Gelman *et al.*, 2004). Frequentist approach regards a parameter as a fixed but unknown quantity while Bayesian regards it as having a distribution of possible values. For the latter, the probability function ( $p(x)$ ) reflects the degree of belief on where the true (unknown) parameters may be. If  $p(x)$  is very narrow around a certain value then the confidence about the location of the parameter is high. On the other hand, a flatter  $p(x)$  translate a less certain prior belief on its location.

The methodologies of data analysis that derive from the frequentist view tend to be computationally simpler and this is one of the main reasons why its use is more widespread. However, the subjective probability view has been acquiring increasing importance due to the development of more powerful computers and algorithms for their processing. Each perspective can be useful and appropriate in different situations.

Bayesian techniques allow one to update random variables when new data is available using a mathematical process in order to reduce uncertainties. This process can be carried out in a sequential way. Therefore, knowledge about the random variable can be consecutively updated

as new information is gathered. The process can be divided in three steps (Ditlevsen and Madsen, 1996).

1. Set up a joint probability distribution for all variables consistent with knowledge about the underlying problem.
2. Calculate the conditional posterior distribution of the variables of interest given new observed data.
3. Evaluate the fit of the model to the data analysing if the conclusions are reasonable and how sensitive are the results to the modelling assumption on step 1.

The posterior distribution is sort of a compromise with reduced uncertainty between the prior information and the one contained in the new data. This compromise is increasingly controlled by the data as the sample size increases in what is sometimes referred to as asymptotic theory (Bernardo and Smith, 2004). As it contains prior and new information the posterior is the updated distribution for the random variable with reduced uncertainty.

### 5.2.2 Bayes theorem

Frequentist statistics provide methods to analyse and process data to draw conclusions about a hypothetical population. However, data may not be the only available source of information. Bayesian methods provide tools to incorporate external information into the data analysis process (Bernardo and Smith, 2004).

In a Bayesian approach, the data analysis process starts already with a given probability distribution. Its parameters may be chosen or estimated based on previous experimental results, experience and professional judgement. This distribution is called prior distribution and represents the uncertainty about the parameter states. The purpose of the prior is to attribute uncertainty rather than randomness to the uncertain variable. When additional data becomes available, the Bayesian data analysis process consists of using it to update the prior distribution into a posterior distribution. The basic tool for this updating is the Bayes theorem which weights the prior information with the evidence provided by the new data. Figure 5.3 resumes this overall process.

If the prior distribution of a parameter  $\Theta$ , with  $n$  possible outcomes  $(\Theta_1, \dots, \Theta_k)$ , is discrete and the new information  $x$  comes from a discrete model, then the Bayes theorem is translated by:

$$Pr(\Theta|x) = \frac{Pr(\Theta_i)Pr(x|\Theta_i)}{\sum_{i=1}^k Pr(\Theta_i)Pr(x|\Theta_i)} \quad (5.1)$$

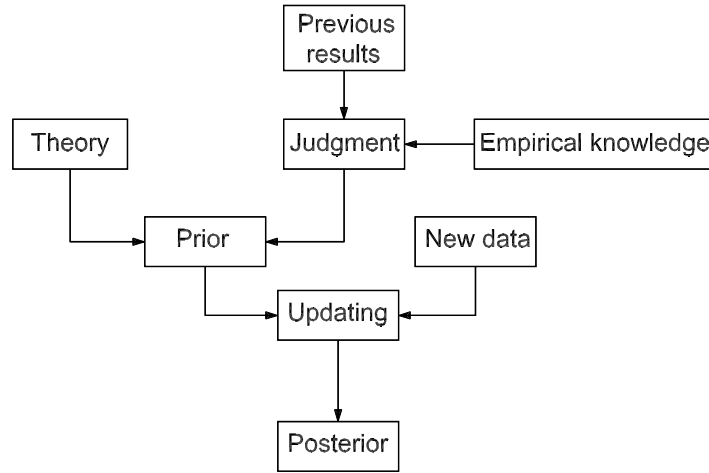


**Figure 5.3:** Scheme of the overall updating process (adapted from Faber (2005)).

where,  $Pr(\Theta_i)$  is the prior distribution of the possible  $\Theta$  values which summarises the prior beliefs about the possible values of the parameter,  $Pr(x|\Theta_i)$  is the conditional probability (or likelihood) of the data given  $\Theta$  and  $Pr(\Theta_i|x)$  is the posterior distribution of  $\Theta$  given the observed data  $x$ .

The more usual form of the theorem is in terms of continuous random variables. The prior and posterior distributions of  $\Theta$  are represented by density functions, respectively  $p(\Theta)$  and  $p(\Theta|x)$ .

$$p(\Theta|x) = \frac{p(\Theta)p(x|\Theta)}{\int p(\Theta)p(x|\Theta)d\Theta} \quad (5.2)$$

The joint probability distribution of the data and the parameter is given by  $p(x|\Theta)$  which is called the likelihood and is defined by:

$$p(x|\Theta) = L(\Theta) = \prod_i p(x_i|\Theta) \quad (5.3)$$

It is assumed that the  $n$  observation of the data are independent. The integral on equation 5.2 acts as a normalizing constant therefore it can be rewritten as:

$$p(\Theta|x) \propto p(\Theta)p(x|\Theta) \quad (5.4)$$

Summarising, Bayes' theorem consists of multiplying the prior with the likelihood function and then normalising (term in nominator), to get the posterior probability distribution, which is the conditional distribution of the uncertain quantity given the data. The posterior density summarises the total information, after considering the new data, and provides a basis for

posterior inference regarding  $\Theta$ . For Bayesian methods, the likelihood function is the instrument to pass from the prior density to the posterior via Bayes' theorem.

### 5.2.3 Choice of a prior

The choice of a prior is part of the modelling process and it is one of the main issues of the Bayesian approach. The prior distribution represents a population of possible parameter values and should include all plausible values.

Several alternatives for the prior are possible, which is a sign of flexibility of the Bayesian approach. However, it is important to check the impact on the posterior distribution stability to different choices of priors. If the posterior is highly dependent on the prior, then the data may not contain sufficient information. On the other hand, if the posterior is relatively stable over a choice of priors, it means that the data contain significant information.

The parameters of the prior distribution can be chosen or calculated in such a way that the prior reflects (Faber, 2005):

1. known (initial) observations of the random variables from which estimates of the parameters in the prior distribution can be calculated;
2. subjective knowledge on the distribution of the parameters.

It is possible to choose a prior distribution, which reflects a range of situations from very good prior knowledge (small standard deviation) to reduced knowledge (large standard deviation) or even no knowledge. In the latter case, the prior is called non-informative. This type of prior is also often called as reference, vague or flat prior. In this case the prior is simply a constant:

$$p(\Theta) = c = \frac{1}{b-a} \text{ for } a < \Theta < b \quad (5.5)$$

Thus a prior  $p(\Theta)$  is non-informative if it has a minimal impact on the posterior distribution of  $\Theta$ . The posterior is just a constant times the likelihood:

$$p(\Theta|x) \propto \text{cons} \times L(x|\Theta) \quad (5.6)$$

Simple Bayesian analysis based on non-informative prior distributions give similar results to standard frequentist approaches.

The use of non-informative priors is often useful. However, it is necessary to perform the mathematical work to check that the posterior density is proper and to determine the sensitivity of posterior inferences to modelling assumptions (Gelman *et al.*, 2004).

A prior density is called proper if it integrates to unity. The usual non-informative priors on continuous, unbounded variables - with interest ranges over  $(0, +\infty)$  or  $(-\infty, +\infty)$  - are improper since the integral does not exist. This way, a prior  $p(\Theta)$  is said to be improper if:

$$\int p(\Theta)d\Theta = \infty \quad (5.7)$$

An improper prior may result in an improper posterior. It is not possible to make inferences from improper distributions. This is not necessarily a problem since improper prior distributions can lead to proper posteriors. It is always necessary to check if the posterior distribution has a finite integral. Improper priors are often used in Bayesian inference as non-informative priors.

A common form of the reference prior is the Jeffrey's prior. To define this prior it is first necessary to define the *Fisher information*.

$$I(\Theta) = -E \left( \frac{\partial^2 \log L(\Theta)}{\partial \Theta^2} \right) \quad (5.8)$$

This is the negative expectation of the second derivative of the log-likelihood. Essentially, it measures the curvature or flatness of the likelihood function. The flatter the likelihood function is, the less information it provides about the parameter values. Jeffrey's prior is then defined as:

$$p(\Theta) \propto \sqrt{I(\Theta)} \quad (5.9)$$

This is always a consistent prior independently of how the parameter is transformed. The Jeffrey's rule allows finding prior distributions that are invariant under reparameterisations. For example, if  $p(\Theta^2) \propto 1/\Theta^2$  then  $p(\Theta) \propto 1/\Theta$ . Other advantage of this prior is that in most cases, Jeffrey's priors are improper priors but posterior distributions are proper.

Specific previous knowledge about the variable can be expressed through an informative prior. This kind of prior is not dominated by the likelihood, and has an impact on the posterior distribution. Informative priors must be specified with care. A reasonable approach is to make the prior a normal distribution.

The property that the posterior distribution follows the same parametric form as the prior distribution is called conjugacy. Conjugate prior distributions have the practical advantage of computational convenience. The results obtained by using conjugate prior distributions are easy to understand and can often be put in analytical form, they are often a good approximation and they simplify calculations.

The conjugate family is mathematically convenient in that the posterior distribution follows a known parametric form. If information is available that contradicts the conjugate parametric

family, it may be necessary to use a more realistic prior distribution (Gelman *et al.*, 2004).

Many common distributions - normal, gamma, Poisson, etc. - are members of the exponential family. When the density or the probability mass function is in the form of an exponential family, a conjugate prior can be found.

#### 5.2.4 Bayesian inference

The process of Bayesian inference involves passing from a prior distribution  $p(\Theta)$  to a posterior distribution  $p(\Theta|x)$  using the likelihood function of the data. Because the posterior integrate information from the data it will be less variable than the prior. The consideration of normal likelihood, i.e. that data follows a normal distribution, has the computational advantage of allowing the use of conjugate or uninformative priors which result in proper posteriors. The central limit theorem helps to justify the use of the normal likelihood and the results are often perfectly acceptable (Ditlevsen and Madsen, 1996). However, the modelling assumptions should always be checked analysing the posterior distribution.

In the Bayesian approach the parameters of interest are assumed to follow certain probability distributions with one or more unknown distribution parameters. These parameters are also considered to have given distributions with known prior hyperparameters (distribution parameters of the distribution parameters). The hyperparameters are then updated given the data and will be used to infer to the parameter distribution. The consideration of variable moments rather than fixed ones intends to incorporate several levels of uncertainty in the model.

The simplest model is the consideration of the parameter mean as an unknown random variable with known deterministic variance. A more complex approach is the multiparameter model that involves the consideration of both mean and variance as unknowns. In the developed Bayesian framework these two models were used to quantify the parameter of interest and correspondent uncertainty. A normal likelihood was considered together with the Jeffreys and conjugate priors. This choice was made in order to evaluate the sensitivity of the posterior to different priors. In this item a synthesis of the priors and posterior for each case is presented (Ditlevsen and Madsen, 1996; Bernardo and Smith, 2004).

#### Normal data with unknown mean ( $\mu$ ) and known variance ( $\sigma^2$ ) - the Jeffreys prior

It can be shown that the Jeffreys prior for ( $\mu$ ) is the improper uniform distribution over the real space in the sense:

$$p(\mu) \propto c, -\infty < \mu < +\infty \quad (5.10)$$



where  $c$  is an arbitrary constant. The posterior distribution is proper. After dropping all constants:

$$p(\mu|X) \propto \exp \left[ -\frac{n}{2\sigma^2} (\mu - \bar{x})^2 \right] \quad (5.11)$$

where  $n$  and  $\bar{x}$  are the number and the mean value of the test results, respectively. Therefore, the posterior distribution of the mean given the data is a normal with mean  $\bar{x}$  and variance  $\sigma^2$ . The posterior Bayes estimates for  $\mu$  and a  $(1 - \alpha)\%$  confidence interval is given by:

$$E(\mu|X) = \bar{x} \quad (5.12)$$

$$\left( \bar{x} \pm z_{\alpha/2} \frac{\sigma}{\sqrt{n}} \right) \quad (5.13)$$

### Normal data with unknown mean ( $\mu$ ) and known variance ( $\sigma^2$ ) - the conjugate prior

The conjugate prior for the mean follows a normal distribution with known initial hyperparameters  $\mu_0$  and  $\sigma_0^2$  (initial mean and variance). This way, the prior of the mean is translated by equation 5.14.

$$p(\mu) \propto \exp \left[ -\frac{1}{2\sigma_0^2} (\mu - \mu_0)^2 \right] \quad (5.14)$$

The posterior is also a normal with the updated parameters  $\mu_1$  and  $\sigma_1^2$ .

$$p(\mu) \propto \exp \left[ -\frac{1}{2\sigma_1^2} (\mu - \mu_1)^2 \right] \quad (5.15)$$

The updated parameters can be computed by expressions 5.16 and 5.17:

$$\frac{1}{\sigma_1^2} = \frac{1}{\sigma_0^2} + \frac{n}{\sigma^2} \quad (5.16)$$

$$\mu_1 = \frac{\frac{1}{\sigma_0^2} \mu_0 + \frac{n}{\sigma^2} \bar{x}}{\frac{1}{\sigma_0^2} + \frac{n}{\sigma^2}} \quad (5.17)$$

The inverse of the variance is called the precision. The above equation shows that for normal data and normal prior distributions, each with known precision, the posterior precision is equal to the sum of prior and data precisions. The posterior mean  $\mu_1$  is expressed as a

weighted average of the prior and sample mean, with weights proportional to the precisions. The posterior Bayes estimates can be found by:

$$E(\mu|X) = \mu_1 \quad (5.18)$$

$$var(\mu|X) = \sigma^2 + \sigma_1^2 \quad (5.19)$$

### Normal data with unknown mean ( $\mu$ ) and unknown variance ( $\sigma^2$ ) - the Jeffreys prior

The simplest option for the joint prior is to assume that the mean and variance can be estimated independently of each other and assume vague prior distributions for the unknown parameters. A common pair of vague priors for the normal model is given by equations 5.20 and 5.21.

$$p(\mu) \propto c, -\infty < \mu < +\infty \quad (5.20)$$

$$p(\sigma^2) \propto \frac{1}{\sigma^2}, \sigma^2 > 0 \quad (5.21)$$

This is equivalent to Jeffreys prior for  $(\mu, \sigma^2)$ :

$$p(\mu, \sigma^2) \propto \frac{1}{\sigma^2}, -\infty < \mu < +\infty, \sigma^2 > 0 \quad (5.22)$$

which is an improper prior. To draw inference on the unknown parameters  $(\mu, \sigma^2)$  it is necessary to derive the posterior distribution given all observations  $X = (x_1, \dots, x_n)$  from Bayes' theorem. This posterior takes the following form:

$$p(\mu, \sigma^2|X) \propto \left(\frac{1}{\sigma^2}\right)^{1/2} \exp\left[-\frac{1}{2}\left(\frac{\mu - \bar{x}}{\sigma/\sqrt{n}}\right)^2\right] \left(\frac{1}{\sigma^2}\right)^{\frac{(n-1)+1}{2}} \exp\left[-\frac{1}{2}\frac{S}{\sigma^2}\right] \quad (5.23)$$

where  $S = \sum (x_i - \bar{x})^2$ . The form of  $p(\mu, \sigma^2|X)$  indicates that the conditional posterior is a normal distribution with mean  $\bar{x}$  and variance  $\sigma^2/n$  and the marginal posterior for  $\sigma^2$  is an inverse  $\chi^2$  distribution in the form:

$$\mu|\sigma^2, X \rightarrow N\left(\bar{x}, \frac{\sigma^2}{n}\right) \quad (5.24)$$

$$\frac{(n-1)s^2}{\sigma^2} \rightarrow \chi_{n-1}^2 \quad (5.25)$$

where  $s = \frac{1}{n-1} \sum (x_i - \bar{x})^2$  is the sample variance. The  $100(1 - \alpha)\%$  credible intervals for  $\mu$  and  $\sigma^2$  are, respectively:

$$\left( \bar{x} - t_{\alpha/2}(n-1) \frac{s}{\sqrt{n}}, \bar{x} + t_{\alpha/2}(n-1) \frac{s}{\sqrt{n}} \right) \quad (5.26)$$

$$\left( \frac{(n-1)s^2}{\chi_{n-1,1-\alpha/2}^2}, \frac{(n-1)s^2}{\chi_{n-1,\alpha/2}^2} \right) \quad (5.27)$$

In this case the main parameter distributions can be obtained by simulation and by analytical solutions. Therefore, the posterior Bayes estimates for the parameters can be obtained by the following expressions:

$$E(\mu|X) = \bar{x} \quad (5.28)$$

$$var(\mu|X) = \frac{n-1}{n-3} \frac{s^2}{n}, \quad n > 3 \quad (5.29)$$

$$\sigma^2 = \frac{n-1}{n-3} s^2, \quad n > 3 \quad (5.30)$$

$$var(\sigma^2|X) = 2 \left( \frac{n-1}{n-3} \right)^2 \frac{s^4}{n-5} \quad (5.31)$$

### Normal data with unknown mean ( $\mu$ ) and unknown variance ( $\sigma^2$ ) - the conjugate prior

The natural conjugate prior has the following form:

$$p(\mu|\sigma^2) \propto \left( \frac{n_0}{\sigma^2} \right)^{1/2} \exp \left[ -\frac{n_0}{2\sigma^2} (\mu - \mu_0)^2 \right] \left( \frac{1}{\sigma^2} \right)^{\nu_0/2+1} \exp \left[ -\frac{S_0}{2\sigma^2} \right] \quad (5.32)$$

where  $n_0$  is the size of the initial sample. This means that the prior is the product of the density of an inverted Gamma distribution with argument  $\sigma^2$  and  $\nu_0$  degrees of freedom and the density of a normal distribution with argument  $\mu$ , where the variance is proportional to  $\sigma^2$ . In other words, it is the density of the so-called normal-gamma distribution. Therefore, the prior for  $\mu$  conditional on  $\sigma^2$  is a normal with mean  $\mu_0$  and variance  $\sigma^2/n_0$ :

$$\mu|\sigma^2 \rightarrow N \left( \mu_0, \frac{\sigma^2}{n_0} \right) \quad (5.33)$$

The prior for the precision ( $1/\sigma^2$ ) is the gamma distribution with hyperparameters  $\nu_0/2$  and  $S_0/2$ :

$$\frac{1}{\sigma^2} \rightarrow \text{gamma} \left( \frac{\nu_0}{2}, \frac{S_0}{2} \right) \quad (5.34)$$

The appearance of  $\sigma^2$  in the conditional distribution of  $\mu|\sigma^2$  means that  $\mu$  and  $\sigma^2$  are necessarily interdependent. The conditional posterior density of  $\mu$ , given  $\sigma^2$ , is proportional to  $p(\mu, \sigma^2)$  with  $\sigma^2$  held constant. After some algebra, it can be shown that:

$$\mu|\sigma^2 \rightarrow N \left( \mu_1, \frac{\sigma^2}{n_1} \right) \quad (5.35)$$

where

$$\mu_1 = \frac{n_0}{n_0 + n} \cdot \mu_0 + \frac{n}{n_0 + n} \cdot \bar{x} \quad (5.36)$$

$$n_1 = n_0 + n \quad (5.37)$$

The parameters of the posterior distribution combine the prior information and the information contained in the data. For example,  $\mu_1$  is a weighted average of the prior and of the sample mean, with weights determined by the relative precision of the two pieces of information. The marginal posterior density of  $1/\sigma^2$  is gamma:

$$\frac{1}{\sigma^2}|x \rightarrow \text{gamma} \left( \frac{\nu_1}{2}, \frac{S_1}{2} \right) \quad (5.38)$$

where,

$$\nu_1 = \nu_0 + n \quad (5.39)$$

$$S_1 = S_0 + (n - 1)s^2 + \frac{n_0 \cdot n}{n_0 + n} (x - \mu_0)^2 \quad (5.40)$$

The posterior sum of squares ( $S_1$ ) combines the prior sum and the sample sum of squares, and the additional uncertainty given by the difference between the sample and the prior mean.

### 5.2.5 Posterior simulation

Obtaining the posterior distribution is the fundamental objective of Bayesian analysis. To obtain the complete posterior distributions of the parameters it is normally necessary to use simulation methods. However, it can be useful to obtain point estimates that resume the overall information like the mean and variance of the posterior distributions. In some cases, this can

be carried out using analytical closed form solutions especially if the prior distributions are properly chosen. Other possible method is to infer from the simulated distributions.

There are several different algorithms to simulate the posterior distributions. One of the most popular is the Markov Chain Monte Carlo (MCMC). The MCMC algorithm was first introduced by Metropolis *et al.* (1953) and sequently generalised by Hastings (1970). Markov chain simulation is a general method based on a sequential draw of sample values with the distribution of the sampled draws depending only on the last value. In probability theory, a Markov chain is a sequence of random variables  $\theta_1, \theta_2, \dots, \theta_n$  for which, for any time  $t$ , the distribution of  $\theta_t$  depends only on the most recent value,  $\theta_{t-1}$ . The description of the mathematical fundamentals of the algorithm are outside the scope of the work but a comprehensive and thorough analysis on this subject can be found in Brooks (1998).

The Metropolis and the Gibbs sampler are particular Markov chain algorithms. The Gibbs sampler is the most popular one and is normally chosen for simulation in conditionally conjugate models, where it is possible to directly sample from each conditional posterior distribution. The Metropolis algorithm can be used for models that are not conditionally conjugate. For parameters whose conditional posterior distribution has standard forms it is better to use the Gibbs sampler otherwise the Metropolis should be used. In this work, the Gibbs sampler was implemented in order to simulate the posterior distributions.

To explain the Gibbs sampler lets consider a problem with two parameters  $\theta_1$  and  $\theta_2$  in which the conditional distributions  $p(\theta_1|\theta_2)$  and  $p(\theta_2|\theta_1)$  are known, and it is necessary to compute one or both marginal distribution  $p(\theta_1)$  and  $p(\theta_2)$ . The Gibbs sampler starts with an initial value  $\theta_2^0$  for  $\theta_2$  and obtains  $\theta_1^0$  from the conditional distribution  $p(\theta_1|\theta_2 = \theta_2^0)$ . Then the sampler uses  $\theta_1^0$  to generate a new value  $\theta_2^1$  drawing from the conditional distribution based on the value  $\theta_1^0$ ,  $p(\theta_2|\theta_1 = \theta_1^0)$ . In mathematical terms the samples are taken from the two conditional distributions in the following sequence:

$$\theta_1^t \rightarrow p(\theta_1|\theta_2 = \theta_2^{t-1}) \quad (5.41)$$

$$\theta_2^t \rightarrow p(\theta_2|\theta_1 = \theta_1^t) \quad (5.42)$$

This sequence of draws is a Markov chain because the values at step  $t$  only depend on the value at step  $t - 1$ . If the sequence is run long enough the distribution of the current draws converges to the simulated distribution.

More specifically, to implement the Gibbs sampler for instance in the case of the Normal model with conjugate priors for unknown mean and variance it is necessary first to obtain draws from the marginal posterior distribution of the variance and then simulate the mean value from

the conditional posterior distribution on the variance and data. The mathematical form of this procedure is the following:

$$\frac{1}{\sigma^{2(1)}|x} \rightarrow \textit{gamma} \left( \frac{\nu_1}{2}, \frac{S_1}{2} \right) \quad (5.43)$$

$$\mu^{(1)}|\sigma^2, x \rightarrow N \left( \mu_1, \frac{\sigma^{2(1)}}{n_1} \right) \quad (5.44)$$

...

$$\frac{1}{\sigma^{2(t)}|x} \rightarrow \textit{gamma} \left( \frac{\nu_1}{2}, \frac{S_1}{2} \right) \quad (5.45)$$

$$\mu^{(t)}|\sigma^2, x \rightarrow N \left( \mu_1, \frac{\sigma^{2(t)}}{n_1} \right) \quad (5.46)$$

## 5.3 Application of the Bayesian framework to update E in a rock mass

### 5.3.1 Introduction

In this work, the developed Bayesian framework is applied to data collected in an underground structure for updating the E value. The data consisted in the results of a Large Flat Jack (LFJ) test performed by LNEC (LNEC, 1983, 2003) in the scope of the Venda Nova II hydraulic scheme project which will be more deeply described in Chapter 7. Figure 5.4 presents a cross-section of the powerhouse caverns of this scheme.

In the performed LFJ test, several loading/unloading cycles were performed in different circumstances. This way, and excluding the values obtained in the first loading cycles, a total of 160 E values were obtained from this test and were used in this application.

The geomechanical parameter was considered a random variable. The original distribution of the population is not known. Normally, in probabilistic approaches, the geomechanical parameters are considered to follow normal or lognormal distributions. In the developed study, both distributions were considered in order to evaluate the impact of prior assumptions on the final results.

The normal distribution presents some drawbacks like the possibility that the random variable assume negative values which is, in this particular case, physically impossible. However, it has the advantage of computational convenience and, normally, good results can be obtained.

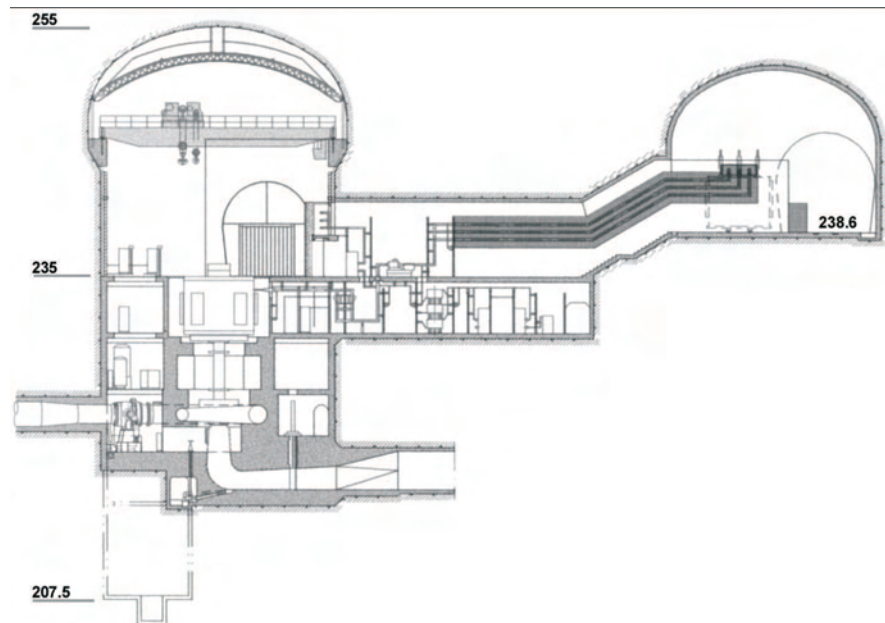


**Figure 5.4:** Cross-section of the Venda Nova II powerhouse complex caverns.

The lognormal distribution has the advantage of not allowing negative values for the random variable and this is one of the main reason of its use for modelling geotechnical data. Moreover, experience shows that normally this distribution is appropriate to describe deformability parameters (LNEC, 1983). The consideration of the lognormal distribution does not raises considerable new computational issues. By its definition, the lognormal distribution is the probability distribution of any random variable whose natural logarithm is normally distributed. It means that if a random variable  $X$  is log normally distributed then  $Y = \text{Log}(X)$  is normally distributed. This way, the updating procedure considering a lognormal distribution of the data was carried out in three main stages.

1. Proceed to a logarithmic transformation of the data and calculation of the main parameters of the distribution (mean and standard deviation).
2. Compute the updated parameters with the formulae for the normal distribution case.
3. Transform the updated parameters for their equivalent ones of the lognormal distribution using the following expressions:

$$\mu_X = \exp\left(\mu_Y + \frac{\sigma_Y^2}{2}\right) \quad (5.47)$$

$$\sigma_X^2 = \exp(2\mu_Y + \sigma_Y^2) \cdot (\exp(\sigma_Y^2) - 1) \quad (5.48)$$

The Bayesian updating calculations were performed considering several situations in terms of uncertainty levels, probability distribution functions for the data and initial knowledge. Concerning the uncertainty for the parameter two different levels were considered, namely: i) unknown mean and known deterministic variance; and ii) unknown mean and variance. For each case, the situations of no prior knowledge translated by the uninformative Jeffreys prior and prior knowledge obtained by analytical solution based on the empirical classification systems application were considered. In conclusion, a total of eight calculations, which are schematized in Figure 5.5, were performed and compared considering different assumptions. The following items start with a brief statistical analysis of the available data. Then, the main results are presented.

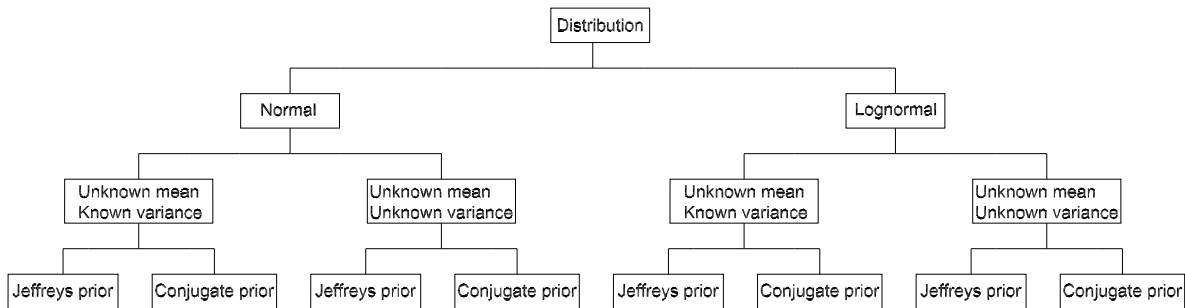


**Figure 5.5:** Scheme of the performed calculations for the Bayesian updating.

### 5.3.2 Statistical analysis of the data

The prior information for the conjugate prior cases was obtained using data from the empirical classification systems application. The calculation procedure was already described in the previous Chapter and used a set of analytical solutions collected in the literature. It was composed of a total of 76 cases gathered in the zone where the LFJ test was performed such that the results could be comparable. Figure 5.6 presents the histograms of the raw data and with the logarithm transformation (to be used in the lognormal case) and Table 5.1 the main parameters of each distribution.

**Table 5.1:** Distribution parameters for the initial values of E (GPa).

Parameter	Distribution (a)	Distribution (b)
$\mu$	38.5	3.486
$\sigma$	17.6	0.665
$\sigma^2$	309.8	0.442



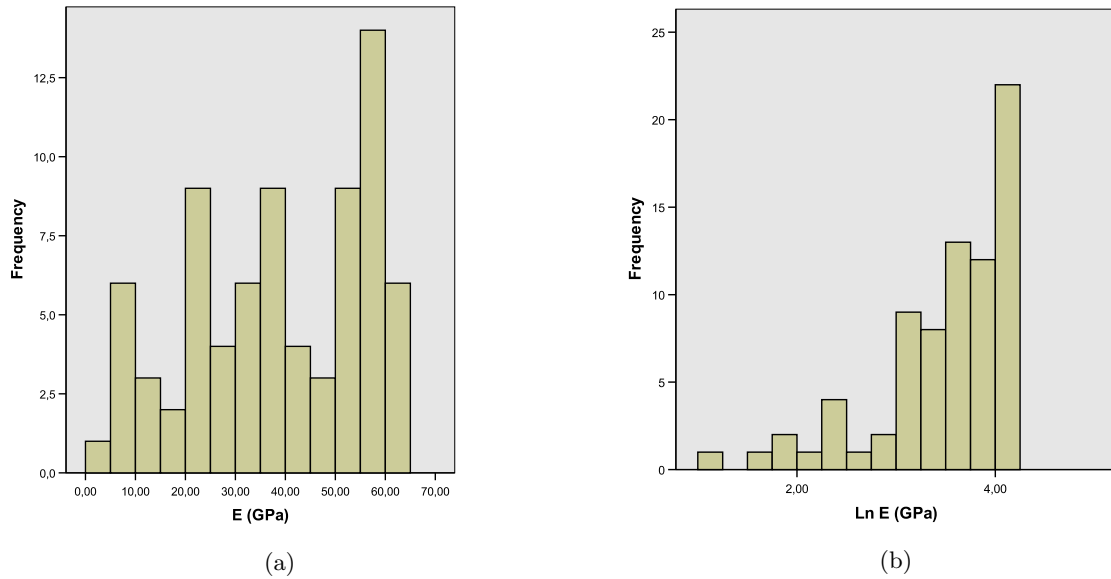


**Figure 5.6:** Histograms of E calculated from the empirical systems application data: (a) raw data (b) logarithmic transformation.

The distributions show high skewness, especially the transformed data and suggest non-normality of the data. The Shapiro-Wilk normality test was performed to test this hypothesis and it shows that they are non-normal for a 95% confidence level. However, based on the central limit theorem, it will be considered that these samples were taken from a population which follow a normal distribution. This assumption is also valid for the data from the LFJ tests.

The histograms of the 160 values of E obtained by the LFJ test are presented in Figure 5.7 in the normal and logarithmic forms. The mean and standard deviation of both distributions are presented in Table 5.2.

**Table 5.2:** Distribution parameters for the values of E obtained by the LFJ tests (GPa).

Parameter	Distribution (a)	Distribution (b)
$\mu$	36.9	3.594
$\sigma$	6.1	0.171
$\sigma^2$	37.2	0.029

The histograms of Figure 5.7 present a normal trend for the data. However, the Shapiro-Wilk normality test showed that for a confidence level of 95%, only distribution a) is a normal distribution.

The mean values of E pointed out by the empirical systems application and the ones given by the LFJ tests are quite close. This means that the initial guess was almost validated by

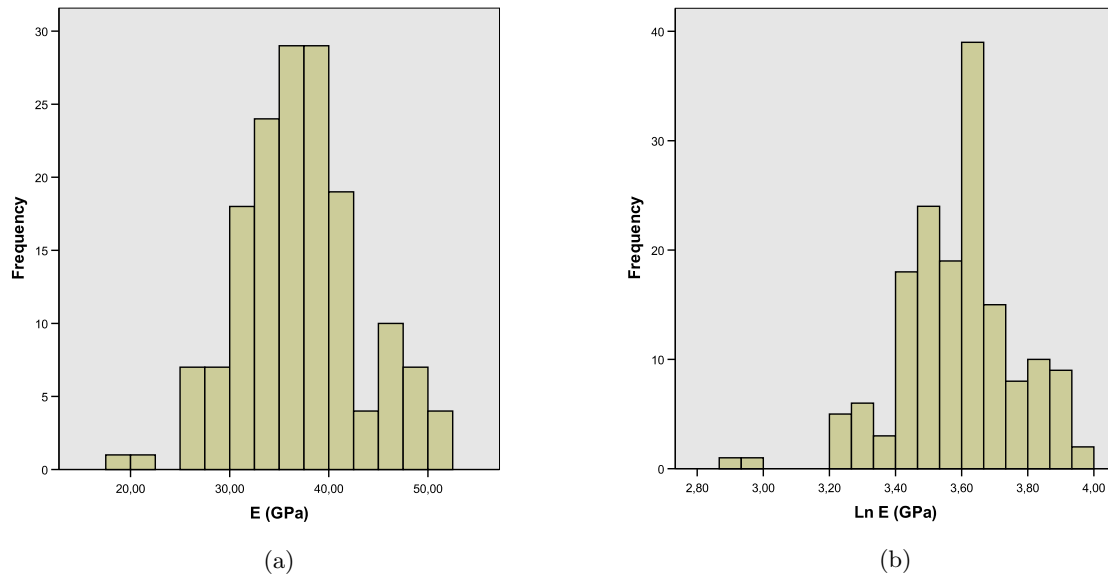


**Figure 5.7:** Histograms of E from the LFJ tests: (a) raw data (b) logarithmic transformation.

the performed *in situ* tests and the updating procedure should not have a significant impact on this value. However, the uncertainty translated by the standard deviation (or variance) is much lower for the LFJ tests so it is expected that its initial value decreases significantly with the Bayesian updating procedure.

### 5.3.3 Updating of E considering unknown mean ( $\mu$ ) and known variance ( $\sigma^2$ )

In the case of using the Jeffreys prior no initial knowledge is considered about E. Nevertheless, in this approach, the value of the population variance is considered to be known. This should not be the current situation and it is used mostly for comparison purposes. For this reason, it is considered a deterministic variance equal to the value of the empirical systems application results.

After obtaining the posterior distribution of the mean values, the Gibbs sampler was used to simulate 10000 population values which showed, in trial calculations, to be a sufficient number of examples to reach convergence. First, mean values for the mean were generated and then used to infer to the population using the known variance. Table 5.3 resumes the values obtained for the posterior distributions of the mean and the simulated population values.

The results obtained for the posterior distributions are comparable in terms of the mean value of the mean which are very similar for both distributions. However, the computed standard deviations have a significant difference with logical impact on the 95% CI. The differences on the standard deviation can be observed in the plots of the probability density functions (Figure 5.8). It can be observed that the mean value of the mean is almost coincident but the

**Table 5.3:** Posterior estimates of the mean value of E considering Jeffreys prior (GPa).

Parameter	Normal distribution	Lognormal distribution
$\mu_1$	36.9	36.4
$\sigma_1$	1.391	1.917
95% CI for the mean	34.2-39.6	32.8-40.3
$\mu_{pop}$	37.0	46.7
$\sigma_{pop}$	19.1	38.2
95% CI for the population mean	5.5-68.5	11.2-117.4

CI - confidence interval

lognormal distribution translates a higher uncertainty about its true location.

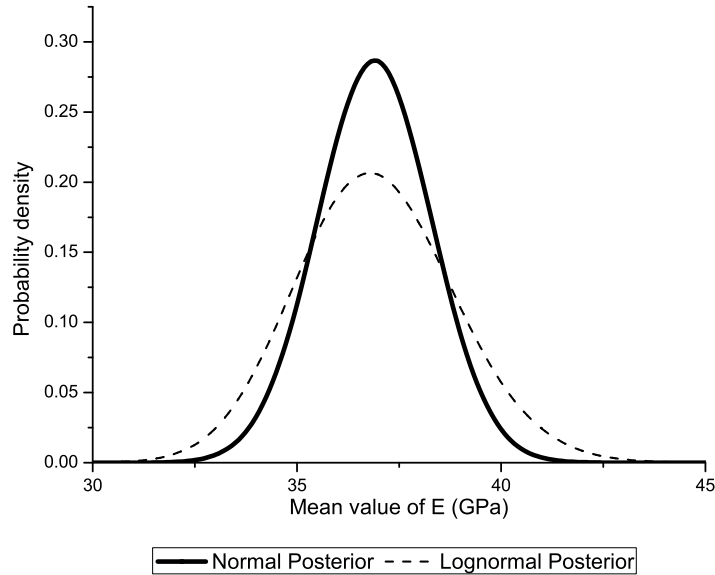


**Figure 5.8:** Posterior probability density functions for the mean value of E for both types of distributions using Jeffreys prior.

The simulated values of the population present significant differences. In the normal case, the mean value for the population is very close to the posterior mean. For the lognormal distribution, the inferred mean value of the population is significantly higher (about 26%) than the one obtained in the normal case. The same trend is observed for the standard deviation and is reflected in the 95% confidence intervals.

Figure 5.9, plotted using the mean value of the mean, shows that the probability density function of the lognormal distribution is highly skewed to the left and, due to the high variance, presents a long tail to the right which reflects on a high value of E on the upper bound of the

95% CI. Another important issue is that the normal distribution, also because of the high deterministic variance, presents positive probabilities for negative values of E.

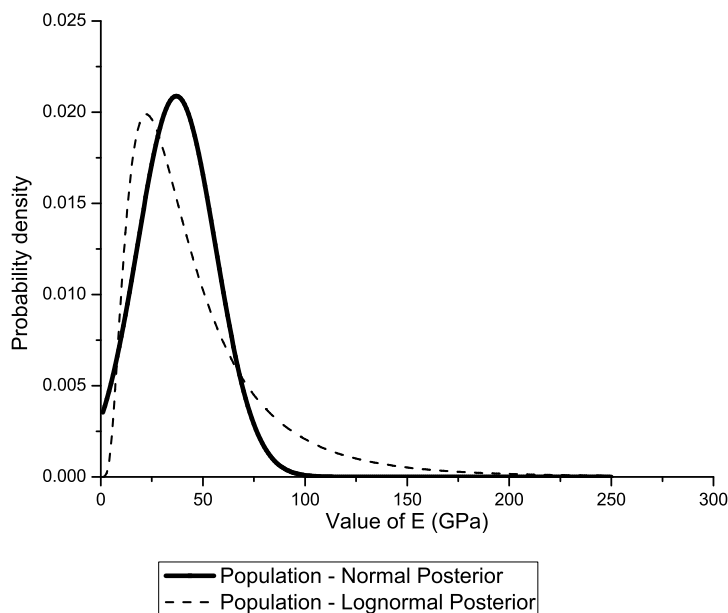


**Figure 5.9:** Posterior probability density functions for the simulated values of E for the both types of distributions using Jeffreys prior (inferred values for the population).

For both cases, the simulated value of the standard deviation is higher than the initial deterministic value since it conveys also the standard deviation (uncertainty) of the mean.

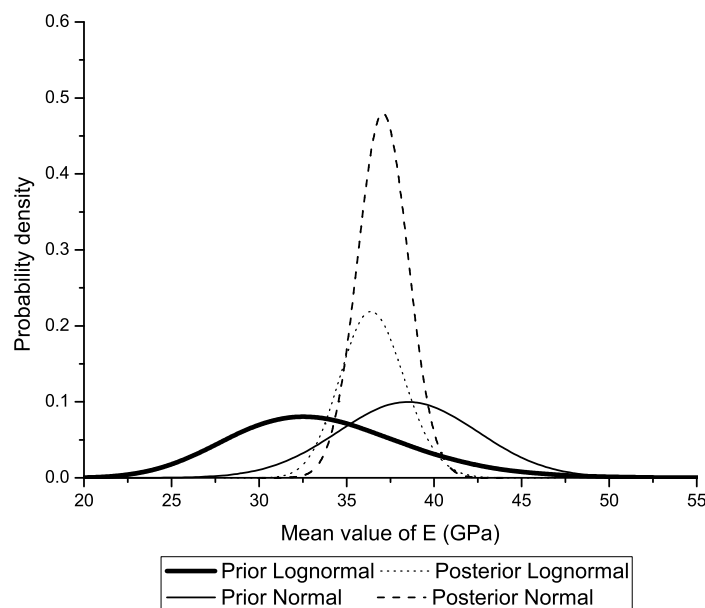
To use the conjugate informative prior it was necessary to define a standard deviation for the initial mean ( $\sigma_0$ ). It was decided to establish this value considering the 95% confidence interval for the mean. For instance, in the normal distribution case, this interval ranged from 34.5 to 42.5, i.e.,  $38.5 \pm 4$ . This way, it was considered 4 GPa to be the standard deviation for the mean. A similar procedure was adopted for the lognormal distribution. Table 5.4 resumes the main parameters of the prior and posterior distributions for this case.

The posterior results are very similar to the previous ones using the Jeffreys prior. Both priors led to almost the same result in terms of the posterior mean with differences lower than 1%. Only a slight reduction (about 6%) is observed in terms of the posterior standard deviation because of the information provided by the prior. The mentioned facts point out for the low impact of the prior in the posterior parameters. In fact, the high uncertainty in the initial data, translated by its high variance, turns the initial distribution little informative. Moreover, and based in the asymptotic theory, as the sample increases the posterior converges to the likelihood. In this case, the sample is composed by 160 cases which can be considered a high

**Table 5.4:** Prior and posterior estimates of the mean value of E considering the conjugate prior (GPa).

Parameter	Normal distribution	Lognormal distribution
$\mu_0$	38.5	33.1
$\sigma_0$	4	5.1
$\mu_1$	37.1	36.0
$\sigma_1$	1.314	1.806
95% CI for the mean	34.5-39.7	32.6-39.7
$\mu_{pop}$	37.1	46.5
$\sigma_{pop}$	18.9	38.4
95% CI for the population mean	5.9-68.2	11.0-117.4

value. Figure 5.10 presents the prior and posterior probability density functions for the mean value of E.

**Figure 5.10:** Prior and posterior probability density functions for the mean value of E.

It can be observed that the effect of the LFJ tests is quite significant and that the prior distribution is relatively flat. The uncertainty about the initial mean value was substantially decreased since its standard deviation was reduced from 4 GPa to 1.3 GPa in the normal case and from 5.1 GPa to 1.8 GPa for the lognormal case. Both posteriors converged to a near location around a higher probability region between 36 GPa and 37 GPa.

The values inferred for the population are also quite close to the previous case. This is also due to the already mentioned fact that these values are mainly controlled by the deterministic

value of the variance. The updating of the mean value distribution has a minor impact on the posterior simulated population.

The confidence intervals for the population mean are very large. They are fundamentally controlled by the high population variance and little by the mean variance.

For comparison purposes, Figure 5.11 shows a plot of the prior and posterior population probability density distribution of E, for the normal case, considering the mean value of the mean. The influence of the mean updating in the population is small due to the deterministic value of the standard deviation. Even though some uncertainty reduction can be observed. An important issue is the existence of negative values with non-zero probability for both prior and posterior distributions.

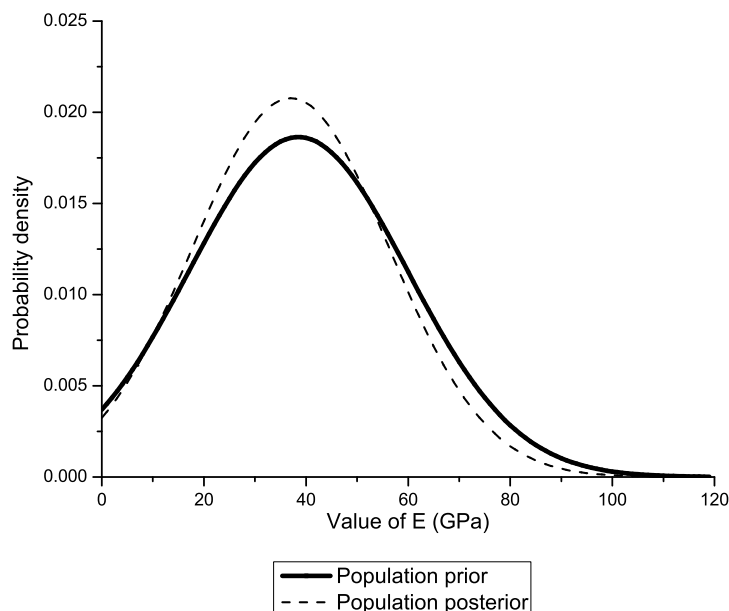


**Figure 5.11:** Prior and posterior probability density distributions for E considering the normal distribution (inferred values for the population).

Figure 5.12 compares the posterior density distributions for the mean value of E. The main aspect is the higher variation for the conjugate prior case for the normal model. This is due to the fact that posterior variance conveys the sample and prior variance while for the Jeffreys case only the sample variance is considered in the model. This increasing variance in the posterior for the conjugate case is negligible for the lognormal distribution. In fact, both approaches led to almost equal posterior distributions showing that, in this case, the prior information had minor impact in posterior results.

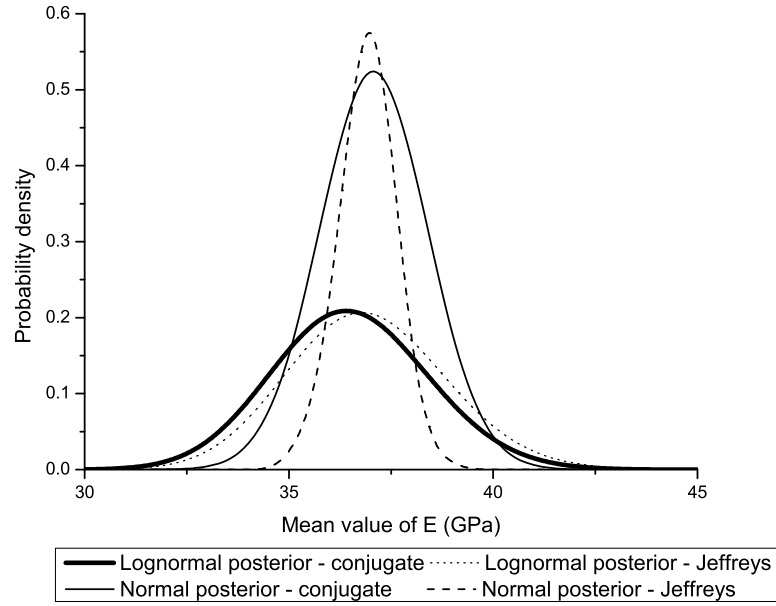


**Figure 5.12:** Posterior probability density distributions for E considering the Jeffreys and conjugate priors.

### 5.3.4 Updating of E considering normal data and unknown mean ( $\mu$ ) and variance ( $\sigma^2$ )

In this case, Jeffreys posterior is conditional on the data and on the unknown variance. This posterior is a normal distribution with mean  $\bar{x}$  and variance  $\sigma^2/n$  and the marginal posterior for  $\sigma^2$  is an inverse  $\chi^2$  distribution. This way, the posterior distributions take the forms presented in Table 5.5. The obtained results for the main parameters of the mean and simulated population posterior distributions are presented in Table 5.6.

**Table 5.5:** Posterior distributions considering Jeffreys prior

Normal distribution	Lognormal distribution
$\mu \sigma^2, X \rightarrow N\left(\bar{x}, \frac{\sigma^2}{n}\right) \Rightarrow N\left(36.9, \frac{\sigma^2}{160}\right)$ $\frac{(n-1)s^2}{\sigma^2} \Rightarrow \frac{5916.39}{\sigma^2} \rightarrow \chi_{n-1}^2$	$\mu \sigma^2, X \rightarrow N\left(\bar{x}, \frac{\sigma^2}{n}\right) \Rightarrow N\left(3.594, \frac{\sigma^2}{160}\right)$ $\frac{(n-1)s^2}{\sigma^2} \Rightarrow \frac{4.649}{\sigma^2} \rightarrow \chi_{n-1}^2$

The posterior values of the mean are equal to the previous case where the variance was considered as a known parameter. In fact, a different approach did not affect this value but had significant impact on its variability. Since the variance was considered a random unknown

**Table 5.6:** Posterior estimates of the mean value of E (GPa)

Parameter	Normal distribution	Lognormal distribution
$\mu_1$	36.9	36.4
$\sigma(\mu_1)$	0.244	0.007
$\sigma_1$	6.13	1.89
$\sigma(\sigma_1)$	0.35	0.012
95% CI for the mean	36.5-37.3	36.37-36.39
$\mu_{pop}$	37.2	37.3
$\sigma_{pop}$	6.38	6.57
95% CI for the population mean	26.7-47.7	27.5-49.0

value, its distribution depended only on the variance of the LFJ tests which was significantly lower than the deterministic variance in the previous case. This fact was most pronounced for the case of the lognormal distribution and is reflected in the 95% CI for the mean which is extremely narrow.

The consideration of a random variance also had significant influence on the population simulated values since it was possible to update its value reducing the uncertainty about E. The updated parameters of the distributions are very similar for both cases. In Figure 5.13 the probability density functions are presented and the similarity of the distributions can be observed.

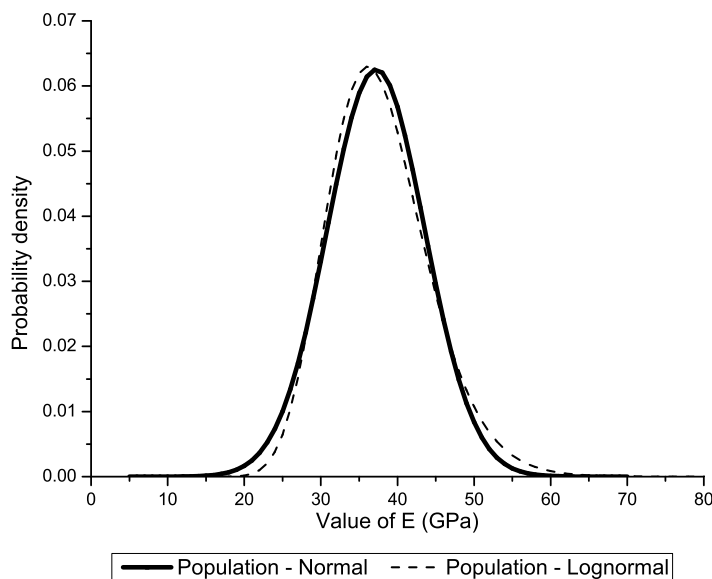


**Figure 5.13:** Posterior probability density distributions for E for the normal and lognormal case using Jeffreys prior (inferred values for the population).



In this case, there are no negative values with positive probabilities in the normal distribution case. The 95% confidence intervals for the mean value of the population appear to be credible in an empirical judgement.

In the case of conjugate prior distributions, the initial data based on the empirical rock mass classifications was used to obtain the priors for the mean and variance. Applying Bayes theorem and using the abovementioned data from the LFJ tests, the conditional posterior distribution for the mean and the marginal posterior for the variance were obtained. The prior and correspondent updated posterior distributions are presented in Table 5.8.

**Table 5.7:** Prior and posterior distributions considering the conjugate prior.

	Normal distribution	Lognormal distribution
Priors	$\mu \sigma^2, X \rightarrow N\left(38.5, \frac{\sigma^2}{76}\right)$ $\frac{1}{\sigma^2} \rightarrow \text{gamma}\left(38.5, \frac{1}{11573.5}\right)$	$\mu \sigma^2, X \rightarrow N\left(3.489, \frac{\sigma^2}{76}\right)$ $\frac{1}{\sigma^2} \rightarrow \text{gamma}\left(38.5, \frac{1}{16.586}\right)$
Posteriors	$\mu \sigma^2, X \rightarrow N\left(37.4, \frac{\sigma^2}{236}\right)$ $\frac{1}{\sigma^2} \rightarrow \text{gamma}\left(118.5, \frac{1}{14597.6}\right)$	$\mu \sigma^2, X \rightarrow N\left(3.560, \frac{\sigma^2}{236}\right)$ $\frac{1}{\sigma^2} \rightarrow \text{gamma}\left(118.5, \frac{1}{19.194}\right)$

As the mean is conditional on the variance, prior and posterior estimates for the mean value and standard deviation were obtained by simulation using the Gibbs sampler similarly to the previous example. The main results for the prior and posterior distributions are presented in Tables 5.8 and 5.9.

The updated mean value of the mean ( $\mu$ ) underwent a small variation from prior to posterior estimates. In fact, this variation was only of about 3% and 7% for the normal and lognormal case, respectively. The initial mean value was already close to the results provided by the LFJ tests. This means that the analytical solutions provided a very good estimate of E.

The most important aspect is the substantial uncertainty reduction at all levels. For the normal distributions case the standard deviation of the mean ( $\sigma(\mu)$ ) has reduced from 2.02 GPa to 0.73 GPa, i.e. only 36% of the initial value. The mean of the standard deviation ( $\sigma$ ) underwent a 37% decrease from 17.5 GPa to 11.1 GPa. Finally, the standard deviation of the standard deviation ( $\sigma(\sigma)$ ) was also significantly decreased from 1.45 GPa to 0.51 GPa.

**Table 5.8:** Prior and posterior estimates of the mean value of E (normal distribution) (GPa).

Parameter	Normal distribution	Lognormal distribution
$\mu$	38.5	37.4
$\sigma(\mu)$	2.02	0.73
$\sigma$	17.5	11.1
$\sigma(\sigma)$	1.45	0.52
95% CI for the mean	35.2-41.8	36.2-38.6
$\mu_{pop}$	38.4	37.5
$\sigma_{pop}$	19.6	11.9
95% CI for the population mean	6.1-70.7	17.9-57.1

**Table 5.9:** Prior and posterior estimates of the mean value of E (lognormal distribution) (GPa).

Parameter	Normal distribution	Lognormal distribution
$\mu$	32.8	35.2
$\sigma(\mu)$	2.47	0.915
$\sigma$	1.943	1.498
$\sigma(\sigma)$	0.105	0.028
95% CI for the mean	28.9-37.1	33.6-36.7
$\mu_{pop}$	42.8	38.3
$\sigma_{pop}$	36.1	17.3
95% CI for the population mean	9.8-109.2	17.2-71.0

The lognormal distribution follows the same trend of uncertainty reduction. The relative reduction of  $\sigma(\mu)$  was very similar to the previous case. In relation to the remaining parameters,  $\sigma$  and  $\sigma(\sigma)$ , they were reduced in 23% and 73%, respectively.

To illustrate this fact, Figure 5.14 shows the prior and posterior probability density functions of the mean value of E considering the mean value of its standard deviation. The uncertainty reduction from the prior to the posterior can be clearly observed.

Using simulation it was possible to infer mean and 95% CI for the population. In relation to the mean value, the updating process only changed significantly the mean of the lognormal distribution which was reduced in about 11%. For the normal distribution case this value remained almost unchanged.

Also for the population values the updating process allowed a significant reduction on the dispersion measures which means less uncertainty. The standard deviation values were reduced in 39% and 52% respectively for the normal and lognormal distributions, with direct impact on a substantial narrowing of the 95% CI for the mean.

In Figure 5.15 the prior and posterior probability distributions of E considering the mean values of the mean and standard deviation is presented. The uncertainty about the parameter

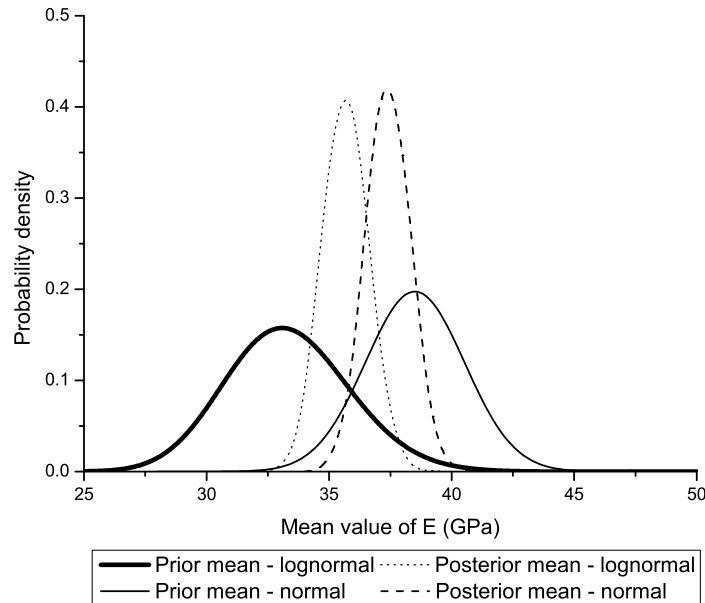


**Figure 5.14:** Prior and posterior probability density functions for the mean value of E.

was clearly reduced using the Bayesian methodology. For the normal distribution case the prior allowed for negative values to have positive probabilities. The updating process corrected this situation. The prior lognormal distribution avoided this situation to happen because it does not allow negative values. The updating enabled to reduce the uncertainty as well as the high skewness of the prior.

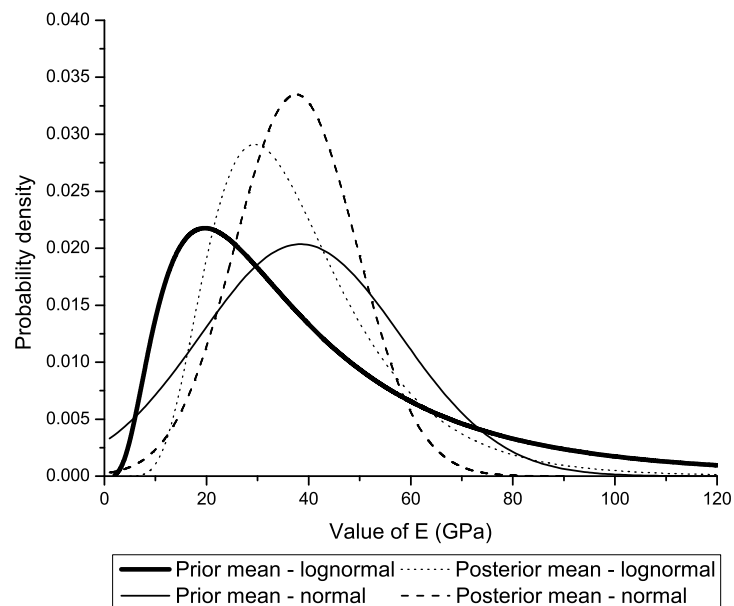


**Figure 5.15:** Prior and posterior probability density functions for E (inferred values for the population).

The main aspect to focus when comparing the posterior results using the Jeffreys and conjugate priors, is that the variance is higher for the latter. In fact, as it is clearly illustrated by Figure 5.16, the uncertainty is higher for the conjugate distributions. This fact was already observed for the case of unknown mean and known variance and is due to the consideration of the prior information uncertainty which does not exist when using Jeffreys prior.

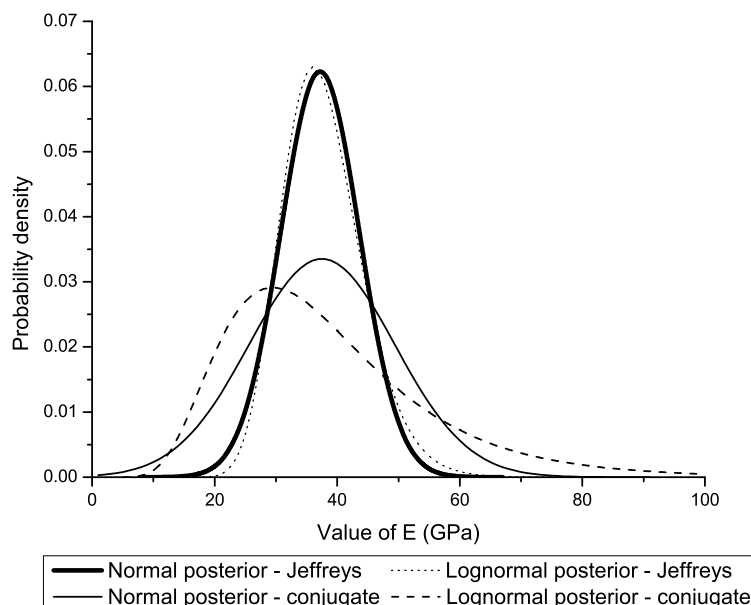


*Figure 5.16:* Posterior probability density functions for E (inferred values for the population).

## 5.4 Alternative updating methodology using the Weibull distribution

### 5.4.1 Introduction

The Bayesian framework presented previously showed good results in the uncertainty treatment especially when both mean and variance of the parameter are considered to be unknown random variables. However, it can be pointed out as the main drawback the relative sensitivity of the posterior results to the prior distribution assumptions.

In this context, a new methodology is proposed which tries to avoid this problem and can be generally applied to most geotechnical parameters updating problems. In this methodology, a two-parameter Weibull distribution is used to model both prior data and the likelihood. The Weibull distribution is a much more flexible distribution which adapts to the available data and

can transform into a normal, Rayleigh or even an exponential distribution depending on the data configuration.

Since Weibull data is not conjugate with Weibull prior there is no closed form solution to the problem. This way, to avoid heavy computations which would transform the method difficult to implement in a practical sense, some acceptable simplifications were performed. The method is then a heuristic approximation to produce a quick method of estimating Weibull parameters assuming that they are normally distributed. This can be considered an acceptable simplification since one of the properties of maximum likelihood estimators is that they are asymptotically normal, meaning that for large samples they are normally distributed.

In the next item the Weibull distribution is briefly described since it is not widely used in geotechnical applications. Then the developed methodology is presented followed by the main results.

#### 5.4.2 The Weibull distribution

The type of Weibull distribution used in this methodology is called the two-parameter Weibull distribution (Weibull, 1951). Its probability density function is defined as:

$$f(x) = \frac{\beta}{\alpha} \left(\frac{x}{\alpha}\right)^{\beta-1} \exp\left(-\frac{x}{\alpha}\right)^{\beta}; x \geq 0 \quad (5.49)$$

where  $\beta > 0$  is the *shape* (or slope) parameter and  $\alpha > 0$  is the *scale* parameter. For  $x < 0$  this function takes a zero value. The correspondent cumulative distribution function is translated by:

$$F(x) = 1 - \exp\left(-\frac{x}{\alpha}\right)^{\beta} \quad (5.50)$$

The reliability of a distribution is simply one minus the cumulative distribution function so the reliability of the Weibull distribution is given by:

$$R(x) = \exp\left(-\frac{x}{\alpha}\right)^{\beta} \quad (5.51)$$

The mean ( $\mu$ ) and standard deviation ( $\sigma$ ) of a Weibull random variable can be expressed as:

$$\mu = \alpha \cdot \Gamma\left(\frac{1}{\beta} + 1\right) \quad (5.52)$$

$$\sigma = \alpha \cdot \sqrt{\Gamma\left(\frac{2}{\beta} + 1\right) - \Gamma\left(\frac{1}{\beta} + 1\right)^2} \quad (5.53)$$

where  $\Gamma$  is the gamma function which is defined as:

$$\Gamma(n) = \int_0^{\infty} e^{-x} x^{n-1} dx \quad (5.54)$$

To obtain the value ( $x$ ) correspondent to a certain reliability degree ( $R(x)$ ) the following expression can be used:

$$x = \alpha \cdot \{-\ln [R(x)]\}^{1/\beta} \quad (5.55)$$

If  $R(x) = 0.50$  one obtains the median value.

The Weibull distribution is one of the most widely used in reliability engineering and failure analysis. It is also very important in extreme value theory, weather forecasting and industrial engineering problems. It is a very versatile and flexible distribution since it adapts to the data and can mimic the behaviour of other types of distributions, based on the value of the shape parameter,  $\beta$ . For instance if  $\beta$  is equal to 3.4 or 1 then the Weibull distribution appears similar to the normal and exponential distributions, respectively.

Weibull analysis is a method for modelling data sets containing values greater than zero. Many methods exist for estimating Weibull distribution parameters from a set of data like the probability plotting, the maximum likelihood estimation or the hazard plotting. To apply any of these methods it is necessary to perform some preliminary calculations.

The probability plotting method, which was used in this work, involves the calculation of a regression line based on the input data. It starts with the organisation of data in ascending order and defining the order number or rank of each data entry. Next, it is necessary to obtain their median rank positions which can be estimated using the following equation:

$$MR(\%) \approx \frac{i - 0.3}{N + 0.4} \cdot 100 \quad (5.56)$$

where  $i$  is the order number and  $N$  is the total sample size. The abscissas and ordinates for the regression line are then obtained using the following expressions:

$$x_i = \ln(X_i) \quad (5.57)$$

$$y_i = \ln[-\ln(1 - MR)] \quad (5.58)$$

where  $X_i$  are the different data values. Then, using the least square method, it is possible to obtain the regression line in the current form  $y = a + bx$ . The Weibull parameters can then be calculated using the following expressions:

$$\beta = b \quad (5.59)$$

$$\alpha = \exp \left[ - \left( \frac{a}{b} \right) \right] \quad (5.60)$$

### 5.4.3 The proposed methodology

In geotechnical engineering, most of the times some prior knowledge about the parameters exist. This knowledge can be based on empirical assumptions, preliminary *in situ* or laboratory tests, data from similar formations, etc. In this methodology it is assumed that a prior distribution can be set up.

It is intended to model both the prior and the new data with Weibull distributions to take advantage of its flexibility to adapt to the data. However, because the parameters of the Weibull prior are not conjugate with Weibull data there is no analytical formula for the posterior probability density of the parameters. The Bayesian updating process can be very complex if conjugate distributions are not used.

To overcome this problem the developed methodology is based on a simple heuristic: the parameters of the Weibull distributions are random variables which follow a multivariate normal distribution and can be updated analytically as such. The main disadvantages are that the method does not use formal Bayesian methods and assumes that the parameter estimates are normally distributed. This can be considered as an acceptable approximation since the maximum likelihood estimators for the Weibull parameters are asymptotically normal, meaning that for large samples they are normally distributed. Even though the used method of parameter estimation was the probability plot it conducts, normally, to similar results to the maximum likelihood approach.

Brennan and Kharroubi (2007) considered the same simplifications in a similar Weibull approach and they reached an approximately 5% error from the full Bayesian calculation. Moreover, the authors stated that its accuracy is context dependent. If the prior information is weak (i.e. based on little knowledge or with considerable uncertainty) and the data is strong (i.e. large sample size) or in the inverse case of strong prior and weak data, then the result can be almost equivalent to formal Bayesian updating. Between these extremes, the simplifications can lead to reduced accuracy.

The developed methodology starts then with the computation of the Weibull parameters ( $\alpha$  and  $\beta$ ) from the prior data. As it was already referred, it is assumed that the uncertainty in these parameters can be correctly characterised by a multivariate normal distribution (*Prior*  $\rightarrow N(\mu_0, \sigma_0)$ ). The value of  $\sigma_0$  was considered to be related to the 95% CI to the mean of the Weibull analysis regression parameters. This way,  $\sigma_0$  was computed as the distance between the mean and the upper or lower bound of the 95% CI. In the cases where the distances were different, the mean of the two values was considered.

Next, the same procedure is applied to the data considering again a multivariate normal distribution to characterise the parameters uncertainty (*Data*  $\rightarrow N(\mu, \sigma)$ ). To combine the prior evidence and the data, the Bayesian updating formulae for the multivariate normal distribution to calculate the posterior parameter estimates are used:

$$\mu_1 = \frac{\frac{\mu_0}{\sigma_0^2} + \frac{\mu}{\sigma^2}}{\frac{1}{\sigma_0^2} + \frac{1}{\sigma^2}} \quad (5.61)$$

$$\frac{1}{\sigma_1^2} = \frac{1}{\sigma_0^2} + \frac{1}{\sigma^2} \quad (5.62)$$

To produce population values a simulation procedure is used. First, 10000 random values for the parameters of the Weibull distribution are generated from their normal distribution parameters. These values are then used to generate Weibull random values which are again fitted to a Weibull distribution which is considered the population distribution. From this distribution it is possible to obtain the probability density function and to calculate moments and values with certain reliability levels which can be of significant interest. Figure 5.17 schematizes the described steps.

This method is relatively simple to use and takes advantage of the versatility and flexibility of the Weibull distribution which adapts to the data and can take on the characteristics of other types of distributions.

#### 5.4.4 Results

In the first stage, a Weibull analysis was applied to the initial data from the empirical systems and to the results of the LFJ tests. As it was referred, it was considered that the distribution parameters of the Weibull distributions followed a normal distribution. This way, the parameters obtained by Weibull analysis are the mean value of the distribution. The standard deviation is related to the 95% confidence interval for the parameter obtained by the linear regression procedure.



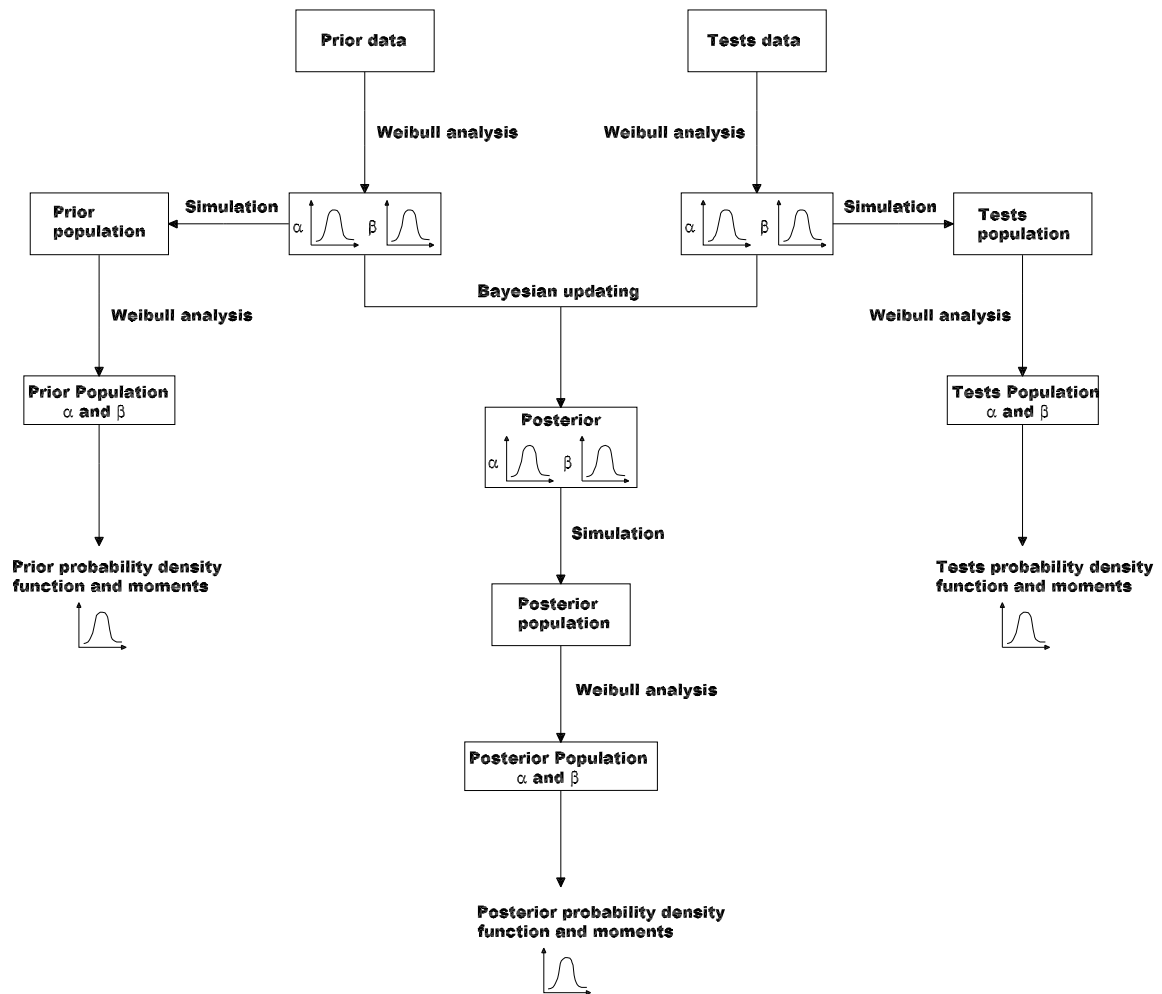


Figure 5.17: Scheme of the alternative Bayesian updating scheme.

Using these parameters it is then possible to produce the posterior estimates. In Table 5.10 the distribution parameters obtained through the Weibull analysis to the prior and tests data and posterior updated values are presented. In the same Table the  $R^2$  parameter values from the regression analysis are presented since they are a measure of the Weibull distribution fitting to the data. The values of these coefficients are near the unity which points out to a good fitting. As expected, the posterior parameters present lower standard deviations which mean that uncertainty was reduced by using the Bayesian updating process.

The population values were generated through simulation. Due to the high standard deviation of the parameter  $\alpha$ , mainly in the prior distribution, the simulated values were truncated to avoid negative values since this parameter can only assume positive ones. The parameters of the Weibull fit to the simulated data are presented in Table 5.11 also along with  $R^2$  of the linear fit.

**Table 5.10:** Mean and standard deviation of the Weibull parameters and determination coefficient from the Weibull analysis fitting (GPa).

	$\alpha$		$\beta$		$R^2$
	Mean	Std. dev.	Mean	Std. dev.	
<b>Prior data</b>	44.303	17.7	1.8282	0.095	0.9523
<b>LFJ tests</b>	39.314	7.9	7.2473	0.198	0.9706
<b>Posterior</b>	40.143	7.2	2.8423	0.086	-

**Table 5.11:** Parameters of the Weibull fit for the simulated population values (GPa).

	$\alpha$	$\beta$	$R^2$
<b>Prior data</b>	36.762	3.0415	0.8428
<b>LFJ tests</b>	37.145	14.357	0.8546
<b>Posterior</b>	37.020	4.6114	0.9578

The  $R^2$  values are a little lower for the prior and the data due to the higher dispersion of the simulated data comparing to the original one. The fitting for the posterior data can be considered very good. Figure 5.18 presents the probability density functions of the prior, likelihood and posterior Weibull population distributions correspondent to the parameters of Table 5.11. In this Figure it is possible to observe the flatness of the prior due to the high uncertainty about the distribution parameters. The posterior updated distribution presents lower uncertainty due to the high reliability of the LFJ tests.

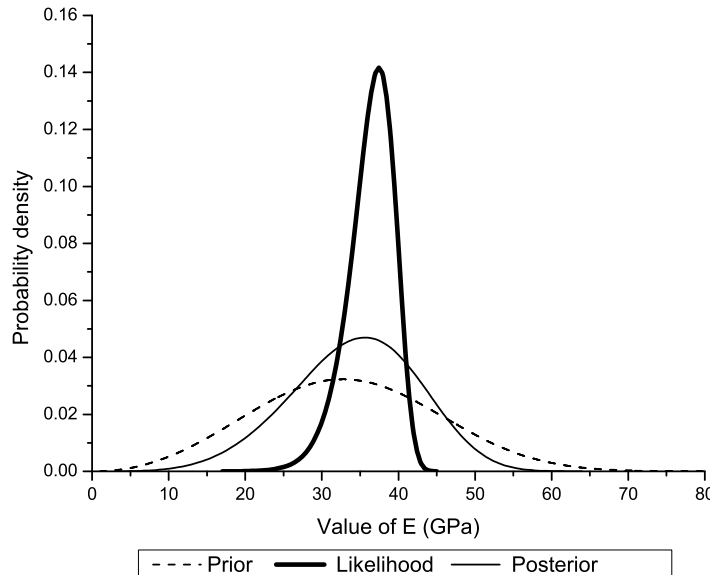


**Figure 5.18:** Weibull distributions for the simulated populations.

The Weibull distribution allows using the reliability concepts in the calculation of parame-

ters. Using the obtained distributions it is possible to calculate values with certain reliability levels. In this case, the reliability of a certain value is interpreted as the probability of the parameter true value to be higher than it. Table 5.12 presents the E values for the prior and posterior distributions considering different reliabilities.

**Table 5.12:** E values for different reliability levels (GPa).

<b>E (GPa)</b>		
<b>Reliability</b>	<b>Prior</b>	<b>Posterior</b>
0.01	60.7	51.6
0.025	56.5	49.1
0.05	52.7	47.0
0.10	48.4	44.4
0.5	32.6	34.2
0.90	17.5	22.7
0.95	13.8	19.4
0.975	11.0	16.7
0.99	8.1	13.7

## 5.5 Conclusions

Bayesian methods have an inherent flexibility introduced by the incorporation of multiples levels of uncertainty and the resultant ability to combine information from different sources. In other words, the major advantages of the Bayesian approach are in its ability to combine different information and its rational way of dealing with uncertainty using probabilistic tools. This methodology allows one to update random variables as new data is collected.

It is believed that the characteristics of the Bayesian data analysis make it well suited to be applied on geotechnical problems where uncertainty is always present at different levels. In geotechnics, the information about the interested formations increases as the project advances for different stages and can be used to update the geotechnical models. Nowadays, this updating is carried out based on empirical knowledge and basic statistic procedures.

In this Chapter, a general Bayesian framework for the geomechanical parameters updating was developed and applied to the updating of E in an underground structure. Different types of probability distributions, initial knowledge and uncertainty levels were considered and tested.

The first approach, which considered the mean value as a random unknown variable and the variance known and deterministic, allowed obtaining good results in what concerns the mean updating. In fact, it was possible to calculate updated posterior values, which were similar for

both distributions, considering the LFJ test results, with reduced uncertainty. The conjugate case provided very similar results which mean that the prior information had very little impact and the posterior was controlled by the new data. The population simulated values showed to have low sensitivity to the mean updating since its behaviour is mostly controlled by the deterministic variance.

The results showed to be sensitive to the type of distribution assumed for the data. Important differences were observed in the posterior distributions for both the mean and the population values considering the normal and lognormal distributions.

The major drawback of this approach is related with the calculation of the characteristic values of  $E$  which is very important for design purposes. The fact that the population variance is considered to be constant significantly influences the characteristic values maintaining them almost unchanged. These values only vary due to the mean updating which has little impact on the population distribution.

The second approach, which considers both mean and variance as unknown variables, even though computationally more complex, allows overcoming this problem. The value of the population variance is also updated which has an important influence on its distribution. This approach allows a more global treatment of uncertainty and presents higher potential to be used for the geomechanical parameters updating.

In this case, and when using the uninformative Jeffreys prior, probabilistic distributions of the population were almost identical for both normal and lognormal case. Using the conjugate prior the mean and population distributions seemed to be more sensitive to the choice of distribution type.

Concluding, the approach of unknown mean and known variance is simpler and can be used when the parameter of interest is the mean value of the geomechanical parameter. In geotechnical engineering, the prior information is often more uncertain and if this data is used to define a deterministic variance, which will certainly be high, the updating of characteristic values for the population can be compromised.

The more complex model that considers both mean and variance as random variables, which can be updated to infer to the population, allows overcoming the main problem raised by the previous approach. It deals with uncertainty in a more global way allowing it to be reduced in several dimensions. In both cases, posterior inferences showed stability to the choice of different priors.

This Bayesian framework provides a consistent way of treating data coming from different sources in order to increase the reliability in the calculated geomechanical parameters. Both approaches are considerable sensitive to the choice of the population distribution which can not be known. However, experience shows that lognormal distributions are more adequate to

model data from deformability parameters and should be considered in the absence of more information.

It is worth emphasising that, in the conjugate prior case, the Bayesian updating procedure did not significantly change the mean value of  $E$ . The preliminary evaluation based on analytical solutions and in the empirical rock mass classification systems application, was almost corroborated by the results of the LFJ test. However, the data led to a very significant decrease in the uncertainty about the parameters.

An alternative methodology was developed to try to overcome the sensitivity of the type of distribution choice by using a much more flexible and general one which can adapt to the available data. In this case, the 2-parameter Weibull distribution was used avoiding the more rigid normal or lognormal distributions.

Since it is not possible to find conjugate distributions for the Weibull, some acceptable simplifications were considered. The methodology is based on a heuristic that the model parameters are random variables which follow a normal distribution and that the Bayesian updating model for such distributions can be applied.

The  $R^2$  values obtained in the regression analysis for the calculation of the Weibull distribution parameters showed that it fitted well the observed data. For the prior and tests population the fit is a little worst but still within acceptable values. To improve the results of this methodology and to get better fits to the data, the 3-parameter Weibull distribution or even mixtures of Weibull with other distributions could be used leading to a more complex approach.

The methodology allowed to reduce the uncertainty concerning  $E$  and to obtain values with different reliabilities. Using this Bayesian framework it is not necessary to specify the type of distribution for the data since it uses a distribution that models the available data and adapts to it. It can approximate a normal, exponential or other skewed distribution.

This work showed how the Bayesian tools can be used in geotechnics. Its main innovative contribution is the definition of general, proper and mathematically consistent methods for the geomechanical parameters updating that can be used in the different stages of an underground work project.

The developed frameworks for the  $E$  updating showed interesting results especially in the uncertainty reduction. These procedures can be sequentially applied as more information about the rock mass is gathered.

These methodologies can be extended to models with more parameters (strength parameters for instance). More complex models could imply the use of Bayesian structures with higher complexity like the mixture or the hierarchical models.



# Application of Inverse Methodologies in Underground Structures

## 6.1 Introduction

Design and construction of underground works is many times based on the observational method (Terzaghi and Peck, 1948) in which field measurements are used in order to overcome uncertainties related to the complexity and unpredictability of geological/geotechnical features. This way, during construction and in some cases also in the exploration stage, displacements and stresses of the underground structure surrounding the rock mass are monitored. Initially, this information was used only for direct interpretation of safety assessment and to evaluate the adequacy of the design and construction methods. Nowadays, with the development of computational methods and observational techniques, it can also be used by practitioners and researchers to validate or update the input data (like the geomechanical parameters for instance) allowing a deeper understanding of the rock mass-underground structure behaviour and providing a sound basis for the adaptation of the initial design and construction method.

The procedure of using field measurements in order to obtain input material parameters is called back analysis in opposition to the conventional forward approach. At this point, it is interesting to mention the main characteristics and differences of both methodologies (Figure 6.1). A forward analysis starts with the definition of a constitutive model and their related parameters which is normally carried out based on geological-geotechnical survey and in experience. This information is used as an input on the numerical models developed for design purposes and to predict stresses, strains, displacements, etc. In the back analysis approach, field

measurements are used together with the models to calibrate their parameters (geomechanical, stress state, etc...) matching, under a defined tolerance, predicted with observed measures. In other words, based on monitoring results of displacements and/or stresses (most of the times only displacements are available) and computational models, geomechanical parameters, loads distribution and geometric conditions can be back analysed.

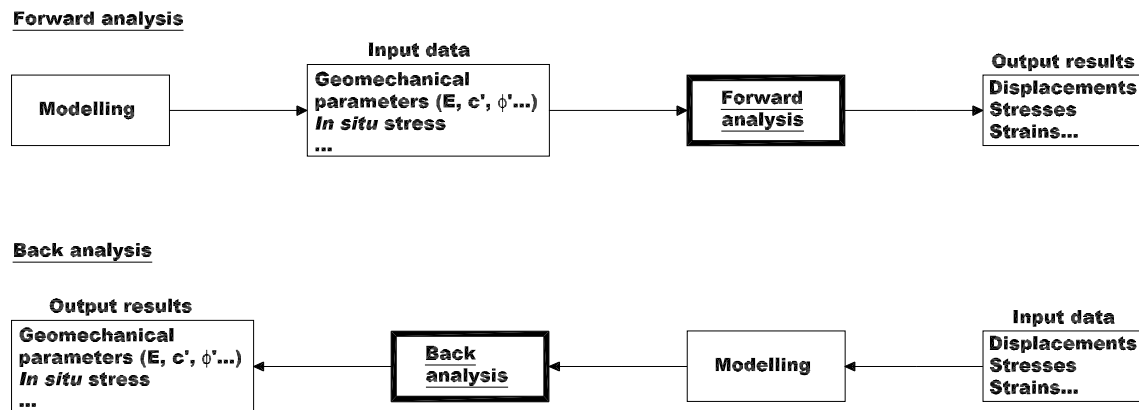


*Figure 6.1:* Scheme of the forward and back analysis (adapted from Sakurai (1997))

Two basic types of problems can be solved using back analysis techniques (Castro *et al.*, 2002):

- inverse problems of the first kind: determination of external loads based on the structural properties and corresponding observed effects;
- inverse problems of the second kind: determination of structural properties as a function of the external loads and corresponding observed effects.

The back analysis of geomechanical parameters in underground structures is within the scope of the latter type of problems. This approach can be formulated as a problem of parameter estimation in which the constitutive model is considered to be known and fixed. A full back analysis procedure should consider all the uncertainties related to the problems therefore the constitutive model should also be determined by back analysis (Sakurai *et al.*, 1995). In the scope of this work, only the identification of geomechanical parameters is carried out and the used constitutive models are considered to be known.

Modelling softwares are not prepared to compute geomechanical parameters from measurement input data. This way, an iterative procedure has to be adopted in order to obtain the required output. Depending on the way the identification problem is solved, the available



back analysis methodologies can be divided in two main categories: the inverse and the direct approach (Cividini *et al.*, 1981; Gioda and Sakurai, 1987).

In the *inverse* approach the equations which describe the system behaviour are rewritten/inverted in such a way that the material parameters appear as outputs and the measured quantities as inputs. The first application of the inverse approach was carried out by Gioda (1980) to identify elastic parameters and earth pressure in a tunnel lining. Murakami and Hasegawa (1987) incorporated the Kalman filter probabilistic procedure in this algorithm in order to consider the measurement errors in the results of back analysis. If the measurement data set is well selected, this approach assures stability and fast convergence in the back analysis process (Venclik, 1994). This approach, in spite of normally being more efficient (demands less iterations to converge), raises however some computational issues. For instance, in order to invert the governing equations, and when a numerical model is used, it demands the access to the software code which most of the times is not possible.

In the *direct* approach the numerical model is not modified. It is used together with an error function (like the least squares), also called cost function, which measures the difference between the observed and computed quantities. This function, which is normally non-linear, is minimised in an iterative process using an optimisation algorithm. The direct approach is more flexible than the previous since the optimisation routine can be programmed independently from the numerical model and the coupling can be carried out using simple programming. However, the iterative process can be time-consuming and convergence to the global minimum is not assured. In the developed studies, the direct approach was used since it is a far more flexible methodology.

Back analysis was introduced by Gioda (Gioda, 1980), Gioda and Maier (1980) and Cividini *et al.* (1981) for the sophistication of the observational method and constitutes an essential tool for assessing design parameters in underground structures. In the broader field of geotechnics, many applications can be found in literature of which the following can be mentioned (Swoboda *et al.*, 1999; Sheu, 2006):

- characterisation of strength and deformability parameters of soils and rocks in underground works (Gioda and Maier, 1980; Gioda, 1980; Sakurai and Takeuchi, 1983; Swoboda *et al.*, 1999; Deng, 2001; Jeon and Yang, 2004; Finno and Calvello, 2005);
- geotechnical structures behaviour prediction by back analysis of an early stage of construction measurements (Asaoka and Matsuo, 1984);
- evaluation of soil and rock mechanics field tests results (Cividini *et al.*, 1981; Gioda and Maier, 1980; Eclaircy-Caudron *et al.*, 2006; Zentar *et al.*, 2001);

- calibration of laboratory tests (Iding *et al.*, 1974; Imre, 1994; Eclaircy-Caudron *et al.*, 2006).

Most of the published studies belong to the first group dealing with the evaluation of geomechanical parameters, particularly applied to tunnels and underground structures. Different material models have been adopted in these studies ranging from linear elastic to elasto-plastic or even to time-dependent models. Some studies considered simultaneously the evaluation of the *in situ* stresses while others a probabilistic view point for this problem. Some of these works are briefly described latter.

In this Chapter, it is intended to present the main components and methods normally used in back analysis applications of geotechnical problems and some of the most important works developed in this field so far. Moreover, an application to a verification problem of three gradient based algorithms to the geomechanical parameters identification is carried out. These algorithms were programmed and coupled with a 3D numerical model that simulates the excavation of a tunnel. Back analysis is performed in elasticity and elasto-plasticity in order to study robustness and efficiency of the algorithms<sup>1</sup>. The main strengths and drawbacks of this approach are highlighted. Finally, an innovative approach based on an evolutionary algorithm (evolution strategies) is applied to a similar problem. In this case, analytical solutions were used because a much higher number of computations was expected. It was found that much of the problems raised by classical optimisation algorithms can be overcome by these algorithms.

For simplicity sake, in this thesis, the expressions "back analysis" and "inverse analysis" will be applied to refer the problem of parameter identification through the direct approach and using different minimisation algorithms.

## 6.2 Main components and methods of inverse analysis

In geotechnical engineering, inverse analysis have been used mainly to estimate rock or soil parameters based on field monitoring (Ledesma *et al.*, 1996). In the particular case of underground works, the measurements performed in the first excavation stages can be used to back analyse the parameters which then can be employed to modify/optimize the design and excavation process.

The main components necessary to perform back analysis through the direct approach are the following (Oreste, 2005):

---

<sup>1</sup>Robustness is seen as the algorithm capability to converge to a satisfactory solution and efficiency is related to the speed convergence is attained

- a representative calculation model that can determine the stress/strain field of the rock mass;
- an error function;
- an optimisation algorithm to reduce the difference between the computed results and the observed values.

In mathematical terms, the current optimisation problem in geotechnical back analysis procedures can be stated as: find a set of  $N_p$  unknown parameters  $x$  in a  $N_p$ -dimension space (the search space) such that the scalar error (objective) function  $f(x)$ , which measures the difference between measured and computed values, is minimised. By minimising  $f(x)$  it is possible to obtain the best set of mean geomechanical parameter values which best fits the *in situ* measures.

The error function can take several forms. Its appropriate definition is very important to obtain good results in the back analysis process (Yang and Elgmal, 2003). The most used error functions in geotechnical inverse analysis are (Ledesma *et al.*, 1996; Tavares, 1997):

- Least-square method: does not implies any previous knowledge and the parameters are obtained by minimising a function depending on the squared difference between the measured and computed values.
- Maximum likelihood approach: probabilistic formulation that can be applied when the probability density function of the measurement errors is known. This is the method with higher applicability when using previous information. It estimates the parameters that maximise the probability of observing the measured data.

The least-square method can be considered a particular case of the maximum likelihood approach when no *a priori* information about the parameters exist and the measurement errors are assumed independent and normally distributed with the same variance. The probabilistic approach is well suited to incorporate previous knowledge about the parameters and treat observation errors in a consistent way. However, it is usually difficult to determine the parameters of the involved probabilistic variables distributions.

Back analysis methods can also be based in uncertain factors like in the Bayesian and Kalman filter approaches. In the probabilistic approach based on the Bayesian rule, the estimated parameters are the ones with higher probability given the available measurements and their precision (Cividini *et al.*, 1983; Gioda and Sakurai, 1987). In the Kalman filter method, measurements, parameters and noise are related through a state equation to estimate an optimal set of parameters (Murakami and Hasegawa, 1987).

Optimisation procedures can be used to systematically search for a set of parameters that can minimise the difference between measured and computed values. In the field of inverse analysis there are two main approaches to carry out the minimisation of the error function: iterative optimisation algorithms form the field of classical optimisation theory such as the Simplex, the Levenberg-Marquardt or gradient methods (Gens *et al.*, 1996; Ledesma *et al.*, 1996; Lecampion *et al.*, 2002; Calvello and Finno, 2004); optimisation methods from the artificial intelligence field like neural networks (ANN), genetic algorithms (GA), evolution strategies (ES), simulated annealing, etc (Haupt and Haupt, 1998; Hashash *et al.*, 2004).

Concerning the classical optimisation methods, the main differences and their applicability are related with the use or not of the first ( $g(x)$ ) and second ( $H(x)$ ) derivatives of the error function. This way, these methods can be divided in the following groups (Yang and Elgmal, 2003):

- Zero-order methods (or direct methods): require only the evaluation of  $f(x)$ . The Simplex, the Gauss method and the Rosenbrock algorithm are examples of these methods.
- First-order methods (or gradient methods): require the evaluation of  $f(x)$  and  $g(x)$ . In case  $g(x)$  can not be explicitly obtained, which happens when numerical models are used for instance, its computation can be a challenging task. It can be approximated by finite-differences or using more complex though accurate methods like the direct differentiation or the adjoint state method. The conjugate gradient method and the steepest descent are two examples of these methods.
- Second-order methods: use information about  $g(x)$  and  $H(x)$  in the optimisation process. Newton's method is typically applied when both can be evaluated directly due to its efficiency. Otherwise, there are several quasi-Newton methodologies to apply indirect approximations to  $g(x)$  and  $H(x)$ .

The performance of the optimisation method is highly dependent on the problem in which it is applied. First and second order methods are normally more efficient. However, in some cases, the error function is not differentiable or the computation of its gradient have a high computational cost. Also, the success of the procedure is strictly connected to the ability of the numerical and constitutive models to accurately predict ground behaviour and to the quality and quantity of measurement data (Mattsson *et al.*, 2001; Sakurai *et al.*, 2003).

These algorithms do not search in the entire parameter space for the optimal solution. They are characterised by a local search for a minimum of the error function, which are only capable to attain under some specific conditions. A highly non-linear error function, which is common in geotechnical problems, may contain several local minima. In this case, different optimised

points can be identified depending on the initial estimation of the parameters (Calvello and Finno, 2002). There is no way to determine whether the set of obtained parameters is also the global minimum of the function. A possible strategy to validate the result is to carry out several runs of the optimisation process with different initial guesses and analyse the outputs (Yang and Elgmal, 2003; Levasseur *et al.*, 2007).

Classical optimisation algorithms present a satisfactory performance in terms of robustness and efficiency, in smooth-shaped error functions, with a clearly defined minimum (Figure 6.2). Moreover, they only can back analyse a reduced number of parameters (two or three) with an important influence on the measured values (Oreste, 2005; Eclaircy-Caudron *et al.*, 2006; Levasseur *et al.*, 2007). As the number of parameters increase, problems concerning the non-uniqueness of the solution and convergence of the process arise. If there are correlated parameters, the problem may be ‘ill-posed’ and an infinity of solutions exist (Zentar *et al.*, 2001). This way, it is advisable to perform sensitivity analysis before the identification process to identify coupled parameters and reduce their number to a manageable level (Calvello and Finno (2004)).

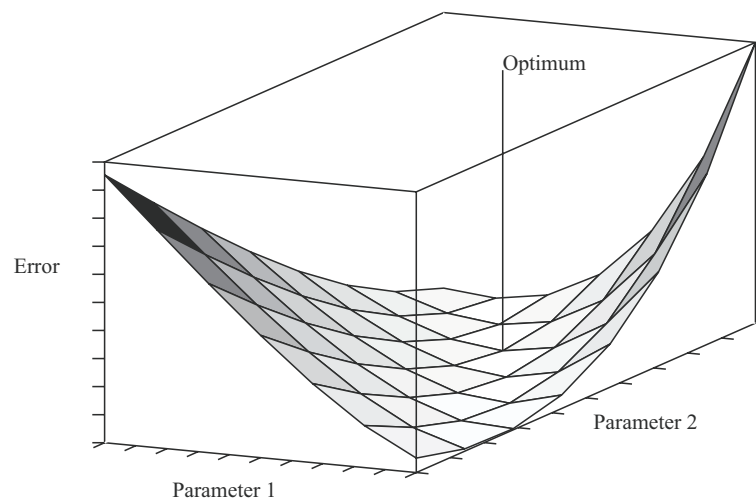


**Figure 6.2:** Typical topology of a smooth-shaped error function (adapted from Lecampion *et al.* (2002))

To overcome much of the classical algorithms mentioned drawbacks, it is possible to use global optimisation techniques from the field of AI. Evolutionary computation is a subfield of artificial intelligence related with metaheuristic optimisation algorithms such as:

- Evolutionary algorithms (e.g. GAs and ESs).
- Swarm intelligence (e.g. ant colony and particle swarm optimisation).

Evolutionary algorithms are robust global optimisation methods, inspired by Darwin's theory of natural selection and survival of the fittest, which try to mimic the natural evolution of the species in biological systems (Costa, 2007). They are characterised by a search of an optimal solution in the entire parameter space. Values of the error function, related to different parameter sets, are evaluated sequentially and compared. These algorithms do not require any continuity or convexity property of the error function. Moreover, only information regarding the objective function and constraints (if they exist) is required to perform the search. Another characteristic that distinguishes these algorithms from the conventional ones is that they start from a set of points (population) of solutions that evolves over time, rather from individual to individual. Figure 6.3 clearly shows this characteristic. It is referred to the identification of three parameters - shear modulus ( $G_{ref}$ ), friction angle ( $\phi'$ ) and  $K_0$  - in a excavation problem using a GA. In this Figure, each point refers to a set of parameters. Along the different generations, the solution is improved and a group of solution near the experimental value (white square) is achieved.

Several evolutionary approaches have been applied to global optimisation problems with success, namely GAs (Holland, 1975; Golberg, 1989; Renders, 1995) and ESs (Rechenberg, 1994; Schefel, 1995). GAs is the most popular type of evolutionary algorithms. A GA is a class of global stochastic optimisation algorithms which does not need the derivative of the error function. They try to mimic the way large populations evolve over a long period of time, through processes such as reproduction, mutation and natural selection. To emulate the natural phenomenon of evolution, GAs create a population of candidate solutions to a particular problem, and through a process of random selection and variation, each generation improves the quality of the solution.

In most GAs, a candidate solution, called an individual, is represented by a binary string. Each binary string is converted into a phenotype that expresses the nature of an individual, and its fitness with respect to the error function is evaluated. Based on fitness of the individuals of a generation, a new one is computed by means of genetic operators such as reproduction, crossover and mutation. In general, new generations are characterised by an increased average fitness of the population.

GAs are well known to be able to solve complex optimisation problems with large, discrete, non-linear and poorly understood optimisation problems (Holland, 1975; Golberg, 1989; Haupt and Haupt, 1998; Marseguerra *et al.*, 2003; Kang *et al.*, 2004; Wrobel and Miltiadou, 2004). They are robust and highly efficient but, since they are based on a heuristic methodology, GAs do not guarantee an exact identification of the optimum solution. However, genetic mechanisms such as reproductions, crossings and mutations, allow to localise an optimum set of solutions close to the global optimum in a given search space even with noisy data (Levasseur *et al.*,

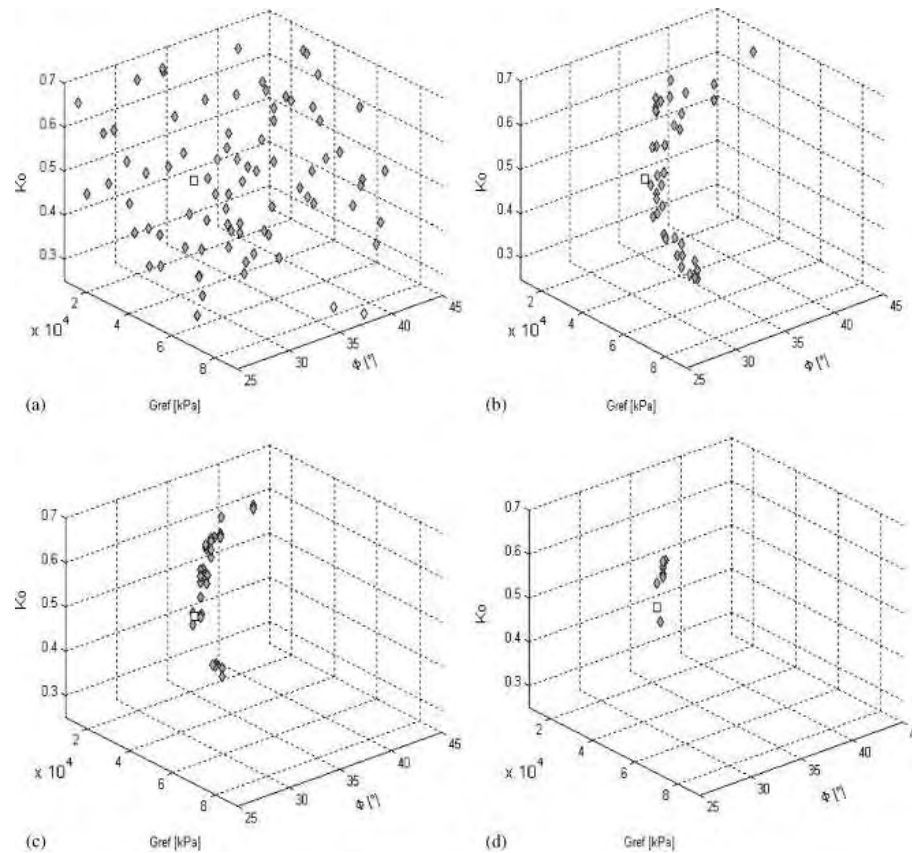


**Figure 6.3:** Optimisation of three parameters ( $G_{ref}$ ,  $\phi'$  and  $K_0$ ) in a excavation problem using a GA (Levasseur *et al.*, 2007). a) Initial population; b) Sixth population; c) Eleventh population; d) Nineteenth population.

2007). Also, GAs are able to deal with linear or non-linear constraints to the objective function.

ESs are also search procedures that mimic the natural evolution of the species in natural systems. They are in many ways similar to GAs. For instance, they only require data based on the objective function and constraints, and not derivatives or other auxiliary knowledge.

Typically, ESs are significantly faster and robust than GAs (Beyer and Schwefel, 2002). This means that, normally, ESs take less evaluations of the error function to reach convergence which can be important in reducing the computational effort when using numerical models. Moreover, ESs are normally more robust algorithms meaning that they are more likely to find the global optimum.

Normally, while GAs have a good performance to solve discrete or integer optimisation problems, ESs are better suited to continuous optimisation problems (Schefel, 1995). This characteristic makes them well adapted to be used for optimisation of geomechanical parameters, which are typically continuous values. Surprisingly, the use of GAs is more widespread and it is not known any application of ESs in the geotechnics field. ESs were recently applied

to problems in many domains (Costa and Oliveira, 2001) and seem to be one of the most competitive and promising global optimisation techniques (Moles *et al.*, 2003).

ESs start searching from an initial population (a set of points) and use deterministic transition rules between generations searching for new points based on mutation and recombination operators. Constraints are handled, normally, using an elimination mechanism (the non feasible points are eliminated). The main differences with GAs, is that ESs use a real coding of decision variables and the adaptation of step sizes for mutation during the optimisation process. This last issue is one of the most promising features of ESs. The performance of ESs is largely dependent on the adjustments of the internal parameters. This way, since also the step sizes of mutation are themselves optimised during the search, the overall procedure is enhanced.

One of the main drawbacks of evolutionary algorithms is the number of error function evaluations to reach convergence. When complex numerical models are used, the computational effort can turn the optimisation procedure infeasible. To overcome this limitation, research is needed to improve the efficiency of these techniques in order to bring the computational time to acceptable levels. These algorithms are particularly well-suited to implementation on parallel computers which can also be used to reduce the time of the process. If the number of processors exceeds the population size, multi-level parallelisation may also be possible.

In spite all the recent advances in numerical methods, availability of affordable high performance computers and novel monitoring techniques and devices, back analysis have not yet become a common task in day-to-day practice of geotechnical engineering. In fact, several research studies can be found in literature about various aspects related with these methodologies, however, very few applied to real works and with direct impact to companies and practitioners. Sakurai *et al.* (2003) presented some justifications for this fact.

- Normally engineers do not have the knowledge nor the time to manage both on site practices and execution of back analysis.
- Back analysis are not included in the contracts' specifications.
- Practical methods for using back analysis results have not been developed and tested to a satisfactory level in order to be accepted by the industry.

### **6.3 Use of classical and new optimisation algorithms in inverse analysis applied to underground structures**

Since the use of optimisation algorithms based on AI is very recent in geotechnical engineering, most applications so far have been developed based on the use of classical algorithms to minimise



the error function.

In the particular case of underground works, several studies have been carried out concerning the identification of geomechanical parameters. The first application developed in this field was presented by Gioda (1980). In the same year, Gioda and Maier (1980) developed a methodology to estimate the strength parameters and the stress state using the interpretation of results of water pressure tests in a tunnel. In the same decade, other important works concerning the use of *in situ* measurements as input for back analysis in geotechnical engineering were proposed (Sakurai and Takeuchi, 1983; Gioda and Sakurai, 1987). After that time, several studies were developed. In this work only some of the most important ones will be mentioned.

Hisatake (1985) proposed a method to estimate initial stresses and mechanical constants of a time-dependent ground, combining the finite element method with the simplex optimisation technique. In their benchmark paper, Ledesma *et al.* (1996) used the Gauss-Newton and the Levenberg-Marquardt methods to minimise the maximum likelihood error function to estimate, within a probabilistic framework, the geomechanical parameters of the rock mass interesting the powerhouse cavern of Estanygento-Sallente in the Spanish Pyrennes (Figure 6.4).

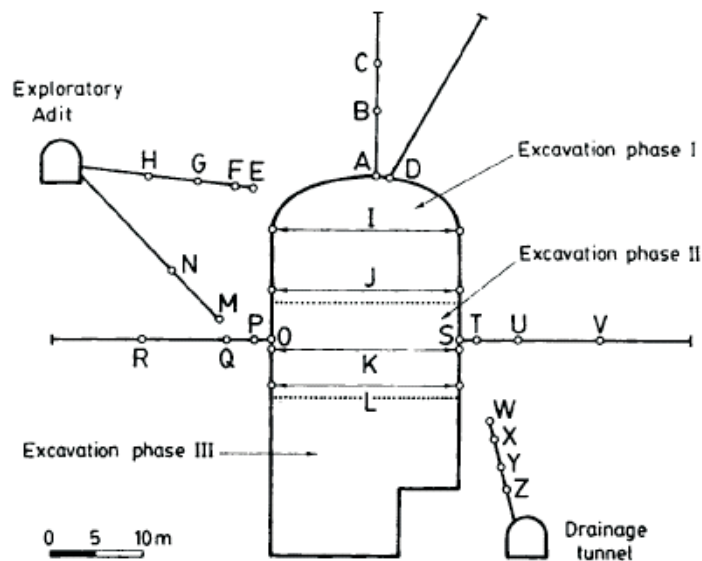


**Figure 6.4:** Excavation sequence and field instrumentation of the Estanygento-Sallente powerhouse cavern (Ledesma *et al.*, 1996).

Swoboda *et al.* (1999) used the boundary control method, which tries to combine the advantages of both direct and inverse approaches, to develop a general code suitable to perform identification on large and complex geotechnical models. The author applied this methodology to the identification of elastic parameters in a shallow subway tunnel (Figure 6.5).

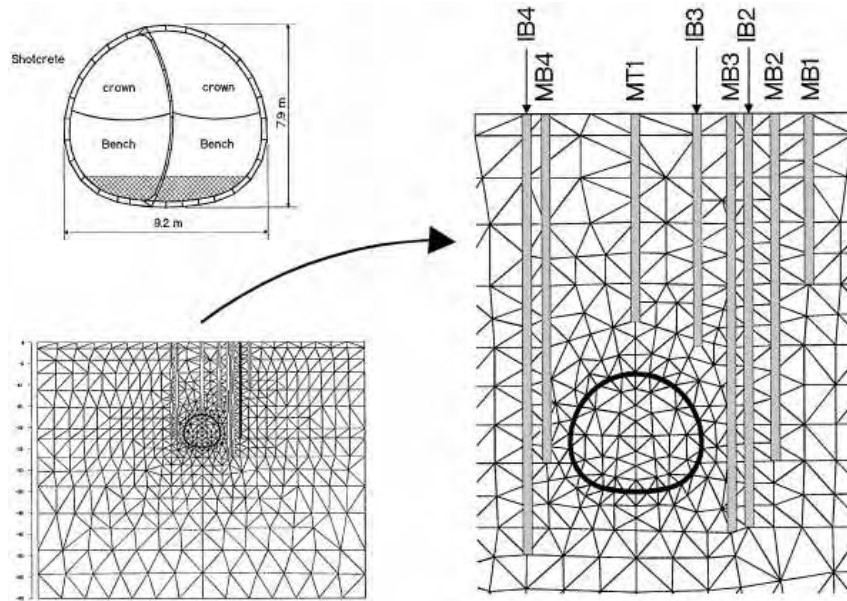


**Figure 6.5:** Tunnel and field instrumentation layout (Swoboda *et al.*, 1999).

Deng (2001) proposed a back analysis method based on the minimisation of the error on the virtual work principle. It showed to be a simple and reliable method which did not use the derivatives of the cost function. The developed methodology was applied to back analyse elastic and elasto-plastic parameters in three case studies, namely: the mining basin of Nord-Pas-de Calais in France, the Cidade Universit ria tunnel of Lisbon Metro and the  gua Vermelha dam in Brasil.

In order to identify the *in situ* state of stress and the deformability of the rock mass for the Alto Lindoso powerhouse complex, Castro *et al.* (2002) developed a methodology which used directly the equations of the finite element formulation. It is an interesting approach since it considers information from the previous excavation stages to compute the actual state allowing to back analyse *ne* different elasticity modulus zones and *ns* different initial state of stresses zones. Moreira *et al.* (2003) also developed an iterative back analysis methodology based on the finite element method together with a maximum likelihood error function and the Gauss-Newton minimisation algorithm. It was successfully applied to identify the parameters of the soils interested to the surface terminus tunnel of the Alameda II station of Lisboa metro. In this work, two types of model were considered, namely: a linear elastic either isotropic and transverse-isotropic and hyperbolic with isotropy.

Considering a more complex elasto-viscoplastic constitutive law, Lecampion *et al.* (2002) identified the parameters from measurements on an underground cavity, using a least-square error function together with the Levenberg-Marquardt algorithm. An innovative approach was

presented by Sakurai *et al.* (2003). The authors developed a back analysis procedure to identify the strain distribution around a tunnel starting from a linear elastic model and adjusting the results numerically by adding a set of forces to translate the non-linear material behaviour and other factors yielding non-linearity to the model (Figure 6.6). Fakhimi *et al.* (2004) estimated soil cohesion and the *in situ* horizontal stress using measures of tunnel convergence.

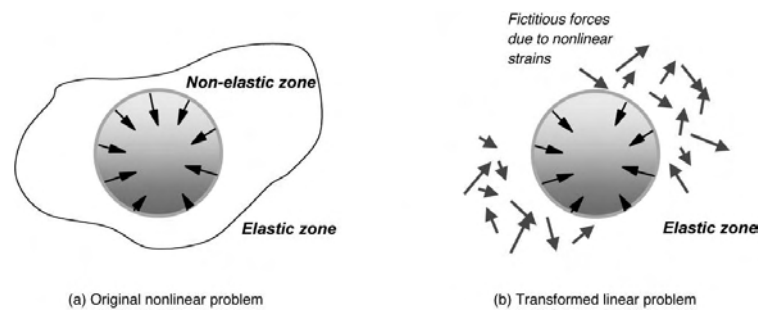


**Figure 6.6:** Approach to back analysis developed by Sakurai *et al.* (2003).

More recently, Eclaircy-Caudron *et al.* (2007) and Jeon and Yang (2004) used the finite difference computer code FLAC coupled with external optimisation programmes and routines. The first authors used the back analysis software SiDolo, which uses a hybrid optimisation algorithm combining a gradient method with a variant of the Levenberg-Marquardt, to identify parameters in the case of an axisymmetric model of a tunnel. Moreover, they performed similar calculations considering results of triaxial and pressurimeter tests. The latter authors, used the same methodology applied to underground works models together with three direct search algorithms.

In spite of the extension of the mentioned cases, many other studies have been conducted to develop different models of displacement-based back analysis (Gioda and Jurina, 1981; Sakurai and Takeuchi, 1983; Sakurai, 1997; Singh *et al.*, 1997; Cai *et al.*, 1998; Zhao *et al.*, 1999; Gioda and Swoboda, 1999; Yang *et al.*, 2000).

To have a broader view of the application range of these methodologies, it is important to mention studies concerning the use of back analysis to other geotechnical engineering problems. Amusin *et al.* (1992) used a theoretical-empirical back analysis approach applied to the results of laboratory tests. For the same purpose, Mattsson *et al.* (2001) developed an optimisation routine using the Rosenbrock and the Simplex methods both belonging to the category of the direct search methods. Yang and Elgmal (2003) applied Newton's method and a optimisation program which uses a quasi-Newton approach to estimate shear stress-strain parameters from

triaxial tests.

Many back analysis applications have been carried out using results from pressuremeter tests (Cambou and Bahar, 1993; Zentar *et al.*, 2001; Rangeard *et al.*, 2003). Calvello and Finno (2004) identified the parameters for the elasto-plastic Hardening Soil model in four clays using results from triaxial tests calibrated by monitoring data given by inclinometers in a supported excavation. Sheu (2006) adopted the meshless local Petrov-Galerkin method and Bayesian statistics to develop a direct back analysis procedure for the particular case of transient problems. This model does not use a finite element mesh since it is derived over a local domain. This way, measured data acquired at discrete points may be directly used into the model.

In a first approach of using AI techniques in back analysis, Shang *et al.* (2002) based on approximately 100 case studies of tunnel projects in China, used an Intelligent Back Analysis to investigate rock mass properties (stresses and rock mass modulus) around tunnels. Using the boundary element method the back analysis is performed under the guidance of experts' knowledge. Also, a case-based system of back analysis was applied to identify probable failure modes for tunnels and underground openings (Lee and Sterling, 1992).

In spite of the current application of evolutionary optimisation algorithms in several field, their use in geotechnical engineering is still scarce. Very few applications of these methods can be found in literature but the results are very promising when compared with the performance of classical algorithms to the typical geotechnical problems of parameter identification. Levasseur *et al.* (2007) presented a study comparing the behaviour of two different optimisation techniques in geotechnical problems, namely, the steepest descent and a genetic algorithm. They applied them to the results of a pressuremeter test and to monitoring results of a sheet pile wall retaining an excavation. They found that the GA is particularly suitable to identify soil parameters when the topology of the error function is complex. The GA worked well in every situation even in the cases where parameters are non-influent or correlated. However, it is computationally expensive and perhaps prohibitive if there are only a few parameters to identify.

Deng and Lee (1981) developed a method for displacement back analysis, based on ANNs and GAs to identify the elasticity modulus in slope stability analysis. The ANN replaces the finite element calculation in order to enhance the calculation efficiency and the GA is used as a global optimisation method. A similar approach was adopted by Pichler *et al.* (2003) to identify parameters of elastic and elasto-plastic models. In this application, the GA was used not only as a global optimisation technique to find the optimal solution but also for the initial choice of the network weights in order to improve the training procedure.

Simpson and Priest (1993) used GAs to identify discontinuity frequency in a fractured rock mass, Goh (1999) to analyse slip surfaces and Pal *et al.* (1996) like Samarajiva *et al.* (2005) to calibrate laboratory test results.

## 6.4 Application of gradient optimisation algorithms to a verification problem

### 6.4.1 Introduction

A synthetic verification example of a tunnel excavation is used to test the capabilities of gradient optimisation algorithms in geomechanical parameters identification both in elasticity and in elasto-plasticity. A least-square error function was used together with three different algorithms, namely: the steepest descent (SD), the conjugate gradient (CG - PR version: unidimensional exact search) and quasi-Newton (QN - DFP version). The gradient of the error function was approximated by finite differences. Parameters like efficiency and robustness of each algorithm were investigated.

A three-dimensional (3D) numerical model of the tunnel, developed with the finite difference software FLAC3D, was used considering the different construction stages. In a first stage, the algorithms were tested in elasticity and afterwards using the Mohr-Coulomb elasto-plastic constitutive model.

The analysis started with the definition of a set of geomechanical parameters which were attributed to the surrounding rock mass to obtain the "monitored" measures in a given section. Then, different perturbations were applied to the parameters to check if the algorithms were able to identify the correct values.

The overall procedure of the back analysis is schematised in Figure 6.7. First an initial set of parameters is defined and introduced in the numerical model. The response of the model is then computed allowing to evaluate the error between computed and "observed" measurements. If the error is below a certain pre-defined tolerance (in this case 0.1%) the process is stopped and the set of parameters is the optimised one. If the error is above the defined threshold, a new set of parameters is calculated based on the considered optimisation algorithm and a new iteration is computed. This process is iteratively repeated until convergence is reached.

### 6.4.2 Numerical model

The developed numerical model is a tunnel composed by a 4 m radius arch and a vertical wall with the same span. The considered sequential excavation steps were the excavation of the top heading followed by the bench excavation. Between these steps the support system composed by 20 cm of shotcrete was installed. The excavation is carried out in 3 m length consecutive advances. The consideration of the excavation sequence is extremely important specially when significant plastic zones occur. In this case, the stress state and displacements of the previous stages have significant impact on the excavation stage being analysed.

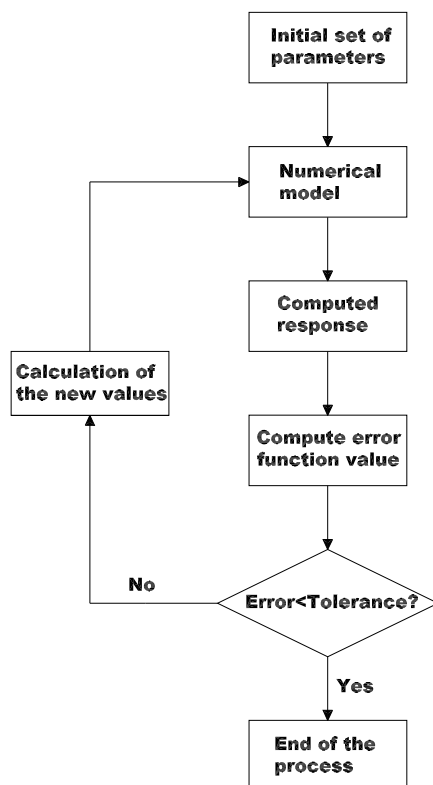


*Figure 6.7:* Scheme of the back analysis procedure using gradient optimisation algorithms.

The initial model presented 40 m depth and 90 m length. It was composed by 31130 zones and 35399 nodes and took approximately two hours to run. Since it was intended to perform several calculations with the model, it was decided to simplify it in order to decrease the computational time. These simplifications were related with the extension of the model, which was reduced to 20 m, and mesh refinement. The tunnel depth was also reduced to 24 m. As a result, the simplified model was composed of 1110 zones and 1375 nodes and took only about two minutes to run (Figure 6.8).

In a first stage, an elastic constitutive model for the rock mass was considered with a deformability modulus ( $E$ ) of 2 GPa and a Poisson coefficient ( $\nu$ ) of 0.1. A gravitational stress state was considered with a horizontal to vertical stress ratio ( $K_0$ ) of 0.8.

In this calculation, a total of five measurements in the reference section were considered through different combinations, namely: vertical displacements at the surface, at the top of the arch and in the tunnel floor; and horizontal (perpendicular to the tunnel axis) displacement and stress in the middle point of the wall. Table 6.1 resumes the results obtained with the initial parameters which were used as monitored values in the back analysis calculations.

In a second stage, calculations were performed to identify the strength parameters of the

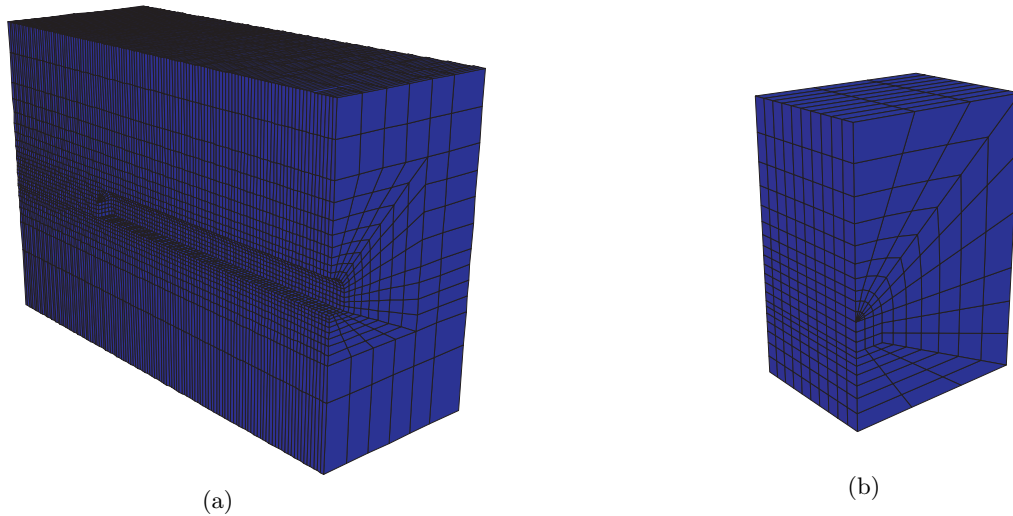


**Figure 6.8:** Initial (a) and simplified (b) models for the back analysis calculations.

**Table 6.1:** Computed values for the elastic calculation.

<b>Horizontal stress in the wall (kPa)</b>		180
<b>Displacements (mm)</b>	<i>Surface</i>	0.493
	<i>Arch</i>	1.278
	<i>Wall</i>	1.045
	<i>Floor</i>	1.810

Mohr-Coulomb failure criterion. The adopted values for cohesion ( $c'$ ) and friction angle ( $\phi'$ ) were, respectively, 50 kPa and  $32^\circ$ . These values are relatively low for a rock mass but their choice is related to the fact that it was intended that plastic zones occurred in the model, namely near the excavation, to check their influence on the back analysis process.

In the calculation using the Mohr-Coulomb constitutive model, four measurements were used. In this case, two displacements and two stresses (one horizontal and one vertical for each) were adopted. In Table 6.2 the results of this calculation are presented.

**Table 6.2:** Computed values for the plastic calculation

<b>Horizontal stress in the wall (kPa)</b>		171
<b>Vertical stress in the arch (kPa)</b>		151
<b>Displacements (mm)</b>	<i>Arch</i>	1.664
	<i>Wall</i>	1.578

### 6.4.3 Used back analysis techniques

The error function used in this verification example was the least square equation translated by equation 6.1.

$$\epsilon = \frac{1}{m} \cdot \sum_{j=1}^m \left[ \frac{\eta_j - f_j(x)}{\eta_j} \right]^2 = \frac{1}{m} \cdot \sum_{j=1}^m \left[ 1 - \frac{f_j(x)}{\eta_j} \right]^2 \quad (6.1)$$

where  $\epsilon$  is the mean squared error,  $x$  is the vector of  $n$  components of the parameters to estimate,  $\eta_j$  is the  $j$  measurement obtained during tunnel construction,  $f_j$  is the computed value correspondent to the  $j$  measurement and  $m$  is the *in situ* measurement number. The iterative process is carried out until  $\epsilon$  is below a pre-defined threshold. In the tested verification example a value of 0.1% was adopted for this parameter.

The minimisation of this function was carried out using three different optimisation algorithms which use the gradient of the error function to guide the search. These methods always start from an initial approximation of the parameters. The next  $(i + 1)$  iteration is computed based on the current one  $(i)$  in the form:

$$x^{(i+1)} = x^{(i)} + \alpha^{(i)} \cdot d^{(i)} \quad (6.2)$$

$x^{(i+1)}$  is the parameter vector of the next iteration,  $x^{(i)}$  is the parameter vector of the current iteration,  $d^{(i)}$  defines the search direction and  $\alpha^{(i)}$  the length of the advancement step. The search direction was defined using three different algorithms: steepest descent (SD), quasi-Newton (QN) and conjugate gradient (CG).

In the SD method, the search direction is dependent on the gradient of the error function in the following form:

$$d^{(i)} = -g(x^{(i)}) \quad (6.3)$$

where  $g(x^{(i)})$  is the error function gradient vector in relation to the parameters which is given by:

$$g(x^{(i)}) = \frac{2}{m} \cdot \sum_{j=1}^m \left[ 1 - \frac{f_j(x)}{\eta_j} \right] \cdot \left[ -\frac{1}{\eta_j} \cdot \frac{df_j(x)}{dx} \right] \quad (6.4)$$

which implies the evaluation of the numerical model gradient vector in relation to the parameters. This is one important issue relating the application of these algorithms. Normally, the gradient is approximated by finite differences. The main difficulty in this approach is to determine the step of the finite difference calculation. The influence of this choice will also be investigated in this study. With this methodology, the gradient is computed as follows:



$$\left(\frac{df}{dx}\right)_{x=x^{(i)}} = \frac{f(x^{(i)} + \Delta x^{(i)}) - f(x^{(i)})}{\Delta x^{(i)}} \quad (6.5)$$

in which  $\Delta x^{(i)}$  is a vector that includes the increment of only one of the parameters.

In the QN method the search direction is obtained in the following way:

$$d^{(i)} = -H^{(i)} \cdot g(x^{(i)}) \quad (6.6)$$

In the DFP method, the  $H^{(i)}$  matrix is determined by equation 6.7:

$$H^{(i)} = H^{(i-1)} - \frac{H^{(i-1)}yy^T H^{(i-1)}}{y^T H^{(i-1)}y} + \frac{ss^T}{s^T y} \quad (6.7)$$

where,

$$s = x^{(i)} - x^{(i-1)} \quad (6.8)$$

$$y = g(x^{(i)}) - g(x^{(i-1)}) \quad (6.9)$$

The  $H^{(i)}$  matrix takes the value of the identity matrix for  $i = (0, n, 2n, \dots)$  in which  $n$  is the number of parameters. This means that, in these iterations, the search direction coincides with the one obtained by the SD method. In the case of the CG method, this direction is defined by:

$$d^{(i)} = -g(x^{(i)}) + \beta^{(i-1)} \cdot d^{(i-1)} \quad (6.10)$$

the  $\beta$  matrix is computed as follows:

$$\beta^{(i-1)} = \frac{g(x^{(i)})^T y}{g(x^{(i-1)})^T g(x^{(i-1)})} \quad (6.11)$$

The  $\beta$  matrix takes the null value for  $i = (0, n, 2n, \dots)$  meaning that, in these iterations, the search direction coincides with the one obtained by the SD method.

The mean squared error condition requires that  $\alpha_i$  is chosen in such a way to satisfy equation 6.12:

$$\frac{d\epsilon(\alpha_i)}{d\alpha_i} = 0 \quad (6.12)$$

where,

$$\epsilon(\alpha_i) = \frac{1}{m} \sum_{j=1}^m \left[ 1 - \frac{1}{\eta_j} f_j \left( x^{(i)} - \alpha_i g(x^{(i)}) \right) \right]^2 \quad (6.13)$$

Developing equation 6.13 in Taylor series in  $x^{(i)}$  until the first order element one obtains:

$$\epsilon(\alpha_i) \cong \frac{1}{m} \sum_{j=1}^m \left\{ \left[ 1 - \frac{f_j(x^{(i)})}{\eta_j} \right] + \frac{\alpha_i}{\eta_j} \left( \frac{df_j(x)}{dx} \right)_{x=x^{(i)}} \left( \frac{d\epsilon}{dx} \right)_{x=x^{(i)}} \right\}^2 \quad (6.14)$$

Taking the derivative of this equation and putting it equal to zero as indicated in equation 6.12:

$$\begin{aligned} \frac{d\epsilon(\alpha_i)}{d(\alpha_i)} \cong \frac{2}{m} \sum_{j=1}^m \left[ \left( 1 - \frac{f_j(x^{(i)})}{\eta_j} \right) + \frac{\alpha_i}{\eta_j} \left( \frac{df_j(x)}{dx} \right)_{x=x^{(i)}} \left( \frac{d\epsilon}{dx} \right)_{x=x^{(i)}} \right] \cdot \\ \cdot \left[ \frac{1}{\eta_j} \left( \frac{df_j(x)}{dx} \right)_{x=x^{(i)}} \left( \frac{d\epsilon}{dx} \right)_{x=x^{(i)}} \right] = 0 \end{aligned} \quad (6.15)$$

From equation 6.15 it is possible to determine the value of  $\alpha_i$ :

$$\alpha_i = - \frac{\sum_{j=1}^m \left\{ \left[ \frac{1}{\eta_j} - \frac{f_j(x^{(i)})}{\eta_j^2} \right] \left[ \left( \frac{df_j(x)}{dx} \right)_{x=x^{(i)}} \left( \frac{d\epsilon}{dx} \right)_{x=x^{(i)}} \right] \right\}}{\sum_{j=1}^m \left[ \frac{1}{\eta_j} \left( \frac{df_j(x)}{dx} \right)_{x=x^{(i)}} \left( \frac{d\epsilon}{dx} \right)_{x=x^{(i)}} \right]^2} \quad (6.16)$$

This equation can be generalised for the case of  $n$  parameters in the following way:

$$\alpha_i = - \frac{\sum_{j=1}^m \left\{ \left[ \frac{1}{\eta_j} - \frac{f_j(x^{(i)})}{\eta_j^2} \right] \sum_{k=1}^n \left[ \left( \frac{df_j(x)}{dx} \right)_{x=x^{(i)}} \left( \frac{d\epsilon}{dx} \right)_{x=x^{(i)}} \right] \right\}}{\sum_{j=1}^m \left\{ \frac{1}{\eta_j} \sum_{k=1}^n \left[ \left( \frac{df_j(x)}{dx_k} \right)_{x=x^{(i)}} \left( \frac{d\epsilon}{dx_k} \right)_{x=x^{(i)}} \right] \right\}^2} \quad (6.17)$$

#### 6.4.4 Obtained results

As it was already referred, in the performed back analysis calculations it was considered an elastic model, with identification of  $E$  and  $K_0$ , and an elasto-plastic model (Mohr-Coulomb), in order to identify  $c'$  and  $\phi'$ .

All the calculations were carried out affecting the parameters with a given deviation in relation to the "real" values, and performing the back analysis procedures to analyse their behaviour under different circumstances. In the elastic model case, the SD algorithm was used, in a first stage, to analyse the importance of these deviations, together with the type and number of measurements, in the convergence of the algorithm. Moreover, the step of the finite difference approximation to the gradient was also analysed in terms of its influence in convergence and speed of the process. The behaviour of this algorithm considering the input of one extra parameter, simulating the 'ill-posed' problem of having more parameters to identify than available measurements was also studied. In a second stage, the performance of the three algorithms was tested considering the measurement of one stress and one displacement and different initial deviations of the parameters.

In the calculation considering an elasto-plastic behavioural model, the three algorithms were used to estimate the Mohr-Coulomb strength parameters considering different number of measurements and deviations for the parameters initial approximations. Moreover, the influence of the finite difference step in the identification process convergence was also tested.

In the first performed example, the SD algorithm was used considering two vertical displacement measurements (surface and arch of the tunnel) and identification of only one parameter ( $E$ ). Several deviations from the "real" values of the parameters were tested. In the text the sign (+) in the deviation means that the values were increased, while (−) means otherwise. Also, two different steps for the gradient calculation were considered (2% and 10%). In Table 6.3 the main results are presented.

**Table 6.3:** Results of the identification process of  $E$  with two displacement measurements.

Deviations	Iterations number		Identified value $E$ (GPa)	
	Step 2%	Step 10%	Step 2%	Step 10%
10% (+)	1	1	2.042	1.996
25% (−)	2	2	1.983	2.010
25% (+)	2	2	2.030	2.022
50% (+)	3	3	2.000	2.008
50% (−)	3	3	2.001	2.011
100% (+)	n.c.	n.c.	-	-

n.c. - no convergence was obtained.

The results show that the identification process converges to the real solution in a reduced iterations number excepting for the case of 100% deviation. In this case, the value of  $E$  was negative in the second iteration which stopped the calculation. The algorithm must be adapted

in order to contemplate the cases where the parameters take values without physical meaning which can be done by using constraints to the parameter values translating *a priori* knowledge about their interval range (for instance by experts' knowledge). However, deviations of this magnitude are not expected to happen often in practice, therefore non-convergence in this case is less important.

The step value of the finite difference calculation did not influence the identification process. The convergence and speed of back analysis, as well as the quality of the results, were unchanged (Figure 6.9). In fact, the final values of  $E$  are the correct ones within the maximum error tolerance ( $\epsilon < 0.01\%$ ).

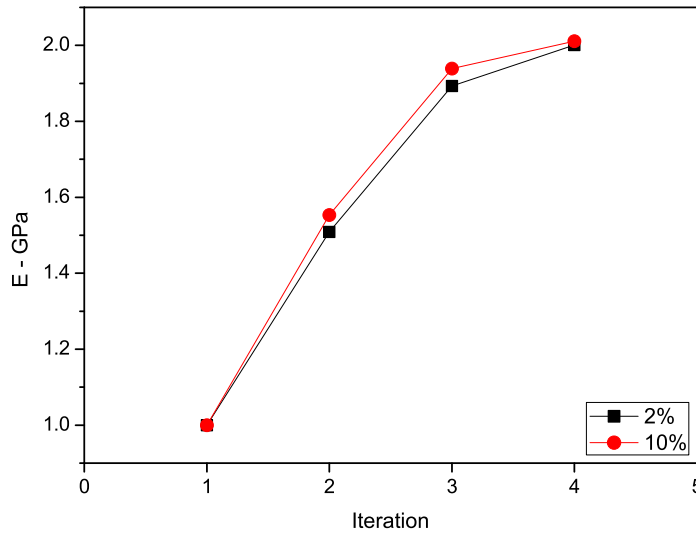


**Figure 6.9:** Convergence of the identification process considering two steps for the finite difference calculation for the case of 50%(-) deviation.

In the following calculation, the same measurements were used in order to identify both  $E$  and  $K_0$ , considering a 10% step for the finite difference. Table 6.4 resumes the overall results.

**Table 6.4:** Results of the identification process of  $E$  and  $K_0$  with two displacement measurements.

Deviations	Iterations number	Identified values	
		$E(\text{GPa})$	$K_0$
25% (+)	2	2.280	0.566
50% (+)	2	2.683	0.233
10% (+)	1	2.085	0.706
50% (+) for $E$ and 50% (-) for $K_0$	1	2.797	0.084

In this case, convergence is reached in a very reduced iteration number but not for the correct values. There are an endless number of possible combinations for the parameters which lead to the same measurement values. The non-unicity of the solution is due to the high correlation between the two used measures (two vertical displacements). The problem is ‘ill-posed’ since, in practice, this high correlation is similar to the use of only one measure to identify two unknown parameters.

In this context, calculations were repeated replacing the vertical measurement at the surface by the horizontal displacement in the wall of the tunnel. It was intended to check the differences in the algorithm performance when using less correlated measures. Table 6.5 presents the obtained results.

**Table 6.5:** Results of the identification process of  $E$  and  $K_0$  with one horizontal and one vertical displacement measurement.

Deviations	Iterations number	Identified values	
		E(GPa)	$K_0$
25% (+)	5	2.012	0.802
50% (+)	3	2.066	0.811
10% (+)	3	2.083	0.810
50% (+) for $E$ and 50% (-) for $K_0$	n.c.	-	-

n.c. - no convergence was obtained.

In three of the tested cases convergence was achieved for the correct parameters. In practical terms, the results show that, in some cases, it is possible to proceed with back analysis using only a few displacement measurements provided that they do not have a high correlation degree. It is worth to mention that the iteration number required for a 50% deviation was less than the one needed for the 25% deviation case. As it is possible to observe from Figure 6.10, for the first case the error function shows an initial higher slope which provides faster convergence.

Other parameters were added to the identification process, namely, the volumic weight of the rock and the deformability modulus of the support system. However, and in line with the conclusions of other studies (Oreste, 2005; Eclaircy-Caudron *et al.*, 2006; Levasseur *et al.*, 2007), it was not possible to identify these parameters since they have reduced influence on the measurements. The optimisation algorithms use the derivative values to determine which are the parameters with higher influence on the error function value. This way, varying the parameters with more influence on the measures allow faster convergence to be attained. Parameters with low influence on measurements, and consequently lower gradient value, will tend to stabilise around a certain value while the algorithm searches for the minimum varying the

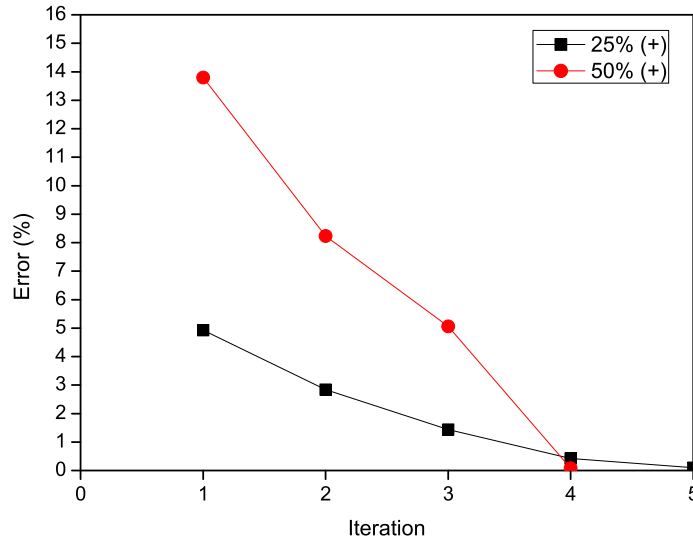


**Figure 6.10:** Error function values during the identification process for two different deviations.

more influencing parameters.

Still considering displacement-based back analysis, calculations were performed using more measurements than parameters to identify. In the process, three measures were used, namely the vertical displacements in the arch and floor of the tunnel and the horizontal displacement in the wall. A fourth measure was then added - the surface vertical displacement - to analyse the effect of the input of a highly correlated measure. The results are presented in Table 6.6.

**Table 6.6:** Results of the identification process of  $E$  and  $K_0$  with three and four displacement measurements

Deviations	Iterations number	Measurements number	Identified values	
			$E(\text{GPa})$	$K_0$
25% (+)	5	3	2.058	0.807
50% (+)	8	3	2.025	0.803
10% (+)	4	3	2.038	0.820
50% (+) for $E$ and 50% (-) for $K_0$	12	3	2.061	0.799
25% (+) for $K_0$ and 25% (-) for $E$	2	3	1.970	0.794
50% (-)	5	3	1.940	0.796
25% (+)	5	4	1.986	0.799
50% (+) for $E$ and 50% (-) for $K_0$	8	4	2.032	0.788

The results show that using three displacements, the identification process is stable and convergent. The correct values were identified in a reduced iterations number. Using the information collected along the several performed iterations it was possible to draw the function

error topology as well as a plan view with isolines of error values. This task was carried out by means of a Kriging algorithm (Journel and Huijbregts, 1978; Cressie, 1991). This is a geostatistical gridding method which can smoothly interpolate the shape of a surface from irregularly spaced data.

Figure 6.11 presents the topology of the error function for the present case. It is a convex-shaped surface with a clearly defined and singular minimum correspondent to the optimum set of parameters. Gradient-based algorithms normally show good performances in optimisation problems with this type of regular error functions.

Normally, higher deviations mean more iterations needed to reach convergence. However, this is not the case when the deviations have different signs for the parameters. In this case, the behaviour is more unpredictable and dependent on the characteristics of the error function surface. When comparing these results with the ones provided in the case using only two displacements (see Table 6.5), it can be stated that the use of more measurements leads to a more time consuming process (more iterations needed to match all the considered displacements). However, when using a higher measurement number the process is more robust since convergence was reached in the case where the process of using only two measures failed.

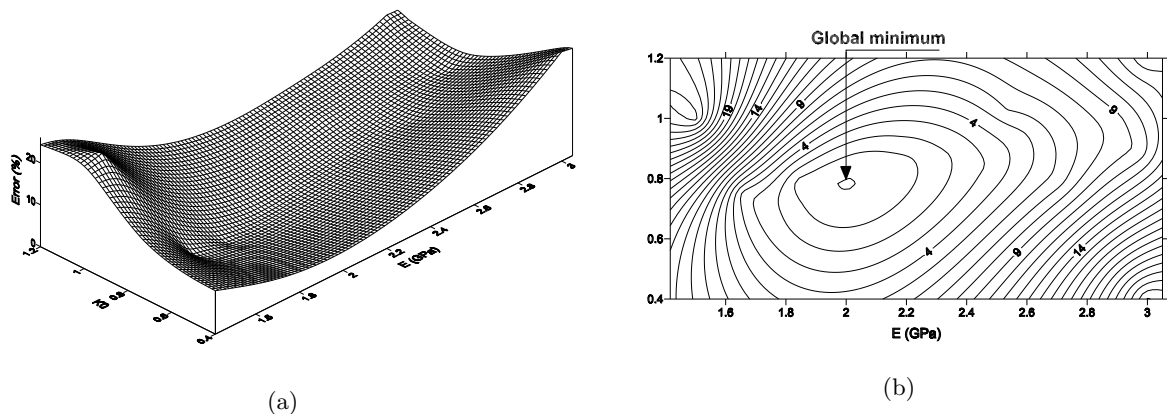


**Figure 6.11:** Topology of the error function on the identification of  $E$  and  $K_0$  for the case of using three measurements. (a) 3D view (b) Plan view.

The consideration of one additional correlated measurement in the identification process increased convergence speed in one of the two tested cases. The number of iterations was reduced meaning that, even though the high correlation, the process can be enhanced by the inclusion of such measurements. It can then be stated that, in displacement-based back analysis in elasticity, a high number of reliable displacements should be used.

The performance of the three algorithms was compared through several simulations, con-

sidering the measurement of one vertical displacement (tunnel arch) and one horizontal stress (tunnel wall) with different initial deviations. All the finite difference approximations to the gradient were computed with a 10% step with the exception of two calculations. For the cases of the QN and CG algorithms, one example was computed with a 2% step in order to check the sensitivity of these algorithms to the variation of this parameter. The results of the simulations are resumed in Tables 6.7, 6.8 and 6.9.

**Table 6.7:** Results of the identification process of E and  $K_0$  with one stress and one displacement measurements using the SD algorithm

Deviations	Iterations number	Identified values	
		E(GPa)	$K_0$
25% (+)	4	2.016	0.774
50% (+)	4	2.107	0.791
100% (+)	10	2.056	0.730
50% (-)	3	2.029	0.789
50% (+) for $K_0$ and 50% (-) for E	10	1.907	0.822
25% (-) for $K_0$ and 25% (+) for E	2	1.992	0.796
25% (+) for $K_0$ and 25% (-) for E	7	1.950	0.837

**Table 6.8:** Results of the identification process of E and  $K_0$  with one stress and one displacement measurements using the QN algorithm

Deviations	Iterations number	Identified values	
		E(GPa)	$K_0$
25% (+)	4	2.029	0.771
50% (+)	6	2.121	0.753
100% (+)	n.c.	-	-
50% (-)	4	1.997	0.791
50% (+) for $K_0$ and 50% (-) for E	8	1.928	0.799
25% (-) for $K_0$ and 25% (+) for E	2	2.150	0.702
25% (+) for $K_0$ and 25% (-) for E	7	1.909	0.820
25% (+) for $K_0$ and 25% (-) for E (step 2%)	6	1.941	0.822

n.c. - no convergence was obtained.

With exception of one calculation, every tested case converged to the correct parameter values, within the established tolerance. Only for a 100% deviation in both parameters, the identification process with the QN algorithm provided a negative value for  $K_0$ . As it was already

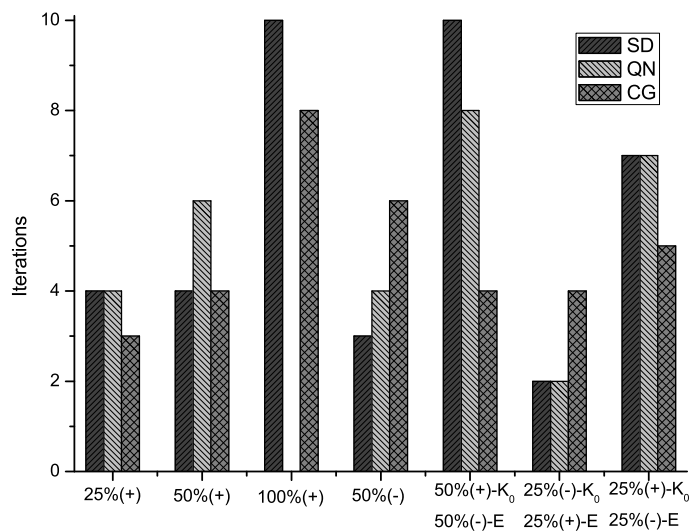


**Table 6.9:** Results of the identification process of  $E$  and  $K_0$  with one stress and one displacement measurements using the CG algorithm

Deviations	Iterations number	Identified values	
		$E(\text{GPa})$	$K_0$
25% (+)	3	2.161	0.739
50% (+)	4	2.094	0.742
100% (+)	8	1.998	0.775
50% (-)	6	1.954	0.817
50% (+) for $K_0$ and 50% (-) for $E$	4	2.020	0.781
25% (-) for $K_0$ and 25% (+) for $E$	4	1.929	0.837
25% (+) for $K_0$ and 25% (-) for $E$	5	1.925	0.850
25% (+) for $K_0$ and 25% (-) for $E$ (step 2%)	6	1.994	0.796

referred, this problem is not very relevant since so high deviations are not expected to happen often in practice and it can be solved with the introduction of simple constrains.

In relation to performance, i.e., the number of iterations required to achieve convergence, the algorithms present some significant differences. This aspect is particularly relevant in back analysis problems using high computational cost numerical models (3D for instance) since a high iteration number can lead to prohibitive computational times. In Figure 6.12 a comparison of the algorithms performance is presented.

**Figure 6.12:** Comparison between the algorithms in terms of efficiency.

The CG algorithm is the most efficient. In a total of seven analysed cases, only in two it is outperformed by the remaining algorithms. It takes a mean of 4.9 iterations to reach

convergence while the SD and QN algorithms, need 5.2 and 5.7 iterations, respectively. It is worth to mention that the last did not reach convergence in one of the studied cases. In Figure 6.13 the evolution of the error function along the iterative process for the three algorithms is presented considering the case of 25% (+) and 25% (-) deviations for  $K_0$  and E, respectively. In this case, the behaviour of the SD and QN algorithms are very similar, while the CG presents an enhanced performance from the third iteration.

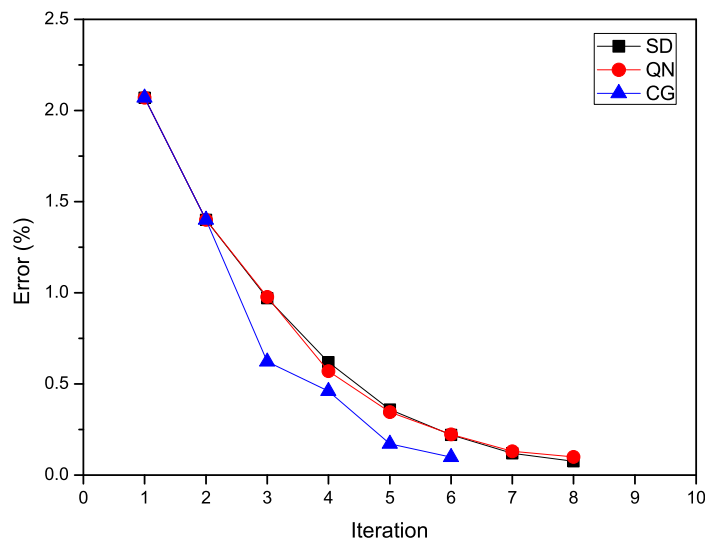


**Figure 6.13:** Evolution of the error function values during the identification process for the three algorithms.

A calculation was performed to check the sensitivity of the QN and CG algorithms to the step of the finite difference calculations. As it can be observed in Tables 6.8 and 6.9 the impact is reduced. The number of iterations only varied one unity considering the two different steps. It can be concluded that, in elasticity, the adopted step for the finite difference approximation to the gradient has a low impact in the convergence speed. However, mainly for the last two algorithms, more tests are needed with different deviations to allow generalising this conclusion and also to check for possible implications on convergence itself.

Using the developed numerical model, several identification processes were carried out to identify the strength parameters of the Mohr-Coulomb failure criterion ( $c'$  and  $\phi'$ ) under different conditions. Using the three algorithms, simulations were carried out considering different deviations and a variable number of available measurements. Table 6.10 resumes the obtained results. Whenever omitted, a step of 10% for the finite difference calculation was used.

As it can be observed, in the cases convergence was obtained, the identified parameters are relatively different from the correct ones. This tendency is more pronounced for  $c'$  where

**Table 6.10:** Results of the identification process of  $c'$  and  $\phi'$ .

Algorithm	Deviations	Iterations number	Measurements number*	Identified values	
				$c'$ (kPa)	$\phi'$ (°)
SD	10% (+)	3	3	54.78	31.20
	25% (+)	6	2	59.14	30.35
	25% (-)	2	2	39.62	33.65
	25% (+)	5	3	60.20	30.33
	25% (+)	3	4	60.17	30.14
	25% (+) 2% step	2	3	59.32	29.97
	25% (+) 15% step	n.c.	2	-	-
	25% (+) for $c'$ and 25% (-) for $\phi'$	2	3	63.67	29.84
QN	25% (+)	n.c.	3	-	-
	25% (+) 2% step	n.c.	3	-	-
	25% (+) 15% step	n.c.	3	-	-
CG	25% (+)	n.c.	3	-	-
	25% (+) 2% step	5	3	58.67	30.35
	25% (+) 15% step	n.c.	3	-	-

\* 2 measurements: vertical displacement in the crown and horizontal stress in the wall; 3 measurements: equal to the previous plus the horizontal displacement in the wall; 4 measurements: equal to the previous plus vertical stress in the crown; n.c.: no convergence was obtained.

higher deviations were found. Figure 6.14 presents the topology of the error function in the case of two measurements. The main characteristic that can be observed is the presence, in the studied parameter space, of two local minima and the low convexity of the function. In this situation, it is expected that gradient-based algorithms perform poorly. In fact, the non-convergence in several cases may be related with the flatness of the error function. In the cases where convergence was achieved, the identified parameters corresponded to the local minima nearer the initial point.

The number of observations did not change substantially the final values of the parameters. However, the convergence speed increased with the available measurement number, which is an important issue. This statement can be observed by the evolution of the parameter values in the identification process considering, for instance, a deviation of 25%(+) (Figure 6.15).

This conclusion is in contradiction to what was verified in elasticity, where a higher number of measurements considered in the back analysis led to a more robust but less efficient (more iterations needed) process. This way, it is necessary to perform complementary calculations to analyse this particular issue.

The QN algorithm never reached convergence while for the case of the CG only in one case

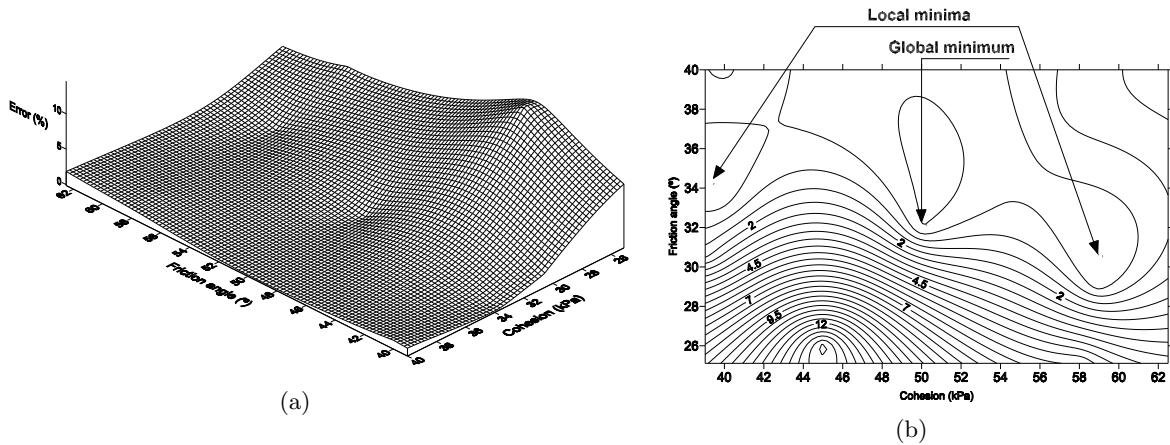


**Figure 6.14:** Topology of the error function on the identification of  $c'$  and  $\phi'$  for the case of using two measurements. (a) 3D view (b) Plan view.

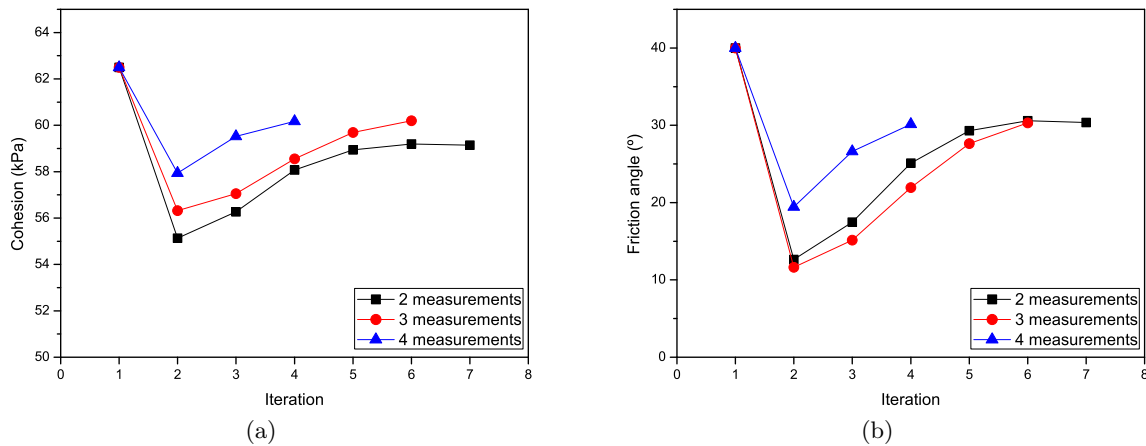


**Figure 6.15:** Evolution of the  $c'$  (a) and  $\phi'$  (b) values during the identification process using the SD algorithm together with different number of available measurements.

it was attained. These algorithms showed a poor performance in elasto-plasticity. The step of the finite difference calculation is very important in this case. The use of a smaller value for the step (2%) allowed, in the case of the SD algorithm, to speed up convergence, decreasing from 5 to 2 the number of iterations required to stop the process. In the case of the CG algorithm it allowed convergence to be obtained. This way, it can be concluded that, in elasto-plasticity, the gradient calculation has a high influence on the back analysis in both speed and convergence of the estimation process. When using the finite difference method to compute its approximate value, a low step should be used in order to increase the process stability.

## 6.5 Application of Evolution Strategies (ES) to analytical verification problems

### 6.5.1 Introduction

To test the performance of ESs in the identification of geomechanical parameters, two verification problems of a circular tunnel in an elastic and elasto-plastic medium were developed. Since a larger number of error function evaluations were expected due to the nature of the algorithm, analytical solutions were used to reduce the computational time. As in the previous application, the least-square error function was used.

Geomechanical parameters were attributed to the rock mass in order to obtain the "monitored" values. These algorithms do not work with an initial approximation to the solution but with constrains to the parameters values. These constrains were used to define interval ranges for the geomechanical parameters to identify. Different magnitude intervals were established in order to evaluate the stability of the algorithm.

The used analytical models were developed by Rocha (1976) and Salençon (1969), for the elastic and elasto-plastic solutions, respectively. The adopted characteristics for each problem are presented in Table 6.11.

**Table 6.11:** Characteristics of the verification problems.

	Elastic case	Elasto-plastic case
Radius	5 m	1 m
Depth	20 m	20 m
Geomechanical parameters	$E = 1500MPa$ and $\nu = 0.34$	$E = 1500MPa$ ; $\nu = 0.21$ ; $\phi' = 30^\circ$ ; $c' = 3.45MPa$ and $\psi = 0$
Stress field	Gravitic: $\sigma_V = 0.75MPa$ and $K_0 = 0.5$	Isotropic: $\sigma_0 = 0.54MPa$

$\nu$  - Poisson coefficient;  $\psi$  - dilation angle;  $\sigma_V$  - vertical stress;  $\sigma_0$  - isotropic stress.

In the elastic case, a total of four measurements, two stresses and two displacements, were used in the identification process, namely: the vertical and horizontal displacements in the arch and wall of the tunnel and horizontal and radial stresses.

In the elasto-plastic case, the initial set of parameters did not cause yielding to happen in the rock mass surrounding the opening. This way, the rock mass behaves elastically, therefore, this case was used mainly to investigate the possibility to identify strength parameters when no plastic zones occur. In a second stage, the isotropic stress was increased to a value of 30 MPa in order to study the effect of yielding and increased non-linearity of the problem in back analysis.

Since an isotropic field stress was used, the measurements located at the same distance from the tunnel centre were equal. This way, a total of three radial measurements, two displacements and one stress, were considered in the back analysis process. The displacements were taken at distances of 1 m and 4 m from the tunnel centre. In relation to the measured stress a 1.5 m distance was assumed.

The back analysis procedure for this case is schematised in Figure 6.16. First a initial generation of ten potential solutions is coded by the algorithm. The response of the analytical model is computed considering these solutions. If the stopping criteria is met (in this case two error values are considered as it will be described latter) the process is stopped and the solution is the set of parameters correspondent to the lower value of the error function within the generation. Otherwise, a new generation is coded by the ES algorithm using genetic operators (like mutation and recombination) and tested again with the analytical model in an iterative process until convergence is achieved.

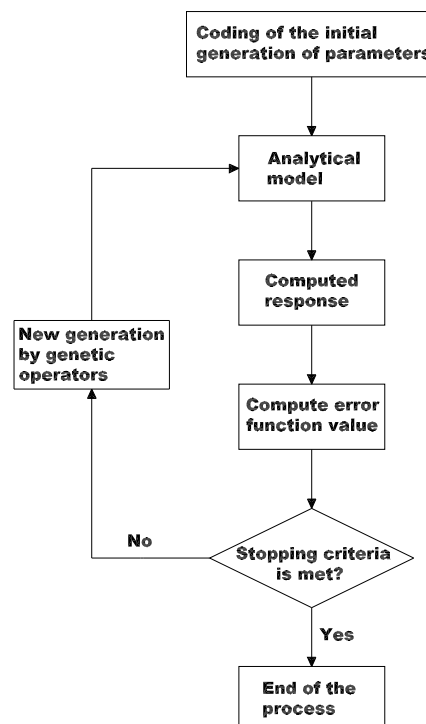


**Figure 6.16:** Scheme of the back analysis procedure using the ES algorithm.

A total of 19 cases were tested in elasticity and elasto-plasticity considering different combinations of measurements and parameters to identify. In each case, 10 different ranges for the parameters were considered for efficiency check of the algorithm. Table 6.12 resumes all the

different combinations of measurements and parameters in the analysed cases.

**Table 6.12:** Adopted combinations of measurements and parameters for the evaluation of the ES algorithm in back analysis.

	Case	Parameters	Measurements
<b>Elastic case</b>	1	E	$u_{arch}$ and $\sigma_H$
	2	E and $\sigma_H$	$u_{arch}$ and $\sigma_R$
	3	E and $\sigma_H$	$u_{arch}$ and $u_{wall}$
	4	E, $\sigma_H$ and $\nu$	$u_{arch}$ and $\sigma_R$
	5	E, $\sigma_H$ and $\nu$	$u_{arch}$ , $u_{wall}$ and $\sigma_R$
<b>Elasto-plastic case</b> No-Yielding	6	$c'$ and $\phi'$	$u_{1m}$ , $u_{4m}$ and $\sigma_{Rpl}$
	7	E and $\phi'$	$u_{1m}$ , $u_{4m}$ and $\sigma_{Rpl}$
	8	E and $c'$	$u_{1m}$ , $u_{4m}$ and $\sigma_{Rpl}$
	9	$c'$ and $\phi'$	$u_{1m}$ and $\sigma_{Rpl}$
	10	E and $\phi'$	$u_{1m}$ and $\sigma_{Rpl}$
	11	E and $c'$	$u_{1m}$ and $\sigma_{Rpl}$
	12	E, $c'$ and $\phi'$	$u_{1m}$ , $u_{4m}$ and $\sigma_{Rpl}$
	<b>Elasto-plastic case</b> With Yielding	13	$c'$ and $\phi'$
14		E and $\phi'$	$u_{1m}$ , $u_{4m}$ and $\sigma_{Rpl}$
15		E and $c'$	$u_{1m}$ , $u_{4m}$ and $\sigma_{Rpl}$
16		$c'$ and $\phi'$	$u_{1m}$ and $\sigma_{Rpl}$
17		E and $\phi'$	$u_{1m}$ and $\sigma_{Rpl}$
18		E and $c'$	$u_{1m}$ and $\sigma_{Rpl}$
19		E, $c'$ and $\phi'$	$u_{1m}$ , $u_{4m}$ and $\sigma_{Rpl}$

### 6.5.2 Evolution Strategies

Due to the lack of knowledge in the geotechnics field concerning the fundamentals of ESs, in this subchapter some of the main issues concerning these algorithms are presented with special emphasis to the ES used in the analysed verification problems. It is not intended to give a thorough insight about the specific features of the ESs (many handbooks were already devoted to this subject e.g. Bäck (1996)) but to provide a general presentation of their characteristics.

The ESs algorithms are search procedures that mimic the natural evolution of the species in natural systems. They work directly with the real representation of the parameter set, searching from an initial population (a set of points) normally generated at random, requiring only data based on the objective function and constrains, and not derivatives or other auxiliary knowledge. Transition rules are deterministic and the constrains are normally handled eliminating the points outside their range.

For differentiation sake, there was the necessity to establish a nomenclature distinguishing

the existent types of ESs. This nomenclature is based on the parents ( $\mu$ ) and offspring ( $\lambda$ ) number and selection type designated as '+' or ','. The most simple form of ES is the so-called two-membered (1+1)-ES (Schwefel, 1965). In this strategy, at a given generation, there are only one parent ( $\mu=1$ ) and one offspring ( $\lambda=1$ ) generated by mutation adding a random quantity  $z^{(k)}$  to the parent. Selection takes place between the two in relation to the error function value, provided that it satisfies all the constraints. The selected one becomes then the parent of the next generation and the process is repeated until the stop criteria is met (Costa and Oliveira, 2001).

Usually, the random numbers  $z^{(k)}$  are generated according to a Normal distribution with mean zero and variance  $\sigma_i^2$ . The initial standard deviations  $\sigma_i$  can be set using equation 6.18.

$$\sigma_i^{(0)} = \frac{\Delta x}{\sqrt{n}} \quad (6.18)$$

where  $\Delta x$  is a rough measure of the distance to the optimum and  $n$  is the dimension problem. However, it can be difficult to estimate  $\Delta x$  therefore the alternative equation 6.19 can be used.

$$\sigma_i^{(0)} = \frac{\beta_i - \alpha_i}{\lambda\sqrt{n}} \quad (6.19)$$

where  $\alpha_i$  and  $\beta_i$  are the lower and upper bounds of the decision variable  $i$ . The standard deviations (or step size) are actualised during the process using different rules and self-adaptation schemes which enhances the algorithm performance (Rechenberg, 1994).

From the appearance of the (1 + 1)-ES algorithm, several developments have been carried out. Nowadays, two main distinct types of ESs, differing basically on the selection procedures, are used: the  $(\mu + \lambda)$ -ES and the  $(\mu, \lambda)$ -ES. In  $(\mu + \lambda)$ -ES, at a given generation, there are  $\mu$  parents, and  $\lambda$  offspring are generated by mutation. Then, the  $\mu + \lambda$  members are sorted according to their objective function values. Finally, the best  $\mu$  of all the  $\mu + \lambda$  members become the parents of the next generation (i.e. the selection takes place between the  $\mu + \lambda$  members). The  $(\mu, \lambda)$ -ES differs from the previous in the point that selection takes place only between the  $\lambda$  members.

Traditionally, the search of new points was based on one single operator, the mutation operator. As it was already referred, mutation consists basically on adding random numbers with mean zero and variance  $\sigma_i^2$  to the vector of decision variables. However, the introduction of a second operator - recombination - benefits ESs performance. Basically, the recombination operator consists on, before mutation, to recombine a set of chosen parents to find a new solution. A given number  $\rho$  of parents are chosen for recombination. Thus, the nomenclature for ESs with recombination are usually referred as  $(\mu/\rho + \lambda)$ -ES or  $(\mu/\rho, \lambda)$ -ES. In the analysed



verification problems a  $(\mu/\rho + \lambda)$ -ES algorithms was used. Figure 6.17 shows the different stages of this ES.

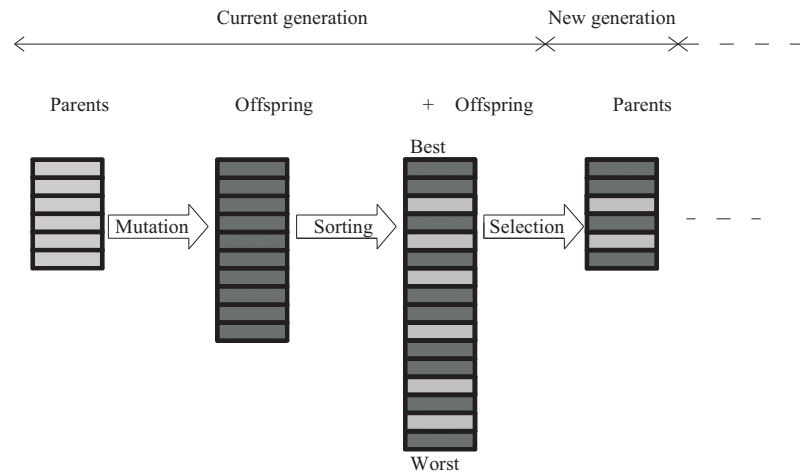


**Figure 6.17:** Evolution stages of the  $(\mu/\rho + \lambda)$ -ES algorithm (Costa and Oliveira, 2001).

In each generation, a set of ten potential solutions was generated. The algorithm stopped its search when one of the following conditions was met:

- the maximum number of generations was reached (a maximum of 100 was assumed);
- the difference between the two extreme values of the error function considering a given generation is lower than  $\epsilon_1$ ;
- the ratio between the previous difference and the mean value of the error function within the generation lower than  $\epsilon_2$ .

In a first attempt, values of  $10^{-4}$  and  $10^{-5}$  were used for  $\epsilon_1$  and  $\epsilon_2$ , respectively. However, these values were too high and, most of the times, the algorithm was kept in local minima. This way, in order to obtain good results, values of  $10^{-5}$  and  $10^{-6}$  had to be considered for  $\epsilon_1$  and  $\epsilon_2$ .

### 6.5.3 Obtained results

In this section the main results are analysed in terms of convergence and performance of the used ES for the different cases considered and presented in Table 6.12. Case 1 is related with the simple case of E identification using two measurements. The results for the different analysis are presented in Table 6.13.

**Table 6.13:** Results of the identification of E with two measurements in the elastic case.

Range of E (MPa)	Number of generations *	Identified value - E (MPa)	Absolute value of the error function
100-10000	3	1498.50	$1.00 \times 10^{-6}$
500-5000	2	1499.64	$5.82 \times 10^{-8}$
1000-3000	2	1499.98	$1.11 \times 10^{-10}$
1000-2000	2	1499.65	$5.44 \times 10^{-8}$
1100-1800	3	1499.62	$6.31 \times 10^{-8}$
1200-1700	3	1500.13	$7.62 \times 10^{-9}$
1300-1650	2	1499.81	$1.58 \times 10^{-8}$
1400-1600	1	1498.70	$7.53 \times 10^{-7}$
1450-1550	1	1499.35	$1.88 \times 10^{-7}$
1499-1501	1	1499.97	$3.39 \times 10^{-10}$

\* - in each generation 10 candidate solutions are generated.

The algorithm presented total convergence even for very high range intervals. Evolutionary algorithms normally take several hundreds or even thousands of error function evaluations to reach convergence. In this case, a maximum of three generations (i.e. 30 evaluations) to reach convergence were needed which can be considered a low value for this type of algorithms.

Cases 2 and 3 are related with the identification of E and  $\sigma_H$  using two measurements. For the first, which used a displacement and a stress measurement, the correct values were identified in every case. The maximum range for E was the same as considered in the previous case while for  $\sigma_H$  it was between 0.1 MPa and 1 MPa. In this case, the algorithm took 12 generations to reach convergence. However, the number of generations rapidly decreased for 3-4 considering more reasonable intervals. Figure 6.18 presents the topology of the error function for this case. In spite of the elastic behaviour, and in contrast with what was verified for the same case using the traditional algorithms, the error function is not strictly convex and present a complex topology with several local minima. The equations of the analytical solution, even though referring to an elastic solution, are highly non-linear. However, the algorithm was able to find the global minimum in every tested case, which would be very difficult if a traditional algorithm was used.

Considering case 3, two displacement measurements were used. In this case, the correct parameters were not identified for the algorithm converged rapidly for local minima with very low error function values. The two displacements seem to be highly correlated and the problem is 'ill-posed'.

In the last two cases,  $\nu$  was added to the back analysis. In case 4, only two measurements were used which is less than the number of parameters to identify. However, convergence was attained to the values of E and  $\sigma_H$  very close to the correct ones which not happened with  $\nu$ .

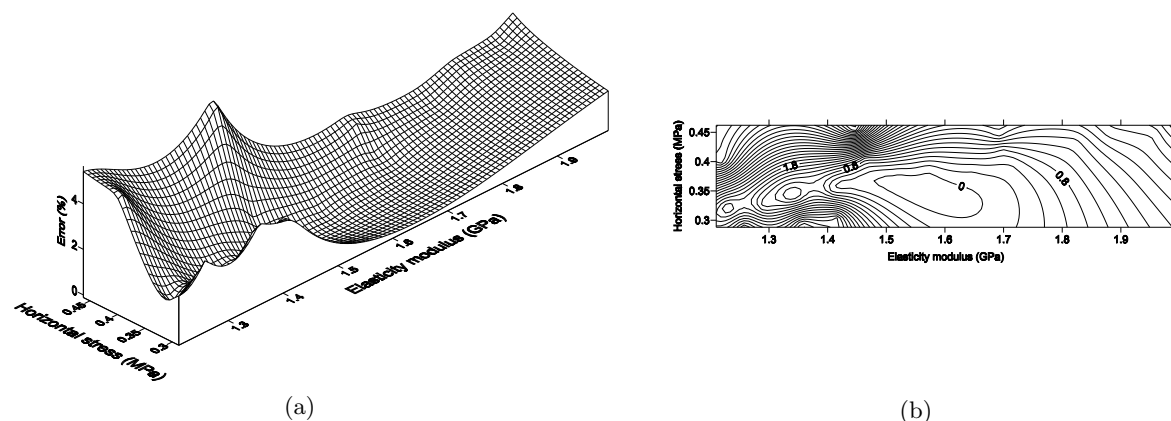


**Figure 6.18:** Topology of the error function on the identification of  $E$  and  $\sigma_H$  for the analytical case in elasticity and using two measurements. (a) 3D view (b) Plan view.

This was probably due to a low importance of  $\nu$  in the computed displacements and stresses which allow to obtain approximate values with a relatively wide range of this parameter. When another measurement was added (case 5), the performance of the algorithm was significantly enhanced even though the high correlation between the two displacement measurements. However, for the larger parameter ranges, a relatively high number of generations were needed as can be observed in Table 6.14

**Table 6.14:** Results of the identification of  $E$ ,  $\sigma_H$  and  $\nu$  with three measurements in the elastic case

Range			Number of gener- ations	Identified value			Absolute value of the error function
E (MPa)	$\sigma_H$ (MPa)	$\nu$		E (MPa)	$\sigma_H$ (MPa)	$\nu$	
100-10000	0.1-1	0.1-0.45	36	1501.01	0.376	0.341	$6.67 \times 10^{-6}$
500-5000	0.2-0.9	0.1-0.45	27	1511.87	0.375	0.342	$2.20 \times 10^{-5}$
1000-3000	0.2-0.8	0.2-0.4	34	1517.85	0.375	0.346	$7.75 \times 10^{-4}$
1000-2000	0.2-0.7	0.2-0.4	33	1477.01	0.372	0.333	$1.28 \times 10^{-4}$
1100-1800	0.3-0.6	0.3-0.4	4	1439.61	0.372	0.336	$4.26 \times 10^{-4}$
1200-1700	0.3-0.5	0.3-0.4	7	1415.62	0.375	0.340	$9.70 \times 10^{-4}$
1300-1650	0.3-0.4	0.32-0.37	2	1462.24	0.371	0.332	$1.95 \times 10^{-4}$
1400-1600	0.35-0.45	0.32-0.36	1	1499.76	0.375	0.341	$3.21 \times 10^{-6}$
1450-1550	0.36-0.38	0.33-0.35	1	1498.50	0.374	0.340	$1.99 \times 10^{-6}$
1499-1501	0.37-0.38	0.33-0.35	1	1499.54	0.375	0.341	$1.54 \times 10^{-6}$

For the elasto-plastic cases with no-yielding it was possible to identify the correct values in every combination of two parameters with both two or three available measurements, i.e. from cases 6 to 11. In fact, it was observed that the measurement number have only minor impact.

Considering all the tested cases, convergence was achieved in a maximum of 11 generations which happened only three times (out of 60 calculations) and for the largest intervals. For reasonable parameter ranges, the identification process only took 4-5 generations to identify the correct values. This good performance is not related with simple topologies of the error function as it can be seen in Figure 6.19 which presents this function for case 6. In fact, it presents an irregular shape with local minima and the algorithm was able to find the optimum solution in different conditions in a reasonable number of error function evaluations.

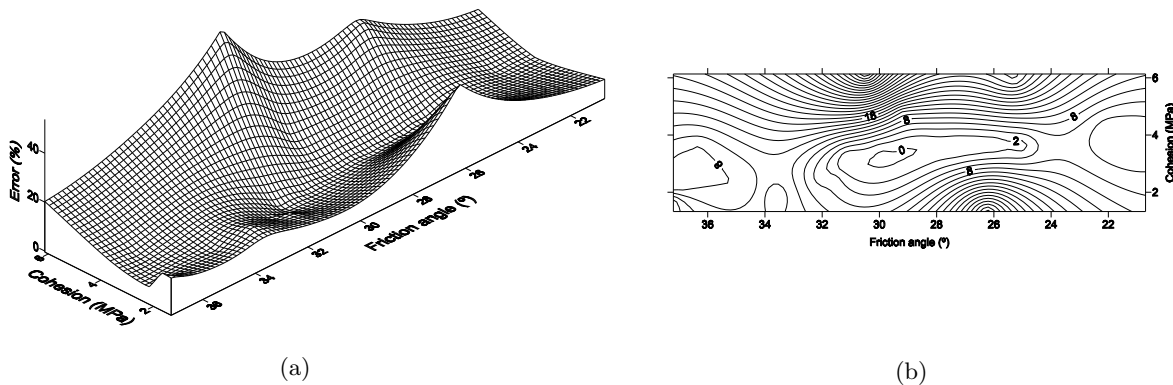


**Figure 6.19:** Topology of the error function on the identification of  $c'$  and  $\phi'$  for the analytical case in elasto-plasticity (no-yielding) and using two measurements. (a) 3D view (b) Plan view.

The remaining case, where three parameters were considered together with the same measurement number, only partial convergence was achieved. In fact, as it can be observed in Table 6.15, the correct parameters were not identified when larger intervals were considered. In these cases, the algorithm was trapped in local minima. In practice, it is expected that the consideration of *a priori* knowledge, experts' opinion and/or site characterisation can keep the interval ranges of the parameters within reasonable ranges and minimise this problem.

For the elasto-plastic cases with yielding the problem becomes more complicated. Besides the high non-linearity of the governing equations, they also present discontinuities. The equations that provide the stresses and displacements are different for the elastic and plastic zones. This fact is clearly reflected on the results. In the cases where two parameters are considered together with three measurements, the behaviour of the algorithm is different. The identification process for cases 14, 15, 17 and 18 was able to reach convergence to the correct parameter values. The impact of the measurement number on the results was low with no recognisable pattern of which cases the algorithm was more efficient. Moreover, the overall behaviour of the algorithm was very similar to the non-yielding cases (7, 8, 10 and 11). However, the identifica-

**Table 6.15:** Results of the identification of  $E$ ,  $c'$  and  $\phi'$  and with two measurements in the elasto-plastic case with no-yielding.

Range			Number of gener- ations	Identified value			Absolute value of the error function
E (MPa)	$c'$ (MPa)	$\phi'$ ( $^\circ$ )		E (MPa)	$c'$ (MPa)	$\phi'$ ( $^\circ$ )	
100-10000	0.1-10	10-50	8	2541.05	6.76	11.86	$4.17 \times 10^{-4}$
500-5000	0.5-5	15-45	8	1605.30	3.75	28.19	$1.04 \times 10^{-5}$
1000-3000	1-5	20-40	7	1657.84	3.90	27.37	$2.35 \times 10^{-5}$
1000-2000	2-5	25-35	2	1495.61	3.46	30.07	$3.11 \times 10^{-5}$
1100-1800	2.5-4	25-35	6	1500.18	3.45	30.00	$3.62 \times 10^{-7}$
1200-1700	3-4	26-34	1	1407.84	3.20	31.38	$2.66 \times 10^{-5}$
1300-1650	3.2-3.8	27-33	1	1446.63	3.32	30.97	$5.54 \times 10^{-5}$
1400-1600	3.2-3.7	28-32	1	1499.08	3.45	30.07	$4.04 \times 10^{-6}$
1450-1550	3.3-3.6	29-31	1	1525.31	3.49	29.69	$4.17 \times 10^{-5}$
1499-1501	3.4-3.5	29-31	1	1499.07	3.44	30.07	$5.78 \times 10^{-6}$

tion of the couple  $c'$  and  $\phi'$  raised more problems. In fact, only partial convergence was achieved independently on the available measurement number. In some of the cases, the algorithm was not able to avoid local minima. To provide a thorough insight of the problem in this specific case, the topology of the error function was drawn (Figure 6.20).

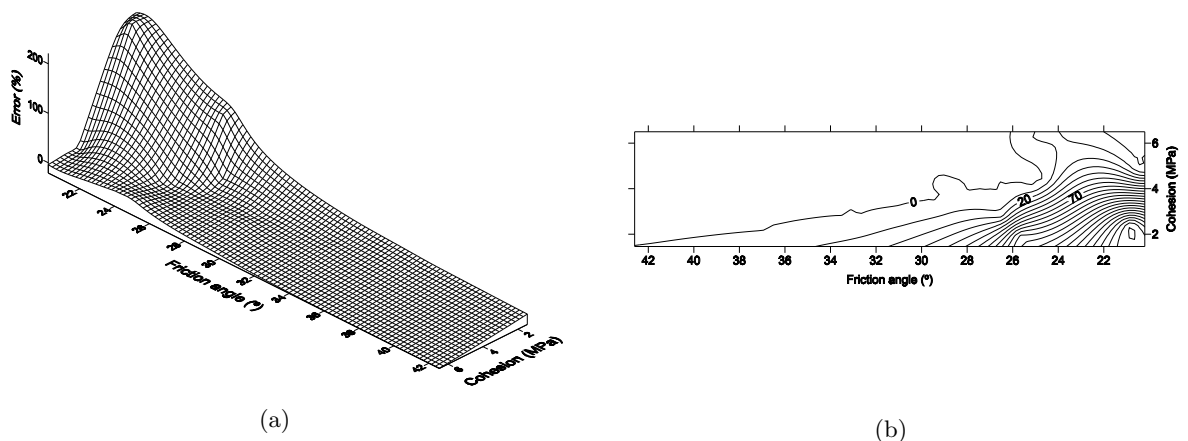


**Figure 6.20:** Topology of the error function on the identification of  $c'$  and  $\phi'$  for the analytical case in elasto-plasticity (with yielding) and using three measurements. (a) 3D view (b) Plan view.

In a first analysis this error function presents a more smooth shape than many of the previously presented ones. This way, it should not be expected an erroneous behaviour of the algorithm. It is however interesting to notice that there is a region in the parameter space for

which the error is extremely high, dropping very rapidly for a large and very flat valley. This region corresponds to very low error function values. This way, there are many combinations of  $c'$  and  $\phi'$  which provide approximately the same measurements. This is probably due to a low influence of these parameters in the considered measurements in comparison with E. To avoid this problem, calculations were repeated considering a new and more restrict limit for the stopping criteria. In these new calculations,  $\epsilon_1$  and  $\epsilon_2$  were put equal to  $10^{-6}$  and  $10^{-7}$ . With this consideration, the results were significantly enhanced as it can be seen in Table 6.16 showing that the limits assumed for the stopping criteria can sometimes be important to avoid local minima and provide better results of the identification process for parameters with lower influence on measurements. However, and as it should be expected, computational cost also increased translated by a higher number of generations needed to reach convergence.

**Table 6.16:** Results of the identification of  $c'$  and  $\phi'$  with three measurements in the elasto-plastic case with yielding

Range		$\epsilon_1 = 10^{-5}$ and $\epsilon_2 = 10^{-6}$			$\epsilon_1 = 10^{-6}$ and $\epsilon_2 = 10^{-7}$		
$c'$ (MPa)	$\phi'$ (°)	Number of generations	$c'$ (MPa)	$\phi'$ (°)	Number of generations	$c'$ (MPa)	$\phi'$ (°)
0.1-10	10-50	13	3.48	29.78	17	3.48	29.81
0.5-5	15-45	7	2.81	33.51	23	3.42	30.12
1-5	20-40	3	3.45	30.01	4	3.44	30.03
2-5	25-35	4	3.08	32.14	13	3.27	30.91
2.5-4	25-35	5	3.41	30.16	6	3.43	30.10
3-4	26-34	3	3.20	31.38	7	3.23	31.19
3.2-3.8	27-33	3	3.49	29.77	3	3.49	29.77
3.2-3.7	28-32	2	3.24	31.09	4	3.33	30.68
3.3-3.6	29-31	2	3.44	30.03	3	3.44	30.03
3.4-3.5	29-31	1	3.45	30.02	1	3.45	30.02

As it was verified that the limits of the stopping criteria could have a significant impact in both the quality of the results and speed of convergence, all the cases of the elasto-plastic case with yielding were repeated for different values of  $\epsilon_1$  and  $\epsilon_2$ . For higher error limits the algorithm could not find the optimal set of parameters in many cases due to local minima. For lower values, results were improved but the computational cost was also significantly increased. This way, it was concluded that the first set of adopted values for  $\epsilon_1$  and  $\epsilon_2$ , and besides the problems presented in the already mentioned cases, provides the algorithm a balance between robustness and efficiency.

Finally, in case 19 in which three parameters are considered together with three measure-

ments, the same problems were detected as in the non-yielding case. The performance of the algorithm is enhanced as the search space is reduced and lower limits of the stopping criteria did not have any influence on the obtained results.

## 6.6 Conclusions

It has passed almost three decades since the first applications of *in situ* measurements in the back analysis of geotechnical parameters. Since then, many studies have been carried out and presented in literature. However, the use of back analysis is still far from being a standard procedure in geotechnical projects. One of the main reasons, between others, is that back analysis is a time-consuming process which demands some expertise. Moreover, in many cases, classical optimisation algorithms fail to provide a solution that corresponds to the global optimum.

In this Chapter, the main components, methods and types of back analysis were briefly described. Special emphasis was given to the direct approach for being a more general and flexible procedure. In the direct approach back analysis is carried out using an error function which measures the differences between observed and computed quantities, and an optimisation algorithm to minimise this function in an iterative process. This way, back analysis can be programmed independently of the model (analytical or numerical) and coupled with it in order to increase the process performance.

Some of the main works related with back analysis in the geotechnics field, with particular relevance to the identification of the geomechanical parameters in underground structures, were presented. Focus was drawn to the type of algorithms normally used in the direct approach distinguishing to main types, namely the classical and new algorithms. The classical ones, developed in the scope of the traditional optimisation field, have been normally used since the first applications. However, as they present some limitations, new algorithms, based on significantly different intrinsic principles, have been developed and applied with success. One example of this type of algorithms are the ESs, which are based on AI techniques, and try to mimic natural principles like natural selection and survival of the fittest.

This Chapter intends to provide a contribution to the definition of a reliable process to perform back analysis specially related with the type of algorithm used in the optimisation process. Using validation problems concerning parameters identification in an underground work, different types of optimisation algorithms, classical and new, were tested in order to highlight their main advantages and drawbacks for this particular case. Three classical gradient-based and one ES algorithms were used considering several different conditions to evaluate their efficiency and robustness.

The classical algorithms were coupled with a 3D model of a tunnel excavation. The performed tests allowed to conclude that gradient-based optimisation algorithms present a very good performance when an elastic model is used. In this situation, these algorithms present a robust and efficient performance since they can, in most of the cases, converge to the optimal solution in a reduced iteration number. In displacement-based back analysis the use of a high number of reliable measurements increase robustness even though some efficiency loss. Moreover, the gradient of the error function can be well approximated by finite differences. The chosen step for this calculation has only minor impact in the process.

Considering the back analysis of strength parameters of an elasto-plastic constitutive model, these algorithms are less reliable. Typically, in these cases, the error function topology is complex presenting one or more local minima. In several cases the algorithms fail to converge or convergence is achieved to the local minimum closer to the initial solution. This way, in order to increase the rate of success when applying gradient based algorithms in elasto-plasticity models, one should be aware of:

- provide the most accurate initial estimation possible to try to avoid local minima;
- use a high number of reliable (specially non/low correlated measurements);
- if using the finite difference method to compute the error function gradient use a low value of the step (typically less than 2%).

It can be then concluded that gradient-based algorithms present significant limitations to perform the identification of geomechanical parameters in underground structures when more complex models are used. Moreover, they are only able to identify a reduced number of parameters which hinders back analysis to be carried out when using a constitutive model composed by a high parameters number.

In order to overcome some of the limitations of the classical algorithms, the ES innovative approach was proposed and applied in two analytical verification problems and proved to be a reliable method in the back analysis of geomechanical parameters. The algorithm showed to be robust in identifying the global minimum even in very complex and noisy error functions and in wide parameter spaces (large intervals for the parameters). Its efficiency is very interesting when compared with other types of evolutionary algorithms (like GAs) that normally take several hundreds or even thousands of error function evaluations to reach convergence. It is worth mentioning that the used algorithm was not optimised for this specific application. This way, further research may be able to improve its behaviour in both robustness and efficiency. The adopted limits for the stopping criteria can have a significant impact on the capacity to achieve



the global minimum of the algorithm in particular in what concerns the identification of parameters with low importance in the considered measurements. In these cases, the error function presents wide valleys corresponding to low values of the error function and it is necessary to use very restrict stopping criteria limits in order to avoid local minima.

Concluding, it is believed that this new approach is a step forward in the development of a generic methodology that can provide an adequate framework for many geotechnical back analysis problems. However, there are still much research work to be performed in order to test and validate this algorithm specially using more complex models. Moreover, another important issues must be consistently contemplated in a global inverse approach using these techniques. A full back analysis approach should consider all uncertainties related to the used model. This way, not only the parameters of the constitutive model but the model itself should be back analysed. Also, the consideration of the previous excavation stages is particularly important in the prediction of the actual stress state and definition of the displacements field. This is valid for both direct and inverse approaches. The measurements observed in the several excavation stages should be considered in the back analysis in order to obtain more consistent results.



# Venda Nova II Powerhouse Complex - Back Analysis of Geomechanical Parameters

## 7.1 Introduction

The EDP - Electricity of Portugal decided to repower the Venda Nova hydroelectric scheme, located in the North of Portugal, by building a new power station, named Venda Nova II, that took advantage of the high existing head - about 420 m - between the reservoirs of Venda Nova and Salamonde dams (Lima *et al.*, 2002) (Figure 7.1).

Venda Nova II is equipped with two reversible units in order to optimise the water resources use for energy production. The scheme, built in a predominantly granite rock mass, is almost fully composed by underground facilities, including caverns and several tunnels and shafts with total lengths of about 7.5 km and 750 m, respectively (Figure 7.2). The Venda Nova II project involved the construction of important geotechnical underground works of which the following can be mentioned:

- the access tunnel to the caverns, with about 1.5 km, 10.9% slope and 58  $m^2$  cross-section;
- the hydraulic circuit with a 2.8 km headrace tunnel with 14.8% slope and a 1.4 km tailrace tunnel and 2.1% slope, with a 6.3 m diameter modified circular section;
- the powerhouse complex located at about 350 m depth with two caverns, for the powerhouse and transforming units, connected by two galleries;
- an upper surge chamber with a 5.0 m diameter and 415 m height shaft and a lower surge chamber with the same diameter and 60 m height.



**Figure 7.1:** General perspective of the power reinforcement scheme (adapted from Plasencia (2003))

Even though the multiplicity of underground structures built in the scope of this scheme, the analysis will focus only on the powerhouse complex. For this caverns, 2D and 3D numerical models were developed considering the different construction stages. The geomechanical parameters of the granite formation for the numerical models were obtained using the software GEOPAT (Miranda, 2003) which is based in artificial intelligence (AI) techniques. This software is a knowledge based system which allows obtaining geomechanical parameters for underground structures modelling in granite formations. *Phases*<sup>2</sup> and FLAC3D were used for the 2D and 3D models, respectively.

This scheme was built in a granite rock mass with overall good quality. In order to have an insight of the main geomechanical characteristics of the rock formation, in the following section some of the geotechnical information gathered during the geotechnical surveys carried out to characterise the rock mass interesting the hydraulic circuit is concisely analysed. The results of some *in situ* and laboratory tests are evaluated using statistical tools which allowed to understand some particular characteristics of the rock mass.

Afterwards, the main characteristics of the powerhouse complex are presented together with the geotechnical survey performed to characterise the rock mass near the caverns and the defined monitoring plan. The main results of the numerical models are analysed and compared with the monitored data in terms of displacements.

Finally, back analysis techniques are applied in order to identify some geomechanical parameters. Two different techniques are used, namely a optimisation software called SiDolo which is based on a hybrid technique which combines two traditional optimisation algorithms and

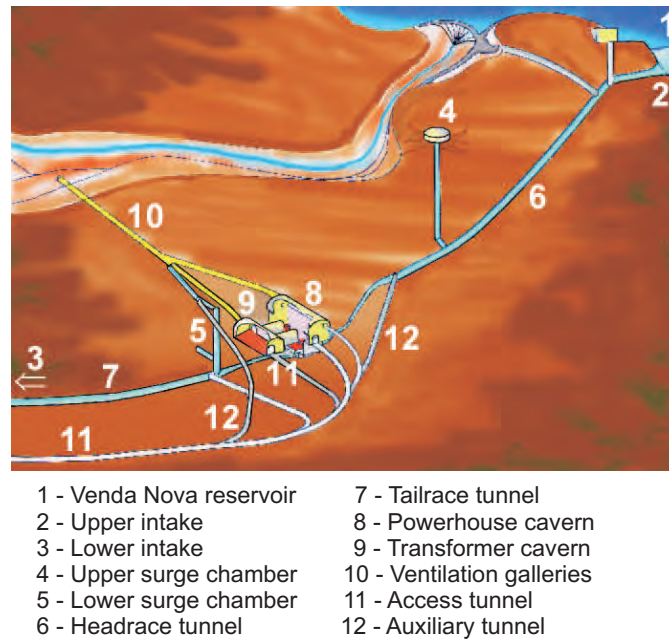


**Figure 7.2:** Scheme of the underground works composing the Venda Nova II complex (adapted from (Lima *et al.*, 2002))

an evolution strategy (ES) algorithm as used in the previous Chapter. Due to the rock mass characteristics the most important parameters in the behaviour (in terms of displacements) of the powerhouse complex are  $K_0$  and  $E$ . Therefore, these parameters were the ones object of the back analysis process. Calculations were performed considering different circumstances.

Part of this work was carried out in cooperation. In particular, the 3D model of the caverns and the back analysis calculations with this model were developed in a joint effort with Professor Daniel Dias and Engineer Stéphanie Eclaircy-Caudron of *INSA-Lyon*.

## 7.2 Analysis of geotechnical information along the hydraulic circuit of Venda Nova II

In order to have a more thorough insight about the rock mass interesting the Venda Nova II project, a succinct analysis of the deformability and strength properties determined by means of *in situ* and laboratory tests performed by LNEC was carried out (LNEC, 1983, 2003, 2005). In this study, the results of the following tests are analysed: dilatometers in boreholes, seismic waves propagation by ultrasounds, uniaxial compressive strength in rock samples and shear tests on discontinuities.

Part of this information was already used and analysed in previous chapters. In particular, the results of the LFJ test was used in Chapter 5 in the scope of the developed Bayesian

approach to update the geomechanical parameters. Just for the record, the results of this test pointed out to a value of  $E$  ranging from 33 GPa to 40 GPa with a mean value of about 37 GPa. Also, in Chapter 4 the results of this test were used to calibrate the analytical methodology based on the empirical system for the calculation of  $E$ .

A coarse porphyritic, both biotitic and moscovitic, granite prevails in the region. The rock mass on which the hydroelectric complex is installed is characterised by a medium-size grain granite of a porphyritic trend with quartz and/or pegmatitic veins and beds, which are occasionally, rose. The rock mass also presents embedment of fairly quartzitic mica-schist.

The geotechnical survey allowed to define three geotechnical zones, namely: ZG1 - correspondent to a very good quality rock mass which is located at variable depths and interests in particular the caverns of the powerhouse complex; ZG2 - a transition slightly weathered rock formation; ZG3 - corresponding to the superficial and unconfined rock. This zonation can be observed in Figure 7.3. Globally, the rock mass interesting these underground works presents good geomechanical quality in spite of the presence of some less favourable geological features like the Botica fault.

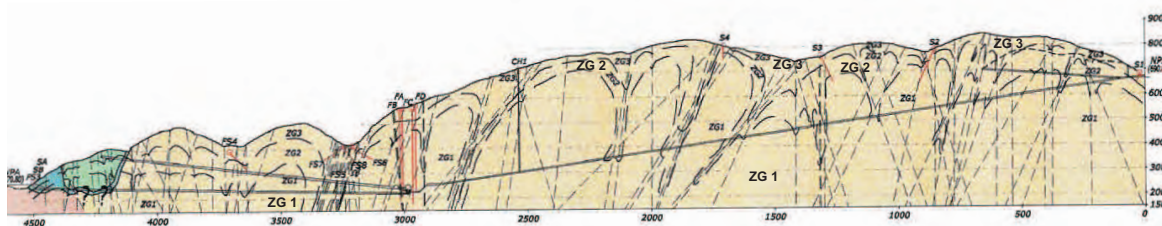


**Figure 7.3:** Geological-geotechnical zones along the hydraulic circuit (adapted from Plasencia (2003))

From the available information it was not possible to distinguish some of the tests to what geotechnical zones they were referred. In these cases, only a global view of the rock mass characteristics is performed. However, it is believed that a substantially higher number of the analysed tests were performed in the ZG1 zone.

In the dilatometer test, the deformations are applied in four diametral directions and in three load cycles. In the analysis of the results, the readings produced by the first cycle were not considered. Table 7.1 presents the results obtained by the analysis of these tests. In this Table, the number of tests ( $n$ ), the mean and standard deviation and the percentiles correspondent to 5% and 95% are presented.

The mean value is about 16 GPa which is substantially lower than the results obtained by the LFJ. In the case of the dilatometers, tests were performed in all types of rock masses (including fault zones) which is translated by the high variability of the results and wide interval

**Table 7.1:** Statistical analysis of E in GPa obtained by the dilatometer tests.

Zone	n	mean	Std. Dev.	5%	95%
All	436	16.14	12.02	2.19	41.92

between the 5% and 95% percentile. In the other hand, the LFJ was performed in a rock mass referred to the ZG1 geotechnical zone. The highest values obtained by the dilatometer tests are close to the mean value obtained with the LFJ.

The Shapiro-Wilk and the Kolmogorov-Smirnov tests were performed to the the overall data collected by the dilatometers. The distribution can not be considered normal nor lognormal for a 95% confidence degree. However, the second one constitutes a better fit as it can be observed by Figure 7.4.

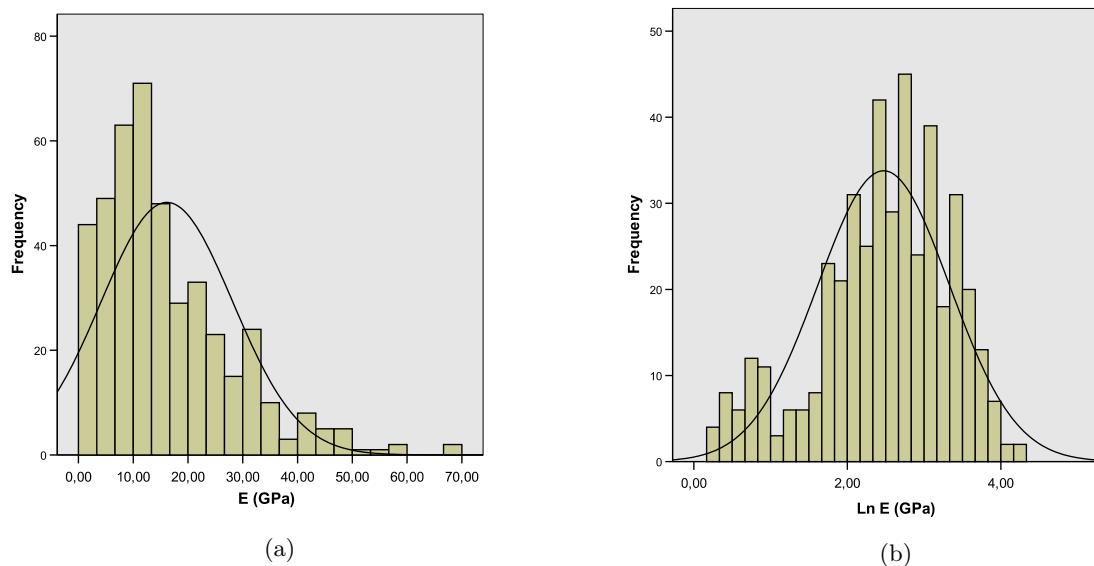


**Figure 7.4:** Histograms of the E values obtained by the dilatometer tests (a) normal distribution (b) lognormal distribution.

To complement the previous analysis, the results from ultrasound tests, which allow obtaining the seismic waves velocity ( $V_p$  and  $V_s$ ) also related with deformability properties, were analysed. Table 7.2 presents the results of these tests. The mean values of  $V_p$  and  $V_s$  translate a stiff formation. The values of the 5% percentile are correspondent to a more weathered/fractured formation.

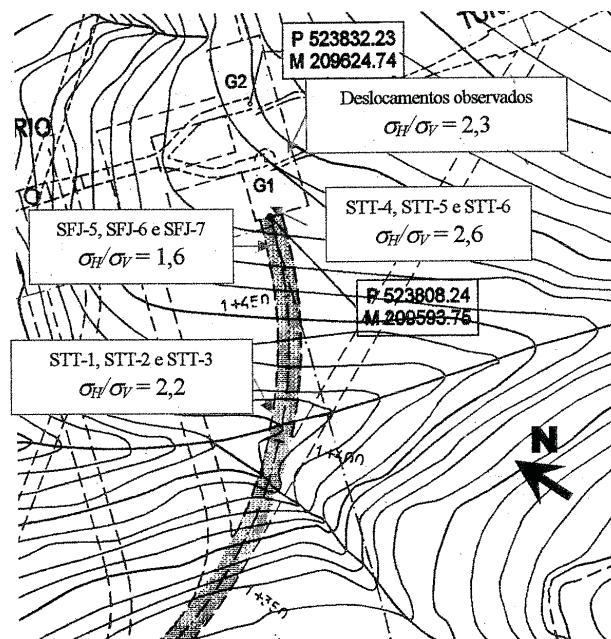
A total of nine SFJ tests were performed. From these, only three (SFJ-5, SFJ-6 and SFJ-7) were considered to be representative of the rock mass with a low disturbance (fracturing) degree caused by the excavation process. The results of these tests ranged from 46 GPa to 51 GPa.

**Table 7.2:** Statistical analysis of  $V_p$  and  $V_s$  obtained by the ultrasound tests.

Zone	n	$V_p$ (m/s)				$V_s$ (m/s)			
		mean	Std. Dev.	5%	95%	mean	Std. Dev.	5%	95%
All	65	4250	760	2688	5314	2631	461	1777	3310

Information about the *in situ* state of stress can also be obtained using the SFJ tests results. In this case, a value of 1.63 was found for  $K_0$  perpendicular to the cavern axis.

Six STT tests were performed in two different locations. The tests, in spite of being carried out in relatively distant test sites, present very similar results. In fact, values of 2.2 and 2.6 were found for  $K_0$  in the same direction as stated for the SFJ tests. The vertical stress corresponds approximately to the overburden gravitic load. Figure 7.5 presents the locations of the SFJ and STT tests and resumes the obtained results. In this Figure, an additional value of  $K_0$  equal to 2.3 is presented which was obtained by back analysis (LNEC, 2003) and will be referred more in detail later in this Chapter.

**Figure 7.5:** Location and comparison between the results of the SFJ and STT tests.

Concerning the laboratory tests, Table 7.3 presents the results obtained by the compression tests, namely the unconfined compressive strength ( $\sigma_c$ ) and the elasticity modulus of the intact rock ( $E_i$ ). The high mean strength and stiffness correspond to a good quality intact rock. In the particular case of  $E_i$ , the mean value is lower than the one obtained by the *in situ* test for the rock mass of better quality which translate the inclusion in these tests of samples collected



in lower quality geotechnical units. However, considering the value correspondent to the 95% percentile, and the previous results of the *in situ* tests, it can be stated that E (for the ZG1 zone) is about 60% to 70% of  $E_r$ .

In terms of  $\sigma_c$ , the overall data collected by the performed tests follows a normal distribution. This was not observed for  $E_i$ . In fact, the Shapiro-Wilk and the Kolmogorov-Smirnov tests rejected the null hypothesis of the data following a normal or a lognormal distribution. However, and as observed before for the case of E determined by the dilatometer tests, the latter distribution presents a better fit.

**Table 7.3:** Statistical analysis of  $\sigma_c$  and  $E_i$  obtained by the laboratory compression tests

Zone	n	$\sigma_c$ (MPa)				$E_i$ (GPa)			
		mean	Std. Dev.	5%	95%	mean	Std. Dev.	5%	95%
All	80	89.6	36.4	24.7	147.7	39.1	19.1	5.9	68.5

The laboratory shear tests on discontinuities were only performed in samples collected in zone ZG1. Besides the Mohr-Coulomb strength parameters ( $\phi'$  and  $c'$ ) also the dilation angle and the stiffness in the normal ( $K_n$ ) and tangent ( $K_t$ ) directions are presented. These results were collected in two different sources LNEC (1983, 2005). In spite of the different criteria for defining the strength parameters values, they correspond approximately to the residual ones. Statistical tests were also performed to the collected data to investigate if the different parameters follow a normal or a lognormal distribution. Table 7.4 presents the results obtained on 40 samples.

**Table 7.4:** Statistical analysis of shear tests on discontinuities results.

	mean	Std. Dev.	5%	95%	Distribution
$\phi'$ ( $^\circ$ )	38.8	6.2	30.4	52.3	Normal and lognormal
$c'$ (KPa)	82.1	56.1	0	184.9	Normal
Dilatance ( $^\circ$ )	8.7	4.7	0.1	17.6	Normal
$K_t$ (MPa/mm)	1.87	0.89	0.83	3.40	Lognormal
$K_n$ (MPa/mm)	32.9	40.4	1.84	106.0	none

The discontinuities present good strength characteristics. In fact, the mean value of the residual  $\phi'$  is high (around  $39^\circ$ ) and they also exhibit, most of the times, some internal cohesion. This parameter is characterised by a high variability which is much less pronounced in what concerns  $\phi'$ . It is interesting to observe the dilatant behaviour of the discontinuities in almost every test. The strength parameters are well described by normal distributions. In the case of

$\phi'$  the lognormal distribution can also be used.

The tangent stiffness, which follows a lognormal distribution is, in mean terms, about 6% of the normal one. However, the results for  $K_n$  show a large dispersion and nor the normal or the lognormal distribution fits to the data. It was observed that the results of the two sets of data were significantly different for this parameter. This was probably due to different approaches in the way this parameter was defined which, in one of the analysed reports, was not detailed. When analysing the two sets of data separately, in both cases, the lognormal distribution fitted well the data.

In conclusion, the rock mass interesting most of the hydraulic circuit present good geomechanical properties which was observed by a large number of *in situ* and laboratory tests. The intact rock and the discontinuities are characterised by high values of strength and stiffness. The stress state is characterised by a vertical stress proportional to the gravitic load and a mean  $K_0$  value in the perpendicular direction of the caverns axis of about 2.5.

In global terms, it was observed that the normal distribution is more adequate to model strength parameters while the lognormal is better suited to describe deformability parameters.

### 7.3 The underground powerhouse complex

The powerhouse complex consists, basically, on two caverns interconnected by two galleries. It is located in a intermediate position of the hydraulic circuit, at an approximately 350 m depth. Figure 7.6 presents two pictures of the powerhouse complex during excavation. In plan, the powerhouse and transforming units caverns are rectangular and have respectively, the following dimensions: 19.0 x 60.5  $m^2$  and 14.1 x 39.8  $m^2$ . The distance between their axes is 45.0 m. Both caverns have vertical walls and scheme arch roofs. In the case of the arch of the powerhouse cavern, the invert of the ceiling is located 20.0 m above the main floor (level 235), whereas in the case of the cavern containing the transforming units, this distance is 10.45 m (Figure 7.7).

The complex was built in a granite rock mass with good geomechanical quality. In order to characterise the rock mass in the area of the caverns, four deep subvertical boreholes with continued sample recovery were performed. Along the boreholes, Lugeon permeability tests were also executed. The lengths of the boreholes varied between 271.0 m and 381.6 m and their positioning was controlled each 50 m. They defined the vertexes of a quadrilateral whose centre was predicted to be close to the central point of the caverns area (Plasencia, 2003). The geomechanical characterisation and the laboratory tests carried out on the 98 collected samples allowed the identification of three geological-geotechnical zones on the rock mass as presented in Table 7.7. Caverns are located in the ZG1C zone corresponding to the zone with best geomechanical characteristics.



Figure 7.6: Pictures of the powerhouse complex caverns during excavation (provided by EDP).

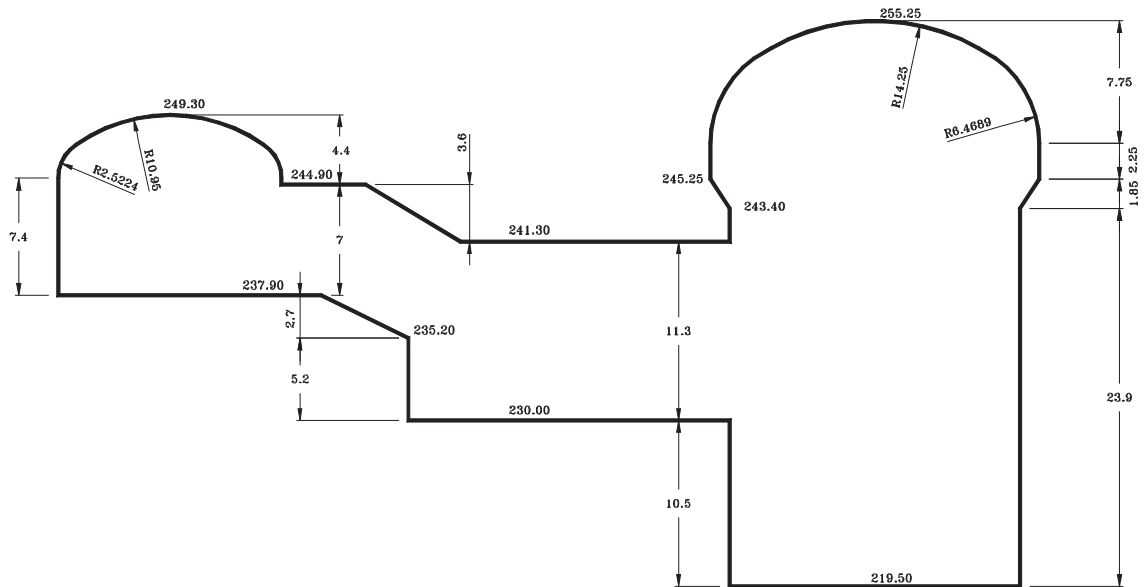


Figure 7.7: Powerhouse complex geometry.

Between the boreholes, seismic tests using longitudinal waves (P waves) were performed in order to obtain tomographies of the rock mass and to detect important geological structures (LNEC, 1997; Plasencia *et al.*, 2000). These tests were executed at depths varying between 95 m and 370 m and the results confirmed the previous zoning. The area where the caverns are located was characterised with P waves velocities between 5250 m/s and 6000 m/s, sometimes 4750 m/s to 5250 m/s. These values confirmed the good geomechanical characteristics of the rock mass.

After the construction of the access tunnel to the caverns, an exploration gallery was excavated in order confirm the previous geomechanical characterisation and to measure the *in situ* stress state. This gallery was excavated from the top of the access tunnel and parallel to

**Table 7.5:** Geological-geotechnical zoning of the rock mass

	<b>Weath.</b>	<b>Disc.</b>	<b>RQD</b>	<b>Perm.</b>	$I_r$ (MPa)	$\sigma_c$ (MPa)	$E_i$ (GPa)
ZG3C	W3/W4-5	F3/F4-F5	0-90	>10 UL	3.8	57.7	42.0
ZG2C	W1-2/W3	F1-2/F3	50-90	0-8 UL	6.3	96.9	51.0
ZG1C	W1/W2	F1/F2	90-100	<2 UL	7.0	110.1	54.9

UL - Lugeon units;  $I_r$  - Point load index.

the caverns axis. As it was already referred, LFJ tests were used to obtain the deformability modulus of the rock mass. These tests led to values ranging from 33 GPa to 40 GPa. The STT and SFJ tests results showed that the vertical and horizontal stress parallel to the caverns axis have the same magnitude and correspond to the overburden dead load. In the perpendicular direction the stress values are approximately 2.5 times higher (LNEC, 1983). From the lithologic characterisation it was possible to identify four main discontinuities sets. In Table 7.6 their main characteristics according to the ISRM (1978) criteria are summarised.

**Table 7.6:** Characteristics of the four main families of discontinuities (Plasencia, 2003).

<b>Family</b>	<b>1</b>	<b>2</b>	<b>3</b>	<b>4</b>
<b>Direction</b>	N81°E	N47°W	N8°E	N50°E
<b>Inclination</b>	77°NW	12°NE	83°NW	80°NW
<b>Continuity</b>	1 to 3 m	1 to 10 m	3 to 10 m	3 m
<b>Alteration</b>	W1-2, occasionally W3	W1-2	W1-2, occasionally W4	W1-2
<b>Opening</b>	closed at 0.5 mm	closed at 0.5 mm	closed at 0.5 mm, sometimes 2.5 mm	closed
<b>Thickness</b>	none at 0.5 mm	none at 0.5 mm	none, sometimes 2.5 mm	none
<b>Roughness</b>	Undulating poorly rough to rough	Undulating poorly rough, sometimes rough stepped	rough plane, sometimes polished	undulating poorly rough
<b>Seepage</b>	Dry	Dry	Dry, occasionally with continuous water flow	Dry
<b>Spacing</b>	2 to 3 m, sometimes 1 or 4 m	2 to 3 m, sometimes 1 m	1 to 2 m	5 to 6 m

In order to evaluate the behaviour of the rock mass and support system during and after construction, a monitoring plan using extensometers and convergence targets was established. The extensometers, in a total number of eleven, were placed in two sections along the caverns axis and their lengths varied from 5 m to 40 m (Figure 7.8). Almost all the extensometers are double. Just the ones installed in the wall of the main cavern (powerhouse cavern) are triple and of larger length (EF1 and EF5). The convergence targets were installed in several sections (5

to 7 each section). The three-dimensional convergence measurement readings were carried out through an optical system based on the total station technology. Six load cells were also installed for the anchors. Figure 7.9 shows the evolution of the measured displacements in extensometers EF5 and EF11 (or extensometers 1 and 5). The observed values in extensometers EF3 and EF4 showed to be unreliable. Therefore, they were discharged for the subsequent analysis.

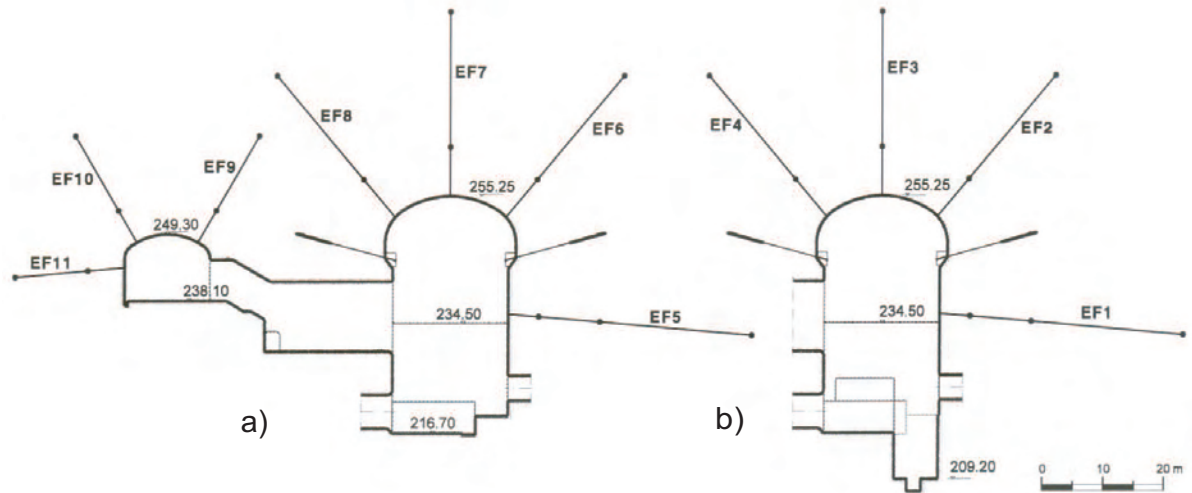


Figure 7.8: Cross-sections of the monitoring plan.

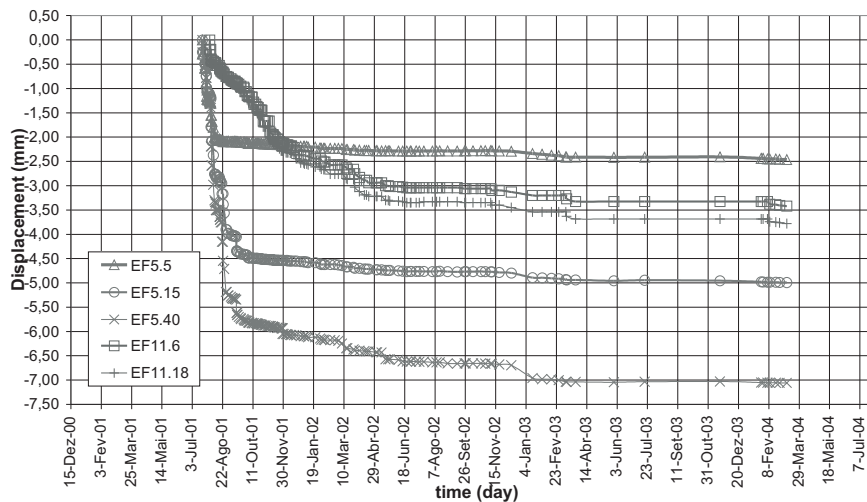


Figure 7.9: Displacements evolution measured by extensometers EF5 and EF11.

For the numerical models developed in this work, the geomechanical parameters were obtained using the Knowledge Based System GEOPAT (Miranda, 2003). It uses well organized and structured knowledge from experts together with AI techniques for decision support in the geomechanical parameters evaluation and has been used with success in different applications. The system is interactive and was implemented using three platforms - Visual Basic, Excel and the object oriented programming software KAPPA-PC (Intellicorp, 1997).

In the case of rock masses, RMR, Q and GSI empirical systems are applied. The system proceeds to the evaluation of strength and deformability parameters, using accumulated knowledge acquired in Metro do Porto and causal nets established for this purpose. In highly heterogeneous rock formations, the KBS system adopts a probabilistic methodology to obtain a distribution of GSI that allows the calculation of mean and characteristic strength and deformability values.

Using the gathered geological-geotechnical information together with GEOPAT, the following geomechanical parameters were obtained:  $E = 45\text{GPa}$ ,  $\phi' = 54^\circ$  and  $c' = 4\text{MPa}$ . A value of 0.2 is adopted for the Poisson ratio and a non-associated flow rule with the dilatancy angle taken equal to  $0^\circ$ .

## 7.4 Numerical modelling

### 7.4.1 Description of the developed models

The 3D model was carried out using the finite difference software FLAC3D (Itasca, 2005) to simulate the complex geometry of the powerhouse complex and its construction sequence. The mesh was developed with the hexahedral-Meshing Pre-processor 3DShop and it is composed by 43930 zones, 46715 grid-points and 1100 structural elements (Figure 7.10). Since the field stress around the caverns was constant it was possible to simplify the mesh in order to increase the computation efficiency. This way, instead of the real 350 m depth of the cavern axis, only 200 m were modelled.

The cross-section analysed through the 2D numerical model, developed using *Phases*<sup>2</sup> (www.roscience.com) software, was section a) referred in Figure 7.8. When comparisons between the two models are performed they are always referred to the results obtained for this cross-section where reliable monitoring values were available.

The sprayed concrete was simulated by shell elements with a linear elastic and isotropic constitutive model, with a Young modulus of 15 GPa and a Poisson ratio of 0.2. The rockbolts were simulated by cable elements, which can yield tensile strength, with two nodes and one axial degree of freedom. An elastic-perfectly plastic constitutive model with a Mohr-Coulomb failure criterion was assumed to represent the rock behaviour.

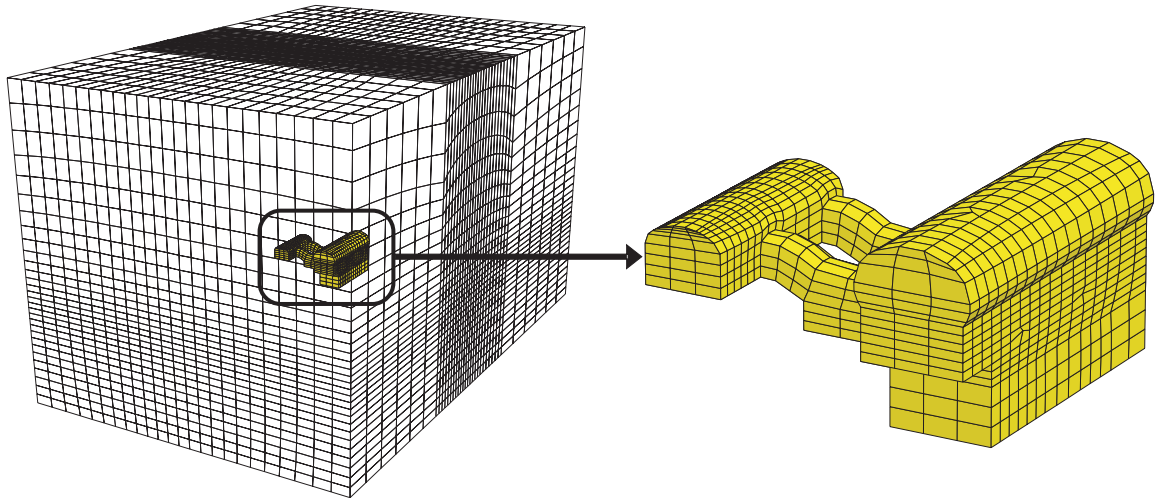


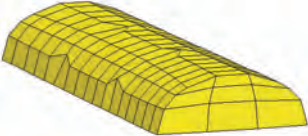
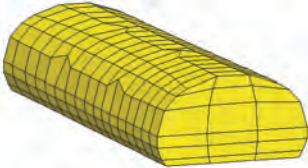
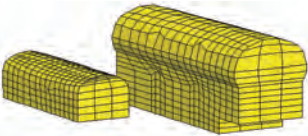
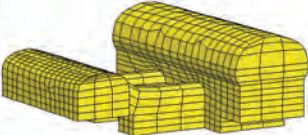
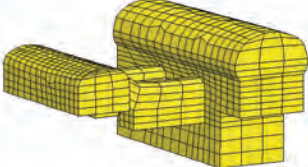
**Figure 7.10:** 3D mesh developed for the Venda Nova II powerhouse complex.

For the 3D numerical modelling, the construction sequence was simplified relatively to the one defined in design. Five excavation stages were considered and are described in Table 7.7. Due to the good geomechanical quality of the rock mass its behaviour during tunnelling was almost elastic. This way, the simplifications considered for the excavation stages had minor impact on the computed displacements.

The construction sequence adopted for the 2D model was very similar. The only difference was the way the two interconnecting galleries were simulated. Three different approaches were carried out in a preliminary analysis: i) considering the total excavation of the galleries; ii) non considering the effect of the galleries excavation due to their small influence in the global behaviour of the structure; iii) replacing the material in the area of the galleries with other material with equivalent lower geomechanical properties. The first approach led to unrealistic results with multiple shearing zones and high displacement levels which were not observed in the field. Since the model was developed considering plain strain conditions this assumption was too unfavourable. The remaining two approaches showed very similar results. The differences were insignificant, therefore, it was chosen not to consider the effect of the interconnecting galleries excavation in the following analysis.

Due to the high depth of the underground complex, a constant stress field was considered and its magnitude was set based on the results of the *in situ*. The vertical stress was computed considering the overburden dead load of the rock mass. The same stress value was considered in the horizontal direction parallel to the cavern axis. In the perpendicular direction the performed tests pointed out for a  $K_0$  coefficient between 2 and 3. Some preliminary calculations allowed to conclude that lower values of this coefficient led to more realistic results. Therefore, in the following analysis, an initial value of 2 was adopted.

**Table 7.7:** Adopted construction stages for the 3D numerical model.

Stage	Model	Description
1		Excavation of the upper part of the main cavern arch. Application of 25 cm of fiber sprayed concrete on the arch and 6 m length and 25 mm diameter rockbolts in a 2x2 m mesh.
2		Excavation of the remaining part of the arch
3		Excavation of the main cavern until the base level of the interconnecting galleries and the transforming units caverns. Application of 25 cm of fiber sprayed concrete on the arch of the second cavern and 6 m length and 25 mm diameter rockbolts in a 2x2 m mesh.
4		Excavation of the two interconnecting galleries and application of 25 cm of fiber sprayed concrete in the roof.
5		Completion of the main cavern excavation.

### 7.4.2 Analysis of the results

In this section, the results of the models are analysed and compared particularly for the last excavation stage. Emphasis will be given to the results in terms of displacements since they can be compared with the real behaviour of the structure observed by the extensometers, allowing the validation of the developed models.

Due to the high  $K_0$  and the span of the main cavern vertical wall, the higher displacements were expected to take place in that area. Figure 7.11 presents the displacement contours computed with the 3D model for the last excavation stage. In fact, the highest displacements are observed in the wall of the main cavern, particularly, between the two interconnecting galleries.

Comparing the results of the two models for the reference cross-section (Figure 7.12), the same qualitative displacement pattern can be observed. The displacement vectors show that the displacements are sub-horizontal near the walls of the main cavern due to the strong influence of the high horizontal stress in that direction.



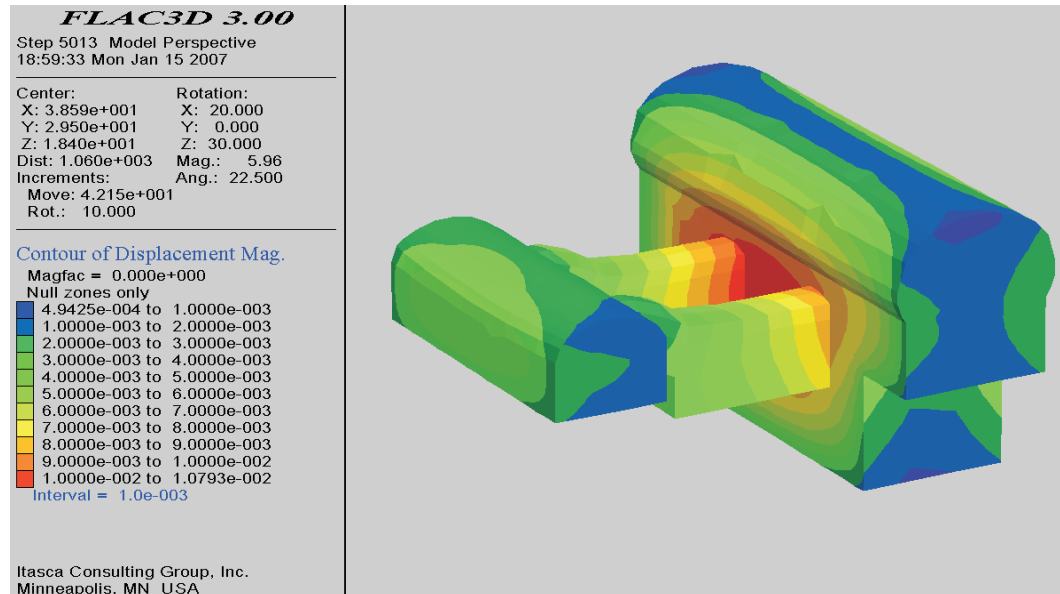


**Figure 7.11:** Displacement contours for the 3D model in the last excavation stage.

For a more thorough analysis, Figure 7.13 shows the computed displacements along lines coinciding with extensometers 5 and 7 (near the wall and arch of the main cavern, respectively). The displacements of the 2D calculation along the sub-horizontal line are much higher than for the 3D model which was expected due to the plain strain consideration. For the 3D model the maximum displacement along this line is, approximately, 10 mm while for the 2D model this value is almost 50% higher. The displacements near the arch of the main cavern are small for both models. In this zone, the gravity loads, which would cause a downward movement, are almost compensated with the high horizontal stress which pushes the arch upwards causing a near-zero displacement.

Due to the good overall quality of the rock mass the displacements magnitude is small. The maximum computed displacements in the rock mass are 15 cm for the 2D model and 10.5 cm for the 3D case. Moreover, there are a small number of yielded zones which are confined to small areas near the arch and wall of the main cavern.

Figure 7.14 compares the results of the models with the measures of extensometers 5 to 11 for the last excavation stage. The results of the 2D and 3D models are very similar for most of the extensometers. Also, the computed values follow the same qualitative trend as the observed ones. The worst results are observed for the inclined extensometers (2, 6 and 8) where the displacement values are clearly overestimated. In the remaining cases the 3D model is more accurate for the measurements of extensometers 5, 7 and 9 while the 2D model slightly outperforms the 3D model for extensometers 10 and 11. In a qualitative perspective it can be concluded that, excepting for extensometers 2, 6 and 8, the results of the models are very

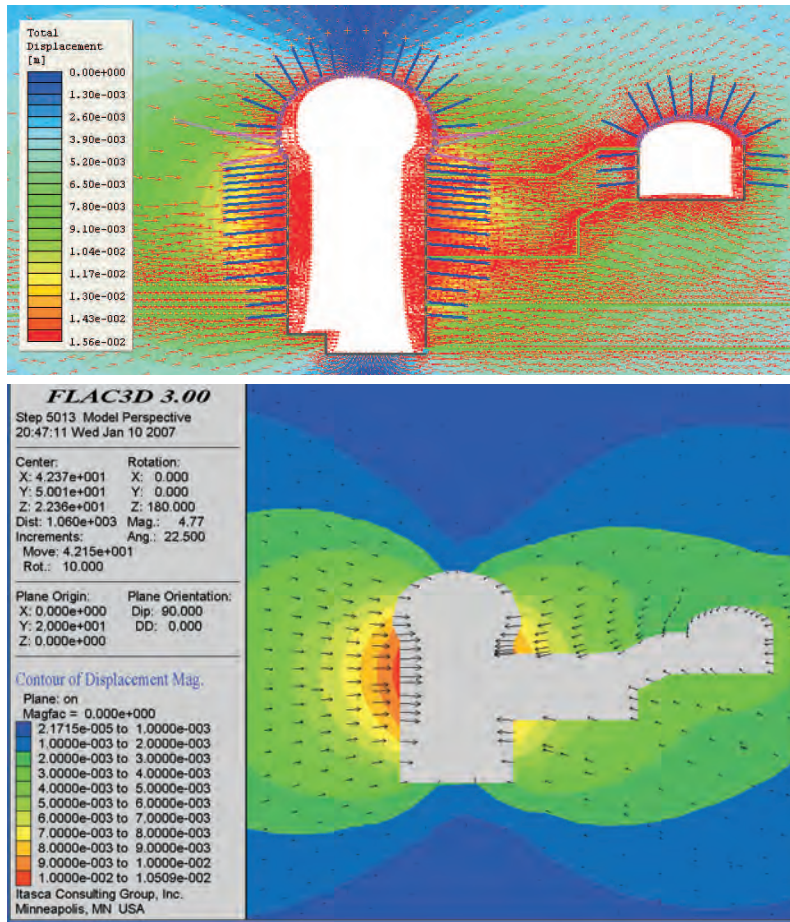


Figure 7.12: Displacement contours and vectors for the 2D (upper image) and 3D models

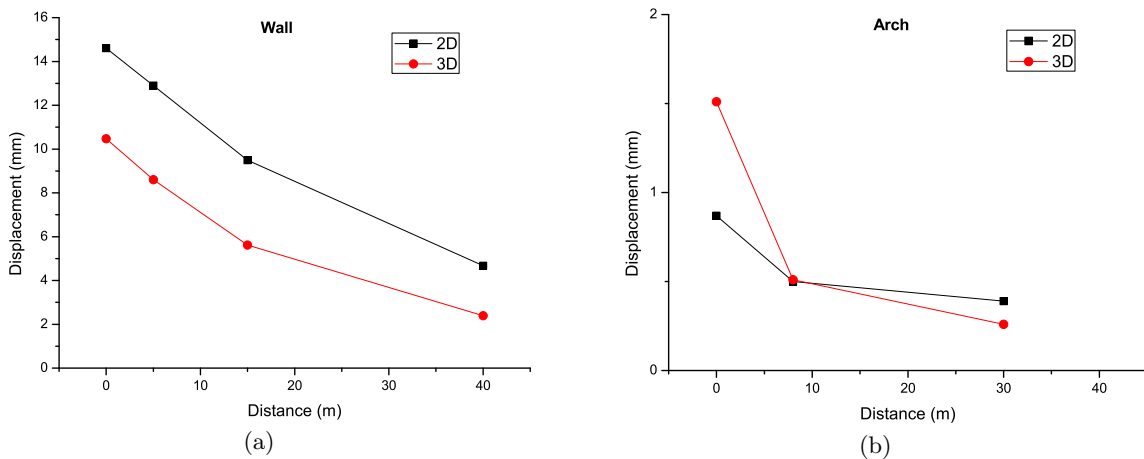


Figure 7.13: Computed displacements near (a) the wall and (b) arch of the main cavern.

acceptable.

For a more thorough insight of the results, some statistical analysis was carried out considering two different situations: a) comparison between the results of both models with the

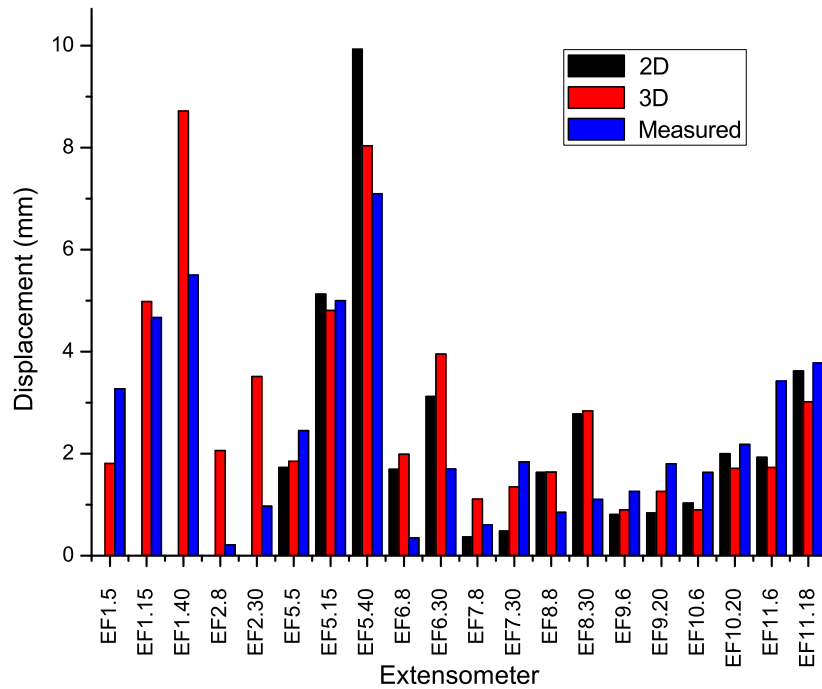


Figure 7.14: Comparison between computed and measured displacements in the last excavation stage.

measurements in the reference cross-section (extensometers EF5 to EF11) and b) comparison between the 3D model results with all considered measures (EF1 to EF11 excepting EF3 and EF4). Table 7.8 presents the mean values of the displacements and mean absolute error (MAD) for both situations.

Table 7.8: Mean displacements and errors for situation a) and b).

	Situation a)			Situation b)	
	2D	3D	Measured	3D	Measured
Mean disp. (mm)	2.47	2.47	2.34	2.91	2.48
MAD* (mm)	-0.135	-0.136	-	-0.425	-

$$MAD^* = \sum_{i=1}^n (computed\ disp. - observed\ disp.)$$

It can be observed that, in mean terms, the results of the 2D and the 3D models are very similar for the reference cross-section showing the same mean displacement and very similar MAD values. The T-test was performed in order to compare the mean displacements of each calculation with the correspondent real values. It was concluded that, for every situation, the mean computed displacements can be considered statistically similar to the mean of the real displacements for a 95% significance level. This conclusion corroborates the previous qualitative idea of a good fit between the results of the models and the real behaviour of the underground

structure. Moreover, the Smirnov test, performed between the computed and observed values, validated for both situations the null hypothesis that these values follow the same statistical distribution.

In order to have a better insight of this fit in each point, Figure 7.15 presents a plot of real versus computed displacements for the 2D model in the reference cross-section and for the 3D model for all the considered extensometers. The values present a reasonable distribution around de 45° slope line with no visible trend also pointing out for a good overall fit of the models to the observed data.

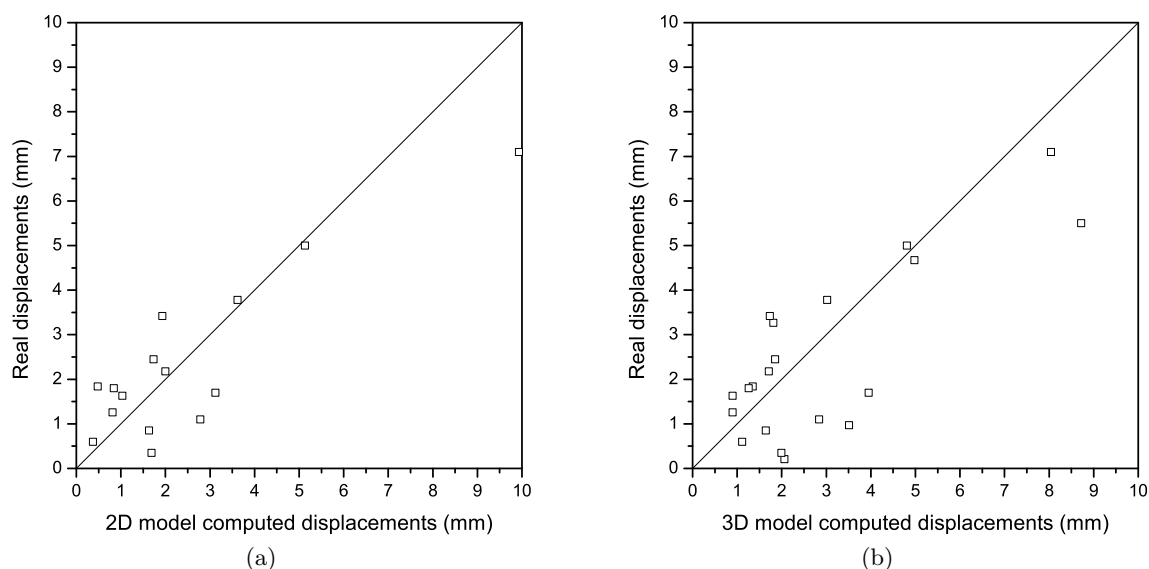


**Figure 7.15:** Computed versus real displacements for (a) the 2D and (b) 3D models.

Figure 7.16 shows the histograms of the errors for the 2D model in the reference section and for the global results of the 3D model. The normal distribution curve as well as some statistical measures are also presented. The histograms represent sets of 15 and 20 error values for the 2D and the 3D model, respectively. The Shapiro-Wilk normality test was performed to the errors of each model and it was concluded that they follow a normal distribution for a 95% significance level suggesting a good distribution of the errors. This fact, in conjunction with the low values of the mean error, point out for the good quality of the results.

In terms of stresses, the rock mass surrounding the caverns is mainly under compression. The maximum compression stress, about 35 MPa, is observed in the upper zone of the main cavern arch (Figure 7.17). Tension stresses only happen near the main cavern wall due to its span and *in situ* state of stress. However, the maximum tension stresses are below 1 MPa. Considering the strength properties of the rock mass it is expected that only a few plastic zones

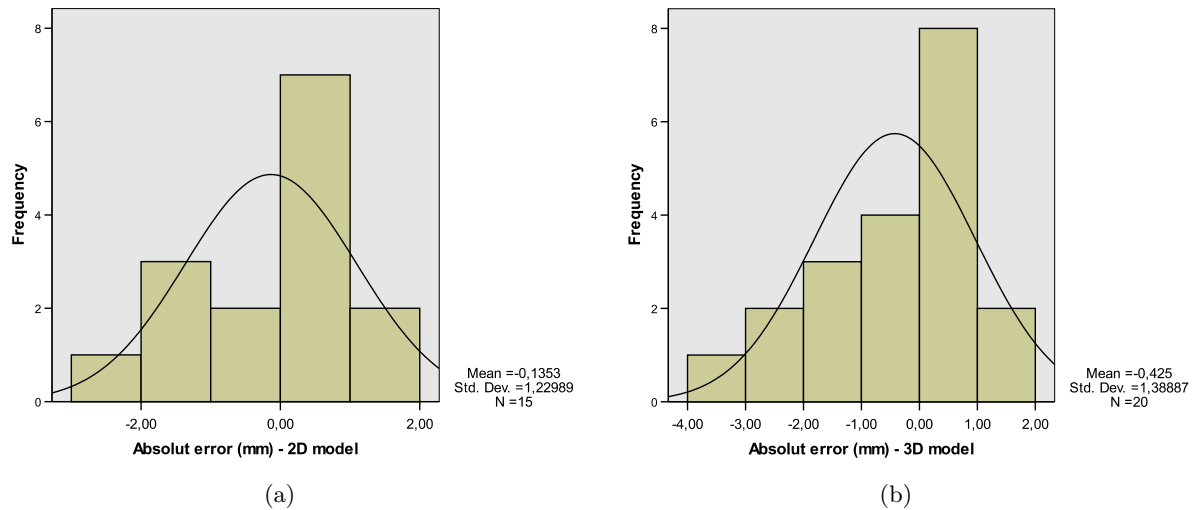


**Figure 7.16:** Absolute error histograms for (a) the 2D and (b) 3D models.

occur and the rock mass behaves almost in elasticity. Figure 7.18 shows the zones in plasticity and, in fact, only a few sheared zones can be observed in the surroundings of the underground structure. This almost elastic behaviour of the structure and surrounding rock mass mean that the adopted construction sequence in the models has a low impact on the final results and that the most important parameters for the structure behaviour prediction are  $E$  and  $K_0$ .

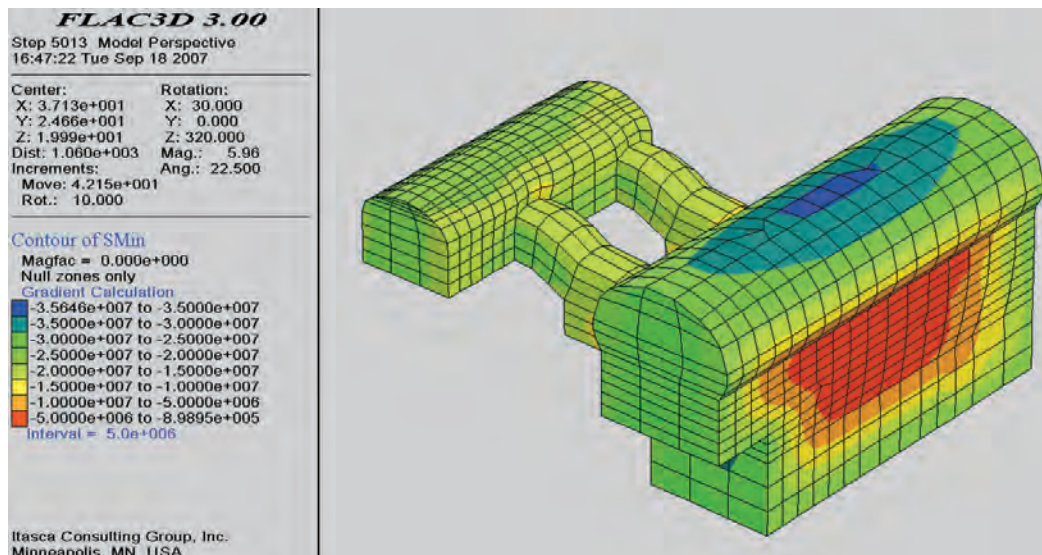


**Figure 7.17:** Computed minimum stresses (negative values translate compression).

The maximum computed shear strains were also low with values ranging from 0.02% and 0.1% for the 2D model and 0.015% and 0.04% for the 3D model. Once more, lower values were

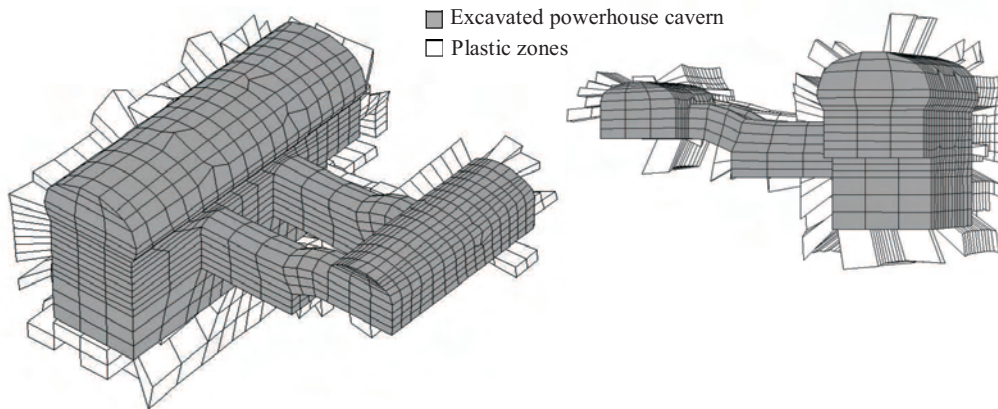


*Figure 7.18:* Plastic zones at the last excavation stage.

obtained for the 3D model. These values are within the expected range considering the quality of the rock mass and the construction method.

Figure 7.19 presents the maximum and minimum principal stresses in the sprayed concrete for the last excavation stage. It can be observed, and in agreement with a previous statement, that the most compressed zone is located near the arch of the main cavern, mainly between the interconnecting galleries. In this area, the computed compression stresses range between 4 MPa and 5 MPa. These values are still far from the limit compression strength of a current sprayed concrete so crushing of the material is not expected to happen. The computed tension stresses are generally low ( $<2$  MPa). However, in the beginnings of the main cavern arch, tension stresses can reach values up to 11 MPa. This is caused by a stress concentration effect in this area and may cause cracking to the concrete. Therefore, it may be necessary to reinforce it in order to avoid this to happen.

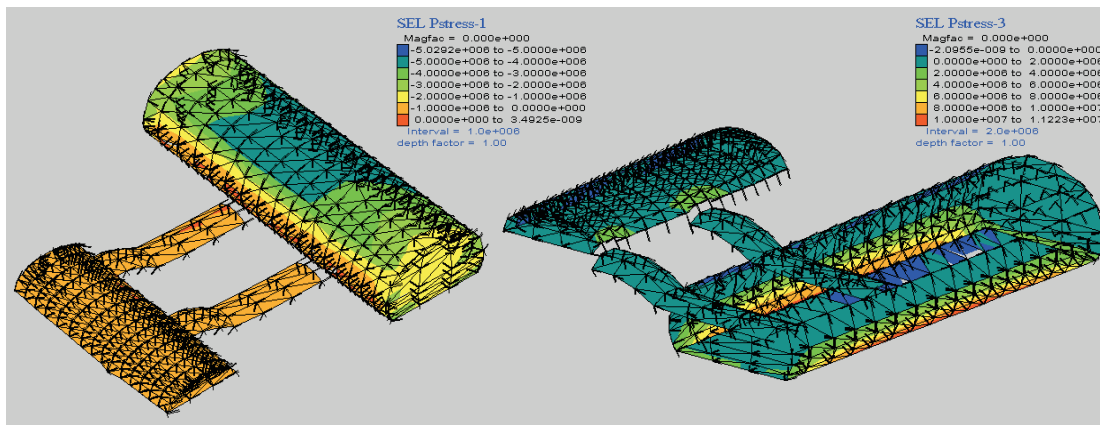


*Figure 7.19:* Stresses in the fiber sprayed concrete.



For the 3D model a calculation of the factor of safety was carried out. FLAC3D uses the method defined by Dawson (1999) in which the strength parameters are consecutively reduced until significant plastic flow appears in some zone of the structure. This way, the computed factor of safety was 4.63 which can be considered satisfactory in terms of security level. Figure 7.20 shows an image of the last non-equilibrium state produced by the methodology of strength reduction applied to calculate the factor of safety. The shear strain contours allow the visualisation of the expected failure mode.

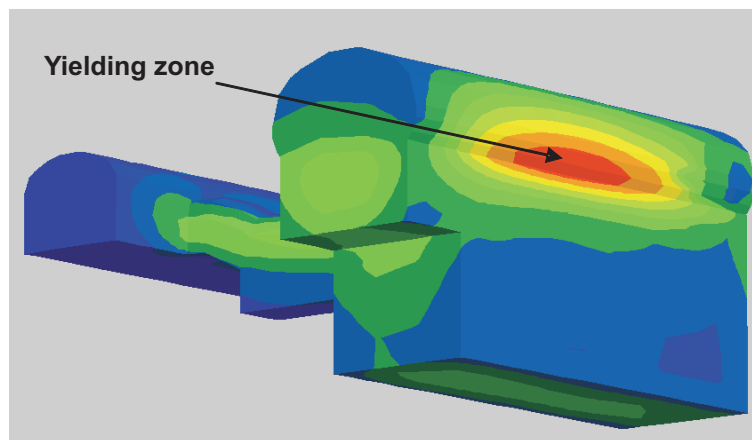


*Figure 7.20:* 3D visualisation of the shear strain contours for the last non-equilibrium state.

Plastic flow appears in the connection zone between the vertical wall and the beginning of the arch which is, as already referred, an area of stress concentration. This fact can be corroborated by the observation of Figure 7.21 where a cutting plane through one of the interconnecting galleries shows the shear strain contours and velocity vectors. It can be seen that potential instability zones are located near the connections between the vertical walls and the arch of the main cavern mainly near the high span vertical wall opposite to the interconnecting galleries.

Annex III is referred for more details about displacements countours and vectors and principal stresses for two different cross-sections.

## 7.5 Back analysis of geomechanical parameters

### 7.5.1 Used optimisation techniques

As it was concluded by the structural analysis of the models, the parameters with more influence on the behaviour of the powerhouse complex are  $E$  and  $K_0$ . In this section, different techniques are applied in order to back analyse these parameters based on the monitored displacements

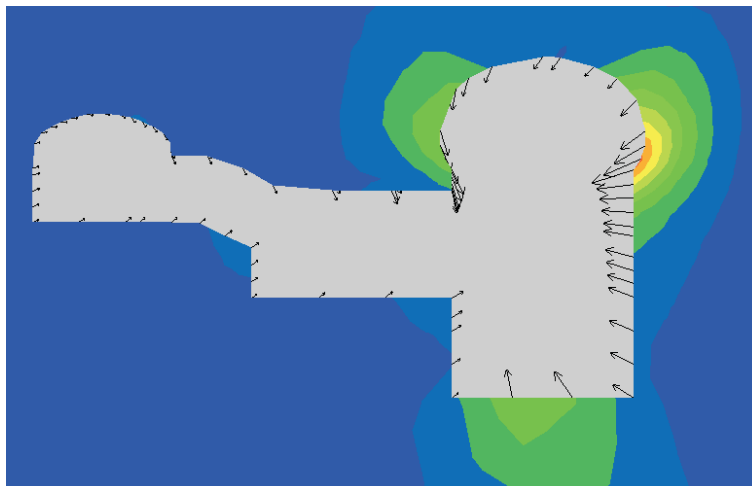


**Figure 7.21:** 2D visualisation of the shear strain contours and velocity vectors.

by the extensometers during the construction of the caverns.

The performed back analysis calculations were carried out in different stages. The first calculations, which were used as a preliminary approach, were performed only for the reference cross-section and using the 2D model. In this case, a least square error function was used together with the steepest descent and conjugate gradient algorithms.

In a more advanced phase, two more optimisation algorithms, a deterministic and a probabilistic, were applied together with the developed 3D model. These algorithms were coupled with FLAC3D in order to perform the identification process in a more efficient way. The algorithms are compared in terms of efficiency and robustness.

The deterministic method was the one provided by the software SiDolo (SiDolo, 2005). This software was created at the *Ecole Normale Supérieure* and, nowadays, is being developed by the laboratory of mechanical and materials engineering of the Bretagne-Sud University in France. It uses an hybrid algorithm that combines two traditional optimisation techniques, namely, a gradient based algorithm and a variant of the Levenberg-Marquardt method to accelerate convergence when the process is close to the solution (Eclaircy-Caudron *et al.*, 2006).

The error function ( $L(A)$ ) used by SiDolo is translated by equation 7.1:

$$L(A) = \sum_{n=1}^N \frac{1}{M_n} \sum_{i=1}^{M_n} [Z_s(A, t_i) - Z_s^*(t_i)] \cdot D_n \cdot [Z_s(A, t_i) - Z_s^*(t_i)] \quad (7.1)$$

where  $A$  represent the model parameters,  $N$  is the number of experimental results,  $[Z_s(A, t_i) - Z_s^*(t_i)]$  is the difference between numerical and experimental results of the  $M_n$  observation at timestep  $t_i$  and  $D_n$  is the weighting matrix of the  $n^{th}$  test.  $D_n$  is a diagonal matrix and its coefficient translate the uncertainties/accuracy of the observed measurements. In practice,



these coefficients correspond, normally, to the square of the inverse measurement error or of its estimation. In this study, these errors were assumed to be equal for all measurements which reduced equation 7.1 to a least square error function.

In the SiDolo software, the process is stopped if one of two conditions is verified: a maximum pre-defined number of iterations is reached or when the relative difference between the error function value obtained at a certain step and the best one obtained during the process is lower than a defined threshold. In this study, a rate of  $10^{-15}$  was adopted which is the default value.

The other used optimisation algorithm was the  $(\mu/\rho + \lambda)$  evolution strategy (ES) presented in the previous Chapter. For comparison sake, the same error function used by SiDolo was considered together with this algorithm. For the stopping criteria, the error values  $\epsilon_1$  and  $\epsilon_2$  were initially considered equal to  $10^{-5}$ . In a more advanced stage, a value of  $10^{-7}$  was also tested in order to analyse the influence of this parameter in the obtained results and in the algorithm efficiency.

### 7.5.2 Validation studies

In order to determine the possibility to identify E and  $K_0$  using the described techniques together with the displacements observed in the extensometers, validation studies were carried out before the optimisation process.

An experimental response of the 24 displacements measured by the extensometers was artificially created using the 3D model and the set of geomechanical parameters initially defined for the structural analysis. Then, the strength parameters, as well as the Poisson coefficient, were fixed while E and  $K_0$  (perpendicular to the caverns axis) were supposed unknown. Both methods need a definition of boundary values for the parameters to identify. This way, the interval values were set between 1 GPa and 100 GPa for E and between 0.5 and 2.5 for  $K_0$ . Moreover, as SiDolo is based on traditional optimisation algorithms, it also needs an initial approximation to the parameters. In this context, values of 60 GPa (+44.4% deviation) and 1.0 (-50% deviation) were adopted for E and  $K_0$ , respectively.

Two identification processes were carried out using SiDolo. In a first approach, just the displacements obtained after the first excavation stage were considered. Afterwards, the displacements measured at every stage were used in the process. The idea of testing these extreme approaches was to investigate the influence of the construction sequence in the identified parameters. If the results did not show significant differences, it meant that indeed the rock mass behaves almost elastically and a more simple model, for instance, considering only the displacements after one construction stage, could be used in the identification process enhancing its efficiency. With the ES algorithm only the first of the described calculations was carried out.

Table 7.9 resumes the obtained results.

**Table 7.9:** Results of the validation studies.

Case	E (GPa)	$K_0$	Error value	Iterations
SiDolo (1 phase)	45.0	2.0	$8.9 \times 10^{-13}$	25
SiDolo (all phases)	45.0	2.0	$1.0 \times 10^{-8}$	50
ES (1 phase)	43.3	1.9	$1.3 \times 10^{-7}$	10 (1 gen.)

It is possible to observe that SiDolo allows obtaining the correct parameter values in both situations. The main difference is the efficiency of each calculation. When the displacements of all excavation phases are considered, the iteration number, and consequently the computation time, is much higher than in the case where the results of a single stage are used. It is once again proved that the rock mass behaviour during the caverns excavation is nearly elastic and the construction sequence has minor impact on the identification process.

The ES algorithm, which used the measurements of only one stage also, reached convergence within a single generation of solutions, i.e. in ten iterations. The identified parameters are close to the correct ones with an error of approximately 4% which is due to the relatively high values adopted for  $\epsilon_1$  and  $\epsilon_2$  ( $10^{-5}$ ). A more restrict stopping criteria would enhance the quality of the results but increase the computation time. Nevertheless, it was concluded that, also with this technique, it would be possible to proceed to the back analysis of the interested parameters considering only the measurements made after one excavation stage.

Figure 7.22 presents the error function topology for the referred case. It is possible to observe that, in spite of being somewhat irregular, the error function presents a clear and singular minimum. This characteristic enables the parameters identification using both algorithms without convergence problems.

This way, it was decided that in the proceeding back analysis calculations, only the displacements observed after the last excavation stage would be used. This option lead to a very important decrease of the identification process computation time with almost insignificant precision loss, in comparison to the option of using the data of all construction stages. The decision of using the results of the last excavation stage (instead of using, for instance, the results of the first stage that would also reduce the computation time) is related with the difficulty of precisely define the time limits between the construction stages and the correspondent displacements after each one of them. In this context, the definition of results after the last stage appears as much more clear and could result in more accurate results of the back analysis process.

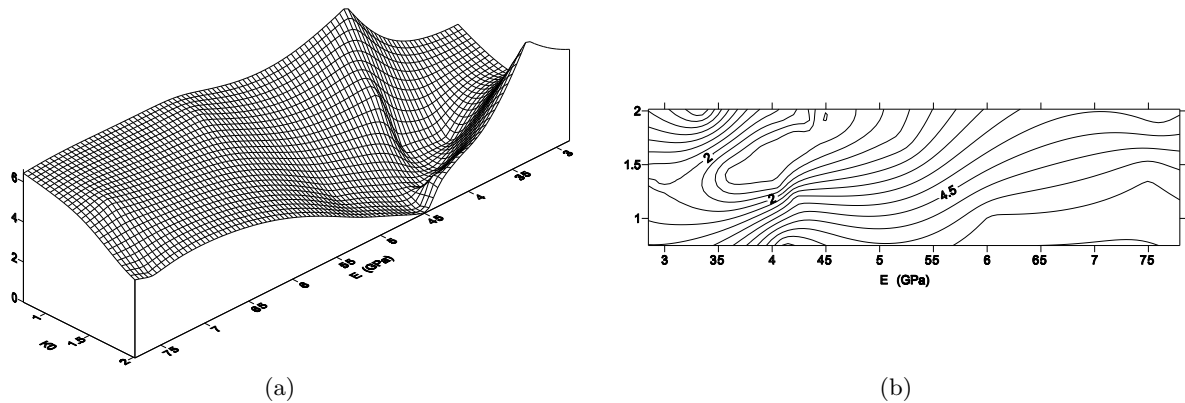


**Figure 7.22:** Topology of the error function on the identification of  $E$  and  $K_0$  for the validation study using only the displacements measured after the first stage. (a) 3D view (b) Plan view.

### 7.5.3 Results

The first preliminary calculations were performed using the previously presented 2D model. Together with a least square error function, the steepest descent and the conjugate gradient algorithms were used in the minimisation process. The gradient of the error function in relation to the parameters was computed using the finite differences method.

Since the computational time of the model was relatively low, several runs were carried out considering all the available measurements on the reference cross-section and different combinations of a limited number of measures. These preliminary calculations constituted a first approach to the problem highlighting possible problems on the identification process and establishing a possible variation range for the interested parameters.

Due to the 2D model plain strain consideration, the computed strains and stresses were higher in this case than for the 3D model. The number of yielded zones were consequently higher and its behaviour aparted, in some way, from the elastic. In the previous chapter, it was concluded that measurement based back analysis using plastic models with yielding and traditional algorithms could lead to the identification of parameters which correspond to local minima near the initial guesses of the parameters. This was normally achieved in a reduced number of iterations. The results obtained from the preliminary calculations resemble this situation.

In fact, the results of the several performed calculations pointed out to parameter values not far from the initial guesses. The values of  $E$  ranged from 40 GPa to 45 GPa while  $K_0$  ranged from 1.90 to 2.45. These values were normally reached in a reduced iterations number. Probably they correspond to local minima. Also, some problems related with the process convergence were identified. The back analysis was "ill-posed" for some measurement combinations which did not allow convergence to be obtained. These results underline once more the problems with

the applicability of traditional algorithms on the identification of geomechanical parameters in underground works.

Concerning the back analysis using the 3D model, as already referred, two different methodologies were used. A back analysis software called SiDolo based on traditional algorithms and an ES were coupled with the model to perform the identification process. The interval range adopted for the parameters was the same used for the validation studies. They seem sufficiently large to contain the optimal solution and to correctly test the algorithms in this real application.

In the calculations performed using SiDolo, the initial approximation for the parameters were the values given by GEOPAT, i.e. 45 GPa for E and 2.0 for  $K_0$ . In the first identification attempt the 20 measurements were considered and convergence was reached. In order to evaluate the process stability and consistency on the results it was decided to perform another calculation in different conditions. These conditions could be defined in a variety of ways and it was necessary to establish a criterion. It was verified that the difference between the computed and observed measurements was always of the same sign before and after optimisation excluding for the values of EF1.15 and EF5.40. This way, a second process was carried out considering as a starting point the optimised values of the first calculation and without the cited measurements. Table 7.10 presents the results of the two identification attempts using SiDolo and compares them with the results obtained with the initial guess provided by GEOPAT.

**Table 7.10:** Results of the identification processes using SiDolo.

Case	E (GPa)	$K_0$	Error value $\times 10^{-6}$	Mean disp. (mm)*	Iterations
Initial values	45.0	2.0	1.76	2.91	-
Results (1)	55.0	1.98	1.26	2.36	25
Initial values	45.0	2.0	1.90	2.51	-
Results (2)	56.7	1.90	1.34	1.93	12

\* - the mean measured displacements are 2.48 mm and 2.11 mm for the first and second calculations, respectively.

Concerning the first identification attempt, convergence is attained in a total of 25 iterations. The optimised set of parameters is not significantly different to the initial guesses specially in what concerns  $K_0$ . The optimised value of E is 22% higher than the initial one. The error function value underwent a 29% decrease and the mean displacement differs only 0.12 mm from the measured values.

Figure 7.23 presents a comparison between the measured displacements with the ones computed with the initial and optimised set of parameters. It is interesting to notice that the results obtained with the optimised parameters only outperforms the fit of the initial calculations in

nine out of twenty measures. However, the errors plot show a more smooth distribution of the errors in the different extensometers for the optimised parameters calculation.

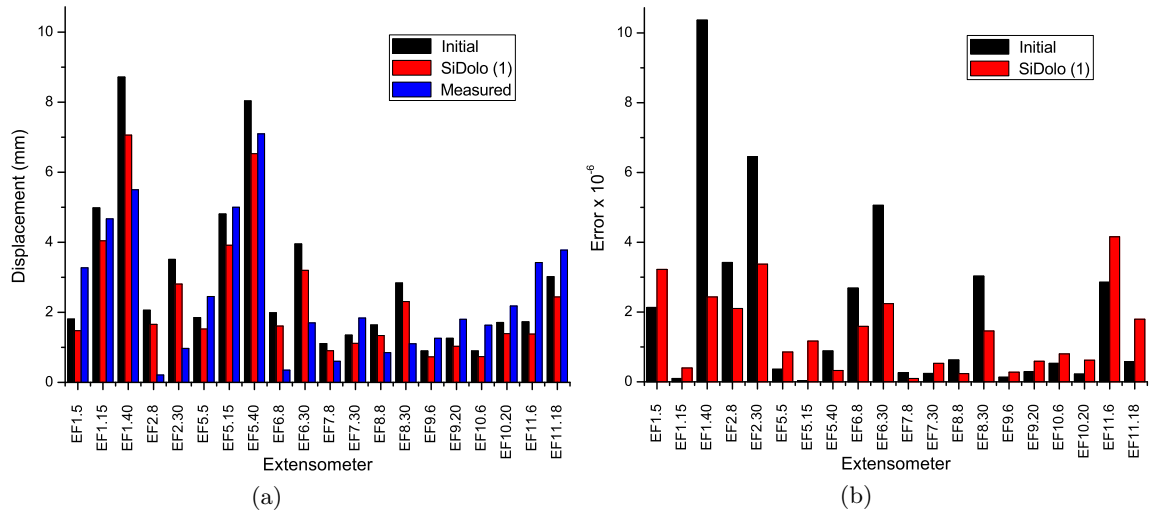


**Figure 7.23:** Comparison between the observed measurements and the computed values with the initial and optimised set of parameters obtained by SiDolo in the first identification attempt. (a) Absolute values (b) Error values.

For the second attempt, additional 12 iterations were necessary to achieve convergence. In spite a higher variation in relation to the initial values given by GEOPAT, the final obtained set of parameters is close to the first attempt. The error function value was reduced in a similar percentage as in the previous calculation. The mean value of the displacement is only 0.18 mm less than the observed values. The results of this calculation point out to a more rigid rock mass and less important horizontal loads translated by the lower value of  $K_0$  in relation to the first calculation. Figure 7.24 presents the fit of the this second identification attempt. The same trend is observed as in the previous scenario. Even though a higher number of initial better fits, the errors for the optimised parameters are more uniform in the considered extensometers.

The initial conditions for the two identification attempts were not considerably different and significant variations in the results were not expected. However, the back analysis process showed to be stable. The second attempt, which considered only 18 measurements instead of the initial 20, presents an absolute error function value (initial and after optimisation) higher than in the first identification process. It means that an overall poorer fit was obtained in this calculation. This way, in the identifications carried out with the ES, only 18 displacement measurements were considered in order to check, under different circumstances, if the obtained results could be improved.

A total of three back analysis processes were performed using the ES algorithm. In the

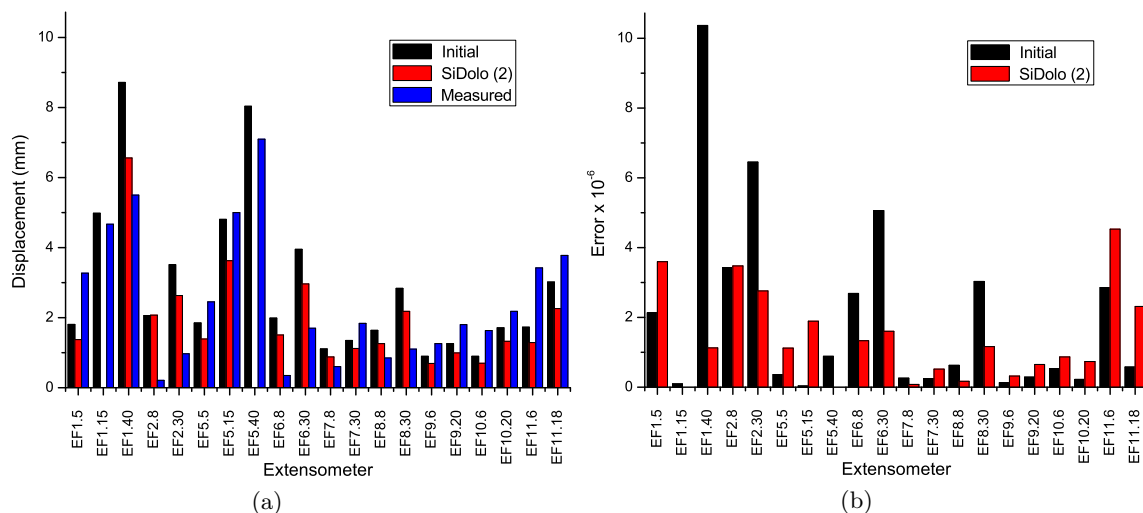


**Figure 7.24:** Comparison between the observed measurements and the computed values with the initial and optimised set of parameters obtained by SiDolo in the second identification attempt. (a) Absolute values (b) Error values.

first identification attempt, a value of  $10^{-5}$  was considered for  $\epsilon_1$  and  $\epsilon_2$ . To evaluate the influence of the stopping criteria, a second process was carried out using a value of  $10^{-7}$  for these parameters. Finally, in the third attempt, an elastic constitutive model was adopted for the rock mass. Table 7.11 resumes the obtained results of these calculations.

**Table 7.11:** Results of the identification processes using the ES algorithm.

Case	E (GPa)	$K_0$	Error value $\times 10^{-6}$	Mean disp. (mm)*	Generations
Initial values	45.0	2.0	1.90	2.51	-
ES ( $10^{-5}$ )	52.1	1.72	1.37	1.91	1
ES ( $10^{-7}$ )	58.0	1.98	1.34	1.97	6
ES ( $10^{-7}$ ) elastic	58.5	2.02	1.36	1.91	7

\* - the mean measured displacement is 2.11 mm.

In the first calculation, and due to the relatively high value for the stopping criteria ( $10^{-5}$ ), convergence was reached in only one generation (10 iterations). The probabilistically created group of solutions by the algorithm allowed to obtain results which reduced the error function value. The optimised set of parameters varied the same relative magnitude in relation to the initial values. In particular, the optimised value of E is 14% higher and  $K_0$  14% lower.

The adoption of a more restrict stopping criteria ( $10^{-7}$ ), allowed to improve the results in relation to the observed measurements. With this new set of optimised parameters, every evaluation criteria was improved. In fact, the value of the error function was decreased and the

mean displacement is closer to the observed value. This improvement was obviously translated with an increased computational effort. In this case, 6 generations (60 iterations) were needed in order to reach convergence.

In comparison with the set of parameters obtained with SiDolo, the error function value is similar but the mean displacement is slightly closer to the observed values in the solution found by the ES. Figure 7.25 presents a comparison between the observed displacements and the ones computed with the initial and optimised set of parameters. As it should be expected, the results are similar to those reported with the set of parameters identified with SiDolo namely in relation to the more smooth distribution of errors obtained with the optimised parameters. However, in this case, the fit is improved in 9 out of 18 cases while for the previous case, that value was 8.

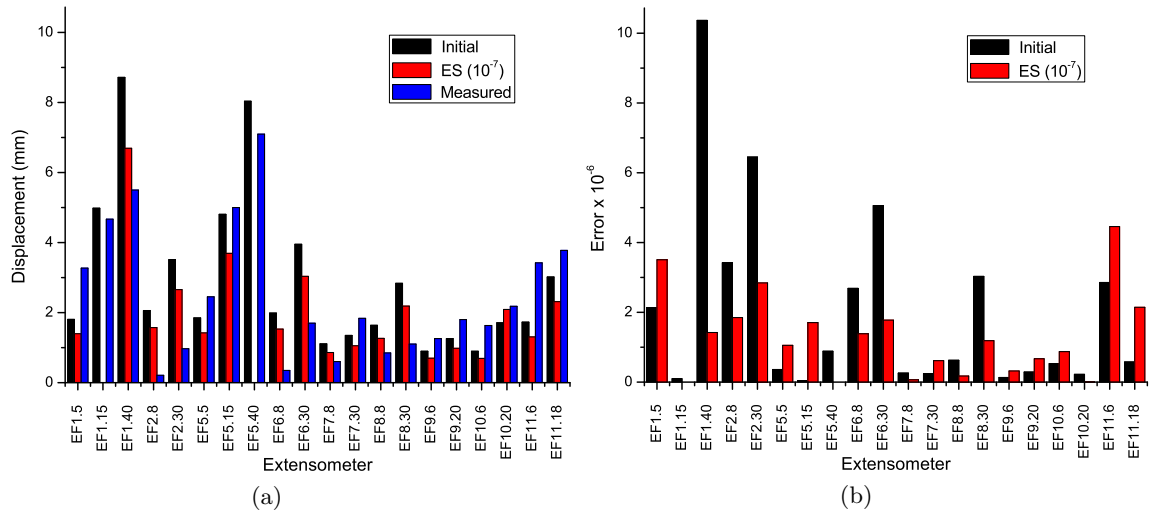


**Figure 7.25:** Comparison between the observed measurements and the computed values with the initial and optimised set of parameters obtained by the evolution strategy considering  $\epsilon_1$  and  $\epsilon_2$  equal to  $10^{-7}$ . (a) Absolute values (b) Error values.

In order to have a thorough insight of the fit, Figure 7.26 presents a comparison between the computed and measured values using the initial and the optimised set of parameters obtained by the ES. It is possible to observe that for the optimised set case, the values are more uniformly distributed around the 45° slope line translating a better fit of the model.

In conclusion, the results obtained by the set of parameters identified by the ES algorithm slightly outperforms the ones obtained by SiDolo. The reason could be one of the following: i) the traditional algorithm based software SiDolo was kept in a local minimum; ii) the stopping criteria of the ES was more restrict. In order to investigate this subject, Figure 7.27 presents the topology of the error function for this case and the location of the identified values by both

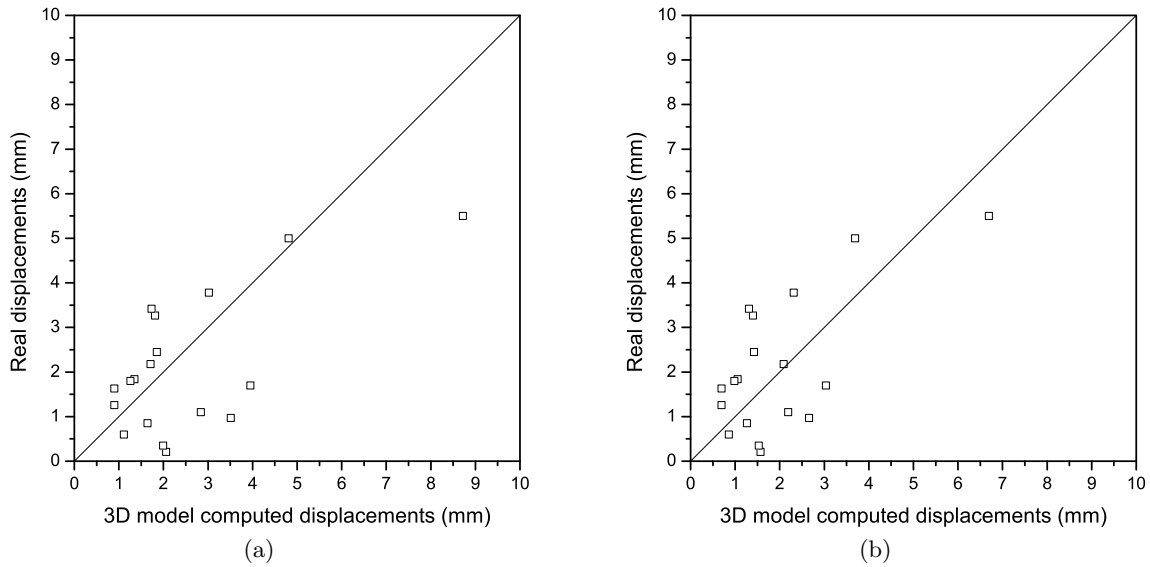


**Figure 7.26:** Comparison between the observed measurements and the values computed using a) the initial set of parameters and b) the optimised set of parameters.

methodologies. In the plan view, it is possible to observe that the solution given by SiDolo and the ES using the more restrict stopping criteria, lay near the same isoline. The remaining solution given by this algorithm corresponds to a higher value of the error function caused not by a local minimum but because of the higher allowed error value to stop the process. This way, it is possible to conclude that the correct hypothesis is the one raised in ii), i.e. the slight differences in the solutions provided by the two methodologies is related with the adopted stopping criteria.

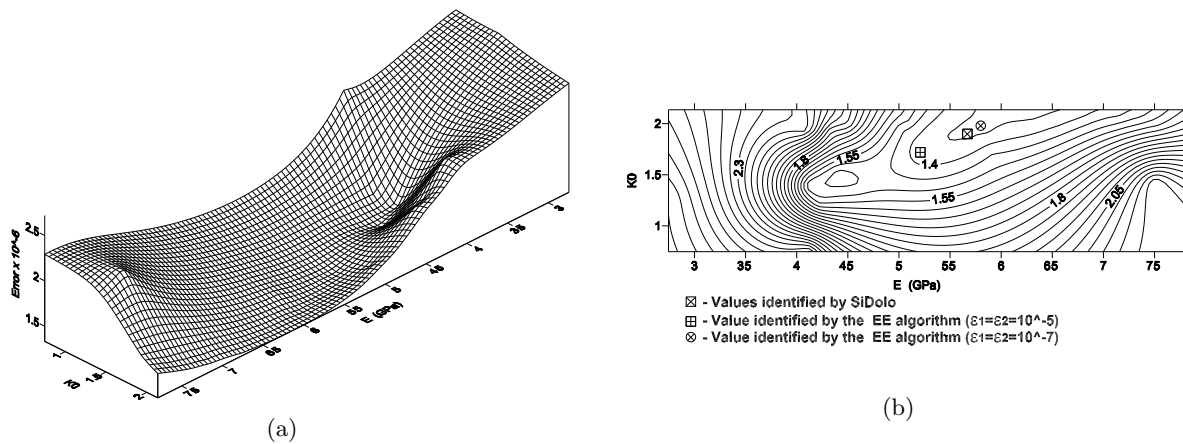


**Figure 7.27:** Topology of the error function for the plastic model of Venda Nova II powerhouse complex. (a) 3D view (b) Plan view.



However, it is also possible to observe a local minimum in the error function near the region corresponding to  $E$  and  $K_0$  values of 45 GPa and 1.5, respectively. Both methodologies were able to avoid this local minimum and converge to the global solution but probably for different reasons: the ES because of its intrinsic characteristics of global optimisation that allows it to avoid local minima as observed in the previous Chapter; SiDolo because of the characteristics of the error function topology but mostly because the initial guess for the identification with SiDolo was already close to the global optimum. These are just hypothesis that need to be tested with additional calculations. In particular, it would be interesting to perform a calculation using SiDolo with an initial approximation close to the local optimum to check for convergence problems.

The first calculation with SiDolo used a starting point close to the value where the local minimum is observed. However, since the initial conditions of the identification process were different, namely in terms of the number of considered measures, there is not enough data to assure that this particular local minimum exists in the error function correspondent to this situation.

Finally, the optimisation procedure was carried out considering an elastic model for the rock mass. The identified set of parameters is rather close to ones obtained with the plastic model. The error function value is only slightly increased. Figure 7.28 presents the plot correspondent to the error function topology. As it should be expected, its topology is very similar from the previous calculation. However, there is one particular issue that is important to mention. In this case, the local minimum is no longer observed. This conclusion points out to the fact that this is a particular characteristic of models with plasticity, meeting the observations of the previous chapter. As there is a minor number of plasticity zones only one local minimum appears in the error function. Probably, in models with a higher plasticity degree, multiple local minima may appear.

As it was stated, the back analysis process allowed to obtain sets of parameters which improved the fit between the computed and measured quantities. For instance, the set identified by the ES algorithm with the more restrict stopping criteria, provide a very good quality fit. However, it is important to discuss to what extent these results really translate the *in situ* conditions of the rock mass. Obviously, the obtained results have to be analysed considering the limitations of the used models. The main limitations and their impact on the results are briefly discussed in the following items.

- Only one value for  $E$  and  $K_0$  was considered when, in fact, their values can vary within the area interested by the caverns. This variation is dependent on the heterogeneity of the rock mass and anisotropy degree of the *in situ* stresses. The relative homogeneity of

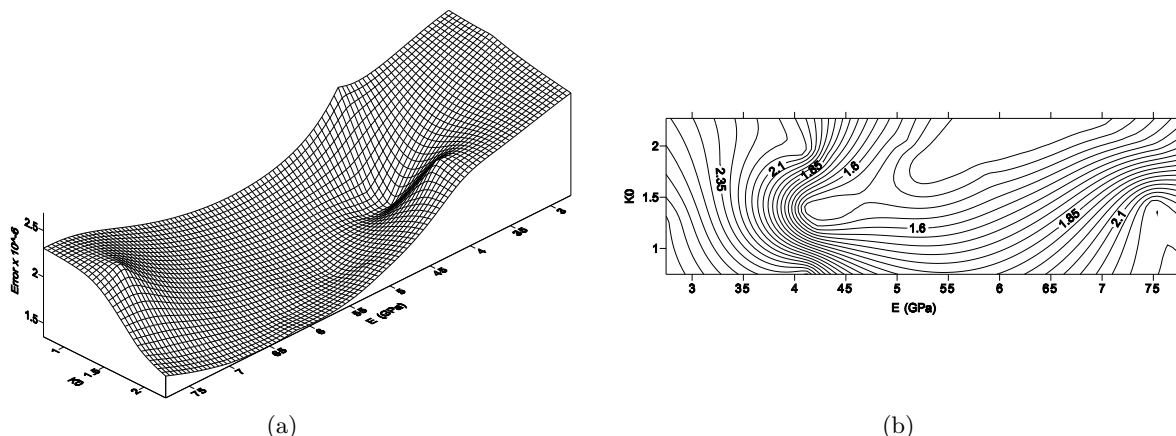


**Figure 7.28:** Topology of the error function for the elastic model of Venda Nova II powerhouse complex. (a) 3D view (b) Plan view.

the rock mass and the results of the STT tests, which resulted in approximate values of  $K_0$  in two distinct test sites, point out to the fact that this issue may not be significantly important in this case and the obtained parameters correspond to mean values with an acceptable accuracy.

- The used field measurements are the total displacements at the end of the last excavation stage. However, when the extensometers are placed, some displacement has already occurred in the rock mass which can not be measured. This way, the total real displacement is higher than the measured one and in this case the back analysis process can point out to a more rigid solution. The alternative was to use an incremental solution considering the measurements between stages as presented in LNEC (2003) for this case. This approach overcomes the previously raised problem and takes in consideration, in a consistent way, the measured displacements and the construction stages. Nevertheless, the correct definition of the time when a certain construction stage is ended and a new one starts is complicated because of the grey areas corresponding to time overlapping between the different construction stages. The definition of this border is, therefore, subjected to judgment errors or, at least, some imprecision. Probably, the best way is to use both approaches in order to validate and compare the results. In the cited study performed by LNEC this incremental back analysis solution was used together with a 2D model and the measures in three extensometers between two stages. In spite of the different approaches and the consideration, in latter case, of a significantly lower measurement number, the results are similar to the ones obtained by the ES algorithm. In particular, the same E value (58 GPa) was identified and for  $K_0$  the difference was about 15% (2.3). Then, it can be concluded that these results point out for the low importance, in this case, of the

displacements occurred in the rock mass before the extensometers placing and validate the obtained results.

- The field measurements were only referred to two cross-section in the extent of the caverns. This way, the results are more related with the rock mass in the vicinity of these cross-sections.

In order to more thoroughly validate the obtained results, some other back analysis calculations may be performed in order to cover some particular aspects: i) use the ES algorithm considering the incremental solution considering the measurements between stages; ii) input more measurements data in the back analysis process, namely convergence measures which were available as well; iii) perform the calculations considering a wider range in particular for  $K_0$  in order to search for other solutions to which correspond a lower error function value.

## 7.6 Conclusions

The Venda Nova II hydroelectric scheme, built in the North of Portugal, includes a set of very important underground structures. In this Chapter a short description of these structures was performed emphasising its main issues.

The scheme was built mainly in a granite rock mass. In order to have a better understanding of the geomechanical characteristics of the interested rock mass, an analysis of geotechnical data gathered in different surveys was carried out. A high number of *in situ* and laboratory tests were statistically analysed. The results allowed to conclude that the rock mass presents good geomechanical properties, both in terms of the intact rock and discontinuities surfaces. Moreover, the performed analysis pointed out to the fact that, in general, strength characteristics are well described by normal distributions while the lognormal presents a better fit for deformability parameters.

The powerhouse complex, composed by two caverns connected by two galleries, was described and object of the development of 2D and 3D numerical models. The different construction stages were considered and their behaviour was analysed and compared with the monitored values by extensometers placed in the caverns along two cross-sections. The geomechanical parameters used in the models were obtained through the GEOPAT system .

The results point out for an almost elastic behaviour of the rock mass due to the small displacements and shear levels induced by the caverns excavation which caused a reduced number of yielding zones. The displacements configuration is very much influenced by the high horizontal stress perpendicular to the caverns axis. This way, the maximum displacement values are observed near the high span vertical wall of the main cavern.

Even though the higher computed displacements in the 2D model due to the plain strain consideration, the fit of the results is acceptable in the developed models in both qualitative and quantitative aspects. In fact, the performed statistical analysis validate the observed good quality of the results. The small measured displacements turn the fit more difficult to obtain (due to lack of precision in the readings, simplifications of the constructions sequence and constitutive models, etc.) which could be one of the reason of a poorer fit in some extensometers.

The stresses in the support system are low and the computed factor of safety on the 3D model is 4.63 which translate an acceptable security level. The most probable failure mode taken from this calculation is plastic flow in the connection between the beginning of the arch and the vertical wall of the main cavern since its an area of stress concentration.

Using the developed models together with different back analysis techniques,  $E$  and  $K_0$  were back analysed based on the displacements measured by the extensometers. In a first stage, validation studies were performed to evaluate the possibility to identify these parameters. It was observed that, due to the almost elastic behaviour, the construction sequence had low impact on the measured response and it was decided to consider only the displacements measured after the last construction stage in the back analysis calculations.

Two different back analysis techniques were used: the software SiDolo based on two traditional optimisation techniques and an ES algorithm. They were coupled with the 3D model to perform the identification of the cited parameters. The use of 3D models for back analysis is not very common and constitutes one important innovative aspect of this work.

The back analysis reached convergence with both techniques. It was possible to identify sets of parameters which improved the fit between measured and computed displacements. It is worth to mention that the initial parameters provided by GEOPAT were close to the real values. The ES slightly outperformed SiDolo when a more restrict stopping criteria was adopted.

The ES was able to avoid a local minimum which was observed in the error function topology even for a higher value of the considered stopping criteria. SiDolo was also able to do it but probably because the initial value was already close to the final solution. Additional calculations are needed to validate this theory. It was also observed that, using an elastic model, the local minimum no longer existed. Probably, the appearance of local minima is more characteristic of plastic models and they are closely related to the plasticity level which occurs in the models.

The capacity of the used models to translate reality was discussed. Three main limitations were pointed out: i) the consideration of only one value for  $E$  and  $K_0$ ; ii) the use of the total displacements measured in the end of the last excavation stage which can cause a stiffer response of the numerical model and iii) the use of measurements in only two cross-sections. It was concluded that, in this particular case, these limitations did not have a very significant impact to the point of severely influencing the reliability of the back analysis results. However,

they should be considered in future analysis.

In conclusion, the main innovative aspect of this work was the use of the ES algorithm combined with a 3D model. In this first approach it was shown that this combination can provide very good results. The 3D model more closely translates the real behaviour of the structures and the ES algorithm allows avoiding many problems of the traditional optimisation algorithms. However, much research is still needed in order to test the algorithm in different circumstances and to improve its efficiency. However, in this case, the identification process was finished in an acceptable number of iterations. It would be interesting also to test other evolutionary algorithms (like GAs) in the same problem to compare the results in this particular aspect.



### 8.1 Summary and main contributions

The evaluation of strength and deformability parameters in rock formations is still a subject where high uncertainty level exists. In the case of underground works these parameters are evaluated and updated in several stages of the project to which correspond different degrees of knowledge about the involved rock formation. This way, different techniques must be used in this evaluation which must be adapted to the available knowledge in each phase.

Three different levels concerning the geomechanical parameters evaluation in an underground structure project were defined. Level 1 is related to the parameters evaluation in the preliminary stages of design where information is still scarce; in level 2 new geological-geotechnical information is available and the preliminary geotechnical model (i.e. the initial geomechanical parameters) can be updated using this information; level 3 is concerned with the back analysis of the parameters when field observation becomes available.

In this thesis, the problematic of geomechanical parameters evaluation (restricted to strength and deformability parameters) in underground structures is addressed. Some innovative developments in the numerical methodologies associated to the evaluation of these parameters are achieved. Instead of focusing on a particular issue of the numerical methodologies, a global approach was carried out in order to improve the way geomechanical parameters are calculated in the several stages of an underground work project.

Concerning the methodologies for geomechanical parameters evaluation in rock masses, and besides a systematic presentation of the main methods with especial emphasis to the most innovative aspects, some innovative contributions were carried out, namely:

- An updating of the main innovative aspects of the RMR,  $Q$ ,  $Q_{TBM}$  and GSI empirical systems. A summary of expressions to compute the deformability modulus ( $E$ ) was carried

out. Concerning the RMR and Q systems, their matrix form and random set theory approach was presented.

- Development of some correlations between classical empirical indexes (RMR-Q and RCR-N) and new ones ( $F_{RMR-FQ}$  which only consider the parameters related with the rock mass, i.e. the common parts of the RMR and Q indexes) based on a large database gathered in a granite rock mass of the North of Portugal.
- Description of some methods especially devoted to the characterisation of highly heterogeneous rock masses like granite rock masses, flysch and block in matrix rocks (bimrocks).

Concerning level 1, related with the preliminary evaluation of the geomechanical parameters, the approach was to take advantage of the great amounts of geotechnical data normally produced in large projects. The idea was to explore this data using innovative and automatic tools, from the fields of artificial intelligence and pattern recognition (in particular Data Mining), in order to discover embedded knowledge which could be useful and reliable.

In this context, the main achieved original contributions were the following:

- Development of new and reliable regression models, based on multiple regression and ANN, for the calculation of the RMR and Q systems indexes and the geomechanical parameters  $\phi'$ ,  $c'$  and E. Several models were developed using different sets of information which allow their use in different conditions of knowledge about the rock mass and can be helpful for the decision-making process. Most of the induced models use less information than the original formulations maintaining a high accuracy level.
- Enhance the understanding of the main parameters related with the behaviour of the granite rock mass and the limitations of some empirical systems. The importance of the discontinuities characteristics in the rock mass behaviour was verified. However, it was pointed out that some of the conclusions, for instance the low importance of the water conditions, were probably due to limitations of the used database or even of the empirical systems themselves, in particular the RMR.
- The results of some expressions concerning the calculation of E were compared and a methodology to define a single final value for this parameter was established and validated with the results of reliable *in situ* tests. It was observed that some expressions may not be adequate to be applied to granite rock masses.
- The establishment of the importance of the Q system value in the strength parameters calculation as a very complete and useful parameter.



- Development of the HRMR-G (Hierarchical rock mass rating for granites). This new empirical rock mass classification system is based on the RMR system and presents a decision tree format. It is called hierarchical because it can be applied with different levels of knowledge. Each level provides a classification for the rock mass with a certain probability degree. It does not need a deterministic definition of each parameter that constitutes the RMR system (which in practice is not realistic) but only a range interval of some of these parameters. As more information is available, it is possible to step to the lower levels of the system providing a classification with a higher probability of being correct.

Level 2 is related with the updating of the geomechanical parameters as new information is available, for instance due to geotechnical survey campaigns performed in different project stages. In underground structures, the geomechanical information is available from several sources and present different reliabilities. In this context, the main goal was to develop a proper, systematic and mathematically valid procedure to update the geomechanical parameters as new information is available, considering the important contribution of experience in order to reduce the uncertainties related to parameters values. This task was carried out in the scope of Bayesian (subjective) probabilities.

The main contributions developed in the scope of this work were the following:

- Development of a Bayesian framework for a formal updating of E in underground works. Different levels of initial knowledge and distributions of the data (normal and lognormal, being the latter the one normally used to describe deformability parameters) were considered.
- Development of an innovative and heuristic Bayesian updating method using the two-parameter Weibull distribution. This approach tries to avoid the sensitivity of the posterior updated results to the consideration of a certain type of distribution to the data. The Weibull distribution is flexible and adapts to the data allowing to transform itself (depending on the characteristics of the data) into a normal, a Rayleigh or an exponential distribution.
- Application of the developed methodologies to real data for the updating of E in an underground structure considering the results of *in situ* tests. Geotechnical data from the Venda Nova II scheme, namely empirical systems applications and results from LFJ tests performed by LNEC, was used in the process. The developed methods presented mathematical consistency and were important mainly in the uncertainty reduction related

to the real value of  $E$ . This example also showed possible applications of Bayesian tools in geotechnics.

Level 3 is concerned with the use of field measurements in order to reevaluate the geomechanical parameters in a process called back analysis. In this procedure, the parameters of the constitutive model (or the constitutive model itself) are fine tuned in order to improve the match between measured and computed values. It can be performed using an error function, which measures the differences between measurements and computed values, together with an optimisation technique. Concerning this problem, the main goal was to test different optimisation techniques in validation and real problems of geomechanical parameters identification in underground works.

The main contribution achieved in this specific field were the following:

- Three traditional gradient-based optimisation algorithms were tested with a 3D model verification problem of a tunnel excavation in elasticity and in elasto-plasticity. This type of algorithms performed very well in elasticity corresponding to smooth-shaped error functions with a clearly defined minimum. In elasto-plasticity, where a great number of local minima may occur, they present convergence problems and identification of the optimal set of parameters is not assured.
- The ES innovative optimisation algorithm was tested in two analytical verification problems of a tunnel also in elasticity and elasto-plasticity. The algorithm proved to be robust even for complex error function topologies with several local minima. In terms of efficiency, it normally takes more iterations than a traditional algorithm but far from the hundreds or thousands calculations that a genetic algorithm normally needs to converge. It is important to mention that the used algorithm was not optimised to the specific application of geomechanical parameters in underground structures. However, the obtained results seem promising to the potential broader application of this algorithm.
- A statistical analysis of geotechnical information gathered in different surveys was carried out. The results pointed out to the overall good geomechanical quality of the granite rock mass in spite of some localised geological features presenting lower characteristics. Moreover, it was possible to conclude that lognormal and normal distributions are better suited to describe deformability and strength parameters, respectively.
- For the caverns of the powerhouse complex 2D and 3D models were developed considering the different excavation stages. The main conclusions of the structural analysis were that the rock mass behaves almost in elasticity due to its good quality and that the displacements (and stresses) field is highly influenced by  $K_0$  in the perpendicular direction of the

caverns axis. The results of the numerical models were compared with field observation, namely displacements measurements in extensometers and the fit was acceptable both in the qualitative and quantitative perspectives.

- The parameters  $E$  and  $K_0$  (perpendicular to the caverns axis) were back analysed using the 3D model together with two different optimisation algorithms, namely the SiDolo optimisation software and the ES algorithm. The optimised set of parameters were not significantly different from the initial values, specially to what concerns the  $K_0$  parameter. These results were analysed at the light of the considered simplifications. It was concluded that, in this particular case, the observed limitations did not affect significantly the results of the back analysis process but should be considered in future calculations. In what concerns the performance of the algorithms, both were able to obtain good results. The ES algorithm slightly outperformed SiDolo in the error function value related with the obtained set of parameters and proved its ability to avoid a local minimum which was observed in the error function topology. The main aspect of this analysis was the coupling of a 3D model with a innovative algorithm that showed good performance.

In conclusion, the main overall innovative contributions of this thesis were the following:

- The application of innovative tools of data analysis (namely Data Mining) to the geomechanical characterisation field, which allowed the development of novel and useful models that can be used mostly in the preliminary stages of the project. Moreover, this study allowed to get an insight of some issues concerning some physical aspects of the analysed granite rock mass, particularly in what concerns the most important parameters in the prediction of its overall behaviour.
- The development of a proper and mathematically valid framework based on Bayesian probabilities which allows the updating of the geomechanical parameters due to the consideration of new knowledge. It contemplates different uncertainty levels and types of knowledge and is able to deal with them consistently.
- To perform inverse analysis of geomechanical parameters considering a 3D model of an underground structures together with an innovative algorithm from the field of evolutionary programming - an evolution strategy (ES) - which allows to overcome some of the main limitations of traditional optimisation algorithms normally used in the back analysis process.

## 8.2 Future developments

In this thesis several issues concerning the geomechanical parameters evaluation were addressed in a integrated way. Some innovative contributions were achieved in different fields concerning the numerical evaluation of geomechanical parameters in underground structures. However, these contributions are not closed form solutions to the problems but almost initial however consistent approaches to possible answers. The use of Data Mining, Bayesian probabilities and inverse methodologies in the evaluation of geomechanical parameters in underground structures raise significant opportunities of open windows for future research. This way, there are a lot that can be done in the addressed areas and only some possible paths are going to be presented in the following items:

- The *in situ* strength evaluation of rock masses is still a problem not satisfactorily solved. This way, more work is necessary to improve the evaluation of strength parameters of rock masses.
- Improve some technological and efficiency aspects related with the LFJ test. There is a large experience in using this test in Portugal, mainly by LNEC, however, some issues must be enhanced.
- Development of the direct and indirect methodologies of geomechanical characterisation in highly heterogeneous rock formations. These type of formations cover important areas (like in the North of Portugal) and in spite of some recent developments in this field, more advances are necessary. The results of some of the current characterisation methodologies are almost meaningless in this type of formations, therefore special methods have to be developed and tested to provide a more accurate characterisation of such formations. Two possible numerical approaches are the development of advanced homogenisation techniques and the use of probabilistic tools like the stochastic random fields approach.
- Increase the used database of geomechanical data in order to overcome some of the pointed out limitations. This process will allow to fine-tune and validate the already developed models.
- Apply the Data Mining techniques to other databases of geotechnical information considering other types of data and different rock masses, for instance the volcanic formations, which present several particular issues. Other possible applications of these tools are the analysis of the data gathered by TBM machines and the validation of the  $Q_{TBM}$  system.
- Establish standard ways of organising the geotechnical information in order to allow applying DM techniques increasing the knowledge about the involved formations. This

is a subject whose importance is already recognised by the scientific community as it can be stated by the creation of the *JTC2 - Joint Committee on Representation of Geo-Engineering Data in Electronic Format* (<http://www.dur.ac.uk/geo-engineering/jtc2>).

- Develop the Bayesian frameworks using more complex models, for instance the hierarchical and the mixture models, and extend them to the consideration of strength parameters and other important issues like the interaction between parameters.
- Improve the efficiency of the ES algorithm by adapting it to the particularities of the constitutive models normally used to characterise rock masses. Efficiency can also be improved using parallel or distributed calculation.
- More thoroughly test and validate the ES algorithm in real and verification problems under different assumptions and circumstances.
- Use other artificial intelligence based optimisation techniques like the simulated annealing and particle swarm intelligence in the back analysis process.



---

## CHAPTER 9

---

### References

- Amusin, B., Shick, V. and Lama, R. “Using back analysis to estimate geotechnical field parameters for the design of support systems of tunnels.” *Tunnelling and Underground Space Technology*, 7(3): 281–284 (1992).
- Asaoka, A. and Matsuo, M. “An inverse problem approach to the prediction of multi-dimensional consolidation behavior.” *Soils and Foundations*, 24: 49–62 (1984).
- Babendererde, S., Hoek, E., Marinos, P. and Cardoso, S. “Characterization of granite and the underground construction in Metro do Porto.” In “Course on Geotechnical Risk in Tunnels,” Aveiro, Portugal (2004).
- Bäck, T. *Evolutionary algorithms in theory and practice*. Oxford University Press, Inc., NY (1996).
- Baker, J. and Calle, E. *JCSS probabilistic model code. Section 3.7: soil properties*. JCSS (2006).
- Bandis, S. “Mechanical properties of rock joints.” In ISRM (editor), “Proc. Int. Soc. Rock Mech. Symp. on rock joints,” 125–140. Loen, Norway (1990).
- Barbero, M., Bonini, M. and Borri-Brunetto, M. “Numerical modelling of the mechanical behaviour of bimrock.” In Sousa, Olalla and Grossman (editors), “11<sup>th</sup> Congress of the ISRM,” 377–380. Lisboa, Portugal (2007).
- Barton, N. *TBM tunnelling in jointed and faulted rock*. Balkema, Rotterdam, 172p. (2000).
- Barton, N. “Fault zones and TBM.” In Matos, Sousa, Klerberger and Pinto (editors), “Course on geotechnical risk in tunnels,” Aveiro, Portugal (2004).
- Barton, N., Lien, R. and Lunde, J. “Engineering classification of rock masses for the design of tunnel support.” *Rock Mechanics*, 6: 189–236 (1974).

- Barton, N., Loset, F., Lien, R. and Lune, J. "Application of Q-system in design decisions concerning dimensions and appropriate support for underground installations." *Subsurface Space*, 553–561 (1980).
- Barton, N. and Quadros, E. "Engineering and hydraulics in jointed rock masses." In ISRM (editor), "EUROCK 2002 - Course A," Funchal, Portugal (2002).
- Basheer, I. and Najjar, Y. "A neural-network for soil compaction." In Pande and Pietruszczak (editors), "Proc. 5<sup>th</sup> Int. Symp. Numerical Models in Geomechanics," 435–440. Davos, Switzerland (1995).
- Bernardo, J. and Smith, A. *Bayesian theory*. John Wiley & Sons, 586p (2004).
- Berry, M. and Linoff, G. *Mastering Data Mining: the art and science of customer relationships management*. John Wiley & Sons, Inc., USA (2000).
- Berthold, M. and Hand, D. *Intelligent data analysis: an introduction*. Springer, Second Edition (2003).
- Beyer, H. and Schwefel, H. "Evolution strategies. A comprehensive introduction." *Natural Computing*, 1: 3–52 (2002).
- Bhattacharya, B. and Solomatine, D. "Machine learning in soil classification." In "Proc. of Int. Joint Conf. on Neural Networks," Montreal, Canada (2005).
- Bieniawski, Z. "Determining rock mass deformability, experience from case histories." *International Journal of Rock Mechanics and Mining Science*, 15: 237–247 (1978).
- Bieniawski, Z. *Engineering rock mass classifications*. John Wiley & Sons (1989).
- Breiman, J., Friedman, R., Olshen, A. and Stone, C. *Classification and regression trees*. Wadsworth (1984).
- Brennan, A. and Kharroubi, S. "Expected value of sample information for weibull survival data." *Health Econ., John Wiley & Sons, Ltd (in press)*, DOI: 10.1002/hec (2007).
- Brooks, S. "Markov chain Monte Carlo method and its application." *The Statistician*, 47, Part 1: 69–100 (1998).
- Bulkley, J., Gayle, S., Hicks, B. and Stephens, R. "Adding the where to the who." In "24<sup>th</sup> SUGI - SAS Users Group International conference," paper 173, 3p. Miami, USA (1999).



- Button, E., Riedmüller, G., Schubert, W., Klima, K. and Medley, E. “Tunnelling in tectonic melanges - accommodating the impacts of geomechanical complexities and anisotropic rock mass fabrics.” *Bull. Eng. Geol. Env.*, 63: 109–117 (2004).
- Cai, J., Zhao, J. and Hudson, J. “Computerised rock engineering systems with neural networks and expert system.” *Rock Mechanics and Rock Engineering*, 31: 135–152 (1998).
- Cai, M. and Kaiser, P. “Obtaining modeling parameters for engineering design by rock mass characterization.” In Sousa, Olalla and Grossman (editors), “11<sup>th</sup> Congress of the ISRM,” 381–384. Lisboa, Portugal (2007).
- Cai, M., Kaiser, P., Uno, H., Tasaka, Y. and Minami, M. “Estimation of rock mass deformation modulus and strength of jointed hard rock masses using the GSI system.” *Int. Journal of Rock Mech. and Min. Sciences*, 41: 3–19 (2004).
- Calvello, M. and Finno, R. “Calibration of soil models by inverse analysis.” In Balkema (editor), “Proceedings of the Int. Sym. on Numerical Methods in Geomech., NUMOG VIII,” 107–116 (2002).
- Calvello, M. and Finno, R. “Selecting parameters to optimize in model calibration by inverse analysis.” *Computers and Geotechnics*, 31: 411–425 (2004).
- Cambou, B. and Bahar, R. “Utilisation de l’essai pressiométrique pour l’identification des paramètres intrinsèques du comportement d’un sol.” *Revue Française de Géotechnique*, 63: 39–50 (1993).
- Carter, T., Diederichs, M. and Carvalho, J. “A unified procedure for Hoek-Brown prediction of strength and post yield behaviour for rock masses at the extreme ends of the rock competency scale.” In Sousa, Olalla and Grossman (editors), “11<sup>th</sup> Congress of the ISRM,” 161–164. Lisboa, Portugal (2007).
- Carvalho, J. “Estimation of rock mass modulus.” *Personal communication* (2004).
- Carvalho, J., Carter, T. and Diederichs, M. “An approach for prediction of strength and post yield behaviour for rock masses of low intact strength.” In “1<sup>st</sup> Can-US Rock Symposium,” 8 pages. Vancouver, Canada (2007).
- Castro, A., Leitão, N., Sousa, L. and Nguyen, D. “The use of inverse methodologies in geotechnical problems.” *ISRM News Journal*, 7(2): 24–32 (2002).

- Chammas, R., Abraham, O., Cote, P., Pedersen, H. and Semblat, J. “Characterization of heterogeneous soils using surface waves: homogenization and numerical modeling.” *Int. Journal of Geomechanics*, 3: 55–63 (2003).
- Chapman, P., Clinton, J., Kerber, R., Khabaza, T., Reinartz, T., Shearer, C. and Wirth, R. *CRISP-DM 1.0. Step-by-step data mining guide*. SPSS Inc., 73p (2000).
- Christensen, R. and Lo, K. “Solution for effective shear properties in three phase sphere and cylinder models.” *J. Mech. Phys. Solids*, 27: 315–330 (1979).
- Cividini, A., Jurina, L. and Gioda, G. “Some aspects of characterization problems in geomechanics.” *International Journal of Rock Mechanics and Mining Science*, 18: 487–503 (1981).
- Cividini, A., Maier, G. and Nappi, A. “Parameter estimation of a statical geotechnical model using a Bayes’ approach.” *Int. Journal for Numerical and Analytical Methods in Geomechanics*, 20: 215–226 (1983).
- Cortez, P. *Models inspired in nature for temporal series prediction (in portuguese)*. Ph.D. thesis, University of Minho, Guimarães, Portugal. 214p (2002).
- Cortez, P. “Data mining opportunities in engineering: what, why and how.” In “Oral presentation to the 5<sup>th</sup> Int. Work. in Applications of Computational Mechanics in Geotechnical Engineering,” Guimarães, Portugal (2007).
- Costa, L. “A new parameter-less evolution strategy for solving unconstrained global optimization problems.” *Personal communication* (2007).
- Costa, L. and Oliveira, P. “Evolutionary algorithms approach to the solution of mixed integer non-linear programming problems.” *Computers and Chemical Engineering*, 25: 257–266 (2001).
- Costa, P., Baião, C., Ribeiro e Sousa, L. and Rosa, S. “Canical tunnel, Madeira island. Geotechnical characterisation and observation.” In “Portuguese-Spanish Congress on Underground Works,” 431–440. Madrid, Spain (2003).
- Cressie, N. *Statistics for spatial data*. John Wiley & Sons, New York, 900p (1991).
- Cruden, D. and Fell, R. *Landslide risk assessment*. Balkema (1997).
- Cunha, A. and Muralha, A. “Scale effects in the mechanical behaviour of joints and rock masses.” Technical report, Technical memorandum n. 763 LNEC, Lisboa, Portugal (1990).

- Dawson. "Slope stability analysis with finite element and finite difference methods." *Géotechnique*, 49(6): 835–840 (1999).
- Deng, D. *Back analysis problems in Geotechnics. A method based on the virtual work principle (in French)*. Ph.D. thesis, École Nationale de Ponts et Chaussées (2001).
- Deng, J. and Lee, C. "Displacement back analysis for a steep slope at the Three Gorges Project site." *International Journal of Rock Mechanics and Mining Science*, 18: 487–503 (1981).
- Dershowitz, W. "Interpretation and synthesis of discrete fracture orientation, size, shape, spatial structure and hydrologic data by forward modelling." In "Proc. of Fractured and Jointed Rock Masses," 579–586. Tahoe, NV (1992).
- Diederichs, M. and Kaiser, P. "Stability of large excavations in laminated hard rockmasses: the Voussoir analogue revisited." *International Journal of Rock Mechanics and Mining Science*, 36: 97–117 (1999).
- Ditlevsen, O. and Madsen, H. *Structural reliability methods*. John Wiley & Sons, 372p (1996).
- Douglas, K. *The shear strength of rock masses*. Ph.D. thesis, UNSW (2002).
- Eclaircy-Caudron, S., Dias, D., Chantron, L. and Kastner, R. "Evaluation of a back analysis method on simple tests." In "Fourth Int. FLAC Sym. on Numerical Modelling in Geomech.," 8p. Madrid, Spain (2006).
- Eclaircy-Caudron, S., Dias, D. and Kastner, R. "Inverse analysis on measurements realized during a tunnel excavation." In "Proc. ITA-AITES World Tunnel Congress," Prague, Czech Republic (2007).
- Einstein, H. "Landslide risk assessment procedure." In "Proc. 5<sup>th</sup> Int. Symp. on Landslides," Keynote paper. Lausanne, Switzerland (1988).
- Einstein, H. "The Decision Aids for Tunnelling (DAT) - an update." *Transportation Research Record*, 1892: 199–207 (2004).
- Einstein, H. "Use of Decision Aids for Tunnelling." In Matos, Sousa, Klerberger and Pinto (editors), "Geotechnical risk in rock tunnels," 63–74. Aveiro, Portugal (2006).
- Einstein, H. and Baecher, G. "Probabilistic and statistical methods in engineering geology. Part I exploration." *Rock Mechanics and Rock Engineering*, 16(1): 39–72 (1983).
- Einstein, H., Indermitte, C., Sinfield, J., Descoedres, F. and Dudt, J. "The Decision Aids for Tunnelling." *Transportation Research Record*, 1656 (1999).

- Eurocode. *Eurocode 7. Geotechnical design - part 1: general rules*. CEN (2004).
- Faber, M. *Risk and safety in civil, surveying and environmental engineering. Lecture notes*. Swiss Federal Institute of Technology. 394 p (2005).
- Fakhimi, A., Salehi, D. and Mojtabai, N. "Numerical back analysis for estimation of soil parameters in the Resalat tunnel project." *Tunnelling and Underground Space Technology*, 19: 57–67 (2004).
- Fardin, N., Stephansson, O. and Jing, L. "The scale dependence of rock joint surface roughness." *International Journal of Rock Mechanics and Mining Sciences*, 38: 659–669 (2001).
- Fayyad, U., Piatetsky-Shapiro, G. and Smyth, P. "From Data Mining to Knowledge Discovery: an overview." In Fayyad (editor), "Advances in Knowledge Discovery and Data Mining. AAAI Press / The MIT Press, Cambridge MA," 471–493 (1996).
- Fenton, A. and Griffiths, D. "Bearing-capacity prediction of spatially random  $c$ - $\phi$  soils." *Can. Geotech. J.*, 40: 54–65 (2003).
- Finno, R. and Calvello, M. "Supported excavations: the observational method and inverse modeling." *Journal of Geotechnical and Geoenvironmental Engineering*, 131(7): 826–836 (2005).
- Gelman, A., Carlin, J., Stern, H. and Rubin, D. *Bayesian data analysis*. Chapman & Hall/CRC. 668p (2004).
- Gens, A., Ledesma, A. and Alonso, E. "Estimation of parameters in geotechnical backanalysis. application to a tunnel excavation problem." *Computers and Geotechnics*, 18(1): 29–46 (1996).
- Gioda, G. "Indirect identification of the average elastic characteristics of rock masses." In "Int. Conf. on Structure and Foundation on Rock," 65–73. Sydney, Australia (1980).
- Gioda, G. and Jurina, L. "Identification of the earth pressure on tunnel liners." In "Proc. 10<sup>th</sup> ICSMFE," 301–304. Stockholm, Sweden (1981).
- Gioda, G. and Maier, G. "Direct search solution of an inverse problem in elastoplasticity: identification of cohesion, friction angle and in situ stress by pressure tunnel tests." *Int. Journal for Numerical Methods in Engineering*, 15: 1823–1848 (1980).
- Gioda, G. and Sakurai, S. "Back analysis procedures for the interpretation of field measurements in geomechanics." *Int. Journal for Numerical and Analytical Methods in Geomechanics*, 16: 555–583 (1987).

- Gioda, G. and Swoboda, G. “Developments and applications of the numerical analysis of tunnels in continuous media.” *Int. Journal for Numerical and Analytical Methods in Geomechanics*, 23: 1393–1405 (1999).
- Goebel, M. and Gruenwald, L. *A survey of Data Mining and knowledge discovery software tools*. SIGKDD Explorations, 1 (1): 20–33, ACM SIGKDD (1999).
- Goel, R., Jetwa, J. and Paithankar, A. “Indian experiences with Q and RMR systems.” *Journal of Tunnelling & Underground Space Technology*, 10(1): 97–109 (1995).
- Goh, A. “Genetic algorithm search for critical slip surface in multiple-wedge stability analysis.” *Canadian Geotechnical Journal*, 536: 382–391 (1999).
- Golberg, D. *Genetic algorithms in search, optimization and machine learning*. Adisson-Wesley: Reading, MA (1989).
- Gomes Correia, A., Viana da Fonseca, A. and Gambin, M. “Routine and advanced analysis of mechanical in situ tests. results on saprolitic soils from granites more or less mixed in Portugal.” In V. da Fonseca and Mayne (editors), “Second Int. Conf. on Site Characterization - ISC’02,” 75–95. Porto, Portugal (2004).
- Goodman, R. *Introduction to rock mechanics*. New York: John Wiley & Sons, 562p (1989).
- Goricki, A., Potsch, M. and Schubert, W. “Probabilistic determination of rock mass behavior and support of tunnels.” In “ISRM 2003 - Technology Roadmap for Rock Mechanics. South African Institute of Mining and Metallurgy,” 405–408 (2003).
- Guo, L., Wu, A., Zhou, K. and Yao, Z. “Pattern recognition and its intelligent realization of probable rock mass failure based on RES approach.” *Chinese Journal of Nonferrous Metals*, 13(3): 749–753 (2003).
- Haas, C. and Einstein, H. “Updating the Decision Aids for Tunneling.” *ASCE Journal of Construction Engineering and Management*, 128(1): 40–48 (2002).
- Han, J. and Kamber, M. *Data Mining: concepts and techniques*. Morgan Kaufmann Publishers, 312p (2000).
- Hand, D., Mannila, H. and Smyth, P. *Principles of Data Mining*. MIT Press, Cambridge, MA (2001).
- Haneberg, W. “Simulation of 3-D block population to characterize outcrop sampling bias in block-in-matrix (bimrocks).” *Felsbau*, 22(5): 19–26 (2004).

- Hanna, A., Morcoux, G. and Helmy, M. "Efficiency of pile groups installed in cohesionless soil using artificial neural networks." *Can. Geotechnical Journal*, 41(6): 1241–1249 (2004).
- Harrison, T. *Intranet Data Warehouse*. São Paulo, Berkeley. Brasil (1998).
- Hashash, Y., Jung, S. and Ghaboussi, J. "Numerical implementation of a neural network based material model in finite element analysis." *Int. Journal for Numerical Methods in Engineering*, 30: 477–488 (2004).
- Hastings, W. "Monte Carlo sampling methods using Markov chains and their applications." *Biometrika*, 57: 97–109 (1970).
- Haupt, R. and Haupt, S. *Practical genetic algorithms*. Wiley: New York (1998).
- Herve, E. and Zaoui, A. "Modelling the effective behavior of nonlinear matrix-inclusion composite." *Eur. J. Mech. A/Solids*, 9(6): 505–515 (1990).
- Hoek, E. "Strength of rock and rock masses." *News Journal of ISRM*, 2: 4–16 (1994).
- Hoek, E. "Rock mass properties for underground mines. Underground mining methods: engineering fundamentals and international case studies." In Hustrulid and Bullock (editors), "Society for Mining, Metallurgy and Exploration (SME)," Littleton, Colorado, USA (2001).
- Hoek, E. and Brown, E. *Underground excavations in rock*. Institution of Mining and Metallurgy, London, 627p. (1980).
- Hoek, E. and Brown, E. "Practical estimates of rock mass strength." *International Journal of Rock Mechanics and Mining Science*, 34: 1165–1186 (1997).
- Hoek, E., Carranza-Torres, C. and Corkum, B. "Hoek-Brown failure criterion - 2002 edition." In "Proc. of the 5<sup>th</sup> North American Rock Mechanics Symposium," 267–273. Toronto, Canada (2002).
- Hoek, E. and Diederichs, M. "Empirical estimation of rock mass modulus." *International Journal of Rock Mechanics and Mining Science*, 43: 203–215 (2006).
- Hoek, E., Marinos, P. and Benissi, M. "Applicability of the geological strength index (GSI) classification for very weak and sheared rock masses. the case of Athens schist formation." *Bull. Eng. Geol. Env.*, 57: 151–160 (1998).
- Hoek, E., Marinos, P. and Marinos, V. "Characterisation and engineering properties of tectonically undisturbed but lithologically varied sedimentary rock masses." *International Journal of Rock Mechanics and Mining Science*, 42: 277–285 (2005).

- Holland, J. *Adaptation in natural and artificial systems*. University of Michigan press: Ann Arbor, MI (1975).
- Holstein, C. *A Tutorial in Decision Analysis. Readings in Decision Analysis*. Howard, Mathe-son, Miller (eds.) SRI, Menlo Park (1974).
- Hungr, D., Fell, R., Couture, R. and Eberhardt, E. “Landslide risk management.” In “Proc. of the Int. Conf. on Landslide Risk Management,” Vancouver, Canada (2005).
- Hush, D. and Horne, B. “What’s new since Lippman?” *IEEE Signal Process Magazine*, 9–39 (1999).
- Iding, R., Pister, K. and Taylor, R. “Identification of nonlinear elastic solids by a finite element method.” *Computer Methods in Applied Mechanics and Engineering*, 4: 121–142 (1974).
- Imre, E. “Model validation for the oedometric relaxation test.” In “Proc. of the 13<sup>th</sup> Int. Conf. on Soil Mech. and Foundation Eng.”, 1123–1126. New Delhi, India (1994).
- Innaurato, N., Mancini, R. and Rondena E, A., Zaninetti. “Forecasting and effective TBM performances in a rapid excavation of a tunnel in Italy.” In ISRM (editor), “Proc. of the 7<sup>th</sup> ISRM International Congress,” Aachen (1991).
- Intellicorp. *KAPPA-PC development software system*. Version 2.4. USA (1997).
- ISRM. “Suggested methods for the quantitative description of discontinuities in rock masses.” *International Journal of Rock Mining Sciences & Geomechanics Abstracts*, 15(16): 319–368 (1978).
- ISRM. *Rock characterization, testing and monitoring - ISRM suggested methods*. Ed. E. T. Brown, Pergamon Press (1981).
- Itasca. *FLAC - Fast Lagrangian Analysis of Continua*. Version 5.0 User’s manual, Minneapolis, USA (2005).
- Jeon, Y. and Yang, H. “Development of a back analysis algorithm using FLAC.” *International Journal of Rock Mechanics and Mining Science*, 41(1): 447–453 (2004).
- Journel, A. and Huijbregts, C. *Mining geostatistics*. Academic Press, 600p (1978).
- Kang, Y., Lin, X. and Qin, Q. “Inverse/genetic method and its application in identification of mechanical parameters of interface in composite.” *Composite Structures*, 66: 449–458 (2004).

- Karam, J. *Decision Aids for Tunnel Exploration*. Master's thesis, Massachusetts Institute of Technology, Massachusetts, USA (2005).
- Kass, G. "An exploratory technique for investigating large quantities of categorical data." *Applied Statistics*, 29: 119–127 (1980).
- Klose, C., Giese, R., Low, S. and Borm, G. "Geological and seismic Data Mining for the development of an interpretation system within the Alptransit project." In "EGS XXVII General Assembly," abstract 2302. Nice, France (2002).
- Kohavi, R. and Provost, F. "Glossary of terms." *Machine Learning*, 20(2/3): 271–274 (1998).
- Kröner, E. "Self-consistent scheme and grader disorder in polycrystal elasticity." *J. Phys. F: Met. Phys.*, 8: 22–61 (1978).
- Lanaro, F., Jing, L. and Stephansson, O. "3-D laser measurements and representation of roughness of rock fractures." In H. Rossmainith (editor), "Proc. Int. Conf. Mech. Jointed and Faulted Rock," 185–189. Vienna, Austria (1998).
- Lecampion, B., Constantinescu, A. and Nguyen, D. "Parameter identification for lined tunnels in a viscoplastic medium." *Int. Journal for Numerical and Analytical Methods in Geomechanics*, 26: 1191–1211 (2002).
- Ledesma, A., Gens, A. and Alonso, E. "Parameter and variance estimation in geotechnical backanalysis using prior information." *Int. J. Numer. Anal. Meth. Geomech*, 20: 119–141 (1996).
- Lee, C. and Sterling, R. "Identifying probable failure modes for underground openings using a neural network." *International Journal of Rock Mechanics and Mining Science*, 29: 49–67 (1992).
- Lee, S. and Siau, K. "A review of Data Mining techniques." *Industrial Management & Data Systems, MCB University*, 101(1): 41–46 (2001).
- Lehman, L. "Mitigating drilling and completion risks through expert planning." *Scandinavian oil-gas magazine*, 11/12: 10–12 (2004).
- Levasseur, S., Malecot, Y., Boulon, M. and Flavigny, E. "Soil parameter identification using a genetic algorithm." *Int. J. Numer. Anal. Meth. Geomech (in press)* (2007).
- Li, Y. and Xia, C. "Time-dependent tests on intact rock in uniaxial compression." *International Journal of Rock Mechanics and Mining Sciences*, 37: 467–475 (2000).



- Lima, C., Resende, M., Plasencia, N. and Esteves, C. “Venda Nova II hydroelectric scheme powerhouse geotechnics and design.” *ISRM News Journal*, 7(2): 37–41 (2002).
- LNEC. “LNEC collaboration in the geological and geotechnical studies concerning the hydraulic circuit of Venda Nova II (in portuguese).” Technical report, LNEC Report 47/1/7084 Lisboa, Portugal (1983).
- LNEC. “Seismic tomography between boreholes in the mass interesting the central cavern of the Venda Nova ii scheme (in portuguese).” Technical report, Technical memorandum LNEC, Lisboa, Portugal (1997).
- LNEC. “Venda Nova II scheme. determination of the state of stress (in portuguese).” Technical report, LNEC Report 371/03 Lisboa, Portugal (2003).
- LNEC. “Venda Nova II scheme. laboratory tests for the characterization of the powerhouse cavern rock mass (in portuguese).” Technical report, LNEC Report 160/05 Lisboa, Portugal (2005).
- Maghous, S., Buhan, P. and Bekaert, A. “Failure design of jointed rock structures by means of homogenization approach.” *Journal of Mechanics of Cohesive-Frictional Material*, 3: 207–228 (1998).
- Mandrone, G. “Engineering geological mapping of heterogeneous rock masses in the Northern Apennines: an example from the Parma valley (Italy).” *Bull. Eng. Geol. Env.*, 65: 245–252 (2006).
- Marinos, P. and Hoek, E. “Estimating the geotechnical properties of heterogeneous rock masses such as flysch.” *Bull. Eng. Geol. Env.*, 60: 85–92 (2001).
- Marinos, V., Marinos, P. and Hoek, E. “The geological strength index: applications and limitations.” *Bull. Eng. Geol. Env.*, 64: 55–65 (2005).
- Marseguerra, M., Zio, E. and Podofillini, L. “Model parameters estimation and sensitivity by genetic algorithms.” *Annals of Nuclear Energy*, 20(7/8): 1229–1236 (2003).
- Martin, C., Kaiser, P. and McCreath, D. “Hoek-brown parameters for predicting the depth of brittle failure around tunnels.” *Canad. Geotechnical Journal*, 36(1): 136–151 (1999).
- Mas Ivars, D., Deisman, N., Pierce, M. and Fairhurst. “The Synthetic Rock Mass Approach - a step forward in the characterization of jointed rock masses.” In Sousa, Olalla and Grossman (editors), “11<sup>th</sup> Congress of the ISRM,” 485–490. Lisboa, Portugal (2007).

- Mattsson, H., Klisinski, M. and Axelsson, K. "Optimization routine for identification of model parameters in soil plasticity." *Int. J. Numer. Anal. Meth. Geomech*, 25: 435–472 (2001).
- McCulloch, W. and Pitts, W. "A logical calculus of the ideas immanent in nervous activity." *Bulletin of Mathematical Biophysics*, 5: 115–133 (1943).
- Medley, E. "Systematic characterization of melange bimrocks and other chaotic soil/rock mixtures." *Felsbau: Rock and Soil Engineering - Journal for Engineering Geology, Geomechanics and Tunnelling*, 3: 152–162 (1999).
- Menezes, A., Varela, F., Ribeiro e Sousa, L. and Moura, F. "Geomechanical studies for a road tunnel in volcanic formations." In ITA (editor), "ITA-AITES World Tunnel Congress," Prague, Czech Republic (2007).
- Metropolis, N., Rosenbluth, A., Rosenbluth, M., Teller, A. and Teller, E. "Equations of state calculations by fast computing machines." *J. Chem. Phys.*, 21: 1087–1091 (1953).
- Min, S., Einstein, H. and Lee, J. "Application of the Decision Aids for Tunnelling (DAT) to update excavation cost/time information." *KSCE Journal of Civil Engineering*, 9(4) (2005).
- Miranda, T. *Contribution to the calculation of geomechanical parameters for underground structures modelling in granite formations*. Master's thesis, University of Minho, Guimarães, Portugal (in Portuguese), 186p (2003).
- Miranda, T., Gomes Correia, A. and Ribeiro e Sousa, L. "Determination of geomechanical parameters in rock masses and heterogeneous formations." *Civil Engineering Journal*, 25: 17–40 (2006).
- Mitri, H., Edrissi, R. and Henning, J. "Finite element modelling of cable bolted stopes in hard rock underground mines." In SME (editor), "SME Annual Meeting," 14–17. Albuquerque (1994).
- Moles, C., Mendes, P. and Banga, J. "Parameter estimation in biochemical pathways: a comparison of global optimization methods." *Genome Research*, 13: 2467–2747 (2003).
- Morales, T., Uribe-Etxebarria, G., Uriarte, J. and Valderrama, I. "Geomechanical characterization of rock masses in alpine regions: the Basque Arc (Basque-Cantabrian basin, Northern Spain)." *Engineering Geology*, 71: 343–362 (2004).
- Moreira, C., Sousa, J. and Lemos, L. "Identification of the parameters of a Miocene clay intersected by a tunnel of the Lisbon Metro (in portuguese)." *Journal of the Portuguese Geotechnical Society*, 102: 5–32 (2003).

- Moritz, B., Grossauer, K. and Schubert, W. “Short term prediction of system behaviour for shallow tunnels in heterogeneous ground.” *Felsbau*, 22(5): 44–52 (2004).
- Motta, C. *Intelligent system for evaluation of risk in roads of terrestrial transport (in portuguese)*. Ph.D. thesis, Rio de Janeiro Federal University, Brazil (2004).
- Murakami, A. and Hasegawa, T. “Back analysis by Kalman filter-finite elements and optimal location of observed points.” In “Proc 22nd Japan National Conf. on Soil Mechanics and Foundation Engng,” 1033–1036. Japan (1987).
- Nicholson, G. and Bieniawski, Z. “A non-linear deformation modulus based on rock mass classification.” *Int. Journal of Mining & Geology Eng.*, 181–202 (1997).
- Normetro. “Geotechnical-geomechanical general report of the underground parts (lines C, S and connection C-S).” Technical report, Execution project. Normetro, Porto, 53p. (2001).
- Oliveira, A., Carvalho, J., Pereira, M. and Costa, R. “Intelligent data analysis: civil mining (in portuguese).” Technical report, Internal Report . Information Systems Department. University of Minho, Guimarães, Portugal, 96p (2006).
- Oreste, P. “Back-analysis techniques for the improvement of the understanding of rock in underground constructions.” *Tunnelling and Underground Space Technology*, 20: 7–21 (2005).
- Pal, S., Wathugala, G. and Kundu, S. “Calibration of a constitutive model using genetic algorithms.” *Computers and Geotechnics*, 19(4): 325–348 (1996).
- Palmstrom, A. *RMI - a rock mass characterization system for rock engineering purposes*. Ph.D. thesis, University of Oslo, Oslo, Norway (1995).
- Palmstrom, A. and Singh, R. “The deformation modulus of rock masses - comparisons between in situ tests and indirect estimates.” *Tunnelling and Underground Space Technology*, 16: 115–131 (2001).
- Peschl, G. and Schweiger, H. “Reliability analysis in geotechnics with finite elements - comparison of probabilistic, stochastic and fuzzy set methods.” In Bernard, Seidenfeld and Zaffalon (editors), “ISIPTA’03,” 437–451. Lugano, Switzerland (2003).
- Pichler, B., Lackner, R. and Mang, H. “Back analysis of model parameters in geotechnical engineering by means of soft computing.” *Int. Journal for Numerical Methods in Engineering*, 57: 1943–1978 (2003).

- Pinto, J. "Determination of the deformability modulus of weak rock masses by means of large flat jacks (LFJ)." In ISRM (editor), "ISRM Int. Symp. On Weak Rocks," Tokio, Japan (1981).
- Plasencia, N. *Underground works - aspects of the engineering geology contribution and design (in portuguese)*. Master's thesis, Technical University of Lisbon, Lisboa, Portugal (2003).
- Plasencia, N., Coelho, M., Lima, C. and Fialho, L. "Contribution of the seismic tomography for the characterization of the mass interesting the central cavern of the Venda Nova ii scheme (in portuguese)." In "7<sup>th</sup> Geotechnical Portuguese Congress," 113–122. Porto, Portugal (2000).
- Popescu, R., Deodatis, G. and Nobahar, A. "Effects of random heterogeneity of soil properties on bearing capacity." *Probabilistic Engineering Mechanics*, 20: 324–341 (2005).
- Potyondy, D. and Cundall, P. "A bonded-particle model for rock." *International Journal of Rock Mechanics and Mining Science*, 41: 1329–1364 (2004).
- Quintela, H. *Knowledge systems based in Data Mining: application to the stability analysis of steal structures*, ". Master's thesis, University of Minho, Guimarães, Portugal (in Portuguese), 199p (2005).
- Rackwitz, R. "Reviewing probabilistic soils modelling." *Computers and Geotechnics*, 26: 199–223 (2000).
- Raiffa, H. and Schlaifer, R. *Applied statistical decision theory*. Harvard Business School, Cambridge, Ma (1964).
- Rangeard, D., Hicher, P. and Zentar, R. "Determining soil permeability from pressuremeter tests." *Int. Journal for Numerical and Analytical Methods in Geomechanics*, 27: 1–24 (2003).
- Rangel, J., Viveros, U., Ayala, A. and Cervantes, F. "Tunnel stability analysis during construction using a neuro-fuzzy system." *Int. Journal for Numerical and Analytical Methods in Geomechanics*, 29: 1433–1456 (2005).
- Read, S., Richards, L. and Perrin, N. "Applicability of the Hoek-Brown failure criterion to New Zealand greywacke rocks." In "Proc. 9<sup>th</sup> Int. Cong. on Rock Mechanics," 655–660. Paris, France (1999).
- Rechenberg, I. *Evolutionstrategie'94*. Stuttgart: Frommann-Holzboog (1994).
- Renders, J. *Algorithmes génétiques et réseaux de neurones*. Hermès: Paris (1995).

- Riedmüller, G. and Schubert, W. “Critical comments on quantitative rock mass classifications.” *Felsbau: Rock and Soil Engineering - Journal for Engineering Geology, Geomechanics and Tunnelling*, 3: 164–167 (1999).
- Rocha, M. *Rock mechanics (in portuguese)*. LNEC, Lisboa (1971).
- Rocha, M. *Underground structures (in portuguese)*. LNEC, Lisboa (1976).
- Russell, S. and Norvig, P. *Artificial intelligence. A modern approach*. Prentice Hall International Editions (1995).
- Rutledge, J. and Preston, R. “Experience with engineering classifications of rocks.” In “Proc. Int. Tunnelling Symposium,” A3.1–A3.7. Tokio, Japan (1978).
- Sakellariou, M. and Ferentinou, M. “A study of slope stability prediction using neural networks.” *Geotechnical and Geological Engineering, Springer*, 23: 419–445 (2005).
- Sakurai, S. “Lessons learned from field measurements in tunnelling.” *Tunnelling and Underground Space Technology*, 12: 453–460 (1997).
- Sakurai, S., Akutagawa, S., Takeuchi, K., Shinji, M. and Shimizu, N. “Back analysis for tunnel engineering as a modern observational method.” *Tunnelling and Underground Space Technology*, 18: 185–196 (2003).
- Sakurai, S., Akutagawa, S. and Tokudome, O. “Back analysis of non-elastic strains based on the minimum norm solution.” *J. JSCE*, 517(III-31): 197–202 (1995).
- Sakurai, S. and Takeuchi, K. “Back analysis of measured displacements of tunnels.” *Rock Mech and Rock Eng.*, 16: 173–180 (1983).
- Salençon, J. “Contraction quasi-static d’une cavité à symétrie sphérique ou cylindrique dans un milieu élastoplastique.” *Annls Ponts Chauss*, 4: 231–236 (1969).
- Samarajiva, P., Macari, E. and Wathugala, W. “Genetic algorithms for the calibration of constitutive models for soils.” *International Journal of Geomechanics*, 5(3): 206–217 (2005).
- Santos, M. and Azevedo, C. *Data Mining. Knowledge Discovery in Databases (In Portuguese)*. FCA - Editora de Informática, Lda. 194p (2005).
- Sapigni, M., Berti, M., Bethaz, E., Busillo, A. and Cardone, G. “TBM performance estimation using rock mass classifications.” *Int. Journal of Rock Mech. and Min. Sciences*, 39: 771–788 (2002).

- Saroglou, H. and Tsiambaos, G. "Classification of anisotropic rocks." In Sousa, Olalla and Grossman (editors), "11<sup>th</sup> Congress of the ISRM," 191–196. Lisboa, Portugal (2007).
- Schefel, H. *Evolution and optimal seeking*. John Wiley & Sons (1995).
- Schwefel, H. *Kybernetische evolution als strategie der experimentellen forschung in der stromungstechnik*,. Master's thesis, Technical University of Berlin, Berlin, Germany (1965).
- Serafim, J. and Pereira, J. "Considerations of the geomechanics classification of Bieniawski." In LNEC (editor), "Proceedings of the International Symposium of Eng. Geol. Underground Construction," II.33–II.42. Lisboa, Portugal (1983).
- Serrano, A., Estaire, J. and Olalla, C. "Extension of the hoek-brown failure criterion to three dimensions." In Sousa, Olalla and Grossman (editors), "11<sup>th</sup> Congress of the ISRM," 289–292. Lisboa, Portugal (2007).
- Shang, Y., Cai, J., Hao, W., Wu, X. and Li, S. "Intelligent back analysis of displacements using precedent type analysis for tunnelling." *Tunnelling and Underground Space Technology*, 17: 381–389 (2002).
- Sheu, G. "Direct back analysis by the meshless petrov-galerkin method and bayesian statistics." *Int. J. Numer. Anal. Meth. Geomech (in press)* (2006).
- SiDolo. *Notice d'utilisation*. Version 2.4495, Laboratoire Génie Mécanique et Matériaux de l'Université de Bretagne-Sud, Lorient, France (2005).
- Silvestre, M. *Geometrical and hydro-mechanical characterization of discontinuities. An experimental study*,. Master's thesis, Technical University of Delft, Delft, Holand (1996).
- Simpson, A. and Priest, S. "The application of genetic algorithms to optimization problems in geotechnics." *Computers and Geotechnics*, 15: 1–19 (1993).
- Singh, B., Viladkar, M., Samadhiya, N. and Mehrotra, V. "Rock mass strength parameters mobilised in tunnels." *Tunnelling and Underground Space Technology*, 12: 47–54 (1997).
- Singh, M. and Rao, S. "Empirical methods to estimate the strength of jointed rock masses." *Engineering Geology*, 77: 127–137 (2005).
- Singh, S. *Time dependent modulus of rocks in tunnels*,. Master's thesis, University of Roorkee, Roorkee, India (1997).
- Solomatine, D. and Dulal, K. "Model trees as na alternative to neural networks in rainfall-runoff modelling." *Hydrological Sciences Journal*, 48(3): 399–411 (2003).

- Sonmez, H., Gokceoglu, C. and Ulusay, R. “Indirect determination of the modulus of deformation of rock masses based on the GSI system.” *International Journal of Rock Mechanics and Mining Science*, 41: 849–857 (2004).
- Sonmez, H. and Ulusay, R. “Modifications to the geological strength index (GSI) and their applicability to the stability of slopes.” *International Journal of Rock Mechanics and Mining Science*, 36: 743–760 (1999).
- Sousa, L., Nakamura, A., Yoshida, H., Yamaguchi, Y., Kawasaki, M. and Satoh, H. “Evaluation of the deformability of rock masses for dam foundations. analysis of deformability investigation results of heterogeneous bedrock.” Technical report, Technical memorandum of PWRI, 45p. (1990).
- Souza, T. *Rio de Janeiro landslides prediction by a Data Mining approach (in portuguese)*. Ph.D. thesis, Rio de Janeiro Federal University, Brazil (2004).
- Stephens, R. and Banks, D. “Moduli for deformation studies of the foundation and abutments of the Portugues dam - Puerto Rico.” In Balkema (editor), “Rock Mechanics as a Guide for Efficient Utilization of Natural Resources: Proc. 30<sup>th</sup> U.S. Symposium,” 31–38. Morgantown, USA (1989).
- Stille, H. and Palmstrom, A. “Classification as a tool in rock engineering.” *International Journal of Rock Mechanics and Mining Sciences*, 18: 331–345 (2003).
- Suwansawat, S. and Einstein, H. “Artificial neural networks for predicting the maximum surface settlement caused by EPB shield tunnelling.” *Tunnelling and Underground Space Technology*, 21: 133–150 (2006).
- Swoboda, G., Ichikawa, Y., Dong, Q. and Mostafa, Z. “Back analysis of large geotechnical models.” *International Journal for Numerical and Analytical Methods in Geomechanics*, 23: 1455–1472 (1999).
- Tavares, C. *Back analysis methods in the interpretation of concrete dams behaviour (in Portuguese)*. Ph.D. thesis, Technical University of Lisbon (1997).
- Terzaghi, K. and Peck, R. *Soil mechanics in engineering practice*. John Wiley & Sons, New York (1948).
- Tonon, F., Bernardini, A. and Mammino, A. “Determination of parameters range in rock engineering by means of random set theory.” *Reliability Eng. and System Safety*, 70: 241–261 (2000).

- Tzamos, S. and Sofianos, A. "A correlation of four rock mass classification systems through their mass fabric indexes." *International Journal of Rock Mechanics and Mining Sciences*, 44: 477–495 (2007).
- Venclik, P. "Development of an inverse back analysis code and its verification." *Numerical Methods in Geotechnical Engineering*, 423–430 (1994).
- Verman, M. *Rock mass - tunnel support interaction analysis*. Ph.D. thesis, University of Roorkee, Roorkee, India (1993).
- Viana da Fonseca, A. and Coelho, S. "Characterization of variable weathered profiles by using DPR." In Sousa, Olalla and Grossman (editors), "11<sup>th</sup> Congress of the ISRM," 187–190. Lisboa, Portugal (2007).
- Wakabayashi, J. and Medley, E. "Geological characterization of melanges for practitioners." *Felsbau*, 22(5): 10–18 (2004).
- Weibull, W. "A statistical distribution function of wide applicability." *J. Appl. Mech.-Tran. ASME*, 18(3): 293–297 (1951).
- Wickham, G., Tiedmann, H. and Skinner, E. "Ground control prediction model - RSR concept." In AIME (editor), "Proc. of the Rapid Exc. and Tunnelling Conference," 691–707. New York, USA (1974).
- Wrobel, L. and Miltiadou, P. "Genetic algorithms for inverse cathodic protection problems." *Engineering analysis with boundary elements*, 28: 267–277 (2004).
- Wyllie, D. *Foundations on rock*. E & FN Spon. (1992).
- Yang, Z. and Elgmal, A. "Application of unconstrained optimization and sensitivity analysis to calibration of a soil constitutive model." *Int. J. Numer. Anal. Meth. Geomech*, 27: 1277–1297 (2003).
- Yang, Z., Lee, C. and Wang, S. "3-D back analysis on one trial adit in Three Gorges, China." *International Journal of Rock Mechanics and Mining Science*, 37: 525–533 (2000).
- Yanjun, S., Yongyue, S., Guangxiang, Y. and Yuanchun, S. "Discontinuity distribution in granites and its effects on rock mass classification." In Sousa, Olalla and Grossman (editors), "11<sup>th</sup> Congress of the ISRM," 227–230. Lisboa, Portugal (2007).
- Yufin, S., Lamonina, E. and Postolskaya, O. "Estimation of strength and deformation parameters of jointed rock masses." In Sousa, Fernandes, Vargas and Azevedo (editors), "5<sup>th</sup>



- Int. Work. in Applications of Computational Mechanics in Geotechnical Engineering,” 3–15. Guimarães, Portugal (2007).
- Zentar, R., Hicher, P. and Moulin, G. “Identification of soil parameters by inverse analysis.” *Computers and Geotechnics*, 28: 129–144 (2001).
- Zhang, L. and Einstein, H. “Using RQD to estimate the deformation modulus of rock masses.” *International Journal of Rock Mechanics and Mining Science*, 41: 337–341 (2004).
- Zhao, J., Zhou, Y. and Hefny, A. “Rock dynamics research related to cavern development for ammunition storage.” *Tunnelling and Underground Space Technology*, 14: 513–526 (1999).
- Zhou, K., Luo, Z. and Shi, X. “Acquirement and application of knowledge concerning stope stability based on Data Mining.” *Mining Research and Development*, 22(5): 1–4 (2002).



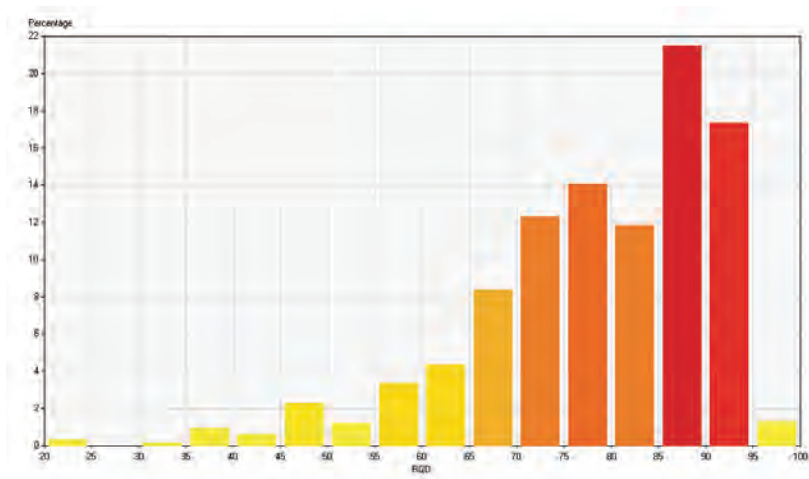
---

# ANNEX I

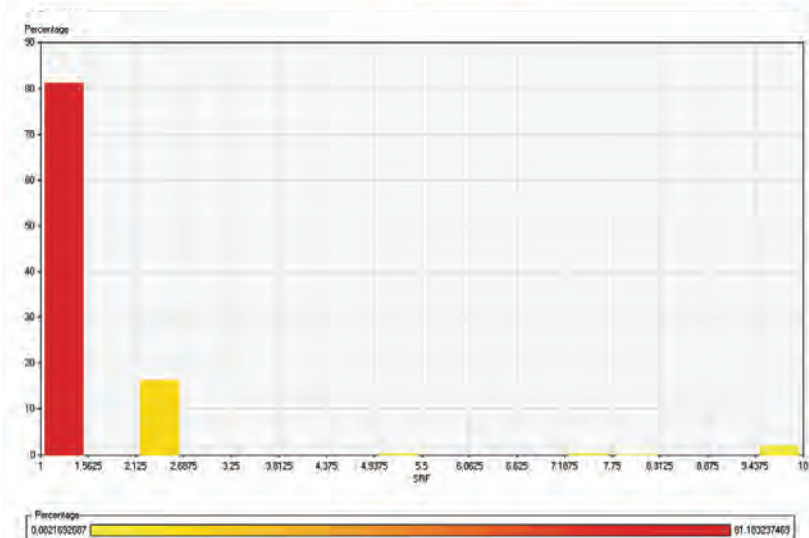
---

## Histograms of the numerical variables used in the DM process

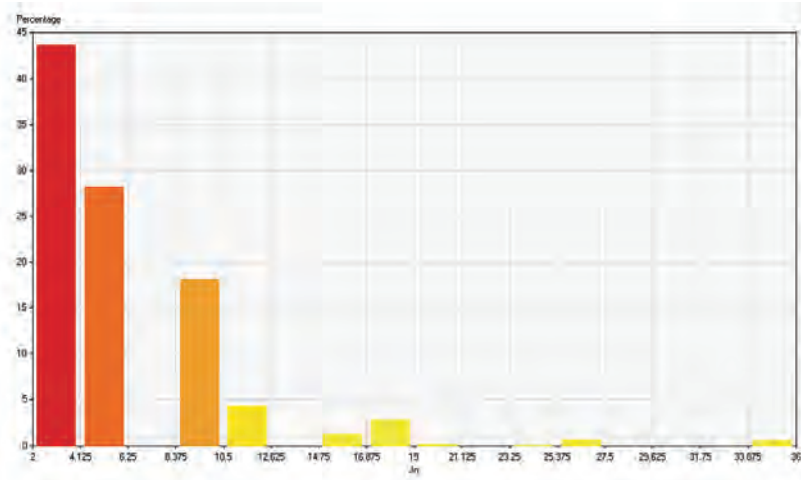
RQD



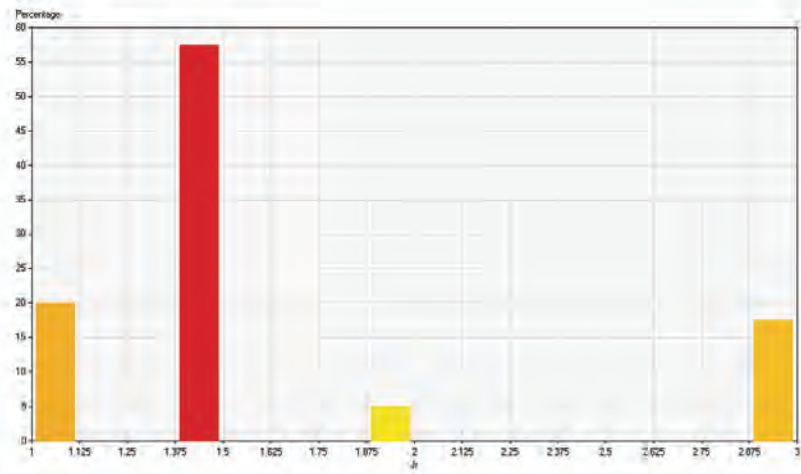
$J_w$



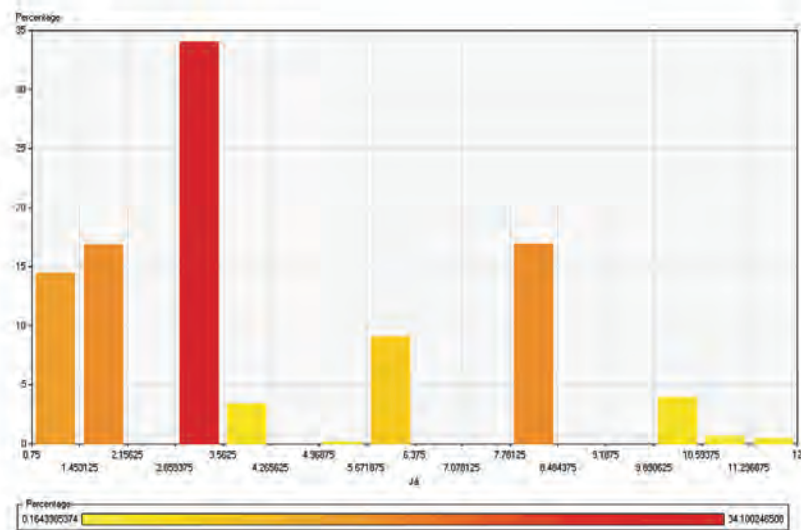
$J_n$



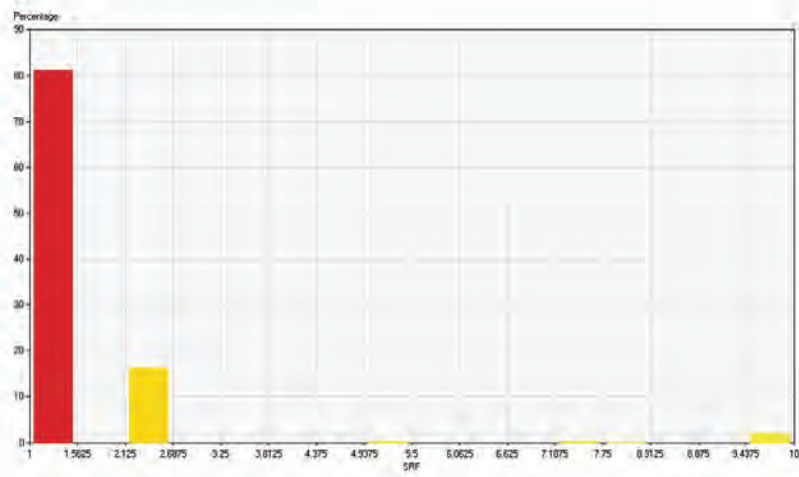
$J_r$



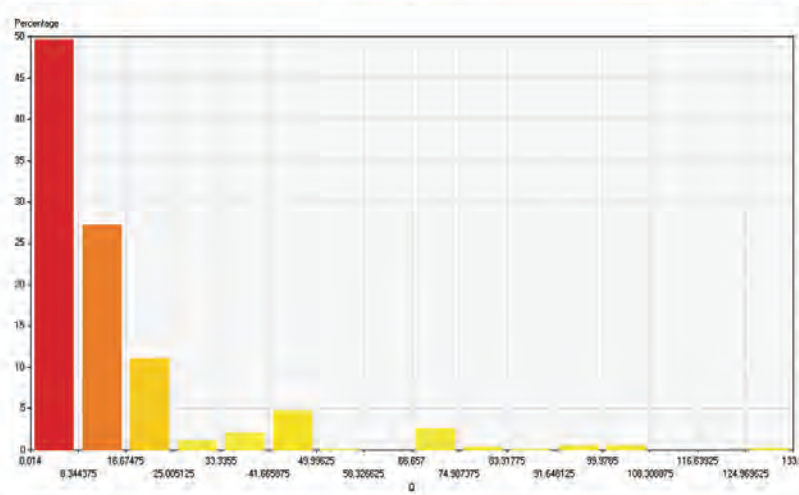
$J_a$



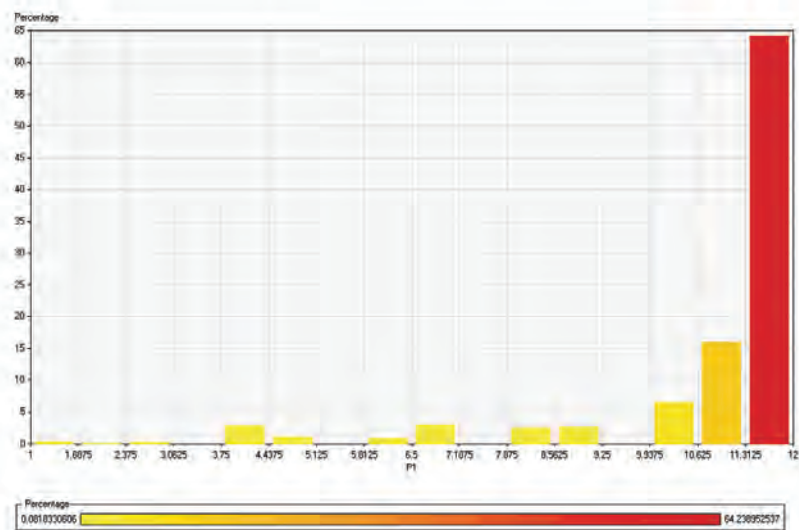
SRF



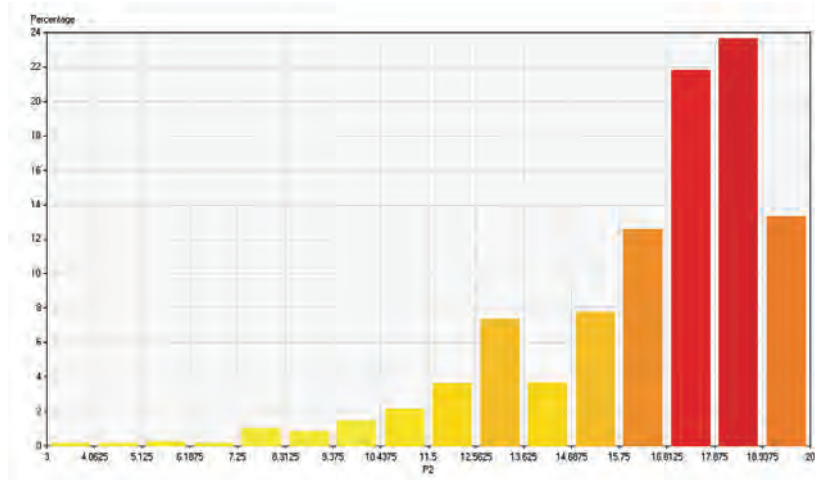
Q



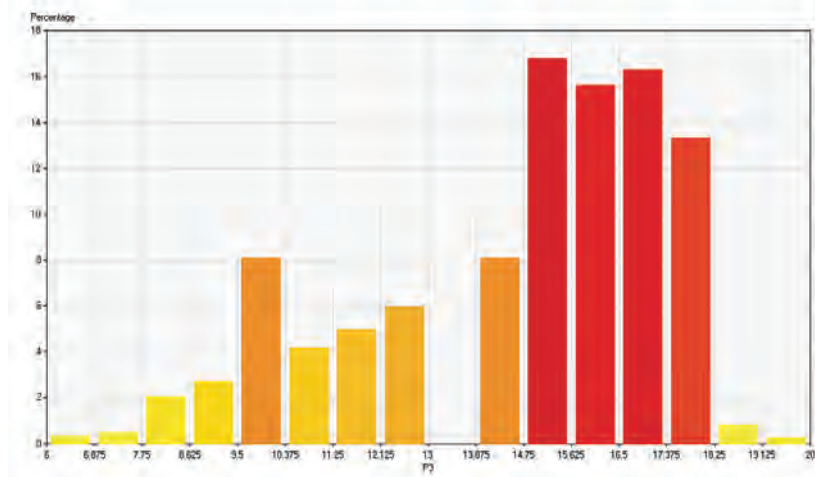
$P_1$



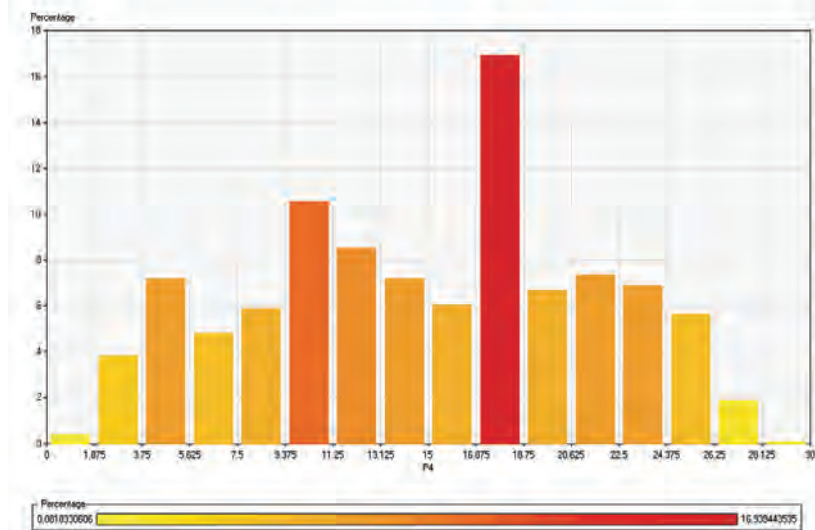
$P_2$



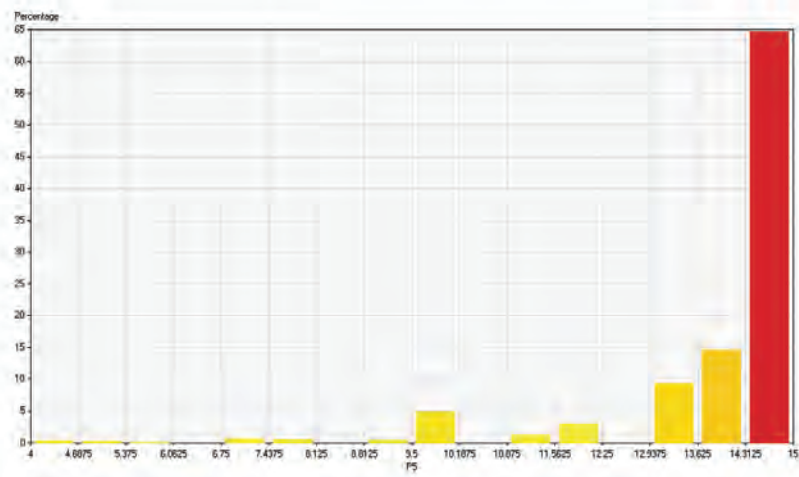
$P_3$



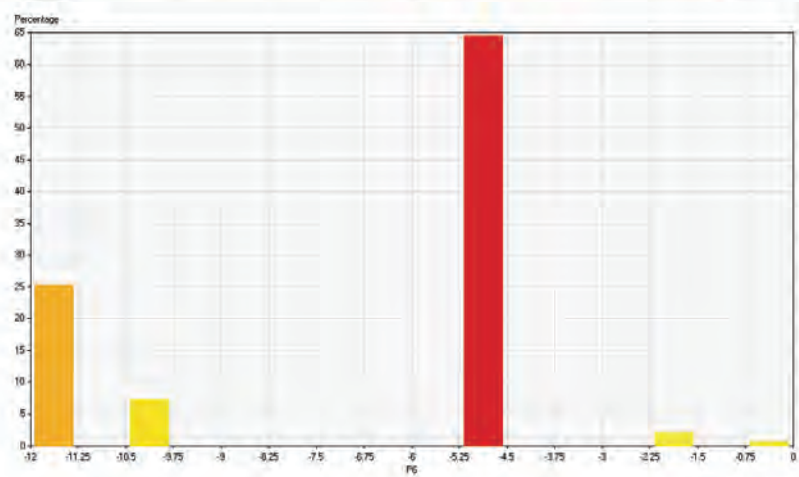
$P_4$



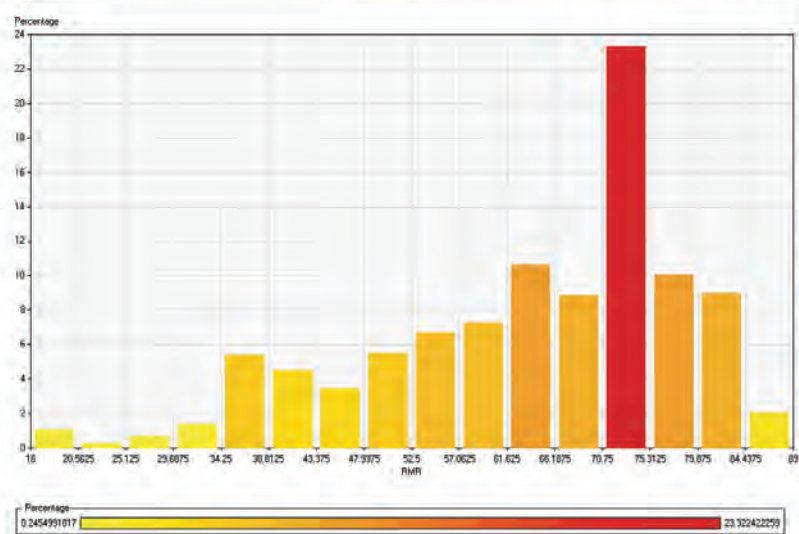
$P_5$



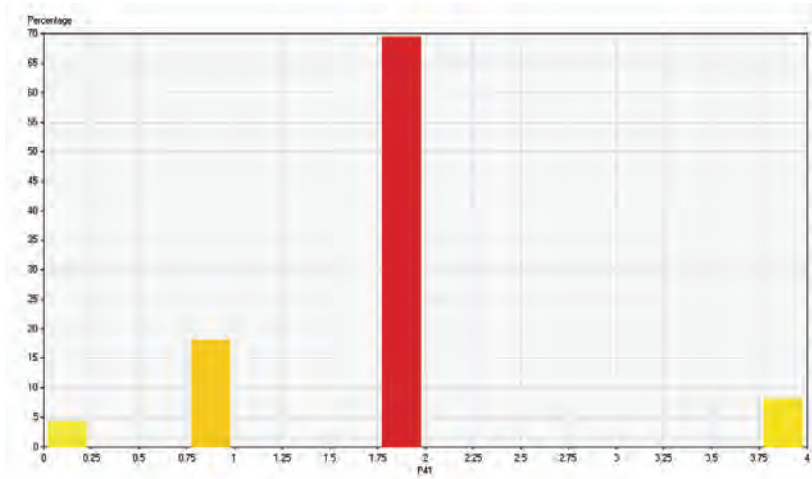
$P_6$



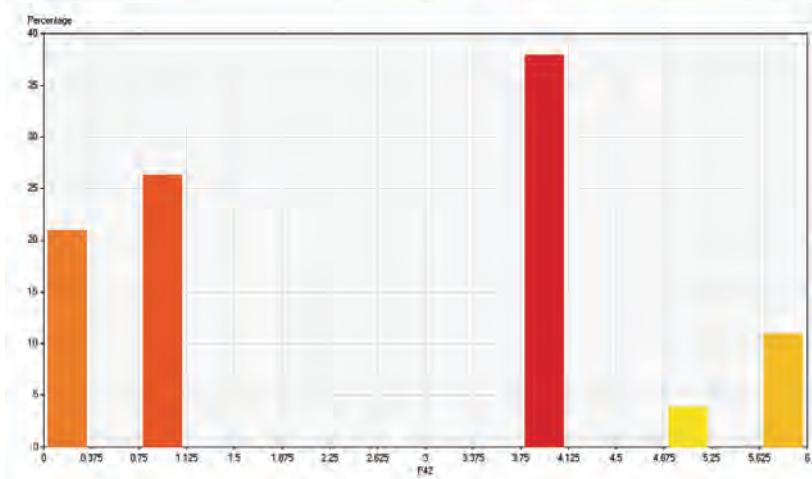
RMR



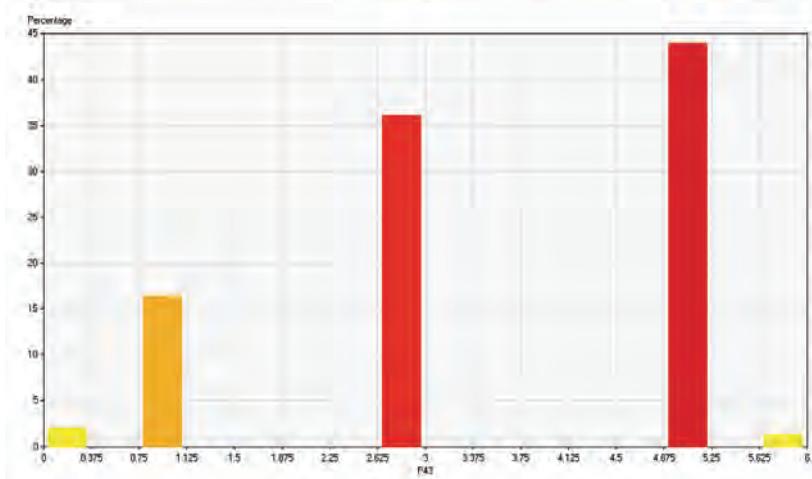
$P_{41}$



$P_{42}$

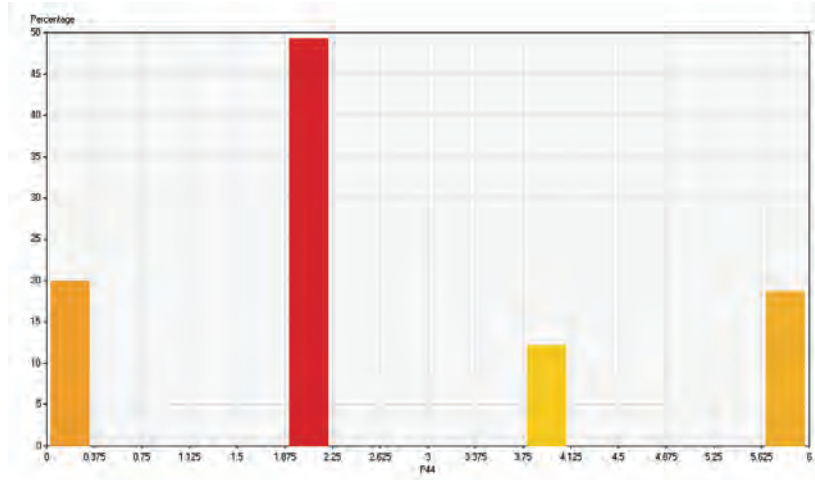


$P_{43}$

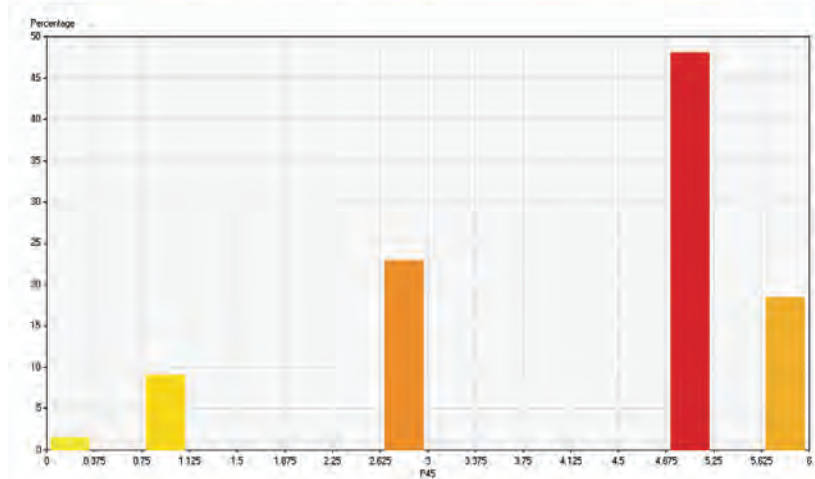




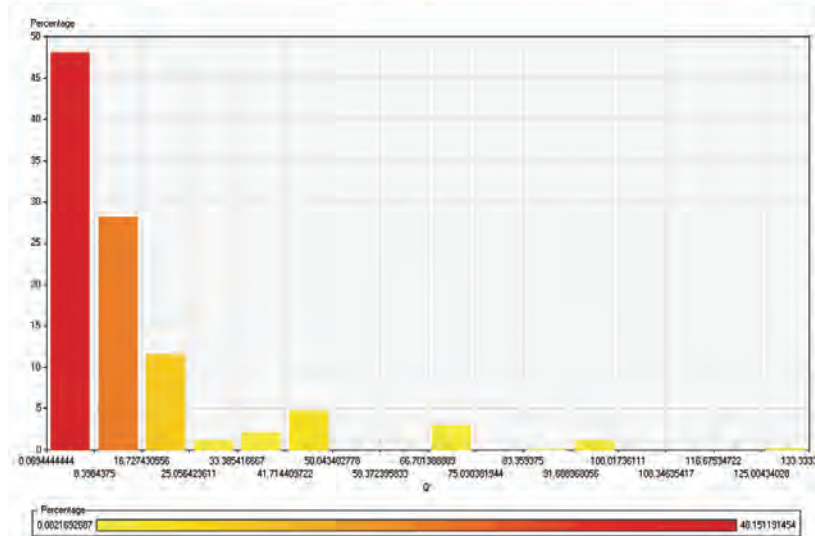
$P_{44}$



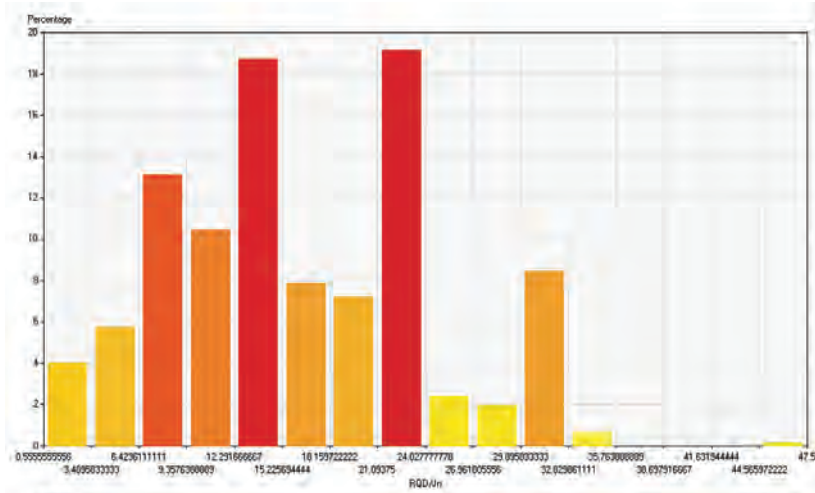
$P_{45}$



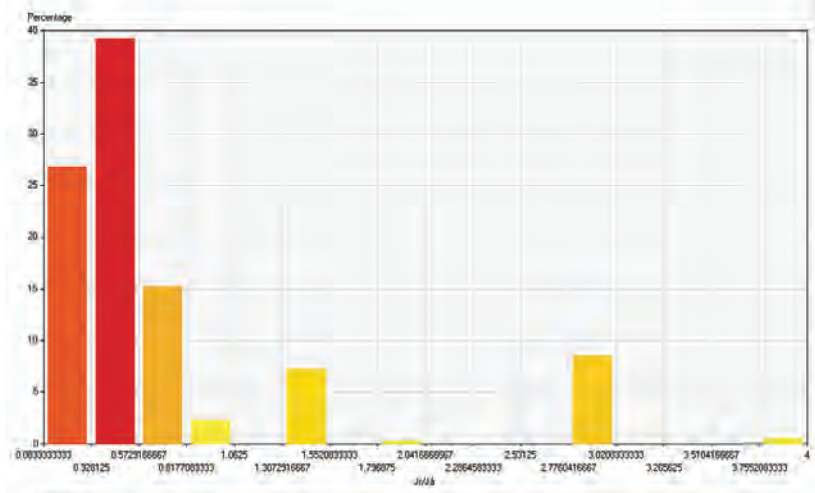
$Q'$



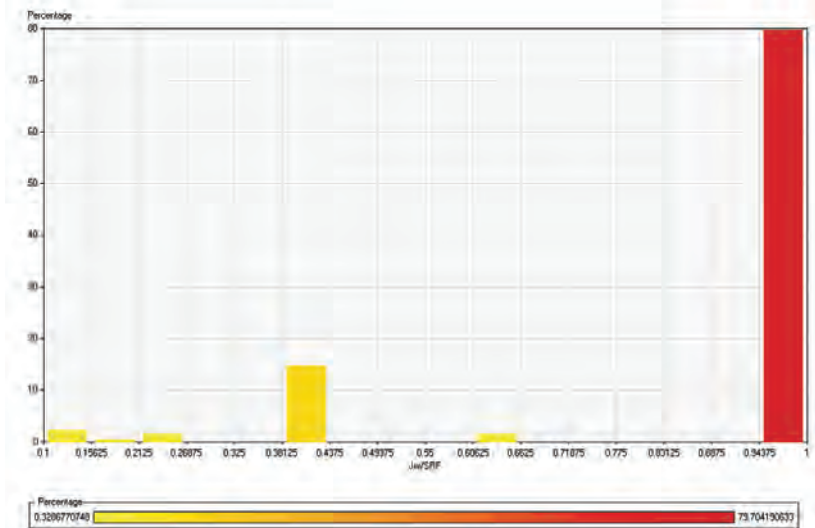
$RQD/J_n$



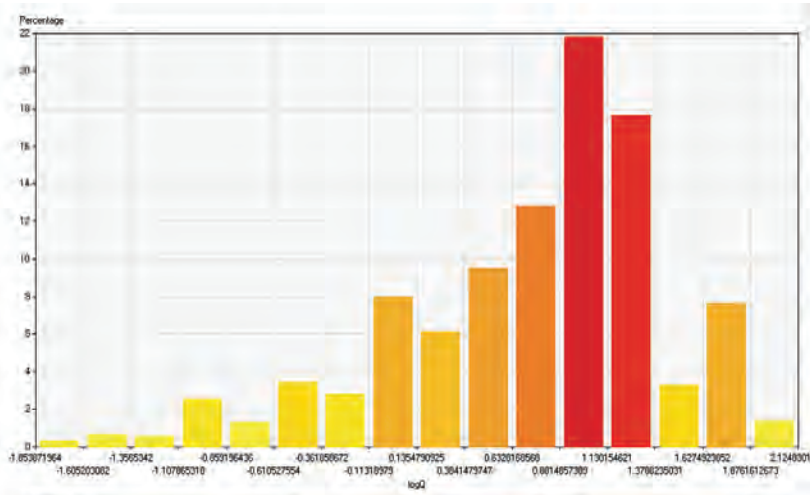
$J_r/J_a$



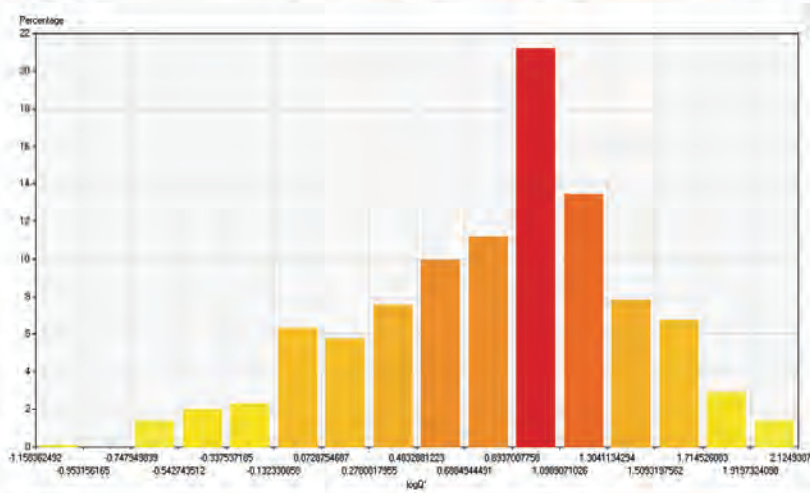
$J_w/SRF$



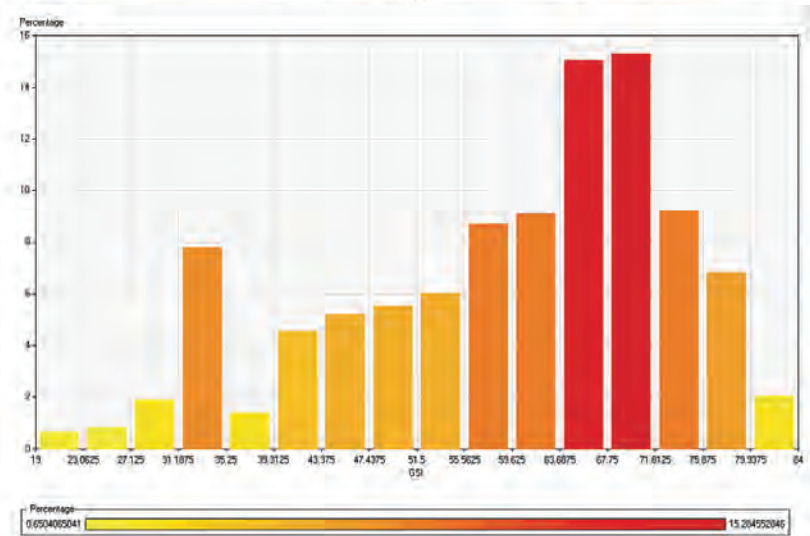
$\log Q$



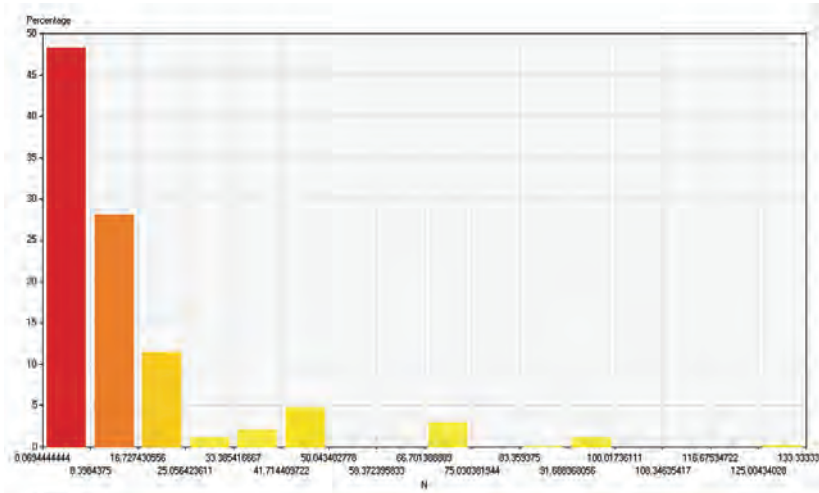
$\log Q'$



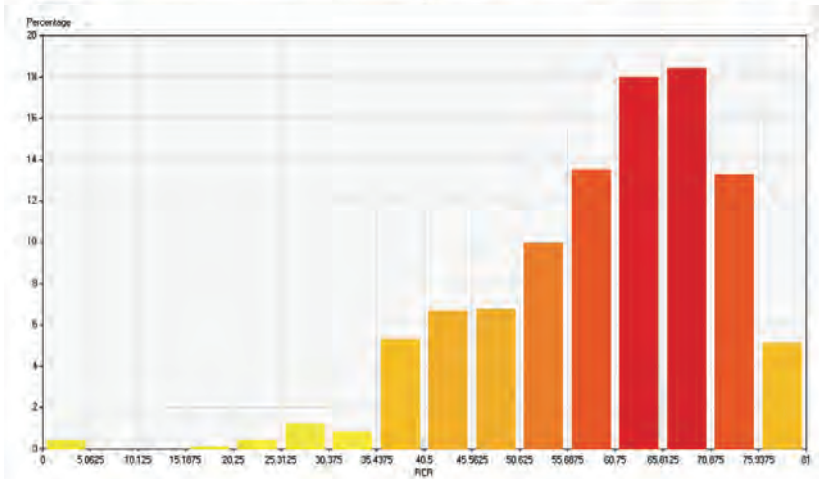
GSI



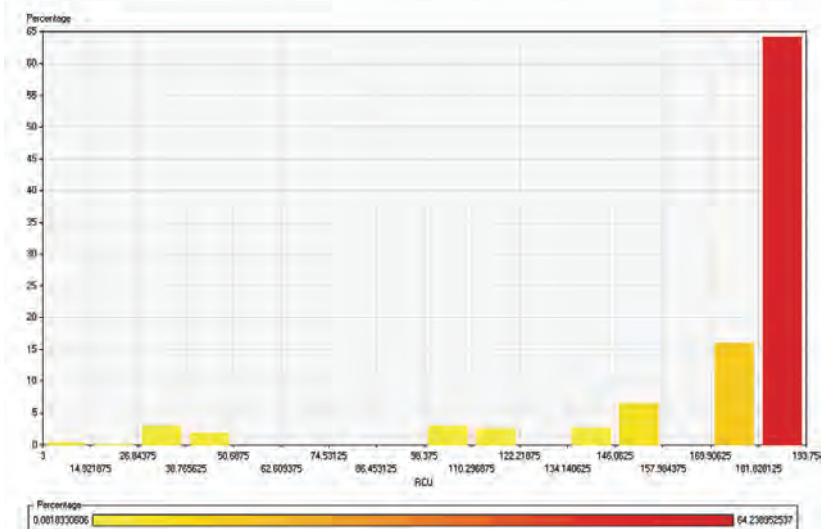
N



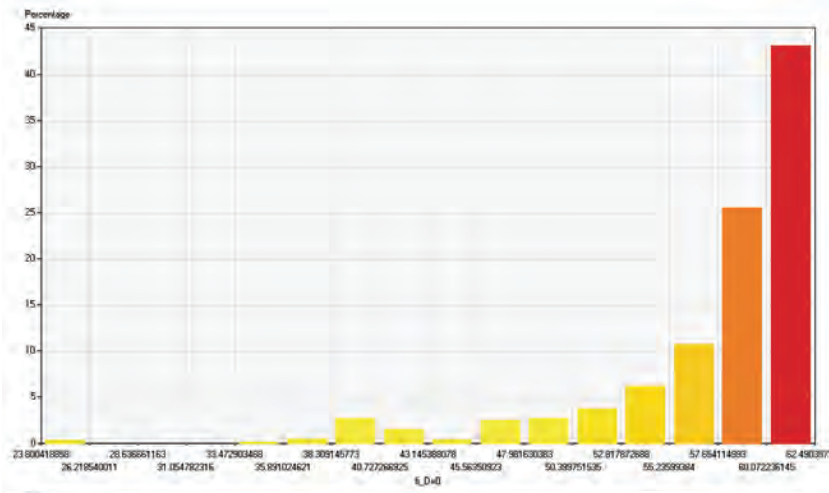
RCR



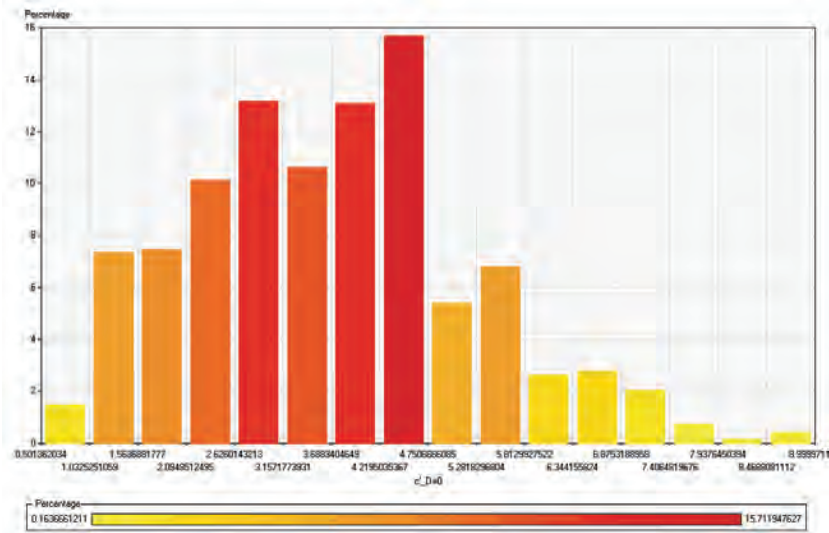
$\sigma_c$



$\phi'$



$c'$



Attribute	Statistical measures				
	Min.	Max.	Mean	Median	Std. dev.
RQD	20.0	100.0	81.0	85.0	12.9
$J_w$	0.66	1.00	0.99	1.00	0.06
$J_n$	2.00	36.00	6.59	6.00	4.38
$J_r$	1.00	3.00	1.69	1.50	0.65
$J_a$	0.75	12.00	4.06	3.00	2.72
SRF	1.00	10.00	1.46	1.00	1.40
Q	0.014	133.300	13.605	8.800	18.341
$P_1$	1.0	12.0	11.0	12.0	2.0
$P_2$	3.0	20.0	16.2	17.0	2.6
$P_3$	6.0	20.0	14.6	15.0	2.8
$P_4$	0.0	30.0	15.0	16.0	6.6
$P_5$	4.0	15.0	14.1	15.0	1.7
$P_6$	-12.0	0.0	-7.0	-5.0	3.2
RMR	16.0	89.0	63.8	68.0	14.8
$P_{41}$	0.0	4.0	1.9	2.0	0.8
$P_{42}$	0.0	6.0	2.6	4.0	2.1
$P_{43}$	0.0	6.0	3.5	3.0	1.6
$P_{44}$	0.0	6.0	2.6	2.0	2.0
$P_{45}$	0.0	6.0	4.3	5.0	1.6
Q'	0.069	133.333	13.972	8.889	18.176
$RQD/J_n$	0.556	47.500	16.249	15.000	7.967
$J_r/J_a$	0.083	4.000	0.757	0.500	0.809
$J_w/SRF$	0.100	1.000	0.873	1.000	0.259
$\log Q$	-1.854	2.125	0.741	0.945	0.709
$\log Q'$	-1.158	2.125	0.836	0.949	0.567
GSI	19.0	84.0	59.1	63.0	14.1
N	0.069	133.333	13.935	8.889	18.192
RCR	0.0	81.0	59.6	62.0	12.3
$\sigma_c$ (MPa)	3.0	193.8	173.8	193.8	39.7
$\phi'$ (°)	23.8	62.5	57.4	59.6	5.7
$c'$ (MPa)	0.501	9.000	3.694	3.623	1.548

# Correction for $\phi'$ and $c'$ due to H and D

In this Annex the developed methodology for a simple correction of the Mohr-Coulomb geomechanical parameters for a given H and D to a different pair of values is described. The main goal is to complement the DM models which give the parameters for reference values of D=0 and H=350 m. First, a general methodology was developed with a broader field of application and then simplified for the particular case of the DM models.

The development of the methodology started with a parametric study of the geomechanical parameters obtained with the Venda Nova II powerhouse complex data. The H-B failure criterion parameters were firstly calculated and then the Mohr-Coulomb geomechanical parameters obtained through the linearisation of that failure criterion for an interest range of stress values. It was considered, as it was for design and modelling purposes, that a gravitic stress field was applied to the rock mass which linearly increased with H. Consequently, for increasing stress (or H),  $\phi'$  decreases while  $c'$  has an inverse trend. In relation to the D factor, increasing values lead to lower values for both  $\phi'$  and  $c'$ . This happens given that higher D values translate a more disturbed rock mass therefore with lower geomechanical parameter values. Figures II.1 and II.2 show the variation of  $\phi'$  and  $c'$ , respectively, for different D and H values.

The variation of  $\phi'$  is non linear for both cases. However, the curves are almost parallel and are well translated by second degree polynomials. The reduction of  $\phi'$  is most pronounced for higher D values. For instance, considering the H=400 m curve, a reduction of approximately 2.5° exist when D varies form 0.8 to 1, while when the variation is from 0 to 0.2 only a 1° reduction is observed. In relation to H, the variation of  $\phi'$  is higher for lower H values. When H varies from 25 m to 50 m, there is an approximately 3° reduction in  $\phi'$ . However, for high H (or stress) values the reduction of this parameter tends to be negligible.

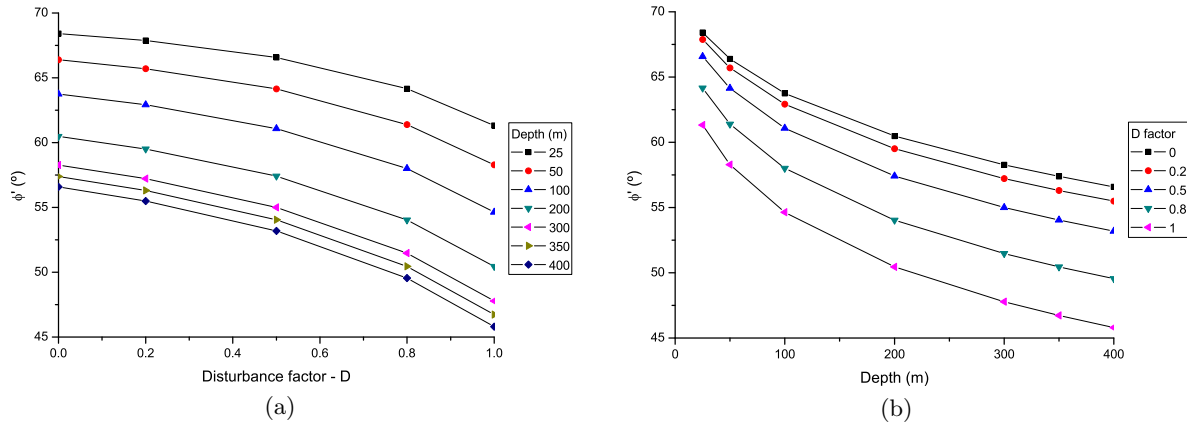


Figure II.1: Variation of  $\phi'$  with a) D and b) H.

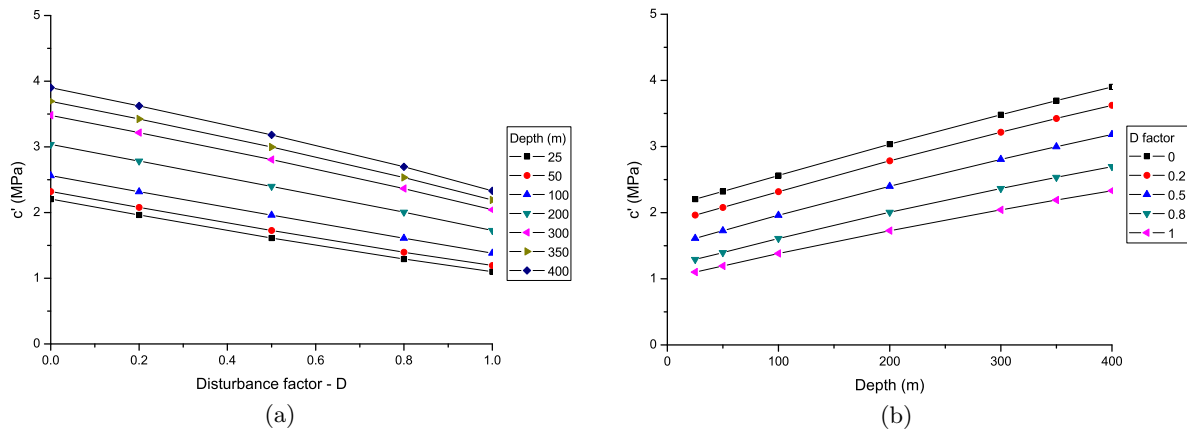


Figure II.2: Variation of  $c'$  with a) D and b) H.

On the other hand,  $c'$  has a nearly linear variation with D and H. This parameter increases with H due to the higher stress field and decreases with D. The variation of D from 0 to 1 means a 1/3 reduction of  $c'$ . In relation to H, its variation from 25 m to 100 m leads to a  $c'$  increase of 15% but if H reaches 400 m the variation is very significant, approximately 80%.

The developed generic methodology is based on the application of two correction factors for each parameter related with D and H. The correction factors can be taken from charts obtained by the normalisation of the previously presented curves for  $D=0$  and  $H=350$  m. This choice was made in order to facilitate its use in the case of the DM prediction models, since they were developed considering these D and H values.

Generically, in the developed methodology, if the geomechanical parameters are available for a given pair  $(D_0; H_0)$  and it is intended to correct them to another pair of values  $(D_f; H_f)$  the process is carried out in two steps:

- first, proceed to the correction for D:  $(D_0; H_0)$  to  $(D_f; H_0)$ ;



- second, correct this value for H:  $(D_f; H_0)$  to  $(D_f; H_f)$ .

This way, the final value of the geomechanical parameters are obtained adding to the initial values the two correction factors. In the particular case of  $\phi'$  its corrected value ( $\phi'_{cor}$ ) is computed by:

$$\phi'_{cor} = \phi'_{ini} + \Delta\phi'_D + \Delta\phi'_H \quad (2.1)$$

where  $\phi'_{ini}$  is the initial friction angle,  $\Delta\phi'_D$  is the correction for D and  $\Delta\phi'_H$  is the correction for H. Attention should be paid that, in this case, the correction values are the difference between the corrections of the final and initial values of D and H:

$$\Delta\phi'_D = \Delta\phi'_{finalD} - \Delta\phi'_{initialD} \quad (2.2)$$

$$\Delta\phi'_H = \Delta\phi'_{finalH} - \Delta\phi'_{initialH} \quad (2.3)$$

where  $\Delta\phi'_{initialD}$  and  $\Delta\phi'_{finalD}$  are the correction factors, related to D, correspondent to  $(D_0; H_0)$  and  $(D_f; H_0)$ , respectively; and  $\Delta\phi'_{initialH}$  and  $\Delta\phi'_{finalH}$  are the correction factors, related to H, correspondent to  $(D_f; H_0)$  and  $(D_f; H_f)$ , respectively. For the particular case of the DM models, the results are already defined for values of H=350 m and D=0 so the initial values are 0. The correction factors for  $\phi'$  can be taken from the charts of Figures II.3 and II.4.

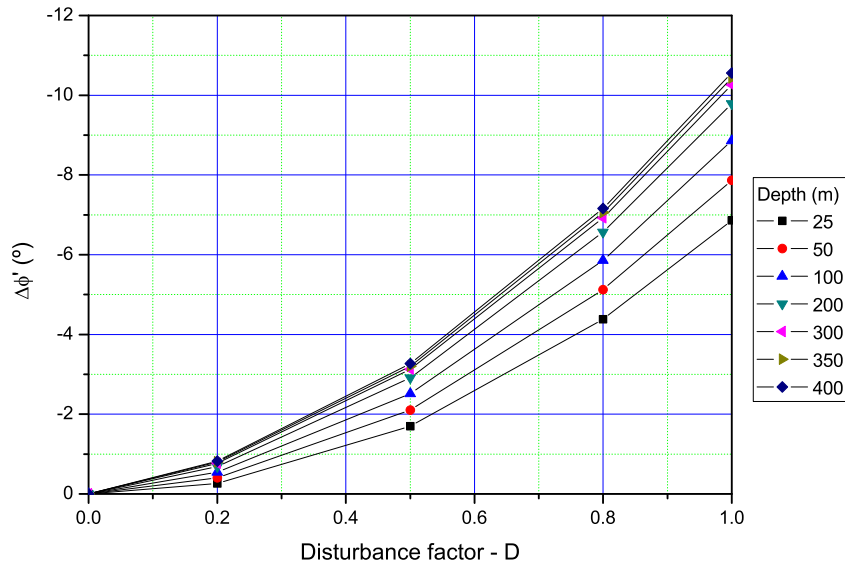
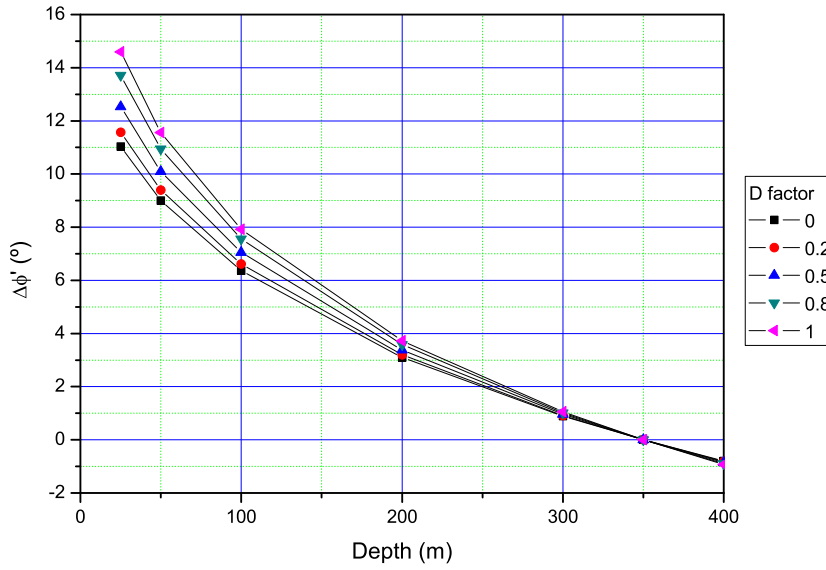


Figure II.3: Correction factor chart for  $\phi'$  concerning D



**Figure II.4:** Correction factor chart for  $\phi'$  concerning H

In the case of  $c'$ , the linear relation with H and D allows establishing a simpler correction process. The expression for computing the final value of  $c'$  is similar to the one developed for  $\phi'$ :

$$c'_{cor} = c'_{ini} + \Delta c'_D + \Delta c'_H \quad (2.4)$$

where  $c'_{cor}$  is the corrected cohesion,  $c'_{ini}$  the initial cohesion,  $\Delta c'_D$  is the correction for D and  $\Delta c'_H$  is the correction for H. The correction factors are proportional to two parameters  $\alpha$  and  $\beta$  in the sense:

$$\Delta c'_D = -\alpha \times \Delta D = -\alpha \times (D_{final} - D_{initial}) \quad (2.5)$$

$$\Delta c'_H = \beta \times \Delta H = \beta \times (H_{final} - H_{initial}) \quad (2.6)$$

where  $D_{final}$ ,  $D_{initial}$ ,  $H_{final}$  and  $H_{initial}$  are the final and initial values for the disturbance factor and depth, respectively. For the particular case of the DM models  $D_{initial}$  and  $H_{initial}$  are 0 and 350, respectively. The  $\alpha$  and  $\beta$  parameters can be taken from the charts of Figures II.5 and II.6.

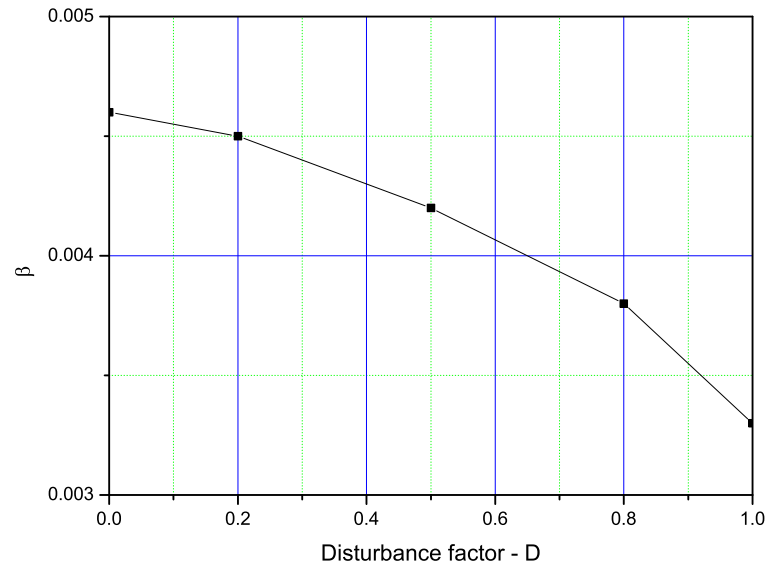


**Figure II.5:** Correction factor chart for  $c'$  concerning D

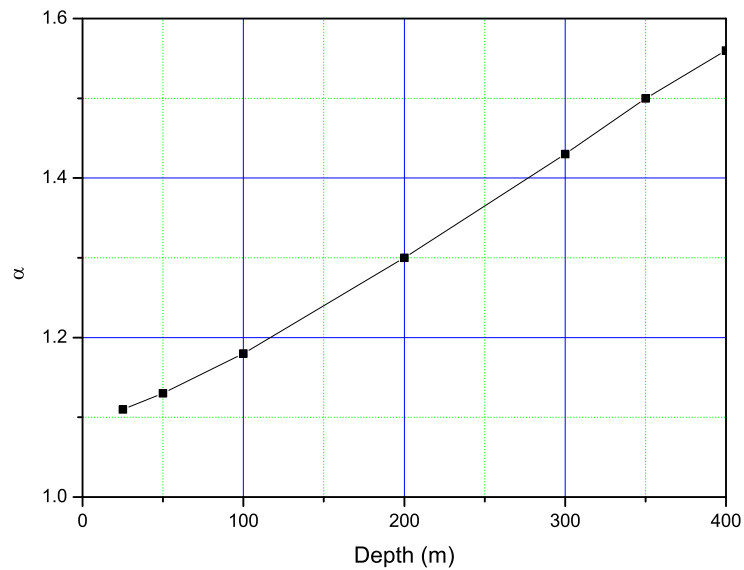


**Figure II.6:** Correction factor chart for  $c'$  concerning H

*Calculation Example:* Lets consider that for  $D=1$  and  $H=100$  m the  $\phi'$  and  $c'$  values were  $54.64^\circ$  and 1,382 MPa, respectively, and it was intended to obtain these geomechanical parameters for  $D=0.5$  and  $H=300$  m.

#### Correction of $\phi'$ :

First, the correction for the D factor.

$$(D = 1; H = 100m) \rightarrow (D = 0.5; H = 100m) \Rightarrow$$

$$\Rightarrow \Delta\phi'_D = \Delta\phi'_{finalD} - \Delta\phi'_{initialD} = -2.51 - (-8.86) = 6.35^\circ \quad (2.7)$$

Second, the correction for H.

$$(D = 0.5; H = 100m) \rightarrow (D = 0.5; H = 300m) \Rightarrow$$

$$\Rightarrow \Delta\phi'_H = \Delta\phi'_{finalH} - \Delta\phi'_{initialH} = 0.96 - 7.04 = -6.06^\circ \quad (2.8)$$

Final value of  $\phi'$ .

$$\phi'_{cor} = \phi'_{ini} + \Delta\phi'_D + \Delta\phi'_H = 54.64 + 6.35 - 6.06 = 54.93^\circ \quad (2.9)$$

The value of the  $\phi'$  obtained directly by the H-B methodology is  $55.01^\circ$  which means that the error is approximately 0.15%.

### Correction of $c'$ :

First, the correction for the D factor.

$$(D = 1; H = 100m) \rightarrow (D = 0.5; H = 100m) \Rightarrow$$

$$\Rightarrow \Delta c'_D = -\alpha \times \Delta D = -\alpha \times (D_{final} - D_{initial}) = -1.18 \times (0.5 - 1) = 0.59 MPa \quad (2.10)$$

Second, the correction for H.

$$(D = 0.5; H = 100m) \rightarrow (D = 0.5; H = 300m) \Rightarrow$$

$$\Rightarrow \Delta c'_H = \beta \times \Delta H = \beta \times (H_{final} - H_{initial}) = 0.0042 \times (300 - 100) = 0.84 MPa \quad (2.11)$$

Final value of  $c'$ .

$$c'_{cor} = c'_{ini} + \Delta c'_D + \Delta c'_H = 1.382 + 0.59 + 0.84 = 2.812 MPa \quad (2.12)$$

The correct value for  $c'$  is 2.805 MPa. This means that the error associated with the correction is 0.25%. Several runs were carried out and the maximum computed error was approximately 2.5% which can be considered acceptable.

---

## ANNEX III

---

# Computed stresses and displacements for the 3D model of Venda Nova II

In this Annex some additional results concerning the 3D model of Venda Nova II powerhouse complex are presented. In particular, the evolution in the different excavation stages of the total displacements (along with displacement vectors) and minimum and maximum stresses are detailed for two different cross-sections. The first, which is designated cross-section 1, intersects one of the interconnecting galleries, while cross-section 2 passes through a zone closer to one extreme of the caverns and does not intersect any gallery. It was thought to present similar results correspondent to the calculation with the optimised parameters. However, the results were qualitatively identical differing only in a stiffer response of the rock mass due mainly to the higher value of  $E$ . This way, in the following Figures, the results are presented.

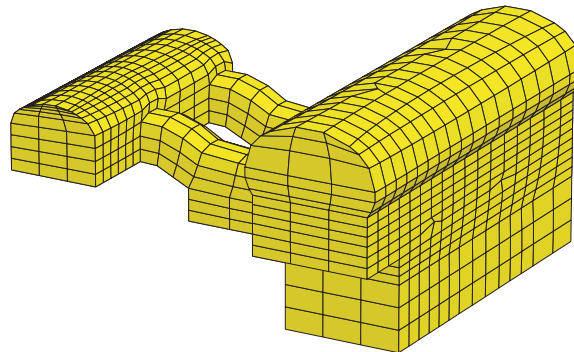


*Figure III.1:* Adopted mesh for the 3D model of the Venda Nova II powerhouse complex

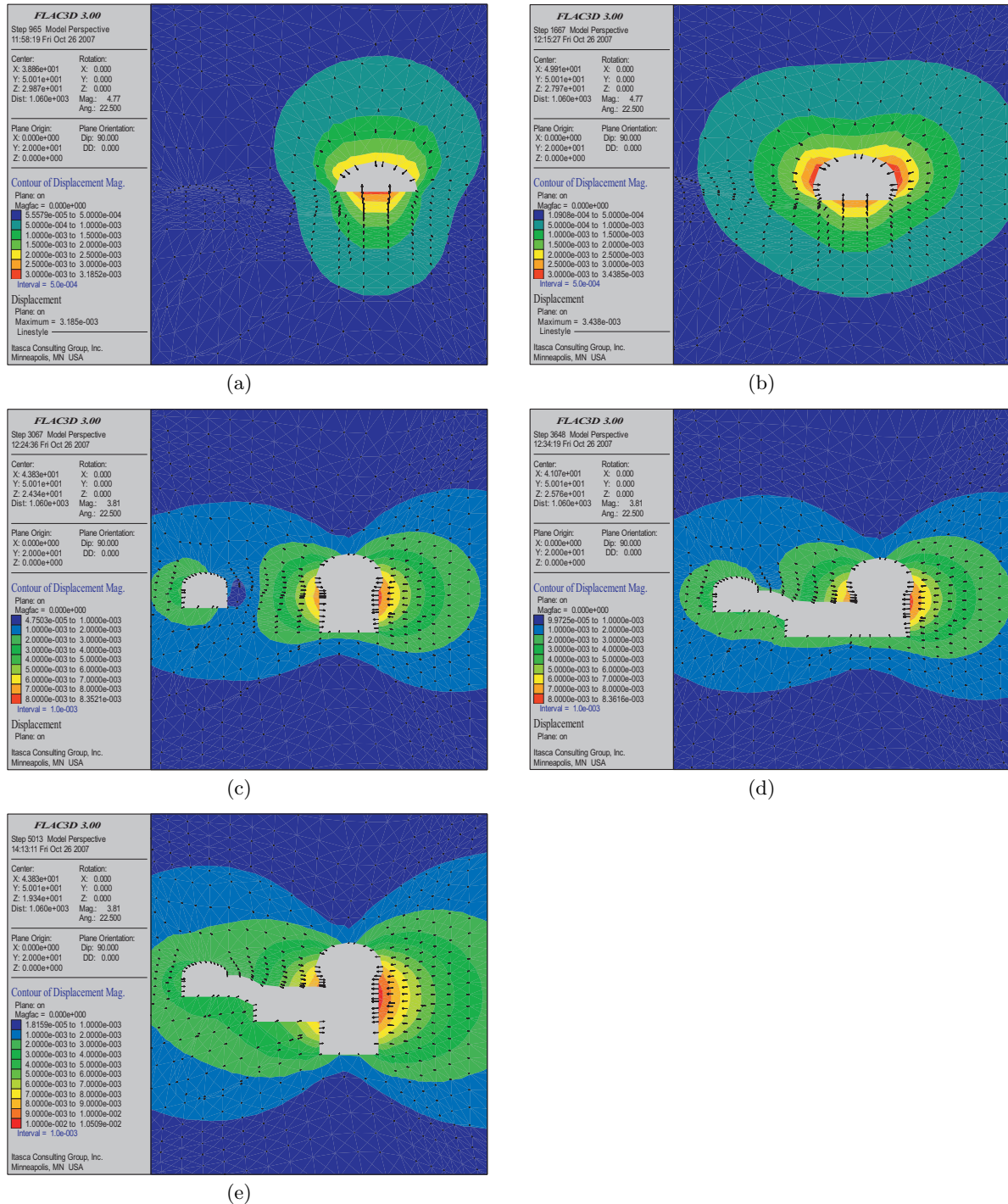
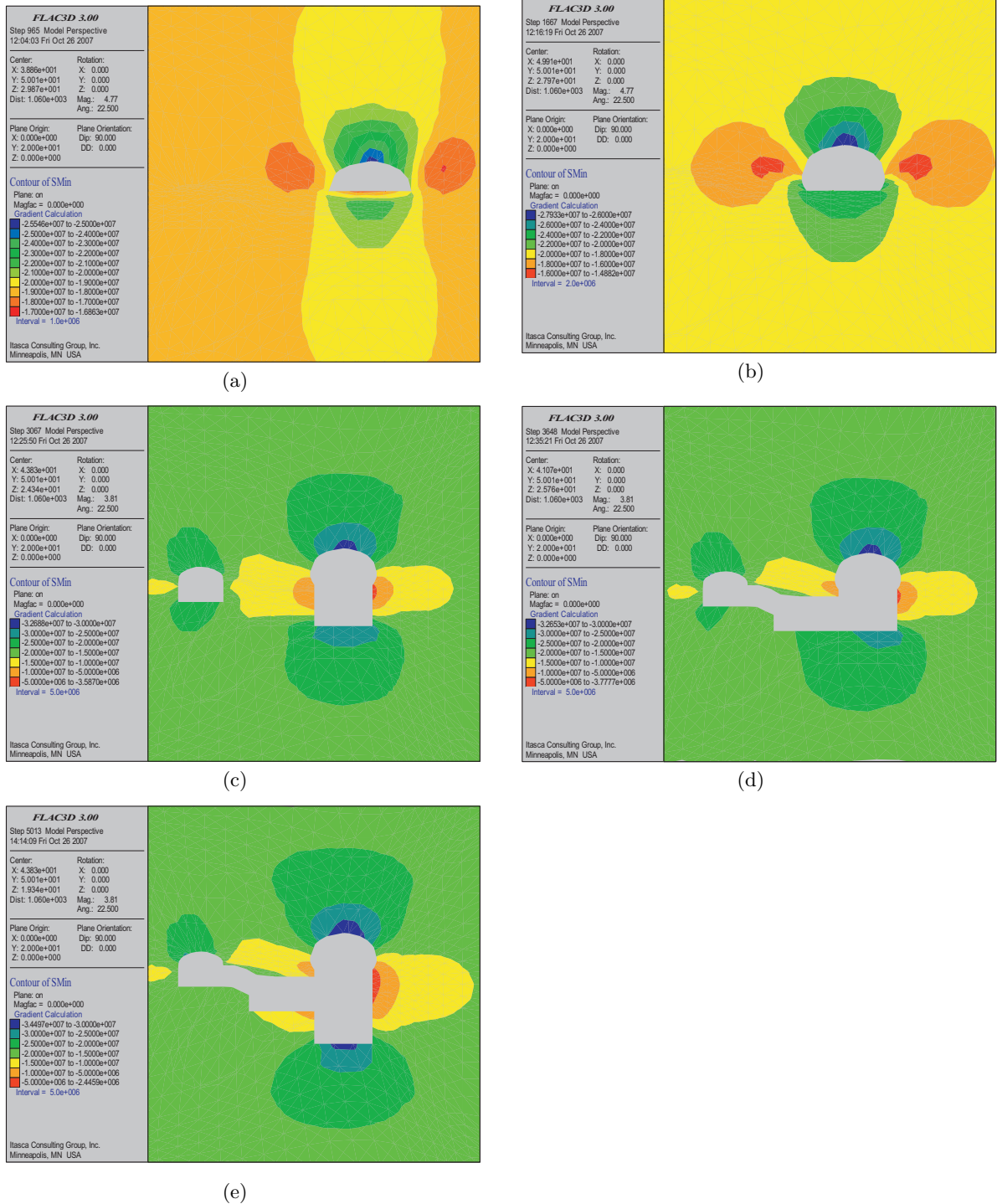


Figure III.2: Total displacements for cross-section 1. a) Stage 1. b) Stage 2. c) Stage 3. d) Stage 4. e) Stage 5.



**Figure III.3:** Minimum stresses for cross-section 1. a) Stage 1. b) Stage 2. c) Stage 3. d) Stage 4. e) Stage 5.



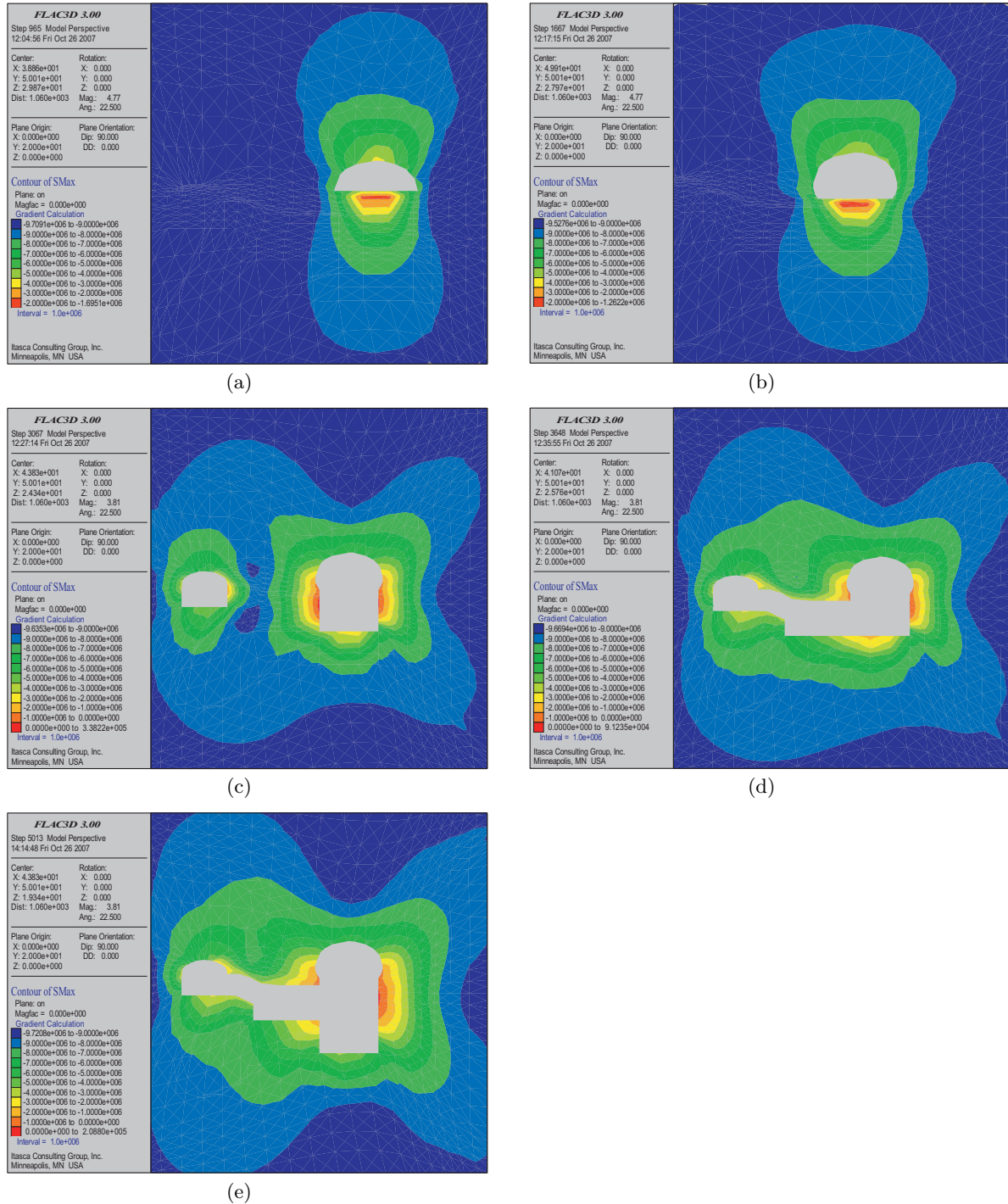


Figure III.4: Maximum stresses for cross-section 1. a) Stage 1. b) Stage 2. c) Stage 3. d) Stage 4. e) Stage 5.



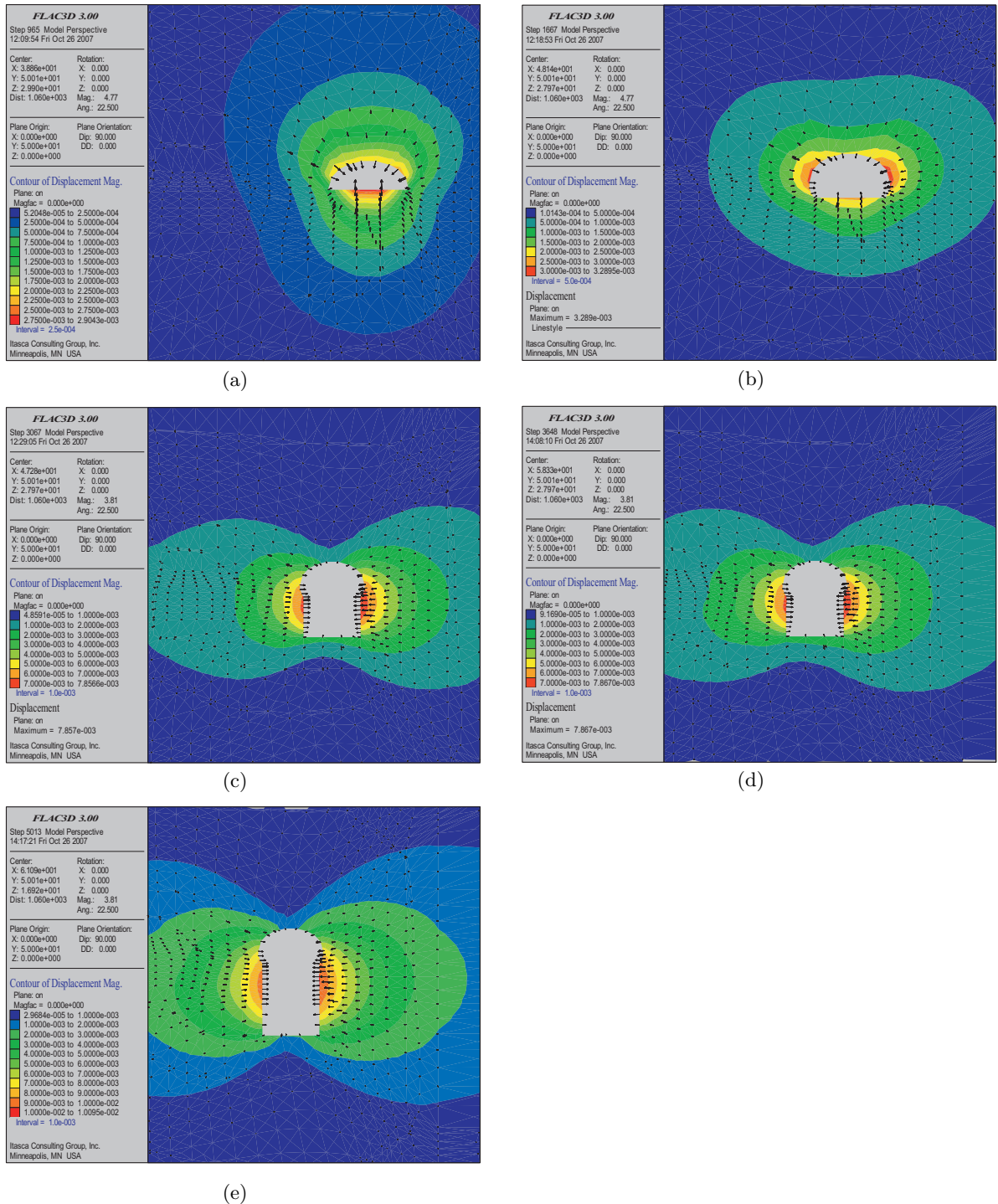


Figure III.5: Total displacements for cross-section 2. a) Stage 1. b) Stage 2. c) Stage 3. d) Stage 4. e) Stage 5.

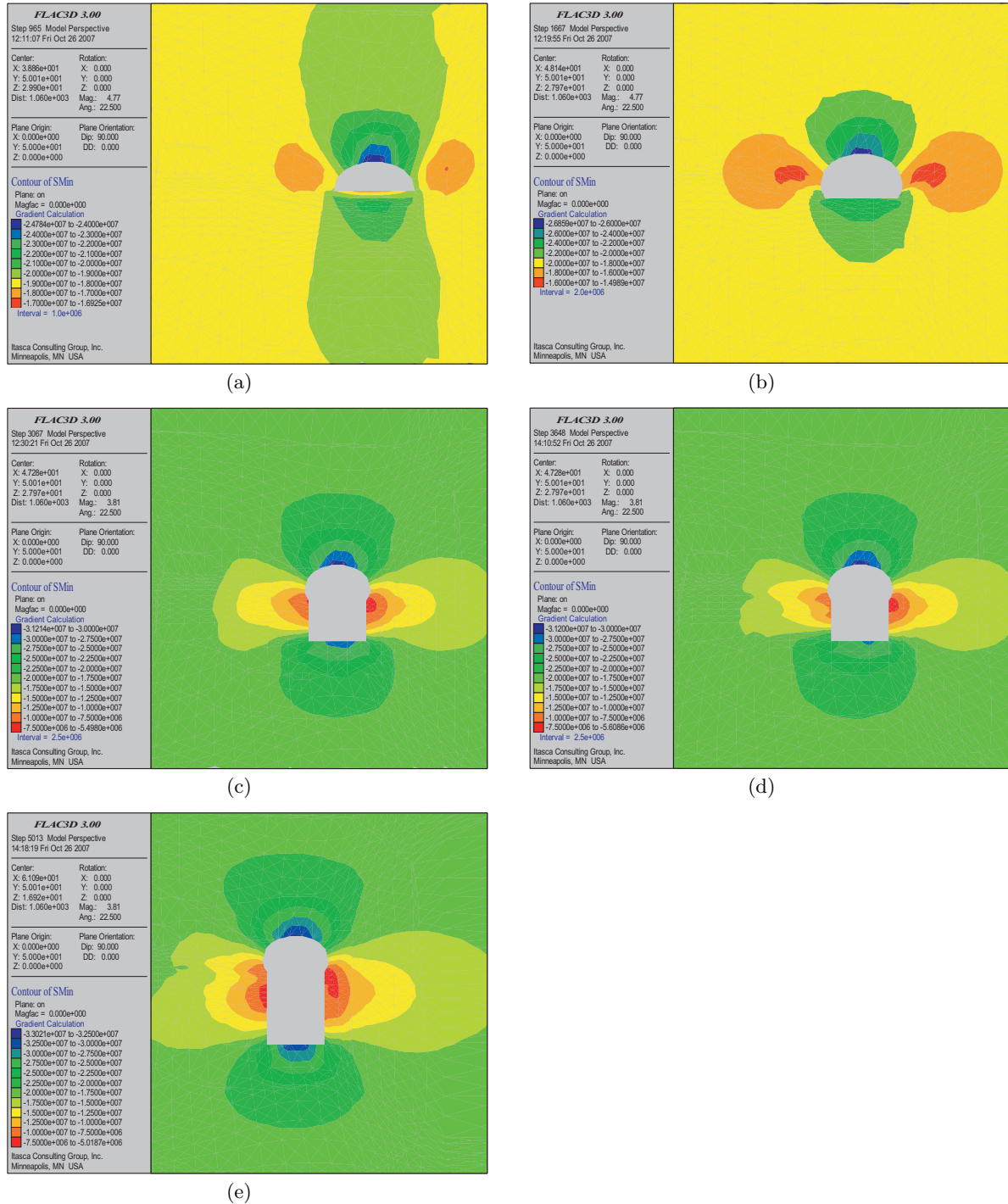
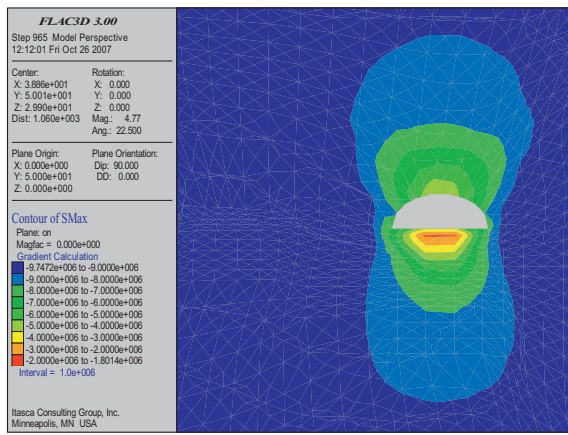
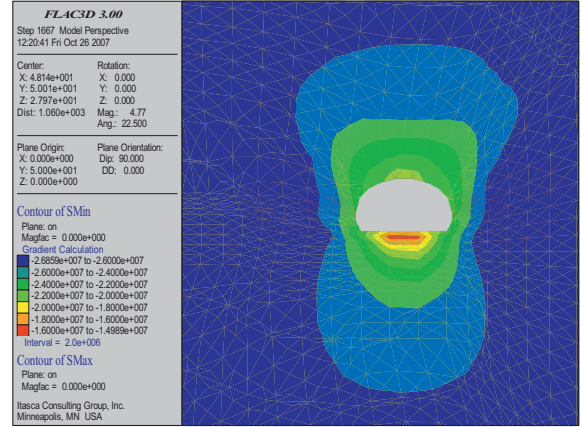


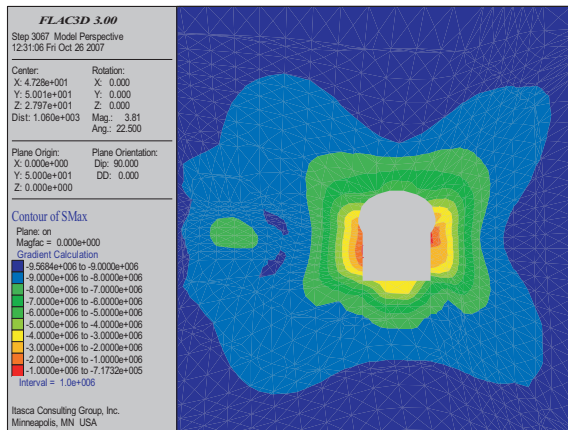
Figure III.6: Minimum stresses for cross-section 2. a) Stage 1. b) Stage 2. c) Stage 3. d) Stage 4. e) Stage 5.



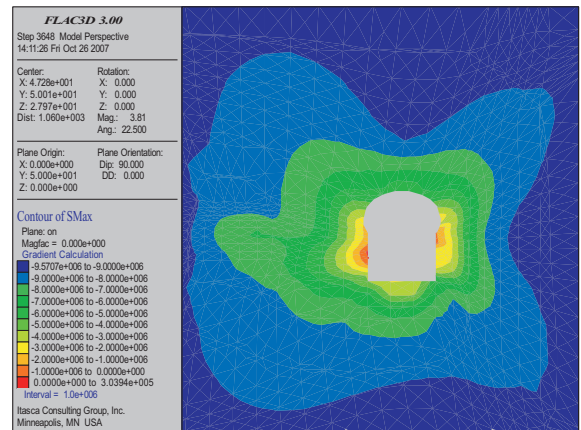
(a)



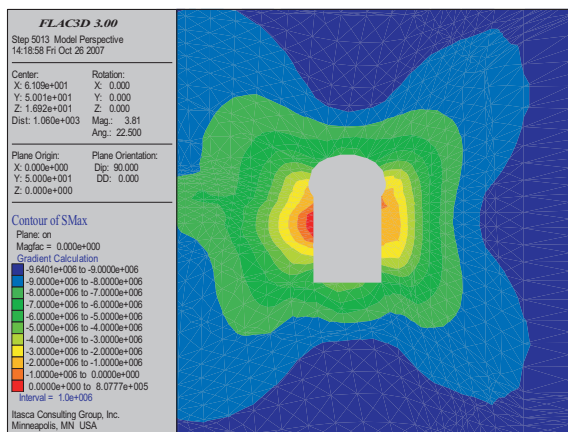
(b)



(c)



(d)



(e)

**Figure III.7:** Maximum stresses for cross-section 2. a) Stage 1. b) Stage 2. c) Stage 3. d) Stage 4. e) Stage 5.